

# **Synthesis of Analogues of Dicoumarol and their Measurement as Inhibitors of NQO1**

A thesis submitted to The University of Manchester for the degree of  
PhD  
in the Faculty of Engineering and Physical Sciences

**2015**

**Juliana Chineze Obi**

School of Chemistry

## Contents

<b>1.0</b>	<b>Chapter 1: Introduction</b>	<b>12</b>
1.1	The cell	12
1.1.1	Carcinogenesis/Tumorigenesis	12
1.1.2	Origin of cancer cells	13
1.1.3	Tumor invasion and metastasis	14
1.1.4	Escaping apoptosis	16
1.1.5	Self sufficient in growth signal	16
1.1.6	Insensitivity to anti-growth signal	17
1.1.7	Sustained angiogenesis	18
1.1.8	Limitless replicative potential	18
1.2.0	Causes of cancer	19
1.3.0	Glucose metabolism	22
1.3.1	Cancer metabolism	23
1.3.2	Advantages of glycolysis to cancer cells	25
1.4.0	Signs and symptoms of cancer	26
1.4.1	Cancer risk factors	26
1.4.2	Treatment of cancer	27
1.4.2.1	Chemotherapy (Chemoprevention)	28
1.4.2.2	Surgery	28
1.4.2.3	Radiotherapy	28
1.5.0	NADH: oxidoreductase quinone 1 (NQO1)	29
1.5.1	Structure of NQO1	34
1.5.2	NQO1 active site	36
1.5.3	NQO1 gene and polymorphism	37
1.5.4	NQO1 inhibitors	37
1.5.5	Consequences of the interaction of NQO1 with dicoumarol	39
1.6.0	NADH: oxidoreductase quinone 2 NQO2	40
1.6.1	Crystal structure of NQO2	40
1.6.2	NQO2 active site	42
1.6.3	NQO2 inhibitors	43
1.7.0	Sources of quinone	47
1.8.0	Consequences of inhibiting NQO1 and NQO2	47
1.9.0	Discovery of potent anti-cancer drugs	48

1.9.1	Isolation of COTC.....	49
1.9.2	The glyoxalase enzymes.....	52
1.9.3	The role of glutathione.....	53
1.9.4	Mechanism of action of COTC and COMC .....	55
1.9.5	Natural ant-tumor agents structurally related to COTC.....	58
1.9.5.1	The antheminones and carvotacetones.....	58
1.9.5.2	The antheminones.....	59
1.9.5.3	Carvotacetone derivatives.....	61
1.9.6	The prodrug concept.....	62
1.9.6.1	Classification of prodrug.....	63
1.9.6.2	Characteristic features of prodrug.....	64
1.10	Aims and objectives.....	65
<b>2.0</b>	<b>Chapter 2: Result and discussion.....</b>	<b>68</b>
2.1	Introduction.....	68
2.2	Previous synthesis.....	69
2.3	New synthesis.....	72
2.3.1	Synthesis of 4-hydroxycoumarin derivatives.....	72
2.3.2	Synthesis of symmetrical analogues of dicoumarol.....	74
2.3.2.1	Non-planarity of symmetrical analogues of dicoumarol.....	76
2.4	Synthesis of the “halfway stage” analogues of dicoumarol.....	78
2.4.1	Reduction of the “halfway stage” analogues of dicoumarol.....	79
2.4.2	Reduction of “halfway stage” analogues using Hantzsch’s ester.....	80
2.5	Reductive cleavage of C-C bond of symmetrical analogues of dicoumarol using NaBH <sub>3</sub> CN.....	83
2.6	Borrowing hydrogen methodology.....	85
2.7	Synthesis of an analogue of ‘antheminone A’ for prodrug design.....	92
2.7.1	Previous synthesis by the Whitehead group.....	94
2.7.2	Synthesis of $\gamma$ -lactone.....	95
2.7.3	Conversion of $\gamma$ -lactone to hydroxyketone.....	96
2.7.3.1	Reductive ring opening in $\gamma$ -lactone.....	96
2.7.4	Oxidative cleavage of triol.....	97
2.7.5	Elimination of $\beta$ -hydroxyl.....	98
2.7.6	1,4-conjugate addition.....	99

2.7.7	The mechanistic cycle of rhodium-catalyzed 1,4-addition.....	104
2.7.8	Eliminative removal of the cyclohexylidene protecting group.....	105
2.7.9	Triethylsilyl (TES) protection of the C-4 hydroxyl group.....	108
2.8.0	Synthesis of Morita-Baylis-Hillman adduct.....	109
2.9.0	Application of Mitsunobu reaction for the prodrug synthesis.....	112
<b>3.0</b>	<b>Chapter 3: Biological evaluation.....</b>	<b>115</b>
3.1	Introduction.....	115
3.2	Determination of IC <sub>50</sub> values.....	116
3.3	Previous work in the Whitehead research group.....	116
3.4	IC <sub>50</sub> values of the novel synthesized compounds.....	119
3.5	Cytotoxicity assay.....	123
3.5.1	MTT cell viability assay.....	124
3.5.2	Evaluation of the IC <sub>50</sub> values of the novel compounds.....	124
<b>4.0</b>	<b>Chapter 4: Conclusion and future work.....</b>	<b>127</b>
<b>5.0</b>	<b>Chapter 5: Experimental procedures.....</b>	<b>132</b>
5.1	Instrumentation.....	132
5.2	Reagents and conditions.....	133
5.3	Experimental.....	133
<b>6.0</b>	<b>Experimental procedures for the enzyme and biological assays.....</b>	<b>191</b>
6.1	Application of menadione and cytochrome c in enzyme assay evaluation..	191
6.2	Preparation of chemicals and reagents for enzyme assay.....	191
6.3	Evaluation of NQO1 inhibition.....	191
6.4	MTT cell viability assay procedure.....	192
6.5	Counting and seeding cells in haemocytometer.....	192
6.6	Treating the cells.....	193
6.7	Ending the viability assay.....	193
	<b>References.....</b>	<b>194</b>
	List of figures, tables and schemes.....	205

**Word count:** 52,707

**Abbreviations:**

ATP	Adenosine triphosphate
ATCC	American Type Culture Collection
A549	Adenocarcinomic human alveolar basal epithelial cells
acac	acetylacetonate
BRCA (1 and 2)	Breast cancer susceptibility gene (1 and 2)
BSA	Bovine serum albumin
b.p	Boiling point
BINAP	2,2'-bis(diphenylphosphino)-1,1'-binaphthyl
<sup>13</sup> C	Carbon-13
δ	Chemical shift (delta)
CAT	Computerized axial tomography
cod	Cyclooctadiene
COSY	Correlation spectroscopy
COTC	2-crotonyloxymethyl-(4 <i>R</i> ,5 <i>R</i> ,6 <i>R</i> )-4,5,6-trihydroxycyclohex-2-enone
COMC	(6-oxocyclohex-1-en-1-yl)methylene ( <i>E</i> )-but-2-enoate
°C	Degree celsius
DBU	1,8-diazabicyclo[5.4.0]undec-7-ene
DIAD	Di-isopropyl azodicarboxylate
DMSO	Dimethylsulfoxide
DMAP	4-N,N-Dimethylaminopyridine
DNA	Deoxyribo nucleic acid
DNQ	Deoxynyboquinone
DCPIP	Dichlorophenolindolphenol
dppp	1,4-Bis(diphenylphosphino)propane
dppb	1,4-Bis(diphenylphosphino)butane
dppe	1,2-Bis(diphenylphosphino)ethane
eq	Equivalent(s)
+ES	positive ion electrospray
-ES	negative ion electrospray
ee	Enantiomeric excess
E1 <sub>CB</sub>	Elimination unimolecular conjugate base
ECM	Extracellular matrix
EDTA	Ethylenediamine tetr-acetic acid

ER	Endoplasmic reticulum
EMP	Emden-Meyerhof Paranas pathway
EtOH	Ethanol
FAS	Fatty acids
FAD	Flavin adenine dinucleotide
FDA	Federal drug agency
FT-IR	Fourier transformed infrared spectroscopy
g	gram
GSH	Glutathione
GSSG	Glutathione disulphide
GST	Glutathione transferase enzyme
h	hour(s)
HPV	Human papilloma virus
HSA	Human serum albumin
hz	hertz
IC <sub>50</sub>	Inhibitory concentration at 50%
IR	Infrared spectroscopy
<i>J</i>	Coupling constant
Lit	Literature
MTT	(3-(4,5-dimethylthiazol-2-yl)-2,5-diphenyltetrazolium bromide)
MMC	Mitomycin C
M.p	Melting point
<i>m/z</i>	mass/charge ratio
mins	minutes
mmol	millimol
M	molar
NRH	N-ribosyl nicotinamide
NAD <sup>+</sup>	Nicotinamide adenine dinucleotide (oxidized form)
NADH	Nicotinamide adenine dinucleotide (reduced form)
NADP <sup>+</sup>	Nicotinamide adenine dinucleotide phosphate (oxidized form)
NAD(P)H	Nicotinamide adenine dinucleotide phosphate (reduced form)
NQO1	NADH quinone oxidoreductase 1
NQO2	NRH quinone oxidoreductase 2
NMR	Nuclear magnetic resonance

PET	Positron emission tomography
PPP	Pentose phosphate pathway
ppm	part per million
Ph	phenyl
ROS	Reactive oxygen species
$R_f$	Retention factor
r.t	room temperature
SDS	Sodium dodecyl sulphate
TESOTf	Triethylsilyltrifluoromethane sulfonate (TES-triflate)
TFA	Trifluoroacetic acid
THF	Tetrahydrofuran
TLC	Thin layer chromatography
TSP	Tumor suppressor protein
Et <sub>3</sub> N	Triethylamine
UV	ultraviolet

## **Abstract**

A variety of novel and effective inhibitors of NQO1 was synthesized. The inhibitors were classified as ‘asymmetrical’ and ‘halfway stage’ analogues of dicoumarol. The synthesis of these inhibitors was achieved through the application of different techniques such as ‘borrowing hydrogen methodology’, thermal and microwave irradiation and reductive C-C cleavage using NaBH<sub>3</sub>CN. One of the most potent analogues was toxic (IC<sub>50</sub> = 9.2 ± 0.3 μM) towards the non-small cell lung cancer cell line, A549.

A selection of the most potent inhibitors was re-modified as prodrugs in order to improve drug penetration through the barrier of the cell membrane. This was achieved by conjugation with a delivery agent related to the natural product antheminone A. The synthesis involved a multi-step reaction sequence involving the use of natural product (-)-quinic acid as a precursor. A range of prodrugs were synthesized which exhibited toxicity towards the A549 cancer cell line.



**Declaration**

No portion of the work referred to in the thesis has been submitted in support of an application for another degree or qualification of this or any other University or other institute of learning.

### **Copyright statement**

- i. The author of this thesis (including any appendices and/ or schedules to this thesis) owns certain copyright or related rights in it (the “Copyright”) and s/he has given The University of Manchester certain rights to use such Copyright, including for administrative purposes.
- ii. Copies of this thesis, either in full or in extracts and whether in hard or electronic copy, may be made only in accordance with the Copyright, Designs and Patents Act 1988 (as amended) and regulations issued under it or, where appropriate, in accordance with licensing agreements which the University has from time to time. This page must form part of any such copies made.
- iii. The ownership of certain Copyright, patents, designs, trade marks and other intellectual property (the “Intellectual Property”) and any reproductions of copyright works in the thesis, for example graphs and tables (“Reproductions”), which may be described in this thesis, may not be owned by the author and may be owned by third parties. Such Intellectual Property and Reproductions cannot and must not be made available for use without the prior written permission of the owner(s) of the relevant Intellectual Property and/ or Reproductions.
- iv. Further information on the conditions under which disclosure, publication and commercialisation of this thesis, the Copyright and any Intellectual Property and/ or Reproductions described in it may take place is available in the University IP Policy (see <http://documents.manchester.ac.uk/DocuInfo.aspx?DocID=487>) in any relevant Thesis restriction declarations deposited in the University Library, The University Library’s regulations (see <http://www.manchester.ac.uk/library/aboutus/regulations>) and in The University’s policy on Presentation of Thesis.

## **Acknowledgements and dedication**

I would like to express my gratitude to God Almighty for a gift of life, protection and guidance throughout the period of this research. Without his intervention I wouldn't have been selected for this research programme at the University of Manchester.

My special gratitude also goes to the 'TETfund' Nigeria for funding this research. I am deeply grateful to my supervisor, Dr Roger Whitehead for his amazing support, continuous co-operation, guidance, suggestions and criticisms throughout this research programme. I am also mostly grateful to Prof. Ian Stratford of School of Pharmacy for his innumerable contributions, particularly for granting me a space in his lab for biological assay evaluation.

I also wish to place on record my personal and deep appreciation to Stephania Christiou, Soo mei Chee, Jak and Mark Little whose initial contributions and assistance made this research a success. The successful completion of this research work would not have been possible without the collaborative efforts of the other members of the Whitehead research group: Chad, Rob, Yiwei, Daniel, Eleanor, Agata and Harry. Additional thanks to Yiwei for carrying out biological MTT assay evaluation.

I would like to thank my family for their unlimited love, support and encouragement through out the period of this research. Their numerous phone calls and prayers kept me happy especially when all hopes are lost.

Finally, a big thank you to all the staff of Chemistry department without their amazing support and help this research programme would not have been achievable.

I dedicate this thesis to the victims of cancer and wish that one day a break through in the treatment of cancer will emerge.

## 1.0 Chapter 1: Introduction

### 1.1 The cell

Cell theory<sup>1</sup> states that all living organisms are composed of cells which replicate themselves and, as a result, they are called the building blocks of life. Modern theory includes other specific roles such as: they provide structures for the body; they synthesize ATP; they contain hereditary information (DNA) which is passed from generation to generation as well as other biomolecules like proteins.<sup>2</sup> Cells are made of protoplasm which is encircled within a cell membrane, and this contains many organelles like the nucleus and mitochondria (also known as the power house of the cell) (Figure 1).

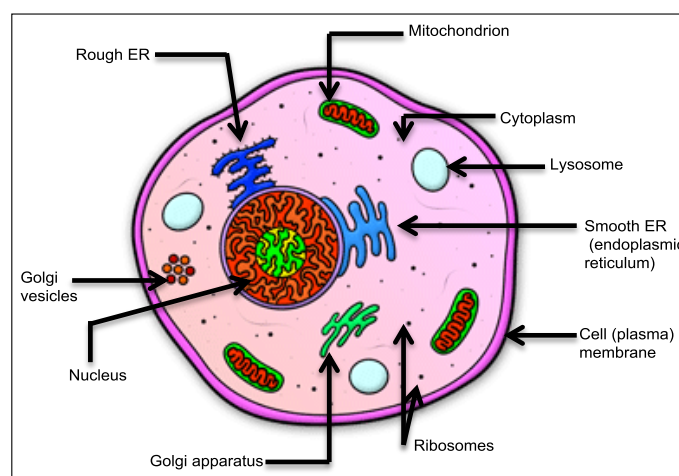


**Figure 1:** Cross section of a human cell. This image is credited to Abhishake Sharma/anatomydiagram.info., posted on October 30, 2015.

Each human cell comprises about 25,000 genes which are used selectively and which can be activated when needed or deactivated when not needed. Some genes are activated at all times to synthesize the proteins needed for normal cell functions (transcription). This process of turning genes on and off is known as gene regulation. The genes therefore control all the functions of the cell.

#### 1.1.1 Carcinogenesis/Tumorigenesis

Carcinogenesis which is also known as tumorigenesis is the real development of cancer, whereby the normal cells are mutated into cancer cells. It is a complex, multi-step process that involves elimination of numerous cell obstructions: such as anti-proliferative responses and programmed cell death-inducing mechanisms. Loss of function of proto-oncogenes and p53 (page 17) occur through genetic mutations, or

through epigenetic mechanisms, such as DNA methylation.<sup>3,4</sup> For example, in epigenetic methylation, the addition of a methyl group to a particular gene results in deactivation so that the transcription process cannot occur. Epigenetic errors can occur, especially when a wrong gene is modified or there is a failure in gene modification. Both errors can lead to abnormal gene activity, or inactivity, thereby causing genetic disorders.

Carcinogenesis comprises three related stages: tumor initiation, promotion and progression.<sup>5</sup> Tumor initiation is rapid and irreversible: it occurs as a result of exposure to carcinogenic agents such as quinones and tumor invasions to the organs and tissues where metabolic and detoxification activities occur. In contrast to initiation, tumor promotion is a slower and reversible process in which the proliferating pre-neoplastic cells accumulate because the immune system fails to destroy them at onset. Tumor progression involves the multiplication of tumor cells with invasive and metastatic effects.

### 1.1.2 Origin of cancer cells

Human bodies comprise a huge numbers of cells which can copy themselves in a specialized manner to produce new cells or daughter cells needed to keep the body healthy. Sometimes this organized process can be affected causing the DNA of a cell to become mutated leading to abnormal cell growth and proliferation. When this occurs, there will be an accumulation of unwanted cells which will not undergo apoptosis (programmed cell death) (Figure 2). When these cells accumulate they form a mass of tissue called a tumor (Figure 3).

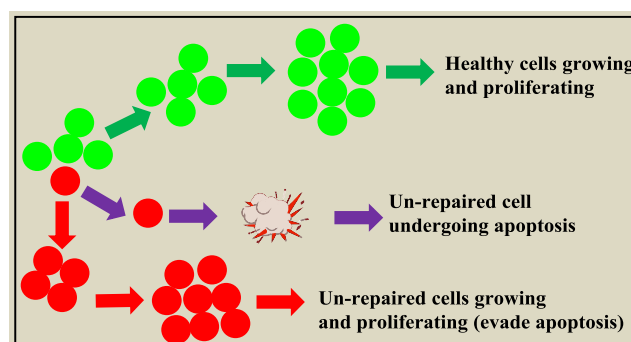


**Figure 2:** Loss of normal cell growth control shown in red. The cells escape apoptosis and therefore progress to a tumor.

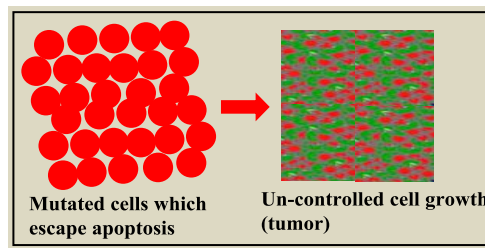


**Figure 3:** Cancer cell division.

### 1.1.3 Tumor invasion and metastasis

Human bodies comprise many different kinds of cells such as nerve cells, blood cells and epithelial cells. Accumulations of cells that perform specific functions are grouped together to form tissues, for example: epithelial tissue, connective tissue, nerve tissue and muscle tissue. The tissues combine to form the organs, for example: skin, eye, breast, liver, etc; and these organs are combined to form a body.

A growing tumor which starts from epithelial cells will eventually produce offspring which migrate out of their original site to invade adjacent tissues and then spread to the organs (Figure 4).

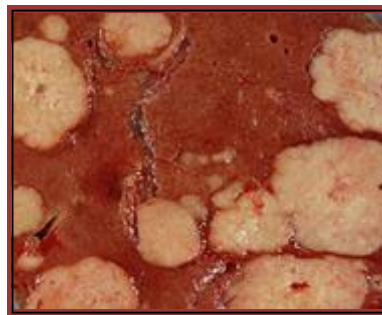


**Figure 4:** Cross section of human liver taken at autopsy examination, showing multiple large pale tumor deposits. This image is credited to Haymani/Wikimedia commons.

Tumor metastasis is a very complex process which involves a systematic interaction between the invasive cells and the extracellular matrix (ECM). The extracellular matrix is an interconnected network of macromolecules (proteins and polysaccharides) which are produced locally by cells in the matrix. Through its functions, it controls some key cellular events such as: cell adhesion, migration, proliferation, differentiation and survival.<sup>6</sup> It has been reported that changes in the ECM rigidity contributed actively to tumor progression.<sup>7</sup> Some enzymes, such as extracellular enzymes, matrix metalloproteinases and proteases, have been identified

in this transformation of the ECM, leading to tumor invasion and metastasis. Thus, drug candidates targeting these enzymes for inhibition have been developed which have potent anticancer activity.

The ability of cancer cells to invade and metastasize to a distant site is an established hallmark of cancer that is, a pathological capability common to most, if not all, cancer cells.<sup>8</sup> The hallmarks of cancer (Figure 5) are the phenotypic adaptations necessary to overcome all the proliferation barriers that a tumor encounters during progression to carcinogenesis.

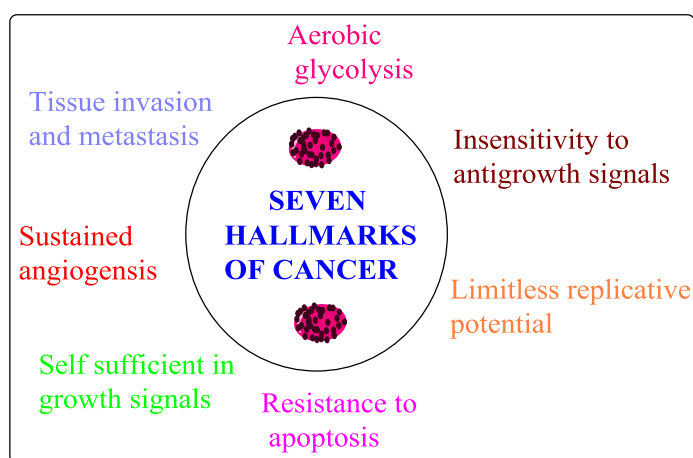


**Figure 5:** Seven acquired capabilities of cancer cells (hallmarks of cancer).<sup>9</sup>

The capability of cancer cells to invade and metastasize enables them to escape the primary mass and to colonize new areas in the body where, at least initially, nutrients and space are not lacking. Metastasis is the most life threatening challenge in patients with cancer this process is the cause of 90% of human cancer deaths.<sup>10</sup>

Not every tumor can be termed to be cancerous and biopsy is used to determine which tumors are harmful. A tumor is referred to as benign when it has not invaded the nearby tissues and hence, does not pose a serious danger to the health of an individual.<sup>11</sup> Malignant tumors grow rapidly and irreversibly due to their having metastasized from the primary site to distant areas.

#### **1.1.4 Escaping apoptosis**

Apoptosis or cellular suicide refers to programmed cell death and is a normal function of cells which occurs inside the mitochondria. The p53 and retinoblastoma proteins control both cell proliferation and cell death. A set of proteins are also known to either support apoptosis (pro-apoptosis: e.g Bax, Bad, Bid, Bok, Bik and Bak) or oppose apoptosis (anti-apoptosis: e.g Bcl-2, Bcl-XL, Bcl-W, Mcl-1 and A1). If there is any response from pro-apoptosis proteins, due to DNA damage, signalling imbalances caused by oncogenes, lack of oxygen supply or insufficient growth factors, the mitochondria release a signalling molecule called cytochrome c. The cytochrome c binds to a protein known as Apaf-1 resulting in formation of the apoptosome. The apoptosome then activates a set of proteins called caspases or 'gate keepers' which in turn activate other caspases leading to selective degradation of the structures of cell components.<sup>9</sup>

For cancer cells to survive and divide uncontrollably however, they must escape apoptotic signalling pathways by either inactivating p53, retinoblastoma proteins or by producing large amounts of anti-apoptotic proteins. For example, human papilloma virus (HPV) produces proteins known as E6 and E7. E6 binds to p53 and inactivates it, while E7 inactivates the retinoblastoma proteins.<sup>9</sup>

#### **1.1.5 Self sufficiency in growth signals**

Growth factors are mostly proteins which are present in very low concentrations in tissues and they are biologically very active. They control most of the important functions within the cell such as growth, proliferation, cell specialization and survival.

Cells communicate with each other in a process known as cell signalling. The behaviour of a cell depends on its microenvironment. There are a variety of growth factors and each carries out its function by binding to a specific receptor. These receptors are proteins found locally on the surface of a cell. The binding of a growth factor to a receptor activates phosphorylation reactions inside the cell and this represents part of the cell signalling pathway.



Cancer cells become independent of growth factors for proliferation by synthesizing their own growth factors and also by mimicking the growth factor receptors. This process can be initiated by an active kinase enzyme which is always switched on. This independence of the growth factor signalling pathway assists them to escape important checkpoints in the cell cycle.

Studies have revealed that a key component of the growth factor signalling pathway, known as *mutant ras*, was found to be permanently switched on in some cancer cells. For example 90% of pancreatic cancer cells showed high expression of *mutant ras*.<sup>8</sup> Therapeutic treatment targeting these proteins therefore, will deprive the cancer cells of the signals required for uncontrolled growth and proliferation.

### 1.1.6 Insensitivity to antigrowth signals

Antigrowth signals are proteins which inhibit cell growth and multiplication whereas growth factors promote them. The growth and proliferation of normal cells are strictly controlled by the antigrowth signals. They block cell growth in a cellular quiescent phase, the G0 and M phase (mitosis). Almost all of the antigrowth signals are guided by a protein known as retinoblastoma which belongs to a class of proteins called tumor suppressor proteins. The retinoblastoma protein prevents uncontrolled growth from the G1 to S phase (Figure 6).

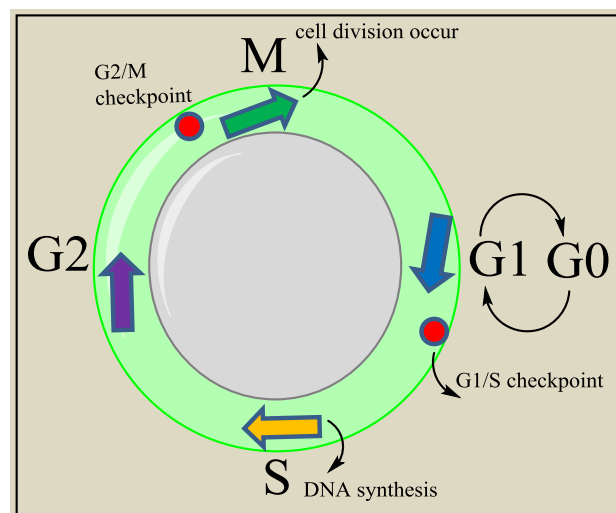


**Figure 6:** The cell cycle, showing G1, S, G2 and M phases. Cell growth occurs during G1 and G2, while DNA is synthesized in S phase. Cell division occurs during M phase (mitosis). G0 is a quiescent phase where the cell exits the cell cycle but can re-enter if the signals from the environment are adequate. Red dots indicate cell cycle checkpoints.

Retinoblastoma protein is active when it is not phosphorylated and inactive when phosphorylated. It binds and inactivates E2F transcription factors which are very important proteins that bind to DNA and activate the genes controlling the cell cycle and DNA replication. Cancer cells interrupt the retinoblastoma pathway by setting free the E2F transcription factors which promote cell growth and division causing uncontrolled cell growth.<sup>8</sup>

### 1.1.7 Sustained angiogenesis

Cells that perform similar functions are grouped together to form tissues. The tissues require oxygen and nutrients to survive and grow otherwise they will ‘suffocate’ and die. They also need to be able to remove metabolic waste and carbon dioxide. The formation of blood vessels a process known as ‘angiogenesis’ helps them to achieve this.

Similarly, a growing tumor requires nutrients, glucose, oxygen and an evacuation system to remove waste and carbon dioxide. Diffusion is insufficient for providing these needs. To achieve this, cancer cells activate the cells of neighbouring blood vessels to grow extensions to form a supply chain and drainage channels (Figure 7).<sup>8</sup> In this way, the normal neighbouring cells play a key role in tumor progression.

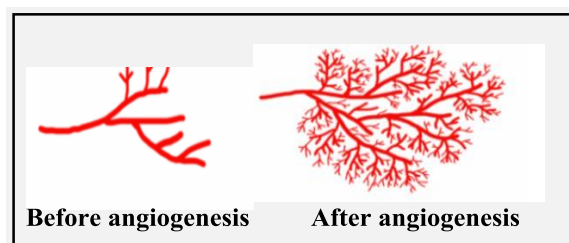


**Figure 7:** Angiogenesis causes blood vessels to grow more branches for transportation of nutrients, oxygen and evacuation of carbon dioxide.<sup>8</sup>

### 1.1.8 Limitless replicative potential

In humans, normal cells have a limited number of un-interrupted growth and proliferation cycles. This limited number is known as the ‘Hayflick Limit’ named after Leonard Hayflick who discovered it.<sup>12</sup> Cells, after having experienced a certain number of divisions, gradually reduce their growth rate and finally stop. In this situation, the cell is said to be in a ‘senescence state’ and this state is irreversible.

The senescence induced p53 pathways are activated by telomeres. Genes are arranged along twisted, double-stranded molecules of DNA known as chromosomes (Figure 8). At the ends of the chromosomes are stretches of DNA called telomeres. These telomeric DNAs determine how often and how long a cell may grow and multiply. The telomere performs its functions by preventing the end to end fusion of the chromosomal DNA or its break down.

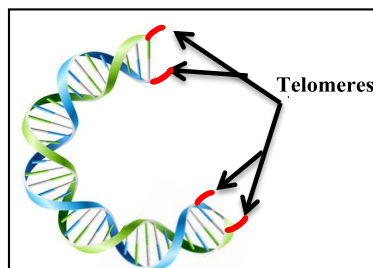


**Figure 8:** Structure of DNA with the protective telomeres at the end of the chromosomes.

As cells undergo successive growth and division cycles their telomeric DNA gets shorter and shorter in length and eventually, the end of chromosomal DNA can no longer be protected. This causes the chromosomal DNA to start fusing with itself and this causes cell death.

Similarly, when cancer cells are progressing into malignancy, they grow and divide very rapidly, causing their telomeres to become very short resulting in the death of the cells. To grow indefinitely however, cancer cells must avoid this pathway and they can achieve this by activating an enzyme called telomerase. Telomerase lengthens the telomeres and this enables the cancer cells to undergo indefinite growth and replication cycles.

*In vitro* inhibition of telomerase activity has been targeted in breast and prostate cancer cells and was found to result in the death of cancer cells but with high associated risks: loss of fertility, adverse affect on wound healing and a weakening of the production of blood and immune system cells.<sup>12</sup>

### **1.2.0 Causes of cancer**

Cancer is a disease of the cells in the body with many possible causes such as genetic or epigenetic factors and exposure to different types of chemicals. Most cancers

occur when certain vital genes, which control how cells divide and proliferate, are damaged or mutated. For example:

#### **(a) DNA mutations**

Mutations either acquired or epigenetic, are irregular changes in the DNA of a gene. The building blocks of DNA are the nucleotide bases and the sequence of these bases regulates the genes and their functions. Mutation involves changes in the sequence of these bases and this can affect the cells in many ways. For example, it can prevent protein synthesis or cause more proteins to be synthesized than usual thus leading to disease or the development of cancer cells. DNA mutations can be caused by environmental factors such as exposure to cigarette smoke, radiation, chemicals, hormones, diet etc, and these are called acquired DNA mutations. Epigenetic mutations are inheritable changes in gene activity and expression that occur without alteration in DNA sequence.<sup>13,14</sup> These include DNA methylation and histone modification.<sup>15</sup>

#### **(b) Oncogenes**

Proto-oncogenes are genes that support the growth of cells. When oncogenes undergo mutation, too many copies are made, resulting in them being continually activated even when they are not needed and this can give rise to unregulated growth, a key hallmark of cancer. Normal cells undergo apoptosis, which is a physiological intracellular process involving a well ordered signalling pathway that leads to cell death and clearance of dead cells by white blood cells (phagocytes), without causing inflammation. Oncogenes cause those cells programmed to die to survive and proliferate uncontrollably, leading to accumulation of tissues which will eventually become cancerous. Proto-oncogenes can be activated through chemical carcinogens such as quinoid molecules (Figure 9).<sup>16</sup> In most malignant tumor cells proto-oncogenes are up-regulated to a high level.

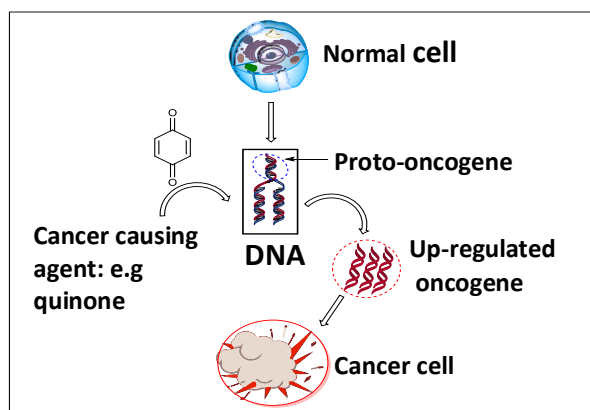


**Figure 9:** Oncogene and cancer cell.

### (c) Tumor suppressor protein (p53)

The tumor suppressor protein (TSP) which is encoded in humans as ‘p53’ is located on the short arm of chromosome 17.<sup>17</sup> It performs numerous functions including the control of cell growth, which is achieved by either repairing damaged DNA when it has undergone mutation, or by inducing damaged cells to die if DNA repair is impossible. The process of programmed cell death is called ‘apoptosis’.<sup>18</sup> DNA, if damaged, will increase the level of p53 which then leads to an increase in cancer cell apoptosis.<sup>19</sup>

The tumor suppressor protein, therefore, controls the cell cycle by preventing replication at the G<sub>1</sub> phase and it then enters the G<sub>0</sub> phase (called a ‘quiescence state’) until the cell repairs itself (Figure 4).<sup>20,21,22</sup> The tumor suppressor protein plays an important role in maintaining the stability of the cell by preventing genome mutations<sup>23</sup> and because of this it has been described as a “genome guardian” because mutation or loss of p53 will cause genetic instability. Abnormal cells take advantage of mutations of p53 to grow uncontrollably leading to cell apoptosis or establishment of neoplastic cells *in vivo*.<sup>24</sup>

### (d) Reactive oxygen species (ROS)

The most characteristic feature of cellular metabolism is the production of toxic by-products, which must be removed for the cell to survive and also to maintain the stability of the genome.<sup>25</sup> These by-products, which are produced from mitochondria or NADH oxidases are known collectively as reactive oxygen species (ROS) which include: hydrogen peroxide (H<sub>2</sub>O<sub>2</sub>), superoxide (O<sub>2</sub><sup>-</sup>), and the hydroxyl radical

(OH)<sup>•</sup>.<sup>26</sup> Reactive oxygen species can be mutagenic, as well as causing damage to the cell membrane, and consequently living organisms have a complex system of antioxidants.

Antioxidants (Figure 10) are molecules that inhibit the oxidation of other molecules, examples include; glutathione (1), vitamin C (2), vitamin E (3) and oxidoreductase enzymes such as the NQOs. The antioxidants terminate chain reactions by removing the free radical intermediates, resulting in themselves being oxidized. Insufficient levels of antioxidants, or inhibition of their activity, can cause accumulation of free radical intermediates leading to oxidative stress, which can result in DNA damage or cell apoptosis.

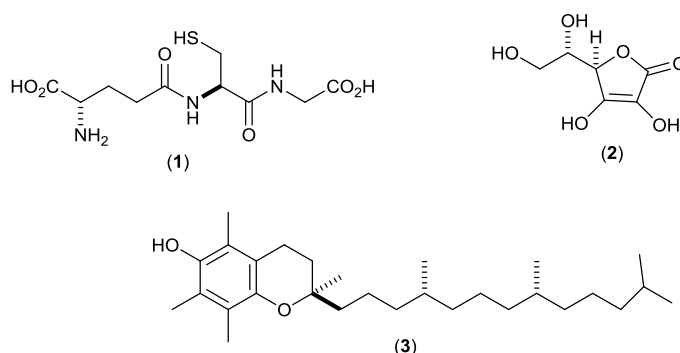


**Figure 10:** Structures of antioxidant compounds: glutathione (1); vitamin C (2); vitamin E (3).

### 1.3.0 Glucose metabolism

The primary function of glucose is to provide energy to the cells in the form of ATP, as an alternative to mitochondrial respiration. Glucose metabolism is essential for the generation of catabolic (eg CO<sub>2</sub> and energy) and anabolic starting materials for virtually all forms of biosynthetic reactions. Glycolysis, which is also referred to as the Emden-Meyerhof Paranas pathway (EMP), is an anaerobic process which can occur in many ways (Figure 11). During this process, pyruvate and several byproducts such as: ATP, NADH/NADPH and fatty acids are produced.

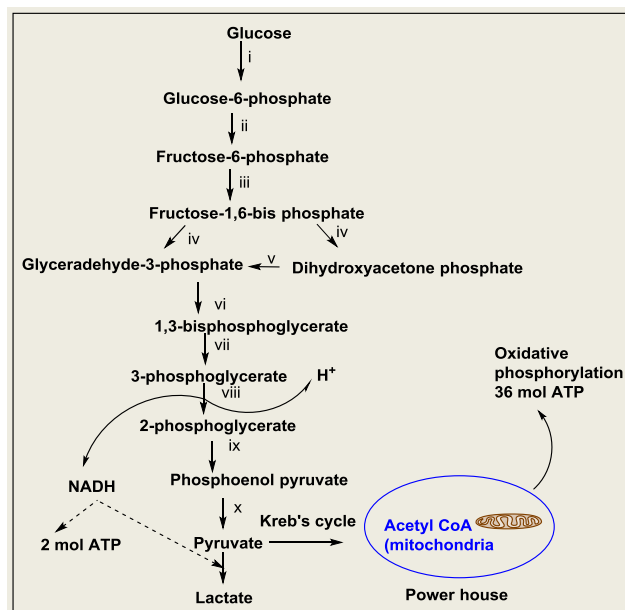


**Figure 11:** Emden-Meyerhof Paranas glycolytic pathways. Steps i and iii consume ATP while steps vii and x produce ATP. Steps vi-x occur twice per glucose molecule and therefore, producing a total of 2 ATP for the complete pathway.

The pyruvate produced can be metabolized to acetyl-CoA, ethanol or lactic acid depending on the microenvironment of the cell. In mammalian cells for example, where oxygen is needed for respiration, pyruvate enters the mitochondria and becomes converted to acetyl-CoA. The acetyl-CoA then enters into the Krebs cycle where it is completely oxidized to  $\text{CO}_2$  and  $\text{H}_2\text{O}$  with formation of 36 moles of ATP through oxidative phosphorylation. Inhibiting effect of oxygen on the fermentation process is called the ‘Pasteur effect’ after Louise Pasteur who reported that glucose fluctuation causes inhibition of lactate production under aerobic conditions.<sup>27</sup>

### 1.3.1 Cancer metabolism

A knowledge of metabolism is crucial when attempting to fight cancer. Normal cell growth and proliferation are controlled by growth regulating signals and also by the cell’s microenvironment. The availability of nutrients and oxygen, which are necessary for cell multiplication and division, depends mainly on blood supply. The initial cancer growth however, occurs in the absence of formation of new blood vessels causing the cancer cells to have insufficient oxygen and nutrients for growth and proliferation.

In order to form metastases, the cancer cells must survive, colonize and proliferate in the host tissue. To achieve this, they develop highly regulated processes for nutrient

consumption and utilization by replacing the glucose metabolic pathway (oxidation of sugar) in normal cells with sugar fermentation. This process represents a cellular phenomenon known as ‘metabolic rewiring’.<sup>28,29</sup> In this process, cancer cells consume high amounts of glucose as clinically evidenced by positron emission tomography (PET)<sup>30,31</sup>, producing a large amount of lactate and  $H^+$  regardless of the availability of oxygen.<sup>32</sup>

Warburg was the first to observe this irregular method of energy production in cancer cells. He reported that tumor tissues *in vitro* convert large amounts of glucose to lactate even in the presence of oxygen and that this is a remarkable difference to normal tissues which display the ‘Pasteur effect’.<sup>33</sup> This is generally known as the Warburg effect,<sup>34,35</sup> and is considered to be the seventh hallmark of cancer. It confers a significant growth advantage because it produces a toxic, acidic environment which is more damaging to adjacent tissues than to the cancer cells themselves.<sup>30</sup>

The Warburg hypothesis was based on mitochondrial malfunction and this has been repeatedly challenged by recent investigations.<sup>36</sup> Aerobic glycolysis in many cancers is the combined effect of many factors such as oncogenes, tumor suppressors, hypoxic microenvironment, mtDNA mutations and genetic background.<sup>37</sup>

Glycolysis in cancer is inefficient in terms of ATP production compared to normal cells which produce 36 moles of ATP through oxidative phosphorylation (Figure 12). Gatenby and Gillies<sup>38</sup> proposed that high glucose consumption in tumor cells is not necessarily for ATP production as it is commonly assumed. Rather it is used to create an acidic environment, which gives the cancer cells a competitive advantage for invasion.

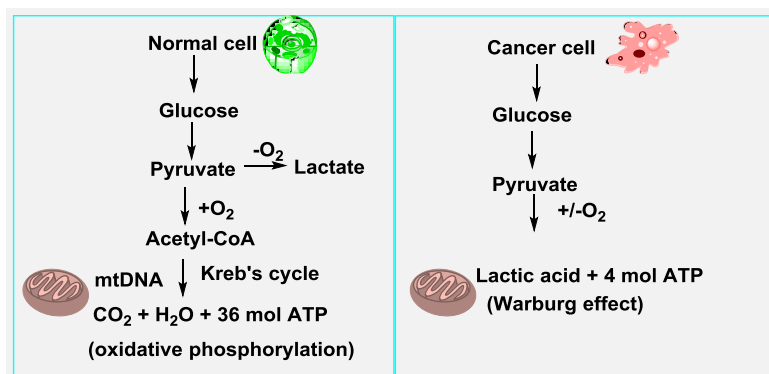


**Figure 12:** Comparison of glucose metabolic pathways in normal and cancer cells.



### 1.3.2 Advantages of glycolysis to cancer cells

A high glycolytic rate in tumor cells has several advantages with regard to proliferation besides enhancing the ability to grow in an hypoxic environment:

- i) The phosphometabolites produced during glycolysis can be processed *via* the pentose phosphate pathway (PPP) for biosynthesis of nucleic acids and lipids as illustrated in Figure 13.

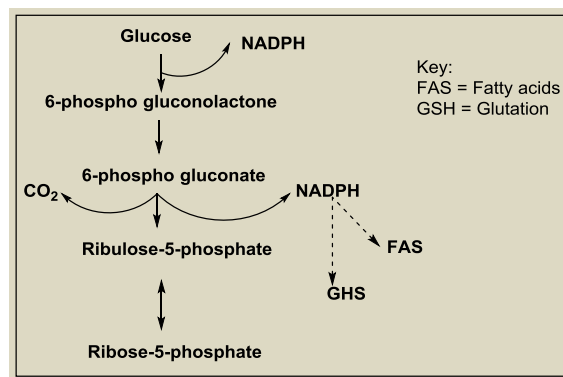


**Figure 13:** Pentose phosphate pathway (PPP).

- ii) It helps the tumor cell to avoid the production of reactive oxygen species through oxidative phosphorylation.
- iii) Cancer cells will no longer rely on mitochondrial function and thus may escape apoptotic signalling which is linked to this function. In other words the genes and the pathways that up-regulate glycolysis are also antiapoptotic.<sup>39</sup>
- iv) High glycolytic activity produces a large amount of lactate and H<sup>+</sup> ions which are transported to outside the cell where they promote aggression.<sup>40</sup>

Indeed, several studies have shown that glucose fluctuation and metabolism stimulates many hallmarks of cancer such as uncontrolled proliferation, anti-apoptotic signalling, cell cycle progression and angiogenesis. Thus with progressive tumorigenesis, cancer cells become highly addicted to high glucose consumption and susceptible to glucose deficiency.<sup>41</sup> Studies have revealed that malignant cells *in vitro* quickly lose ATP and undergo apoptosis in the absence or shortage of glucose.<sup>42,43,44</sup>

#### **1.4.0 Signs and symptoms of cancer**

The signs and symptoms of cancer depend on where the cancer is located, how big it is, and how much the tissues and organs have been affected. If the cancer has metastasized, the signs and symptoms may appear in different parts of the body. Occasionally, however, cancer starts in places where signs and symptoms will not be observed at an early stage, for example, pancreatic cancer. The signs or symptoms are observed when it has spread beyond the place it started (the pancreas). Generally, some common symptoms of cancer include:<sup>45</sup>

- Unexplained bleeding
- Unexplained weight loss
- Unexplained pain
- A lump or swelling

#### **1.4.1 Cancer risk factors**

A cancer risk factor is anything that affects the chances of getting the disease. Different cancers have different risk factors and these include:

- Old age: half of the people diagnosed with cancer are those at the age of 60 and above;<sup>46</sup>
- Obesity,<sup>47</sup> lack of exercise, excessive drinking of alcohol, unhealthy eating (consuming a lot of saturated fat);<sup>48</sup>
- Genetics: people with inherited traces of gene mutation are at high risk of developing cancer;<sup>49</sup>
- Medicinal factors: radiation therapy especially at a younger age is a high risk factor for the development of cancer. Radiation exposure during routine screening tests is generally only of a low dose, however cumulative effects from repeated exposure can lead to cancer;<sup>50,51</sup>
- Changes in hormone levels;
- Infections such as human papilloma virus (HPV) can increase the risk of cancer;
- Prolong exposure to air pollution.

### **1.4.2 Treatment of cancer**

Early detection of cancer increases the chance of survival because it is still at a primary stage and has not spread to other parts of the body. For example, breast cancer survival rates are increasing and this is partly as a result of high awareness programmes established to discover cancer at an early stage before it has metastasized. Early detection rates make treatment easier leading to an improved prognosis.

There are various standard treatments for cancer, each of which is matched to the particular type of cancer. Before the treatment is decided upon, staging is carried out to determine the location, size and the metastasized areas of the tumor. Staging is done using different scanning techniques such as (i) CAT scans, (ii) BONE scans and (iii) PET scans.

#### **(i) CAT scan**

This is a procedure that gives a detailed picture of areas inside the body, pictured from different positions. The pictures are linked to an X-ray machine. Dyes may be injected into a vein or swallowed so as to help organs or tissues to show up properly. This process is called ‘computerized axial tomography’ (CAT).

#### **(ii) BONE scan**

This is a procedure used to check if there are rapidly replicating cancer cells in the bones: a small amount of radioactive material is injected into the bloodstream which is then detected by a scanner.

#### **(iii) PET scan**

This is a positron emission tomography scan which is used to find metastasized cells in the body. A small amount of glucose is injected into the vein, while the scanner rotates around the body collecting pictures where the glucose is being used in the body. Metastasized cells show brighter colours because they are more active and hence take up more glucose than the normal cells.

#### 1.4.2.1 Chemotherapy (Chemoprevention)

One way of controlling cancer is by inhibition, reversal or delay of genetic and epigenetic agents that cause the neoplastic modification of cells.<sup>52</sup> Chemoprevention, therefore, is the use of natural or synthetic, non-toxic substances to destroy the cancer cells or prevent them from proliferating at an early stage.<sup>53</sup>

To treat breast cancers that are estrogen hormone dependent, warfarin (**4**) and tamoxifen (**5**) (Figure 14) are the drugs usually administered and their potency with respect to the prevention of likely reoccurrence of breast cancer among women is high. These drugs are especially effective for the treatment of BRCA 1 and BRCA 2.<sup>54</sup>

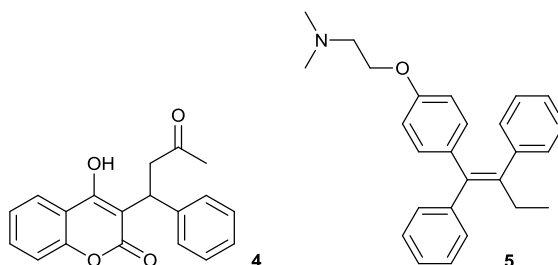


**Figure 14:** Structure of warfarin (**4**) and tamoxifen (**5**).

#### 1.4.2.2 Surgery

Surgery is still regarded as the most effective treatment for the majority of cancers because the affected areas can be removed while the tumor is still within its primary stage. For example, breast cancer invades the body through the tissue and passes through the lymph systems and metastasizes to other areas through the blood. During surgery, therefore, some of the affected lymph nodes and a small amount of unaffected tissues are removed (lumpectomy), or the whole breast is removed (mastectomy), after which an adjuvant therapy is used as a follow up. Adjuvant therapy is a treatment given after surgery to lower the risk of reoccurrence of cancer cell growth.

#### 1.4.2.3 Radiotherapy

Radiotherapy is the most commonly used adjuvant therapy which is given after surgery. It involves the use of high energy rays to destroy the malignant cancer cells that are still present after the surgery.<sup>55</sup> Many cancer patients are not happy to be

treated using radiotherapy because of its side effects, which include: lack of energy and pains in the affected areas.

### 1.5.0 NADH: oxidoreductase quinone 1 (NQO1)

NQO1 is a ubiquitous flavoprotein, meaning it contains flavin adenine dinucleotide (FAD) (**6**) (Figure 15). As a protein, it functions in a catalytic manner and can therefore be called a flavoenzyme. It belongs to a group of enzymes called oxidoreductases which protect cells against toxic metabolites by catalyzing the transfer of hydrogen or electrons to their co-enzymes. The co-enzymes accept the hydrogen and or electrons and transfer them to co-substrates during the cell's metabolic processes.

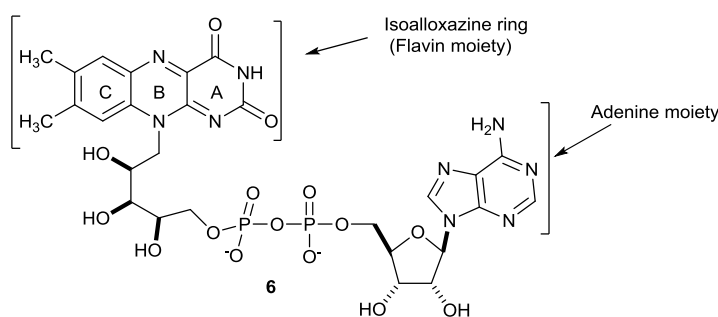


**Figure 15:** Structure of flavin adenine dinucleotide (FAD) (**6**).

The enzymatic activity of NQO1 was first described by Ernester and Navazio in 1958 who revealed it catalysed the reduction of 2,6-dichlorophenolindophenol in the rat liver cytosol.<sup>56</sup> It was originally called DT-diaphorase<sup>57</sup> to demonstrate that the enzyme uses NADH or NADPH as a source of reducing equivalents<sup>58</sup> and it is currently designated as NAD(P)H:oxidoreductase quinone 1, and in humans, it is encoded as 'NQO1 or QR1'. It is ubiquitous and about 84% of the enzyme is found in the cytosol of human cells,<sup>59</sup> while the remaining fractions can be found in mitochondria, ribosomes and the Golgi apparatus.<sup>60</sup>

NQO1 has attracted significant attention because of its ability to not only detoxify a number of natural and unnatural compounds,<sup>61,62</sup> but also to activate certain anti-tumor agents such as mitomycin C (MMC) (**7**), quinolinquinone (**8**), aziridinylbenzoquinone (**9**) and CB1954 (**10**) (Figure 16).<sup>63,64</sup> These findings therefore, prompted considerable interest among many researchers around the world

to study the enzyme and its analogues, and their role in protection against free radical formation and cancer development.

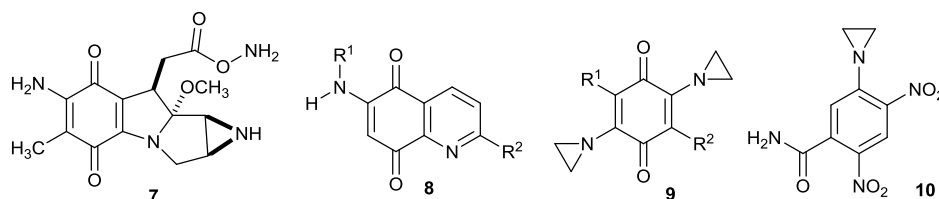
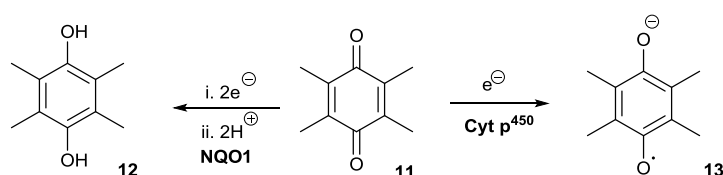


**Figure 16:** Compounds generally considered as NQO1-directed antitumor agents; mytomycin C (**7**), quinolinequinone (**8**), aziridinylbenzoquinone (**9**) and CB1954 (**10**).

As a detoxification enzyme, NQO1 catalyses an obligate 2-electron reduction of quinones (**11**) to stable hydroquinones (**12**)<sup>65</sup> using NADH or NAD(P)H (Figure 17) at equal efficacy as electron donor. The formation of hydroquinones occurs *via* a single step process, by-passing toxic semi-quinone intermediate (**13**) which can be formed by one electron reduction by cytochrome p450 reductase, cytochrome b<sub>5</sub> reductase, ubiquinone oxidoreductase and xanthin oxidase.<sup>66</sup> Spin resonance studies have revealed the absence of the semi-quinone radical intermediate (**13**) (Scheme 1) thus demonstrating the importance of NQO1 in cellular protection against toxic metabolites.<sup>65</sup>



**Scheme 1:** One electron reduction of quinones (**11**) by cytochrome p450 reductase results in formation of semi-quinone radical intermediates (**13**) whereas two electron reduction forms hydroquinones (**12**).

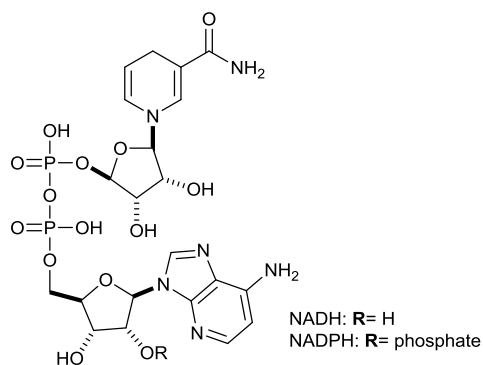


**Figure 17:** Structure of NADH and NADPH.

18).<sup>67,68</sup>



**Figure 18:** Structure of UDP-glucuronic acid (**14**).

reaction occurs *via* a ‘ping pong’ mechanism (Scheme 19). NADH binds and reduces the FAD cofactor and the reduced FAD is released prior to the binding of the substrate (Figure 19).



**Scheme 2:** Mechanism of two electron reduction of quinone to hydroquinone by NQO1.<sup>70</sup>

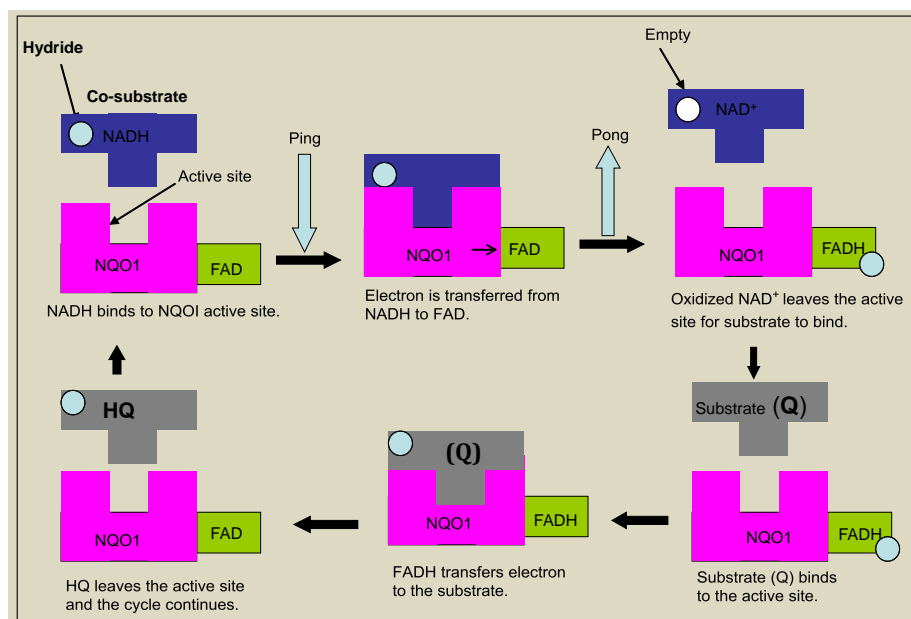


**Figure 19:** Diagrammatic representation of the 'ping-pong' mechanism of NQO1

Evidence in support of this mechanism of action of NQO1 has been gained from electron spin resonance experiments which did not detect the presence of semiquinone radicals during the metabolism of benzoquinone (**15**) or naphthoquinone (**16**) substrates (Figure 20).<sup>71</sup> Reports revealed that, in addition to *ortho* and *para* quinones,<sup>72</sup> NQO1 is capable of reducing a wide range of substrates such as quinone-imines (**17**, **18**, **19**), dichlorophenolindolphenol (DCPIP) (**20**), methylene blue (methylthioninium chloride) (**21**), glutathionyl-substituted naphthoquinone (**22**) and nitro compounds such as 1,3-dinitropyrene (**23**).<sup>73,74,75,76</sup>

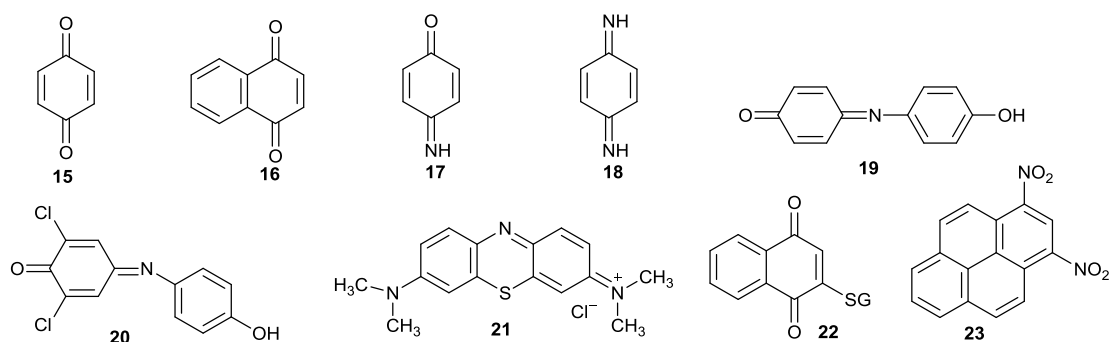
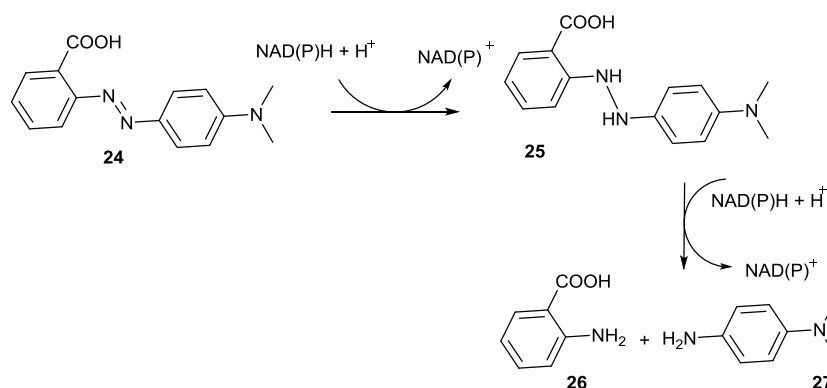


**Figure 20:** Structures of NQO1 co-substrates.



In addition to two electron reduction, NQO1 also catalyses a four electron reduction of azo dye (**24**) to 2-amino benzoic acid (**26**) and *N,N'*-diamethylbenzene-1,4-diamine (**27**) (Scheme 3) and other nitro-aromatic compounds.<sup>70,77</sup> A number of reports show that NQO1 plays additional roles apart from its usual metabolic functions,<sup>78</sup> for example it controls the stability of p53 by inhibiting its degradation.<sup>79</sup>



**Scheme 3:** Flavin mediated electron transfer from NAD(P)H to an azo dye (**24**) to give the products: 2-amino benzoic acid and *N,N'*-dimethylbenzene-1,4-diamine.<sup>70</sup>

Recent work with NQO1 has revealed that the enzyme plays an antioxidant role through the reduction of natural quinones which helps in the protection against oxidative damage.<sup>80,81</sup> It also reduces the oxidized form of vitamin E into an antioxidant product.<sup>82,83</sup> The antioxidant role played by NQO1 is further demonstrated by immunohistochemical studies in humans which have shown over expression of NQO1 in many tissues requiring a high level of antioxidant protection.<sup>84</sup> Such tissues include: epithelial cells of lung, breast and colon.

Synthetic anti-oxidants, like butylated hydroxyanisole (BHA) (**28**) (Figure 21) as well as some natural extracts from broccoli have been reported to be potent inducers of the NQO1 enzyme.<sup>85,86</sup> Broccoli contains isothiocyanates which induce carcinogen detoxifying enzymes.<sup>87</sup> Glutathione undergoes conjugate addition with isothiocyanates, leading to their excretion. This inducibility has led to the suggestion that NQO1 plays a key role in cancer chemoprevention.<sup>88</sup>

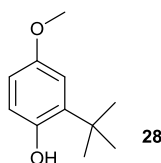
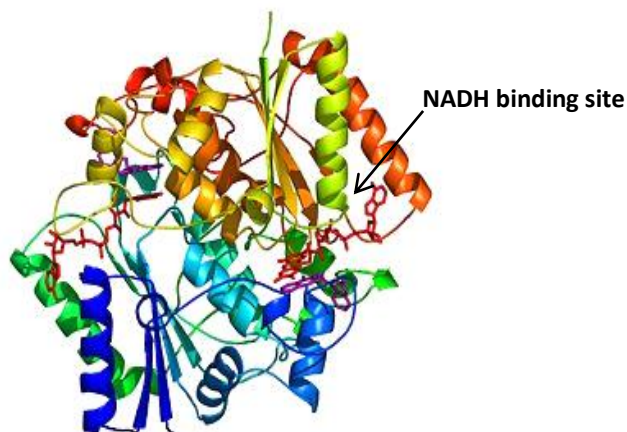


**Figure 21:** Structure of butylated hydroxyanisole: an anti-oxidant.

The X-ray structure of NQO1 (Figure 22 and 23) was first reported by Li and co-workers.<sup>89</sup> The 2.1-Å crystal structure revealed that the enzyme is a homodimer comprised of two connecting monomers oriented in a head-to-tail manner to ensure stability of the dimer. The FAD cofactor is non-covalently bound at the boundary of each monomer, giving rise to two active sites which are identical and independent of each other. Thus each active site is made up of parts of both monomers.



Each monomer unit of NQO1 is comprised of 273 amino acid residues. Experiments carried out by Chen and co-workers<sup>91</sup> revealed that each monomer consists of two separate domains: a solid N-terminal (1-220 residues) and an elastic C-terminal domain (221-273) which forms the active site of the enzyme.<sup>92</sup> The whole NQO1

unit forms a twisted central parallel  $\beta$ -sheet surrounded on both sides by connecting helices (Figure 24).<sup>93</sup> The catalytic domain contains an antiparallel hairpin motif along with one helix and some loops.

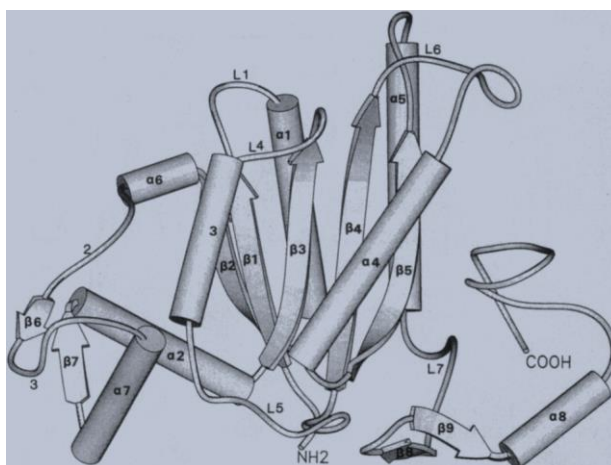


**Figure 24:** A single unit of NQO1 showing  $\alpha$ -helices and twisted  $\beta$ -sheet.<sup>93</sup>

The isoalloxazine ring of FAD is bound tightly to the catalytic site *via* non-covalent interactions involving residues in loops 1 and 4 in one monomer and loops 3 and 5 from the other monomer. The FAD is largely secured by Tyr-104, Trp-105, Phe-106 and Leu-103.<sup>89</sup> The two oxygen atoms attached to ring 'A' of the isoalloxazine form hydrogen bonds with the main chain NH groups of the protein: O4 with Phe-106 and O2 with Gly-150 (Figure 25).

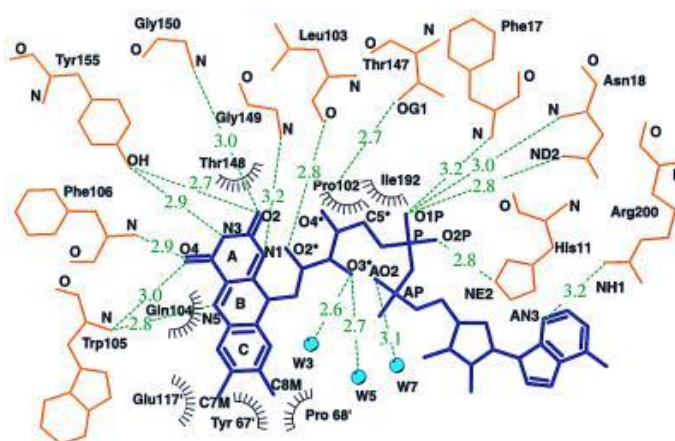


**Figure 25:** Representation of FAD-NQO1 interactions showing residues involved in hydrogen bonds (dashed lines) to the cofactor. FAD is secured by Tyr-104, Trp-105, Phe-106 and Leu-103.<sup>89</sup>

The FAD-NQO1 interactions in human and mouse differ from those in rat: the bulky aromatic residue Tyr-104 in rat is replaced with the smaller aliphatic Gln in human NQO1, resulting in an increase in size of the FAD binding pocket. An example of the effect of this change is the efficacy of NQO1 in human towards prodrug CB1954 (10).

### 1.5.2 NQO1 active site

The crystal structure of NQO1, with deoxynyboquinone (DNQ) as the electron accepting substrate, reveals the active site as a pocket at the dimer boundary (Figure 26).<sup>89</sup> The entrance to the site is restricted by Gly-149, Gly-150, His-194 and Pro-68 from the N-terminal of the *alpha*-helix of the second monomer. The amino acid residues: Phe-106, Phe-178, Trp-105 and Gly-174 form the internal wall, while Tyr-126 and Tyr-128 form the roof and the isoalloxazine ring of FAD forms the floor of the cavity (Figure 27). His-161 and two molecules of water form the opposite side of the pocket.

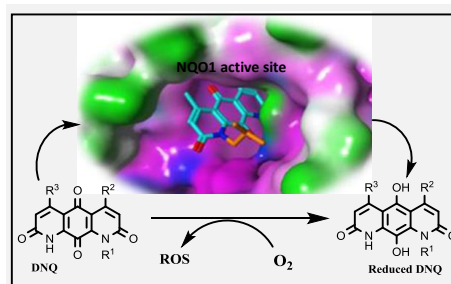


**Figure 26:** Structural image of deoxynyboquinone in the NQO1 active site. DNQ is reduced by NQO1, thus preventing one electron reduction by cytochrome c reductases which would produce ROS.<sup>93</sup>

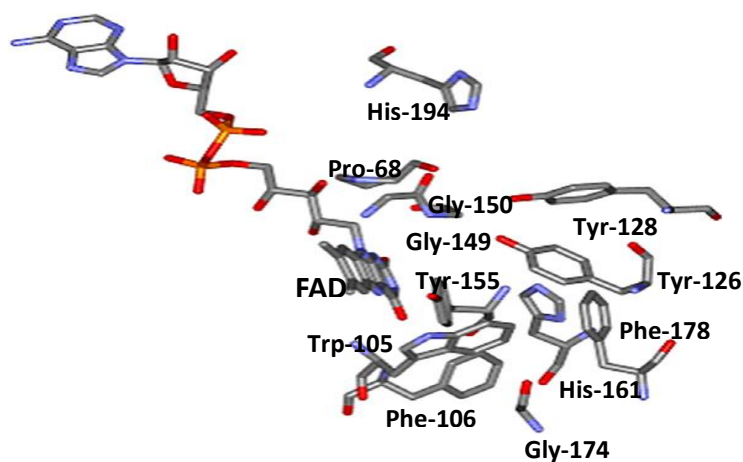


**Figure 27:** The active site residues of human NQO1.<sup>94</sup>

The optimal location of Tyr-128 in the absence of substrate, is one in which its side-chain is close to Phe-232 and His-161 of the other monomer. This position helps to protect the region from possible attack by water and oxygen molecules.<sup>92</sup> The quinone binds to the active site through contacts with the flavin moiety and several hydrophobic and hydrophilic residues. C-2 of the quinone lies almost on top of the phenyl moiety of the isalloxazine ring of FAD. The quinone oxygen is 3.5 Å away from flavin N(5) which is ideal for hydride transfer from FADH to the quinone.<sup>95</sup>

Kinetic and docking studies have proved that the NQO1 active site is very elastic<sup>96</sup> and its elasticity enables a large variety of quinones (with one, two or three fused rings) to bind. This is significant in terms of chemotherapeutic targeting of NQO1 using compounds of different sizes and chemical properties.

### 1.5.3 NQO1 gene and polymorphism

The NQO1 gene is a single copy gene located on chromosome 16q22.1.<sup>97,98</sup> The gene consists of six exons and five introns which span approximately 20 kb. Polymorphism is used to explain certain point mutations in the genotype of an organism giving rise to different forms of genes. Two polymorphisms have been characterized in NQO1: the NQO1\*2 allele which represents a base change from cytosine (C) to thymine (T) at base pair 609 in the cDNA coding for a proline (P) 187 to serine (S) change in the enzyme. This mutation results in a decrease of NQO1 concentration. Individuals who have this allele are susceptible to different forms of cancer such as urothelial tumors,<sup>99</sup> acute myeloid leukaemia<sup>100</sup> and child leukaemia.<sup>101</sup> The second form of polymorphism is the NQO1\*3 allele, representing a C465T change in cDNA coding for an arginine 139 to tryptophan substitution in the enzyme.<sup>102</sup>

### 1.5.4 NQO1 inhibitors

Both human and rat NQO1 can function physiologically as vitamin K reductases which are involved in the modification of vitamin K hydroquinone-dependent blood coagulation factors.<sup>69</sup> Liu and co-workers reported that flavones such as 7,8-dihydroxyflavone (**29**) and chrysin (**30**) (Figure 28), isolated from the Chinese herb *Scutellariae radix*, have anti-coagulant activities and are potent inhibitors of NQO1.<sup>103</sup>

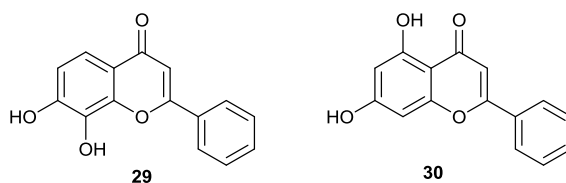


**Figure 28:** Structure of flavones; 7,8-dihydroxyflavone (**29**) and chrysin (**30**).

Presusch and Smalley in 1990 also observed that NQO1 is capable of reducing vitamin K<sub>3</sub> (menadione, **31**) but not vitamin K<sub>1</sub> **32** (Figure 29).<sup>104</sup>

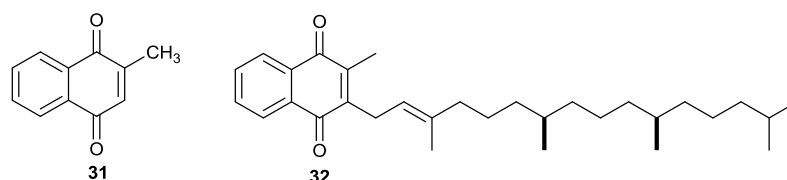


**Figure 29:** Structure of menadione (**31**), and vitamin K<sub>1</sub> (**32**).

Oral anti-coagulants such as dicoumarol (**33**) have been shown to be potent competitive inhibitors of NQO1 with respect to nicotinamide coenzymes (NADH/NADPH).<sup>105</sup> Results obtained from inhibition studies with dicoumarol illustrate that the strong affinity of dicoumarol with human and rat NQO1 ( $K_i = 2.0$  nM and 0.5 nM respectively) was due to a  $\pi$ - $\pi$  interaction of one ring with the isoalloxazine ring of the FAD cofactor (not shown) and another  $\pi$ - $\pi$  interaction of the second ring with the phenol ring of Tyr-128,<sup>106</sup> (Figure 30).

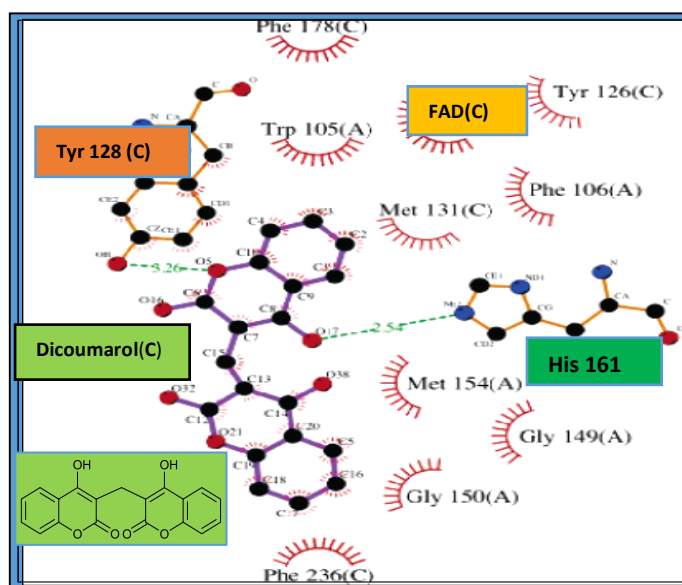


**Figure 30:** Interaction of dicoumarol with NQO1. Protein amino acid, FAD and dicoumarol are labelled (C) and (A) to represent the 1<sup>st</sup> and 2<sup>nd</sup> NQO1 monomers respectively. Nitrogen atoms are coloured in blue, oxygen in red and carbon in black. Residues making Van der Waals interactions with

the dicoumarol are represented by a decorated arc. Hydrogen bonds are represented by dashed green lines along with their distances.<sup>90</sup>

Other inhibitors of NQO1 which are less potent than dicoumarol include: warfarin (**4**), CB 1954 (**10**), DCPIP (**20**), phenindone (**34**), ES936 (**35**) and cibacron blue (**36**) (Figure 31). These inhibitors bind differently to the NQO1 active site with dicoumarol (**33**) having the strongest binding affinity ( $K_I = 170$  nM).<sup>90</sup>

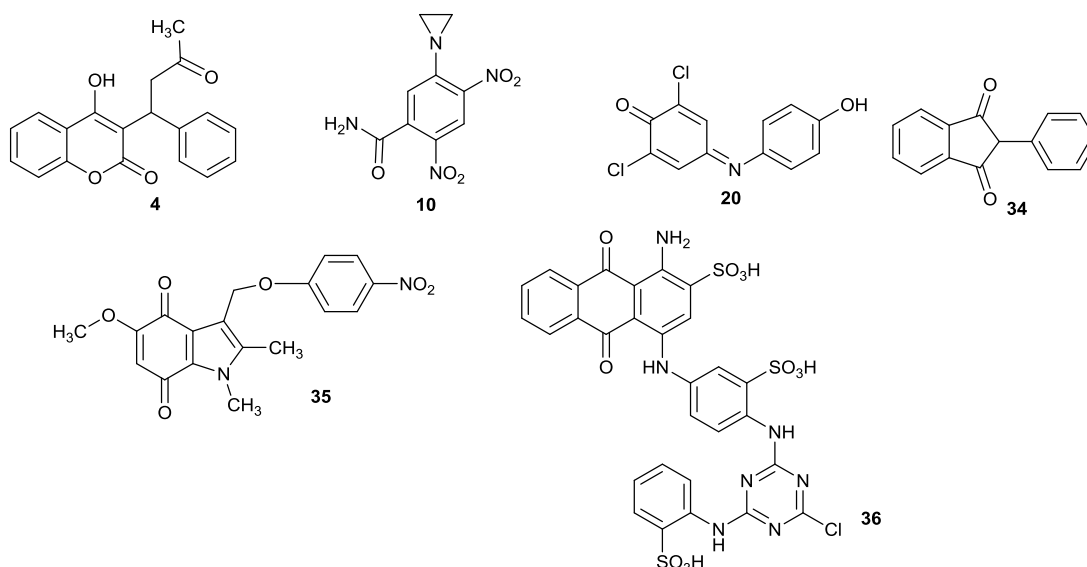


**Figure 31:** Structures of warfarin (**4**), CB 1954 (**10**), DCPIP (**20**), phenindone (**34**), ES936 (**35**) and cibacron blue (**36**).

### 1.5.5 Consequences of the interaction of NQO1 with dicoumarol

The proteasome is a protein complex containing many subunits that plays an important role in regulating the concentration and degradation of misfolded proteins in the cell. This degradation results in the formation of shorter peptides or even individual amino acids that make up that protein. The misfolded proteins are tagged for degradation with a small protein called ubiquitin, and this signals other ubiquitin molecules to start attaching resulting in the formation of a polyubiquitin chain (Figure 32).

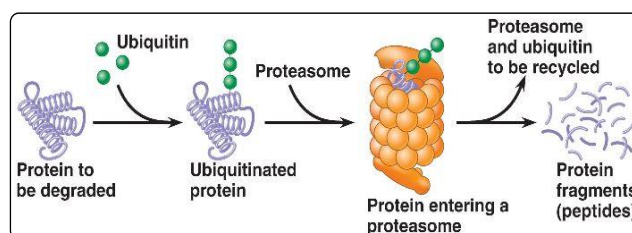


**Figure 32:** Misfolded proteins and its degradation by proteasome.

Wild-type/mutant p53 is a labile protein and its cellular role depends on the level of proteasomal degradation. The degradation can occur either by ubiquitin-dependent or ubiquitin-independent processes. The ubiquitin-independent process is controlled by NQO1 and it is facilitated by the 20S proteasome.<sup>107</sup> NQO1 stabilizes p53 by inhibiting its degradation. Over expression of NQO1 consequently will enhance p53 activity, whereas NQO1 knockdown will reduce the level of p53. Binding of NQO1 with the inhibitor dicoumarol, will prevent p53 from binding and this will cause ubiquitin-independent proteasomal degradation of p53. This has led to the targeting of the proteasome for anti-cancer therapy.

#### **1.6.0 NRH: oxidoreductase quinone 2 (NQO2)**

The systematic name of this enzyme is NRH: oxidoreductase quinone 2 and it is encoded as NQO2 or QR2 in humans. It was first discovered by Liao and co-workers in 1961,<sup>108</sup> and later rediscovered by Jaiswal in 1990 while trying to uncover other members of the oxidoreductase family.<sup>109</sup> It is a ubiquitous cytosolic flavoprotein which, like NQO1 plays an antioxidant role that protects cells against redox cycling. Human NQO2 is mostly up-regulated in skeletal muscle, liver, kidney and heart<sup>110</sup> but it is not expressed simultaneously with NQO1.<sup>111</sup> Studies conducted by Harada and his co-workers revealed that genetic polymorphisms of NQO2 are associated with several diseases, such as Parkinson's disease and Schizophrenia.<sup>107,112</sup>

##### **1.6.1 Crystal structure of NQO2**

The X-ray crystal structure of NQO2 (Figure 33) shows that it has structural similarity with NQO1 with which it shares 49% similarity at the amino acid level.<sup>95,113</sup> Analogously to NQO1, it forms a homodimer with one molecule of non-covalently bound FAD per monomer resulting in two identical active sites on the enzyme interface.



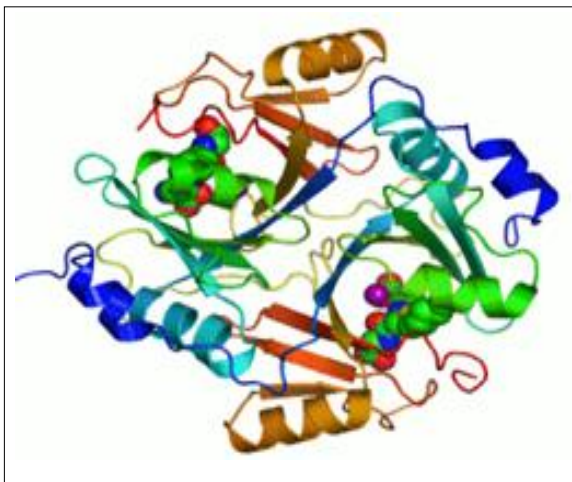


**Figure 33:** X-ray structure of NQO2. Zinc/ copper metal is represented in purple colour.<sup>90</sup>

In contrast to NQO1, the biological function of NQO2 is still ambiguous. It comprises 230 amino acid residues: the catalytic domain (N-terminal) contains residues 1-220, while the carboxy terminal contains 43 amino acid residues. The missing residues from the C-terminal in NQO2 provide the binding site for the adenine monophosphate (AMP) moiety of NAD(P)H in NQO1 and this explains the inability of NQO2 to use NADH/NAD(P)H as electron donor.

NQO2 catalyses its reactions using reduced N-ribosyl nicotinamide (NRH) (**37a**) (Figure 34) which is not synthesized in the body, but may be formed from the breakdown of NAD(P)H or NADH *in vivo*.<sup>114</sup> Knox and his co-workers synthesized several analogues of NRH (**37b-f**) (Figure 31) and these compounds were found to be more efficient than the NRH for the enzymatic reduction of quinones *in vitro*.<sup>115</sup>

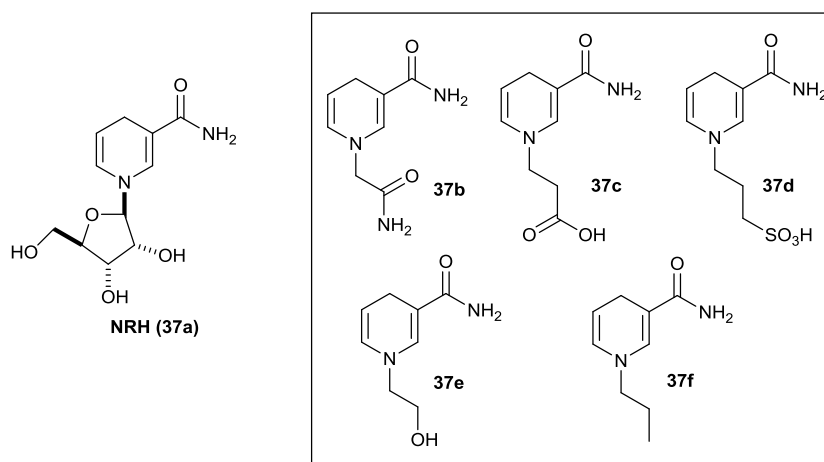


**Figure 34:** Structure of NRH (**37a**) and its analogues (**37b-f**).

The crystal structure of NQO2 also reveals that the enzyme contains a metal binding site which is tetra co-ordinated with two histidine residues (His-173 and His-177), one cysteine residue (Cys-222) and the main chain carbonyl. This finding lead to the assumption that NQO2 is a copper enzyme in which the metal may be used in electron transfer instead of providing structural stability.<sup>95,114</sup> This hypothesis was recently proved wrong by Kwiek and co-workers<sup>116</sup> who carried out research with EDTA (**38**) (Figure 35). Their studies revealed that EDTA does not affect the functioning of the enzyme meaning that the metal is not vital for catalytic activity.

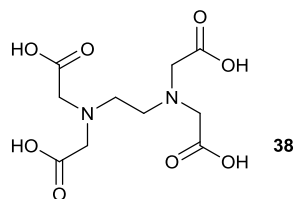


**Figure 35:** Structure of ethylenediamine tetra-acetic acid (EDTA; **38**).

### 1.6.2 NQO2 active site

The active sites of both NQO1 and NQO2 are relatively similar. Residues from both monomers line the active sites, which are deep cavities. This is not surprising since both enzymes catalyse reactions with similar mechanisms ('a ping-pong' mechanism) with one molecule of FAD bound to each monomer.<sup>117</sup> The active site of NQO2 (Figure 36), however, is slightly larger and more hydrophobic<sup>118</sup> than that of NQO1: this is a consequence of replacement of three residues; Tyr-126, Tyr-128 and Met-131 with Phe-126, Ile-128 and Phe-131 in NQO2.<sup>95</sup>

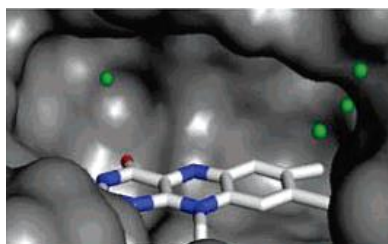


**Figure 36:** Representation of the deep cavity of the active site of NQO2 in its apo-form with non-covalently bound FAD.<sup>119</sup>

During the catalytic reaction of both NQO1 and NQO2, Tyr-155 is involved: a proton is transferred from the OH of Tyr-155 to FAD. In NQO1, the negative charge formed on Tyr-155 is stabilized by His-161.<sup>92</sup> In contrast, in NQO2, His-161 is

replaced by Asn-161 however a reason for the involvement of asparagine in the NQO2 reaction mechanism is not known, since it cannot stabilize a developing negative charge on Tyr-155 in the same way as His-161.

Research carried out by Zhang and his co-workers<sup>120</sup> demonstrated that the active site cavity of NQO2 is about 1.9 Å longer than that of NQO1 and it allows only molecules that can adopt a parallel orientation with respect to the FAD molecule to bind. This explains why dicoumarol and other NQO1 inhibitors do not potently inhibit NQO2.

### 1.6.3 NQO2 inhibitors

The active sites of both NQO1 and NQO2 are sufficiently similar that they not only have the same catalytic mechanism but also share similar substrates. For example, studies have revealed that both enzymes catalyse the reduction of menadione (**31**), DCPIP (**20**) and other 1,4 para-quinones at equal rates.<sup>121</sup> The slight difference in the enzymes active site residues (such as, His-161 for NQO1 and Asn-161 for NQO2) still affect the potency towards some of their substrates. For example, Asn-161 plays an important role in the interaction of NQO2 with CB1954 (**10**) and resveratrol (**39**) (Figure 37).

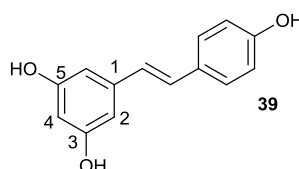


**Figure 37:** Structure of *trans*-resveratrol (**39**).

In the NQO2-CB1954 complex (Figure 38 and 39), the side-chain of Asn-161 forms a hydrogen bond with the 2-nitro group of CB1954 and this gives it a better orientation for reduction of the 4-nitro group.

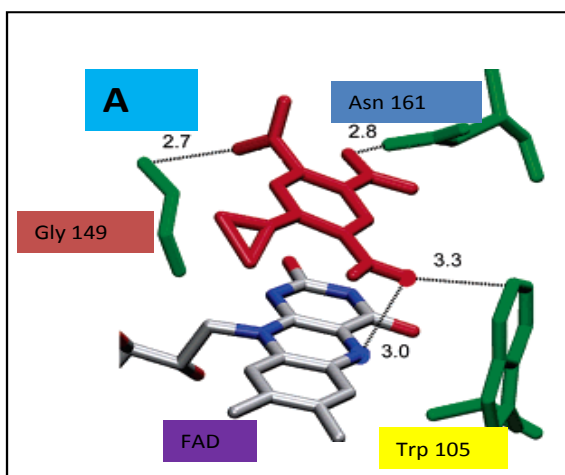


**Figure 38:** Representation of FAD interaction with CB1954 (**10**) in the NQO2 active site. CB1954 makes two important electrostatic interactions with the protein residues such as Gly 149 and Asn 161. The site of reduction is in proximity to the FAD N5 (3.0 Å). Gly 149 holds the CB1954 strongly and thereby places the 4-nitro group in a better orientation for hydride transfer.<sup>119</sup>

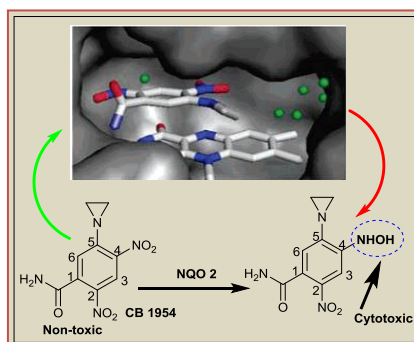


**Figure 39:** CB1954 at the active site of NQO2 in a parallel position with respect to the FAD moiety.<sup>119</sup>

In contrast, in the NQO2-resveratrol complex (Figure 40), the side-chain of Asn-161 forms a hydrogen bond with the 5-hydroxy group of resveratrol and this helps to prevent the interaction of the hydrophobic cavity with water molecules.

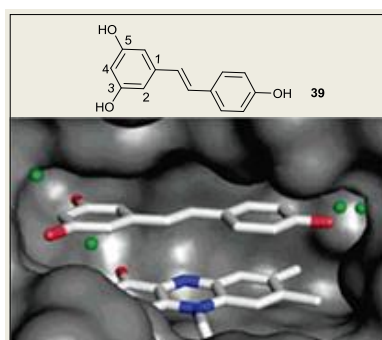
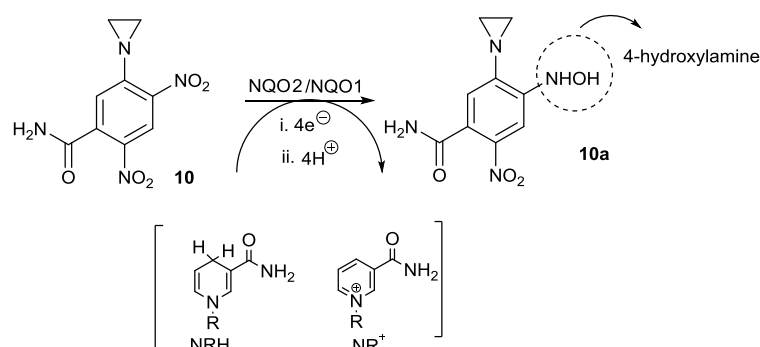


**Figure 40:** Resveratrol (**39**) in the binding pocket of the NQO2 active site. The structure illustrates the  $\pi$ - $\pi$  interaction of the FAD moiety with the resveratrol inhibitor. The green colour represents water molecules.<sup>119</sup>

Currently, research is being conducted into the use of CB1954 (**10**) as a prodrug for the treatment of certain cancers such as prostate. As a prodrug, it is moderately non-toxic to cells. It is not a quinone or a derivative thereof and therefore cannot be reduced by quinone reductases such as cytochrome p450 reductase or xanthine oxidase. The reduction of CB1954 by the oxidoreductases produces a potent cytotoxic compound: 5-(aziridin-1-yl)-4-(hydroxyamino)-2-nitrobenzamide (**10a**) as depicted in Scheme 4. The presence of 5-(aziridin-1-yl)-4-(hydroxyamino)-2-nitrobenzamide (**10a**) in the cells causes the formation of DNA-DNA interstrand cross-links which can result in the death of cancer cells.<sup>115</sup>



**Scheme 4:** Reduction of CB1954 (**10**) to 5-(aziridin-1-yl)-4-(hydroxyamino)-2-nitrobenzamide (**10a**) catalysed by NQO1 and NQO2.

Human NQO2 was reported to be 300 times more effective than human NQO1 in catalysing the reduction of CB1954 *in vitro*.<sup>115</sup> The difference in reactivity of the two enzymes towards CB1954 may be due to the side-chain of residue 161. The side-chain of His-161 in NQO1 is larger than that of the Asn-161 in NQO2 and this may obstruct the binding of CB1954 if it binds to NQO1 in a similar parallel orientation to NQO2 (Figure 34a). If CB1954 binds to the NQO1 active site, the position of the 4-nitro group will be affected by His-161 for the hydride transfer (Figure 41).<sup>122</sup>

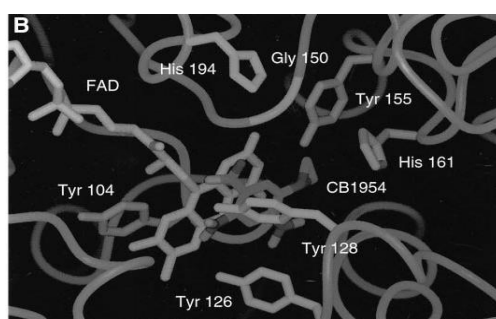


**Figure 41:** Predicted binding orientation of CB1954 (**10**) in the active site of NQO1. The diagram suggested different orientation of CB1954 in NQO1 compared with that of NQO2.<sup>122</sup>

In order to confirm the role of Asn-161 in the activation of CB1954 by NQO2, Zhang and his co-workers<sup>115</sup> conducted research with a mutant NQO2 in which Asn-161 had been mutated to His-161. In comparison to the wild type NQO2, the mutant NQO2 showed no detectable activity for the reduction of CB1954 even up to a maximum concentration of 150  $\mu$ M. Zhang and his team therefore concluded that Asn-161 plays an important role in the positioning of CB1954 at the NQO2 active site. The team carried out further research into the activity of mutant NQO2 with menadione as substrate. They observed that the mutation of Asn-161 to His-161 did not affect the binding or the orientation of menadione at the NQO2 active site.

The most potent NQO2 inhibitor reported in the literature is resveratrol (**39**) which is competitive with respect to the N-ribosyl derivative of dihydronicotinamide (NRH). The potency of resveratrol as a NQO2 inhibitor was reported by Zhang and co-workers who measured a binding affinity ( $K_1$ ) of 35 nM.<sup>123</sup> Resveratrol, a phytoalexin produced by many plants, has been reported as an inhibitor of other enzymes but a nanomolar inhibition concentration towards NQO2 makes it unique.

Furthermore, anti-malaria drugs such as quinacrine (**40**) and chloroquine (**41**) (Figure 42) have also been reported as potent inhibitors of NQO2 with activities in the 500 nM to 1  $\mu$ M range.<sup>124</sup>

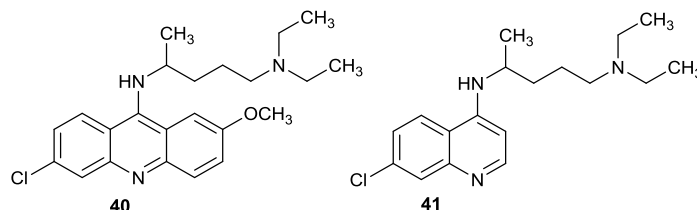


**Figure 42:** Structure of quinacrine (**40**) and chloroquine (**41**).

Other potent inhibitors of NQO2 that have been reported include: chrysoeriol (**42**), quercetin (**43**) and primaquine (**44**) (Figure 43).

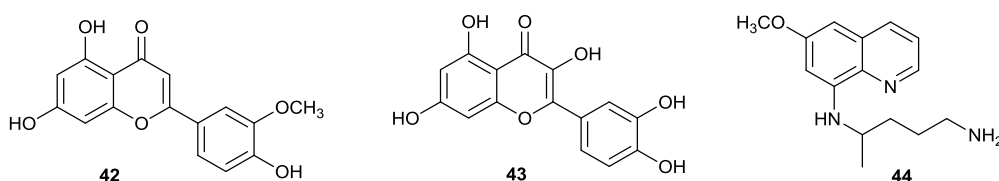
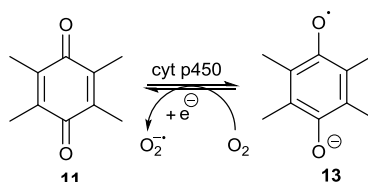


**Figure 43:** Structures of chrysoeriol (**42**), quercetin (**43**) and primaquine (**44**).

It is noteworthy that NQO1 and NQO2 inhibitors both contain aromatic ring systems that are needed for  $\pi$  binding with the isoalloxazine ring moiety of the flavin cofactor.

### 1.7.0 Sources of quinones

Quinones, especially *para*-quinones, belong to a class of ubiquitous and naturally occurring compounds. Quinones obtained from polycyclic aromatic hydrocarbons are found abundantly in all burnt organic materials such as, urban air particulates, automobile exhaust, cigarette smoke and many foodstuffs.<sup>125,126</sup> Generally, compounds containing a quinoid nucleus are potent as cancer causing agents. They are highly reactive as electrophiles and also generate unstable semi-quinone radicals (**13**) *via* one electron reduction by cytochrome p450 reductases as depicted in Scheme 5.



**Scheme 5:** One electron reduction of quinone (**11**) to a semiquinone (**13**) caused by cytochrome p450 reductases.

The semi-quinone radicals subsequently undergo redox cycling in the presence of molecular oxygen forming highly reactive oxygen species (ROS). This leads to oxidative stress and consequently, tissue degeneration, apoptosis, premature aging, cellular transformation and neoplasia.<sup>127</sup> Obligate two electron reduction by the NQOs prevents these harmful effects by producing more stable hydroquinones, which can be removed from the cell by conjugation with glutathione or glucuronic acid thus providing cellular protection.

### 1.8.0 Consequences of inhibiting NQO1 and NQO2

Inhibition of the NQO enzymes may have some important consequences as there will be a resulting over accumulation of reactive oxygen species resulting in oxidative stress and cell apoptosis. Inhibition will be effective, however, in terms of anti cancer therapy if there is up-regulation of these enzymes in cancer cells. The data in (Table 1) indicates the upregulation of NQO1 activities in tumor tissues compared with the

corresponding normal tissues. Findings such as these have lead to the chemotherapeutic targeting of NQO1 in some cancer treatments.

Tissue	Normal	Tumor
Breast	50 ± 11	165 ± 43
Colon	17 ± 4	66 ± 13
Liver	17 ± 4	64 ± 32
Lung	10 ± 2	150 ± 45

**Table 1:** Level of NQO1 activity in normal and tumor tissues. The values represent the activity inhibited by 1  $\mu$ M dicoumarol with dichloroindophenol (DCPIP) as the substrate. Units are nmol/min/mg protein.<sup>128</sup>

### 1.9.0 Discovery of potent anti-cancer drugs

Compounds screened as possible anti-cancer agents can be either natural or synthetic in origin. Natural compounds have provided many useful leads and their structural identification has afforded numerous compounds with good pharmacological activity and therapeutic potential. The search for novel natural bioactive compounds has therefore intensified over recent years.

This effort has led to the discovery of several natural compounds and their synthetic analogues which have been identified as possessing a wide range of remarkable antitumor properties, such as:

- Induction of cell cycle arrest,
- Induction of apoptosis and cell division, and
- Inhibition of cell growth and proliferation.<sup>129</sup>

A number of anti-tumor compounds have been obtained from *Streptomyces*, the largest genus of actinobacteria (Gram-positive bacteria) which grow in different locations. A remarkable property of *Streptomyces* bacteria has emerged to be their ability to produce a variety of bioactive secondary metabolites which include: antitumor agents, immunosuppressive agents and antibiotics.<sup>129</sup> This has increased interest in the search to discover more novel bioactive secondary metabolites from the *Streptomyces* genus. One outcome of this research interest has been the discovery of the anti-cancer compounds: 2-crotonyloxymethyl-(4*R*,5*R*,6*R*)-4,5,6-



trihydroxycyclohex-2-enone (COTC, **45**), gabosine E (**46**), antheminone A (**47**) and phorbacin B (**48**) (Figure 44). COTC was found to demonstrate remarkable toxicity towards some cancer cell lines in culture as well as in tumor bearing mice.<sup>130</sup>

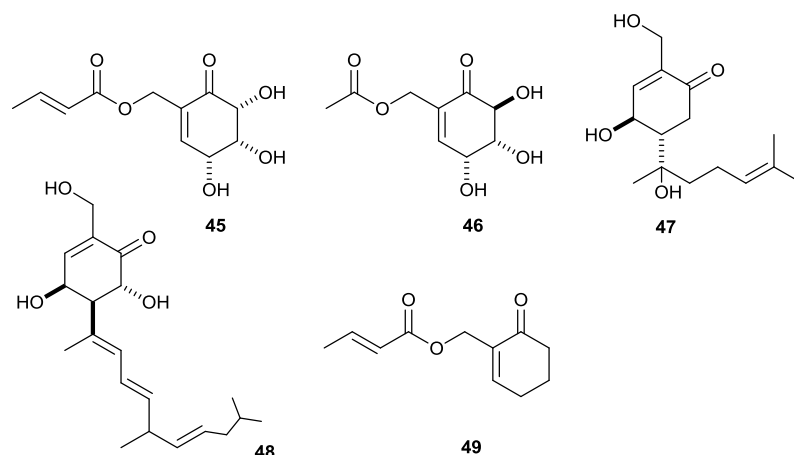


**Figure 44:** Structures of COTC (**45**), gabosine (**46**), antheminone A (**47**), phorbacin B (**48**) and COMC (**49**).

### 1.9.1 Isolation of COTC

In 1975, Takeuchi and his co-workers isolated COTC (**45**) from the cultures of *Streptomyces griseosporus*.<sup>130</sup> After conducting a preliminary chemical analysis, the compound was identified as 2-crotonyloxymethyl-(4*R*,5*R*,6*R*)-4,5,6-trihydroxycyclohex-2-enone (**45**). The stereochemistry and the absolute configuration were assigned by X-ray crystallography.<sup>130</sup> COTC (**45**) and its synthetic analogue COMC (**49**) have been found to exhibit potent antitumor activity against murine and human tumors in culture.

Takeuchi and his team conducted further investigations into the anti-tumor activity of COTC. They observed that glyoxalase 1 enzyme obtained from the rat liver and yeast was inhibited by COTC. Glyoxalase enzymes have been reported to support cell growth and regulation by controlling the level of toxic methylglyoxal (**50**) (Figure 45) produced by normal body metabolism.<sup>131</sup> Such inhibition will result in a carcinostatic effect by preventing the metabolism of methylglyoxal in tumor cells and hence leading to cell apoptosis.<sup>132</sup>

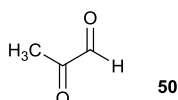


**Figure 45:** Structure of methylglyoxal (**50**).

Further studies also proved that daily injections of COTC into mice that had been intraperitoneally inoculated with cancer cells led to strong inhibition of growth of Hela cells and EHRlich ascites carcinoma and a weak inhibition of L-1210 leukaemia cells, with low toxicity.<sup>133</sup>

The fact that many biological agents that either initiate or retard cancer growth react with -SH containing molecules such as, thiophenol (**51**), 2-mercaptoethanol (**52**) and cysteine (**53**) (Figure 46), indicates that there may be some form of relationship between cancer and GSH.<sup>133</sup> The antitumor properties of both COTC (**45**) and COMC (**49**) indeed, were actually based on this property. In view of this, Takeuchi and his team conducted further research into the bioactivity of COTC by studying its reaction with a series of sulfhydryl containing compounds.

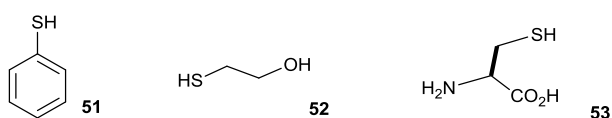
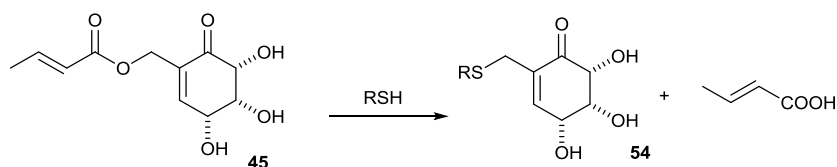


**Figure 46:** Structure of thiophenol (**51**), 2-mercaptoethanol (**52**) and cysteine (**53**).

The team observed a rapid replacement of the crotonate group in COTC by 2-mercaptoethanol (**54**) as depicted in Scheme 6.<sup>130</sup> The team therefore, concluded that the anti-cancer activity of COTC was a result of the nucleophilic substitution of the crotonate group by an intracellular sulfhydryl (-SH) group, such as that present in glutathione (GSH).



**Scheme 6:** Nucleophilic displacement of the crotonyl moiety of COTC (**45**) by sulfhydryl containing compounds.

The potent antitumor activity of COTC prompted efforts to carry out further investigations into compounds of this nature.<sup>111</sup> Analogues of the natural product were synthesized in an attempt to improve potency and/or the cytotoxicity profile. For example, studies conducted by Douglas and Shing demonstrated that the non-hydroxylated synthetic compound COMC (**49**), was more toxic towards cancer cell lines than the trihydroxylated natural product.<sup>134</sup>

In 2007, Whitehead and co-workers investigated the influence of the degree of hydroxylation of the carbacyclic core on *in vitro* toxicity towards non-small lung cancer cell lines (A549 and H460).<sup>135</sup> The result revealed that the mono-hydroxylated products (**55**), (**56**) and (**57**) (Figure 47), showed notable toxicity towards cancer cell lines in comparison to COMC (**49**) (Table 2).

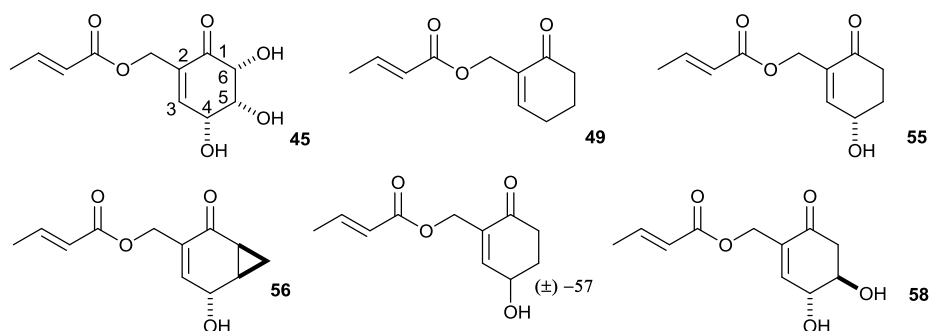


**Figure 47:** Structure of mono-hydroxylated analogues of COTC (**45**).<sup>135</sup>

Compound	IC <sub>50</sub> (μM)	
	A549	H460
<b>49</b>	54.5	40.4
<b>55</b>	16.7	10.9
<b>56</b>	18.1	20.4
(±)- <b>57</b>	23.6	10.5
<b>58</b>	147.4	158.0

**Table 2:** Bioactivity of COTC (**45**) analogues.<sup>135</sup>

Compounds (**55**) and ((±)-**57**) which differ only in their absolute configurations, have IC<sub>50</sub> values almost the same, which suggests that the absolute configuration at C-4

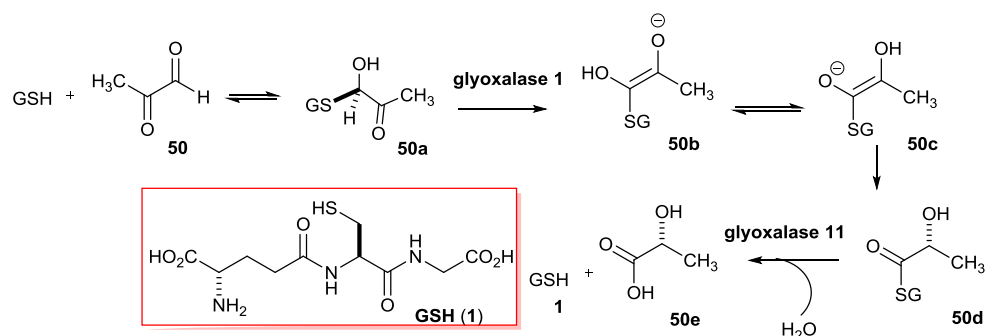
has an insignificant effect on the potency of the compounds. Introduction of a second hydroxyl group at C-5 as in compound (**58**), decreases the efficacy of the compound towards the cell lines.<sup>135</sup>

### 1.9.2 The glyoxalase enzymes

The glyoxalase system, which is comprised of two ubiquitous enzymes (glyoxalase 1 and 11) and their related cofactor, reduced glutathione (GSH), was discovered in 1913.<sup>136</sup> The system is part of a detoxification network necessary for cellular protection against toxic metabolites. Such metabolites include  $\alpha$ -keto aldehyde (**50**), and other reactive aldehydes produced in the body by normal metabolism (catabolism of threonine).<sup>137</sup>  $\alpha$ -Keto aldehydes are highly carcinogenic<sup>138</sup> and can chemically damage a number of important components of the cell, such as proteins and nucleic acids.

The major physiological role of the glyoxalase system is detoxification of toxic methylglyoxal<sup>139</sup> which will accumulate if the glyoxalase system is inhibited. It has been reported that glyoxalase 1 is frequently overexpressed in malignant tissues and tumor cell lines compared with the corresponding normal tissues. Inhibition of glyoxalase 1 therefore, could be effective as a therapeutic treatment of malignant cancers.<sup>140,141</sup>

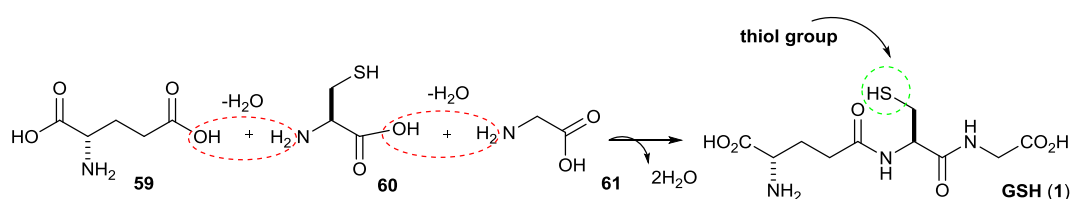
In its enzymatic reaction, glyoxalase 1 (lactoylglutathione lyase) catalyses the isomerisation of the monohemithioacetal (**50a**), formed spontaneously between glutathione and methylglyoxal, into *S*-lactoylglutathione (**50b**).<sup>142</sup> The thioester (**50d**) is then hydrolysed by glyoxalase 11 (hydroxyl-acylglutathione hydrolase) to produce D-lactic acid (**50e**) and reduced glutathione (GSH) as depicted in Scheme 7.



**Scheme 7:** The mechanism of detoxification of methylglyoxal (**50**) detoxification by the glyoxalase system.<sup>136</sup>

### 1.9.3 The role of glutathione

Glutathione (GSH, **1**) is a tripeptide (L- $\gamma$ -glutamyl-L-cysteinyl-glycine) that is synthesized in the cytosol from the amino acids L-glutamic acid (**59**), L-cysteine (**60**) and glycine (**61**) as shown in Scheme 8. GSH, a ubiquitous non-protein molecule found in all parts of the cell, acts both as an anti-oxidant and a reducing agent, that prevents damage to cells caused by the formation of ROS.<sup>143</sup> The two unique structural features of GSH, the  $\gamma$ -Glu linkage and the thiol group, promote its intracellular stability and are also linked with its functions. It is involved in the synthesis of proteins, nucleic acids and detoxification of free radicals and peroxides.



**Scheme 8:** Synthesis of reduced glutathione from its precursor amino acids; L-glutamic acid (**59**), L-cysteine (**60**) and glycine (**61**).

Cells contain about 10 mM concentrations of glutathione which is maintained in its reduced form (GSH) by a cytosolic NADPH/dependent reaction catalysed by glutathione reductase (GSR). GSH serves as an electron donor for the reduction of protein disulphide bonds formed during the enzymatic reduction of damaging peroxides such as  $\text{H}_2\text{O}_2$  and  $\text{ROOH}$ .<sup>144</sup> In this process, GSH is converted to its oxidized form, glutathione disulphide (GSSG), (**62**) (Figure 48) which can be readily reduced back to GSH by GSR using a FAD prosthetic group and NADPH as electron donor. The ratio of the oxidized and reduced form of glutathione can be used as a

measure of cellular toxicity<sup>145</sup> with an increase in the oxidized state over the reduced state being an indication that a cell is under oxidative stress.

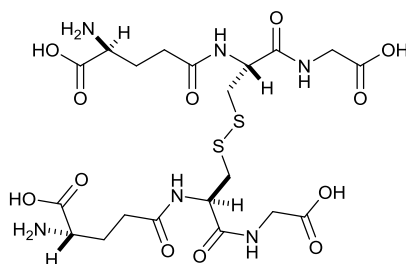


**Figure 48:** glutathione disulphide (GSSG) (**62**).

Although glutathione is part of a detoxification system, up-regulation in cancer cells may lead to insensitivity towards alkylating chemotherapeutic agents. For example, studies have shown that there is high level of GSH in cell lines resistant to alkylating chemotherapeutic agents such as cisplatin (**63**), melphalan (**64**) and chlorambucil (**65**) (Figure 49).<sup>146</sup> This occurs as a result of an interaction of the thiol group of GSH with the chemotherapeutic agents, leading to tumor therapy failure. Conjugation of GSH and the alkylating drugs *via* the thiol group causes detoxification of the chemotherapeutic agents, thereby making malignant cancer cells drug resistant.<sup>147,148</sup>

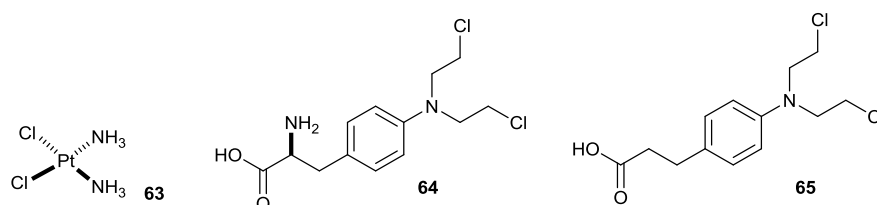


**Figure 49:** Chemotherapeutic anti-cancer agents: Cisplatin (**63**), Melphalan (**64**) and Chlorambucil (**65**).

The importance of glutathione is also apparent from the inhibition of glyoxalase 1 by the COTC-GSH conjugate (**66**) (Figure 50). In the absence of GSH, glyoxalase 1 was not inhibited by COTC alone.<sup>149</sup>

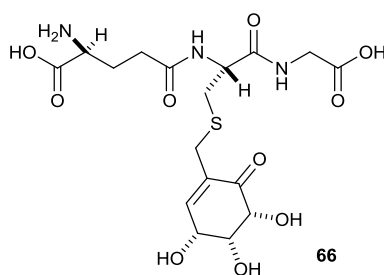


**Figure 50:** Structure of COTC-GSH conjugate adduct (**66**).

In 2005, Ichikawa and co-workers intensified their research to find novel potent anticancer drugs targeting GSH and the glyoxalase 1 enzyme. The team investigated apoptosis induction using COTC in apoptosis-resistant human pancreatic adenocarcinoma cells (AsPC-1).<sup>150</sup> They evaluated the content of GSH in AsPC-1 cells, and observed a high level of GSH in AsPC-1 ( $352.5 \pm 128.2$  nmol/mL) compared to other cell lines under study. In view of this, the group concluded that the high level of GSH could be a major factor in the apoptotic resistance of the cells.

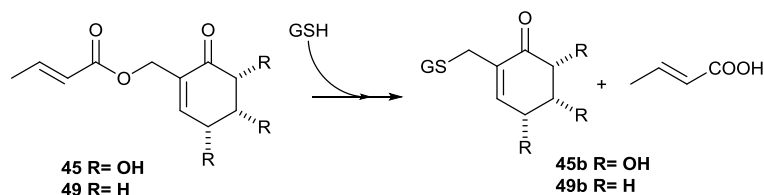
The group also investigated the effects of COTC on cellular GSH levels in AsPC-1 cells. The GSH level in AsPC-1 dropped to 40% of its initial level 1-2 hours after addition of 30  $\mu$ g/mL of COTC. The fact that cancer cells use GSH as part of a drug-detoxifying system, led to a comparative analysis of the reaction between GSH and COTC in the presence of the alkylating agent melphalan (**64**). It was discovered that the COTC-GSH conjugate was formed faster than that of melphalan-GSH, consequently leading to increased cytotoxicity of the alkylating agent.

In conclusion, the depletion of GSH and inhibition of glyoxalase 1 by COTC, may lead to high concentrations of intracellular anticancer drugs as well as toxic methylglyoxal and other reactive aldehydes. The inhibition of glyoxalase 1 by COTC in the presence of GSH, may lead to an increase in chemotherapy-mediated apoptosis.<sup>150</sup>

#### 1.9.4 Mechanism of action of COTC and COMC.

It was originally thought that the potent antitumor properties of COTC and COMC against murine and human cancer cell lines in culture was as a result of the inhibition of glyoxalase 1 by glutathione adducts. The suggested mechanism proceeded *via* an

overall  $S_N2$  displacement of the crotonate group by GSH, to give GSH-conjugated adducts (**45b**) and (**49b**), which were believed to inhibit glyoxalase 1 (Scheme 9).<sup>133</sup>



**Scheme 9:** Nucleophilic displacement of crotonate group by GSH.

This ‘prodrug hypothesis’, put forward by Takeuchi and co-workers, was not verified until 2002, when Hamilton, Ganem, Creighton and co-workers undertook research into the mechanism based antitumor activities of both COTC and COMC. Authentic samples of GSH-conjugated adducts (**45b**) and (**49b**) were prepared and tested against erythrocyte glyoxalase 1. The two samples proved to be poor competitive inhibitors of human glyoxalase 1<sup>151</sup> and also lacked substantial antitumor activity towards B16 melanotic melanoma *in vitro*.<sup>152</sup> The Takeuchi hypothesis of antitumor property of COTC and COMC was consequently put into question.

In 2003, Ganem, Creighton and co-workers<sup>153</sup> proposed that the GSH-conjugated adducts may be toxic to tumor cells through an alternative mechanism consisting of a multistep sequence of reactions.<sup>152</sup> Further studies by the team showed that the human glutathione transferase isozyme of the class  $\pi$ (hGSTP1-1) (Figure 51) catalyses the conjugate addition of GSH to the cyclohexenone to give an exocyclic enone (**68**) as depicted in Scheme 10.

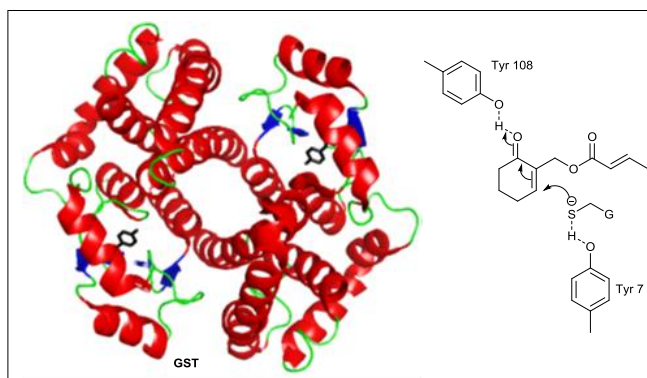
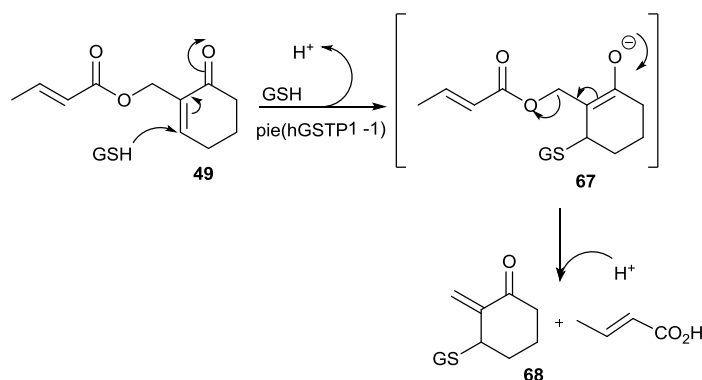


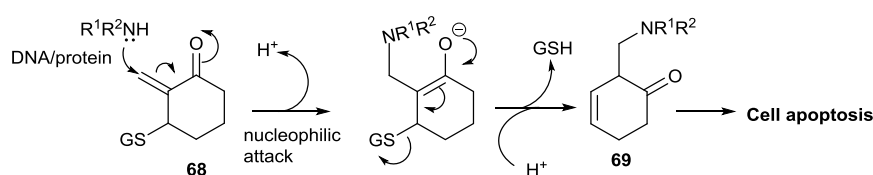
**Figure 51:** X-ray crystal structure of  $\pi$ GSTP1-1 showing the Tyr 108 residue in black colour which was proposed to be involved in the activation of glutathione (GSH).<sup>152</sup>





**Scheme 10:** Mechanism of formation of an intermediate electrophilic exocyclic enone (**68**).

The fact that the exocyclic enone (**68**) is a better Michael acceptor than COMC itself, suggests that the former might be the actual toxic species in tumor cells. The exocyclic enone may undergo alkylation reactions with reactive groups on intracellular proteins and/ or nucleic acids which are vital to cell function, leading to cell apoptosis (Scheme 11).

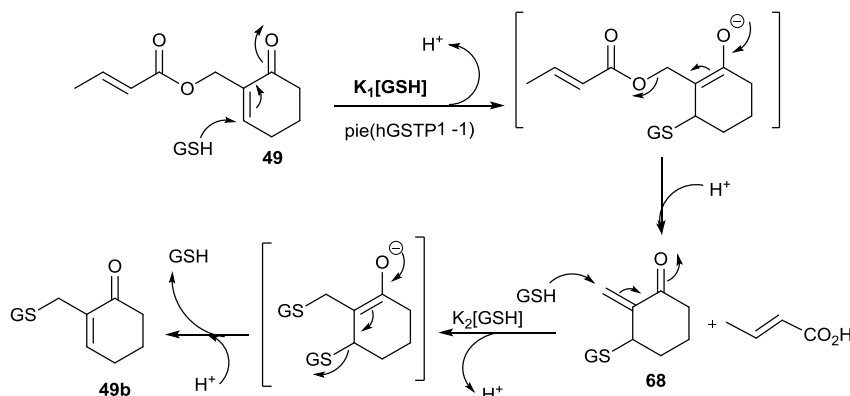


**Scheme 11:** Mechanism of alkylation of nucleic acids / proteins by an exocyclic enone (**68**) to give (**69**).

Fundamental kinetic studies and trapping experiments were also carried out to monitor the mechanism of formation of GSH-conjugated adduct (**49b**). Ganem, Creighton and co-workers reported that the non-enzymatic reaction of COMC and GSH followed a smooth first order conversion to GSH-conjugated adduct (**49b**) without any detection of intermediate species. In the presence of human placental glutathione transferase ( $\pi(hGSTP1-1)$ ) however, the reaction rate profile changed into a double exponential decay.

The reaction profile comprised of a rapid, enzyme-depended initial step which involved COMC, followed by a slow enzyme-independent first-order phase.<sup>153</sup> These findings therefore, led to the conclusion that an enzyme catalysed Michael addition of GSH to COMC produced an exocyclic enone (**68**). The exocyclic enone after

dissociation from the enzyme reacts with GSH non-enzymatically to form GSH-conjugated adduct (**49b**) (Scheme 12).



**Scheme 12:** An alternative mechanism for the reaction of COMC (**49**) and GSH in the presence of  $\pi(hGSTP1-1)$ .

Based on the fact that the conjugate addition of COMC with GSH is a multistep reaction, Ganem, Creighton and co-workers suggested that the cytotoxicity of COMC could be a consequence of the ability of the exocyclic enone to undergo alkylation reactions with the reactive groups of nucleic acids and proteins. Such reactions may disrupt the vital functions of biomolecules leading to the death of tumor cells. This hypothesis was supported by monitoring the *in vitro* reaction of COMC and GSH with oligonucleotides or dinucleotides using mass spectrometry.

In these experiments, COMC formed stable adducts *in vitro* with both GSH and the exocyclic amino groups of the nucleotide bases. Mass spectroscopic studies indicated that the alkylation of exocyclic amino groups of nucleotides by COMC could occur either in the presence or in the absence of GSH.<sup>154</sup> Due to high level of GSH in most cancer cells, it is suggested that it may be involved in the mechanism of action.

## 1.9.5 Natural anti-tumor agents structurally related to COTC

### 1.9.5.1 The antheminones and carvotacetones

The antheminones and carvotacetones are different bioactive natural products that have been extracted from plants.<sup>155,156</sup> Similarly to COTC, both the antheminones and carvotacetones contain the  $\alpha$ -oxymethyl- $\alpha,\beta$ -cyclohex-2-enone moiety and their anticancer properties have prompted more interest in the compounds of this nature.

### 1.9.5.2 The antheminones

In 2008, Collu and his colleagues<sup>155</sup> isolated antheminones A, B and C from the leaves of *Anthemis maritimum*, an organic herb which grows on sandy beaches along the western Mediterranean coastline. Collu and his teams were the first to conduct research into the chemical composition of the antheminones. The phytochemical analysis conducted resulted in the isolation of the two new cyclohexenones (**47**) and (**69**) and a new cyclohexanone (**70**) as shown in Figure 52.

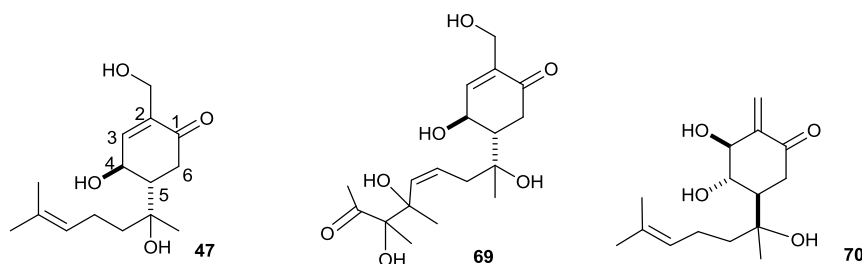


**Figure 52:** Structures of antheminone A (**47**), antheminone B (**69**) and antheminone C (**70**).

The use of 1D and 2D NMR spectroscopy combined with mass spectrometry enabled the team to investigate the structures of these new compounds. Consequently, the structure of compound (**47**), isolated as a colorless oil, was established as 4-hydroxy-5-(1-hydroxy-1,5-dimethyl-4-hexenyl)-2-cyclohexen-1-one which was given the common name, antheminone A.

Likewise, antheminone B (**69**), was isolated as a colorless oil and was designated as 4-hydroxy-2-(hydroxymethyl)-5-[(3Z)-1,5,6-trihydroxy-1,5,6,7-tetramethyl-3,7-octadienyl]-2-cyclohexen-1-one. The structure of antheminone C (**70**), which was also isolated as a colorless oil, was determined to be 3,4-dihydroxy-5-(1-hydroxy-1,5-dimethyl-4-hexenyl)-2-methylene cyclohexanone. The absolute configurations of antheminones A-C, however, have yet to be established due to difficulties with the isolation of crystalline derivative suitable for X-ray structure determination.

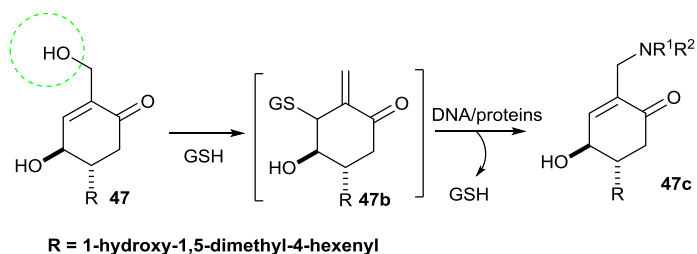
Collu and his teams conducted further research into the cytotoxicity of the three antheminones towards some human cancer cell lines. Antheminones A (**47**) and C (**70**) revealed a remarkable toxicity against all cancer cell lines. They were more potent than antheminone B (**69**) and also displayed substantial antigrowth activity toward the cells which are related to immune system, such as HL-60, U-937, and Jurkat T. The cell lines that were assayed and the IC<sub>50</sub> values (μM) are summarized

in (Table 3).<sup>155</sup> The data showed that antheminone C with an IC<sub>50</sub> value of 3.2  $\mu$ M toward HL-60 cells was the most potent.

$\mu$ M					
Antheminones	HCT- 116 (Colon)	MCF-7 (Breast)	HL-60 (Leukemia)	U-937 (Leukemia)	Jurkat T (Leukemia)
A ( <b>47</b> )	15 $\pm$ 2	21 $\pm$ 2	7.6 $\pm$ 0.6	6.2 $\pm$ 3	9.0 $\pm$ 0.4
B ( <b>69</b> )	29 $\pm$ 4	29 $\pm$ 5	11 $\pm$ 0.9	12 $\pm$ 0.4	14 $\pm$ 2
C ( <b>70</b> )	19 $\pm$ 2	15 $\pm$ 1	3.2 $\pm$ 0.6	7.4 $\pm$ 1.3	8.4 $\pm$ 0.3

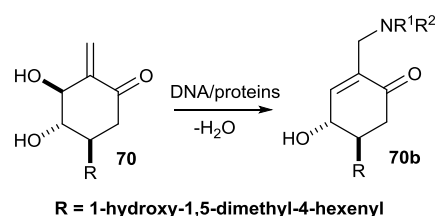
**Table 3:** Cytotoxic activities ( $\mu$ M) of antheminone A (**47**), antheminone B (**69**) and antheminone C (**70**) determined after 72h.<sup>155</sup>

The mode of action of antheminone A (**47**) is still unknown, but since it has a structural relationship with COTC (**45**), it might be assumed that it may react in a similar manner with GSH to COTC and COMC (Scheme 13). This assumption is chemically unlikely because the hydroxyl (OH) is a poor leaving group in comparison to a crotonate group and hence will be less readily displaced by the glutathionyl (SG) group.



**Scheme 13:** The assumed mechanism of action of antheminone A (**47**). The reaction is not chemically favourable because OH is a relatively poor leaving group and thus not readily displaced by GSH. The mechanism by which antheminone A exerts its antitumor effects is thus still unknown.

Antheminone C (**70**), interestingly, has a cyclohexanone moiety instead of a cyclohexenone and was more potent than antheminone A toward HL-60 cells. Collu and his teams explained that the reason that antheminone C was more cytotoxic, could be related to its exocyclic enone structure, and consequently, doesn't require activation by GSH for the alkylation of nucleic acids to give (**70b**) (Scheme 14).



**Scheme 14:** The proposed mechanism of action of antheminones C (**70**) by Collu and co-workers.<sup>155</sup>

### 1.9.5.3 Carvotacetone derivatives

Many carvotacetone derivatives have been isolated from the aerial parts of *Sphaeranthus suaveolens*.<sup>157</sup> The genus *Sphaeranthus*, which comprised about forty species, is found mainly in tropical and subtropical areas of Africa, Asia and Australia.<sup>158,159</sup> Some of these species have been popular due to their significant contribution towards traditional medicine. For example, they have been used in the treatment of skin infections, glandular swellings, bronchitis, jaundice and nervous disorders.<sup>157</sup>

Some of the carvoacetone derivatives that have been isolated and studied chemically (**71-75**) are summarized in Figure 53. The structures and the stereochemistry were confirmed by <sup>1</sup>H NMR, <sup>13</sup>C NMR and 2D NMR spectroscopy.

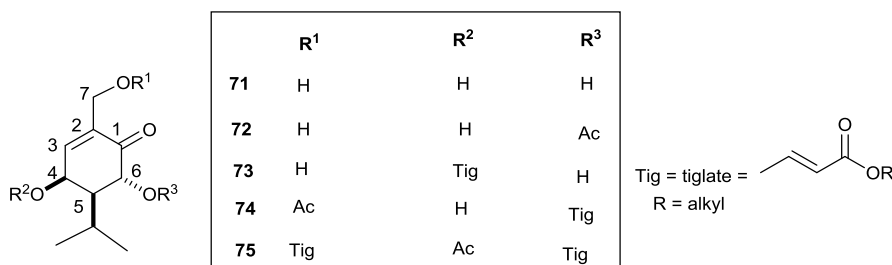


**Figure 53:** Structures of some of the carvoacetone derivatives isolated (**71-75**).<sup>159,160</sup>

In 2012, Midiwo and co-workers were the first to report the anti-plasmodial, antileishmanial and anticancer properties of carvotacetone derivatives isolated from *Sphaeranthus bullatus* (**76-79**) (Figure 54).<sup>160</sup> During the course of their investigation, the researchers observed that compounds (**76**), (**77**) and (**78**) displayed higher activity compared to compound (**79**) with IC<sub>50</sub> values ranging from 1.1- 5.3 µg/mL.<sup>160</sup> The high activities of compounds (**76**), (**77**) and (**78**), were due to the

presence of acetyl or tigloyl substituents at C-4 and C-6 respectively which are lacking in compound (79).

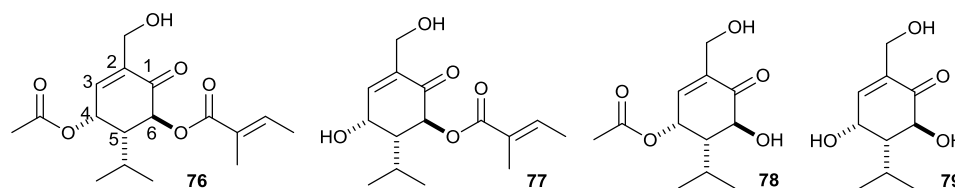


**Figure 54:** Chemical structures of carvotacetone derivatives (76-79) that display antiplasmodial, antileishmanial and anti-cancer properties.

### 1.9.6 The pro-drug concept

The use of modern technologies has empowered the invention of numerous novel compounds with high pharmacological efficiency but low physicochemical and biopharmaceutical efficacy. Schwartzmann and co-workers noted that out of 600,000 anticancer drugs screened in 1988, only 40 were routinely used in the clinic<sup>161</sup> and most of them were not selectively toxic to tumor tissues. Instead they acted by anti-proliferative mechanisms which are aimed at disrupting specific cellular processes occurring during cell growth and proliferation.<sup>162</sup>

One of the limitations of many anti-cancer drugs is their toxicity to healthy tissues and organs rather than being selectively toxic to tumor tissues. In order to overcome this difficulty, and to obtain target based drugs, prodrugs have been designed in order to increase the efficiency of the parent drug.<sup>164,165</sup>

The term prodrug was first introduced by Albert in 1958<sup>166</sup> to describe any compound that is toxicologically and pharmacodynamically inactive but is transformed *in vivo* into an inactive product by an enzyme. Prodrugs provide possibilities to overcome several barriers to drug formulation and delivery. These include poor solubility, chemical instability, insufficient oral absorption, inadequate penetration and irritation. This can be accomplished by numerous mechanisms, such as a change of temperature or salt concentration, natural decomposition of the drug, internal ring- opening or cyclization, change of pH and oxygen tension.<sup>167</sup>

### 1.9.6.1 Classification of prodrug

Prodrugs are classified into two major types based on their solubility, method of bioactivation, type of catalyst used in bioactivation and chemical composition. These are; i) carrier linked prodrugs and ii) bioprecursors or metabolic precursors.<sup>168</sup>

- (a) Carrier linked prodrugs consist of the active parent drug covalently linked to an inert carrier or transporter moiety *via* an ester or amide.<sup>169</sup> The parent drug is released by either hydrolytic cleavage or by degradation by an enzyme (Figure 55).

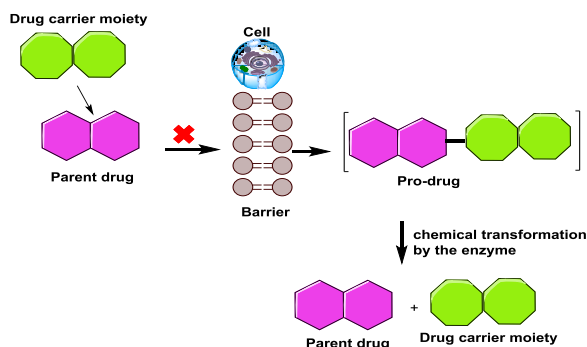


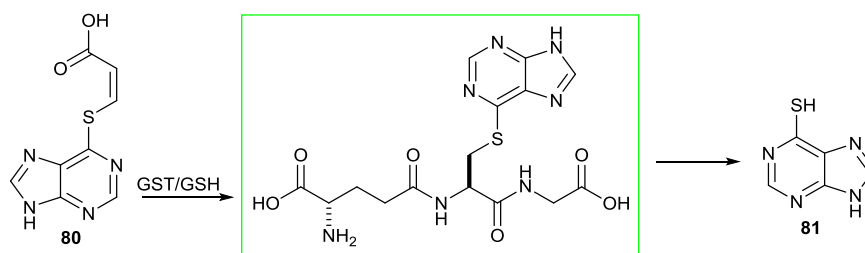
**Figure 55:** A simplified illustration of the pro-drug concept. Barriers are any limitations that prevent optimal efficiency of the parent drug which has to be overcome for the development of a marketable drug. This is achieved by coupling the drug with a drug carrier moiety. The ideal prodrug yields the parent drug with high recovery ratios with the drug carrier moiety being either toxic or non-toxic.

- (b) Bioprecursors or metabolic precursors are inert compounds synthesized by chemical modification of the parent drug. In this case the prodrug has almost the same solubility as the parent drug and it is activated by enzymatic biotransformation.<sup>170</sup>

The key approach to prodrug synthesis for cancer chemotherapy includes the synthesis of inactive compounds that will be converted to active products by enzyme action. In cancer treatment however, the inactive prodrug is converted to a highly toxic compound by enzymes which are highly up-regulated in tumor cells. In research conducted by O'Brien and co-workers,  $\pi$ (GSTP1-1) is frequently overexpressed in almost all human tumors. These include, carcinoma of the colon, lung, kidney, ovary, pancreas, breast, liver, esophagus and stomach.<sup>171</sup>

In 1999, Gunnarsdottir and Elfarra reported the first GSH-dependent prodrug activation in which they found that a prodrug (Z)-3-((9H-purin-6-yl)thiol)acrylic (**80**)

releases the cytotoxic agent 9H-purin-6-thiol (**81**) upon reaction with GSH as shown in Scheme 15.<sup>172</sup>



**Scheme 15:** Prodrug (**80**) activation by GSH which releases cytotoxic thiopurine (**81**).

### 1.9.6.2 Characteristic features of prodrug

An ideal prodrug should possess the following properties:<sup>173</sup>

- (i) It should be pharmacologically unreactive.
- (ii) It must undergo rapid transformation, chemically or enzymatically, into the active form at the target site.
- (iii) It must generate non-toxic metabolic fragments which undergo quick elimination.

Currently, 5-7% of the drugs approved worldwide can be grouped as pro-drugs, while 15% of all the new drugs approved in the years 2001 and 2002 were pro-drugs.<sup>164</sup>



### 1.10 Aims and objectives

Studies conducted by Ernester in 1967 established that dicoumarol (**33**) was a potent inhibitor of NQO1 with an  $IC_{50}$  value of 2.6 nM.<sup>72</sup> Similarly, the Whitehead and Stratford groups at Manchester also reported that symmetrical analogues of dicoumarol (**92a**) and (**92b**) (Figure 56) were the more competitive inhibitors ( $IC_{50}$  values  $2.8 \pm 0.42$  and  $0.16 \pm 0.16$  nM respectively) of NQO1<sup>174</sup> with respect to NADH as electron donor and menadione as co-substrate.

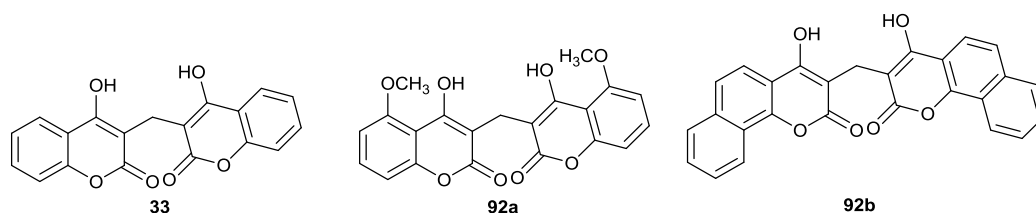


**Figure 56:** Structures of symmetrical dicoumarol (**33**) and its derivatives (**92a**) and (**92b**).

In addition, the team also conducted extensive research into developing an efficient route for the synthesis of asymmetric analogues of dicoumarol (Figure 57) and assaying their biological potency as NQO1 inhibitors.

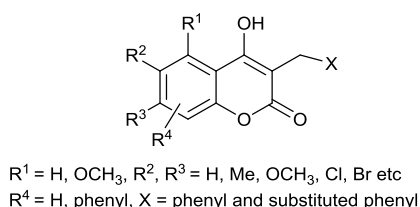


**Figure 57:** General structure of asymmetrical analogues of dicoumarol used as NQO1 inhibitors.

The aim of the research project described herein was to synthesize a range of symmetrical and asymmetrical analogues of dicoumarol with better inhibitory potency than dicoumarol itself. The target compounds, based on the general structure shown in Figure 58, were derived from the precursor 4-hydroxycoumarin and its derivatives. It was intended that these compounds would be synthesized using techniques previously developed by the Whitehead group with modifications in some cases.

Following the syntheses, enzyme assays were to be carried out to determine their potency as NQO1 inhibitors. An ideal enzyme inhibitor, in the context of a potential therapeutic agent, would have high specificity and potency but would also have few side effects and low toxicity.

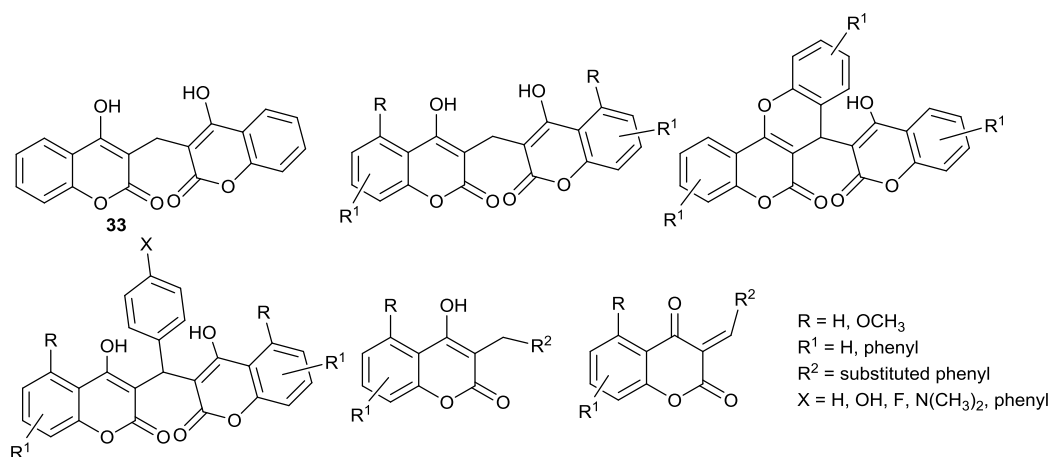


**Figure 58:** General structure of target compounds.

Conversely, there may be the possibility of drug barriers to the target site with all these inhibitors, therefore the target compounds were modified in order to overcome some of these barriers such as chemical instability and poor penetration which may lead to low toxicity to cancer cells (Figure 59).

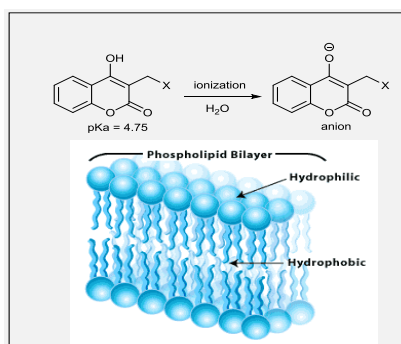


**Figure 59:** Ionization of the inhibitors leading to their inability to penetrate the cell membrane which contains a hydrophilic phospholipid layer.

Since the  $\pi$ GSTP1-1 enzyme, which uses GSH (**1**) as a cofactor, is over expressed in most solid tumors, coupling of these inhibitors with an analogue of antheminone A (**84a**) could produce compounds which will serve as prodrugs (example (**84b**) and (**84c**)) (Figure 60). These compounds could be activated by GSH in the presence of

GST which would result in release of the inhibitors of NQO1 as well as the cytotoxic exocyclic enone derived from (**84a**), thus leading to cell apoptosis.

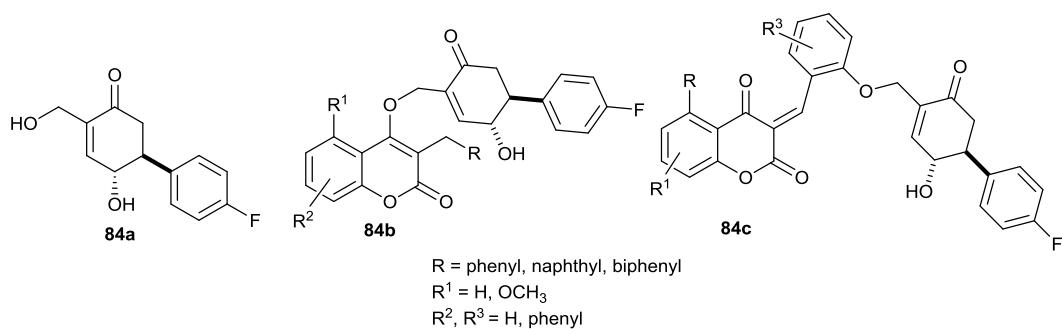


**Figure 60:** Structures of an analogue of antheminone A (**84a**), utilized for prodrug synthesis (**84b**) and (**84c**).

In order to determine cytotoxicity of these potential prodrugs, MTT assays were carried out in A549 cancer cell line which has a high level of NQO1 activity.

## 2.0 Chapter 2: Results and discussion

### 2.1 Introduction

Coumarins and flavonoids belong to a group of compounds known as benzopyrones, which consist of a benzene ring fused to a pyrone ring. The benzopyrones are further categorized into  $\alpha$ -benzopyrones (**85a**) and  $\gamma$ -benzopyrones (**85b**) (Figure 61). Coumarins substituted in the pyrone ring such as 4-hydroxycoumarin (**86**), 7-hydroxycoumarin (**87**) and their derivatives like warfarin belong to the family of  $\alpha$ -benzopyrones, whereas the flavonoids such as quercetin (**43**) belong to the  $\gamma$ -benzopyrones (Figure 62).

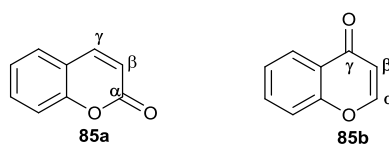


**Figure 61:** Structure of  $\alpha$ -benzopyrone (**85a**) and  $\gamma$ -benzopyrone (**85b**).

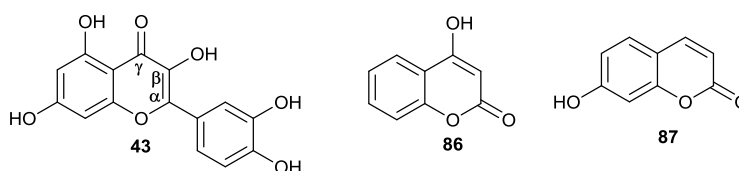


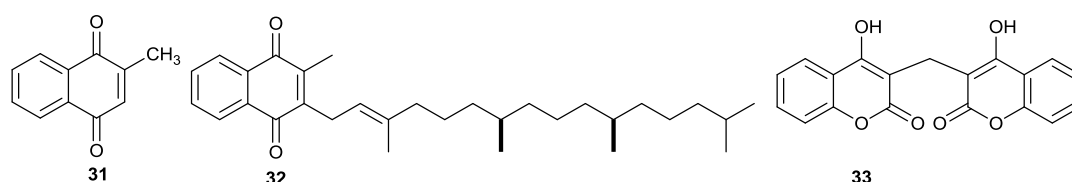
**Figure 62:** Structures of quercetin (**43**), 4-hydroxycoumarin (**86**) and 7-hydroxycoumarin (**87**).

Coumarins are of great importance to synthetic organic chemists due to their biological properties, such as anticoagulant,<sup>175</sup> antioxidant, antibacterial, antiviral<sup>176</sup> and anti-tumor activities.<sup>177</sup> They are consequently highly utilized as precursors for the syntheses of a variety of therapeutic agents. For example, research conducted by Weber and co-workers revealed that coumarin and some of its metabolites display anti-tumor properties towards many human cell lines.<sup>177</sup> Similarly, compounds derived from the benzopyrones have proven to be potent inhibitors of the proliferation of several carcinoma cell lines: for example, 4-hydroxycoumarin (**86**) and 7-hydroxycoumarin (**87**) inhibited cell growth in a gastric carcinoma cell line.<sup>178</sup>

In related research, Velasco-Velazquez reported<sup>179</sup> the *in vitro* effects of 4-hydroxycoumarin in murine melanoma cell lines (B16-F10) and non-malignant fibroblastic cell lines (B82). It was discovered that 4-hydroxycoumarin disordered the actin cytoskeleton of B16-F10 cells without any significant effect on the fibroblasts. 4-Hydroxycoumarin also serves as a useful precursor for the syntheses of

compounds that can be used as adjuvant therapy for melanoma and also for other cancer treatment.

Coumarin anticoagulants are also antagonists of Vitamin K (**32**), an enzyme cofactor essential for the biosynthesis of prothrombin factors vii, ix and x.<sup>180</sup> Overproduction of prothrombin causes excessive clotting of the blood (hypercoagulation) which can lead to deep vein thrombosis. Interestingly, vitamin K<sub>3</sub> (**31**), being an NQO1 co-substrate has a structural relationship with coumarin which makes it possible for dicoumarol (**33**) and its analogues to bind with NQO1.<sup>174</sup> In view of this, dicoumarol is often used to study the importance of the absence, or presence, of NQO1 activity in cells.



## 2.2 Previous synthesis

Three types of dicoumarol analogues have been reported in the literature<sup>181</sup> which can be described as unsymmetrical dimer (**88**), symmetrical dimer (**89**) and asymmetrical (**90**) as shown in Figure 63.

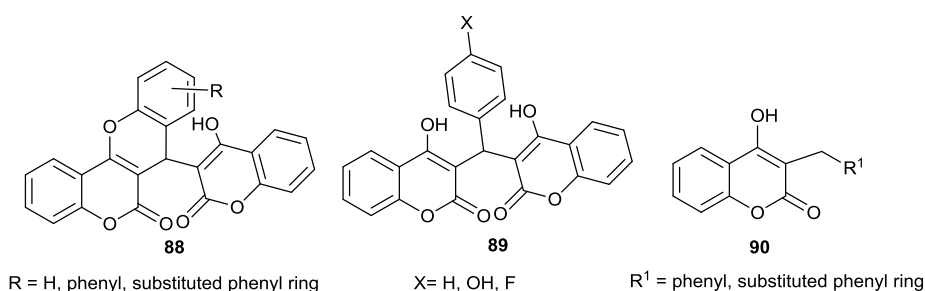
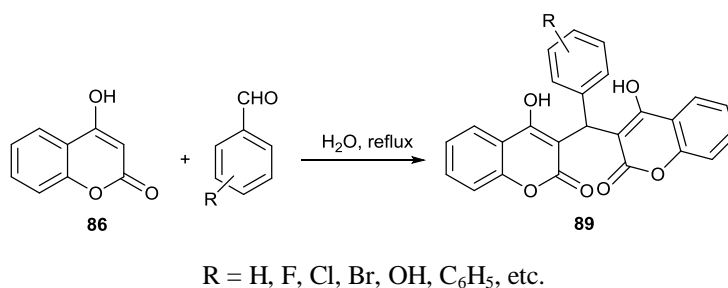


**Figure 63:** Structures of the analogues of dicoumarol.

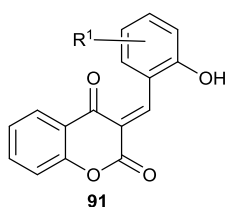
Over three decades ago, Sullivan<sup>182</sup> reported the syntheses of a variety of symmetrical dicoumarols by reacting 4-hydroxycoumarin with different aldehydes in ethanol as solvent. The products were obtained in mostly poor yields.

Zeba and co-workers<sup>183</sup> also reported the syntheses of symmetrical dimer (**89**) by coupling 4-hydroxycoumarin (**86**) with aromatic and heteroaromatic aldehydes, in a range of media, such as water, methanol, acetic acid, dichloromethane and acetonitrile (Scheme 16). The team observed that using less polar aprotic solvents such as DCM, resulted in low yields (< 30%) after a prolonged period of time (24 h). Performing the reaction in polar aprotic solvents, such as acetonitrile, gave only a trace of the products and in some cases no reaction was observed. The use of polar protic solvents such as methanol (85%) and acetic acid (65%) gave high yields under thermal conditions and there reactions took a relatively short time period (35-45 mins). The best yield however, was obtained (96%) using an aqueous medium and a very short reaction time (5 mins). The teams concluded, therefore, that for the syntheses of symmetrical analogues of dicoumarol, water was the optimal solvent from a ‘green chemistry’ point of view.



**Scheme 16:** Synthesis of symmetrical dimer using 5 mol% Zn(proline)<sub>2</sub>.

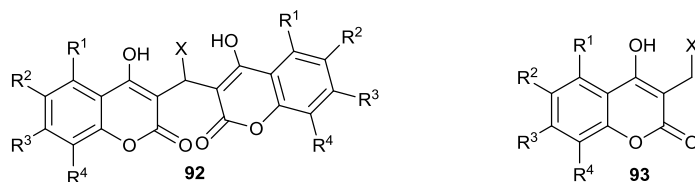
Manolov<sup>180</sup> and co-workers described the syntheses of dicoumarol analogues by reacting 4-hydroxycoumarin (**86**) with different substituted aromatic aldehydes under various conditions. Using 2 equivalents of coumarin and 1 equivalent of aromatic aldehyde gave the dimeric products in excellent yields (> 66%). In contrast, a 1:1 ratio of coumarin and aldehyde gave the “halfway stage” product (**91**) shown in Figure 64 in poor yields (18-39%).



R<sup>1</sup> = H, phenyl ring.

**Figure 64:** General structure of “halfway stage” (**91**) analogues of dicoumarol analogue.

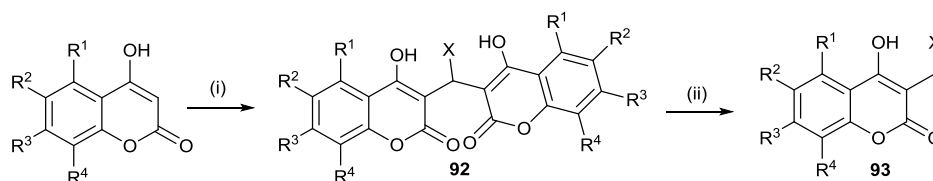
In 2009, members of the Whitehead research group conducted similar syntheses of symmetrical (**92**) and asymmetrical (**93**) analogues of dicoumarol (Figure 65) using simple aldol condensation reaction techniques.<sup>174</sup>



$R^1, R^2, R^3, R^4 = \text{H, alkyl, halo, alkoxy and phenyl ring; } X = 1\text{-naphthyl, 2-naphthyl, phenyl.}$

**Figure 65:** Structures of symmetrical (**92**) and asymmetrical (**93**) analogues of dicoumarol.

The syntheses of asymmetrical compounds (**93**) proceeded in two steps as depicted in Scheme 17. In the first step, dimers (**92**) were obtained by coupling 2 equivalents of coumarin and 1 equivalent of the appropriate aldehyde. The second step involved reductive cleavage of one of the bridging carbon-carbon bonds with sodium cyanoborohydride. Unfortunately, the asymmetrical analogues (**93**) were obtained in poor yields (<40%), although the investigators noted the improved solubility of these compounds compared with the members of the symmetrical series (**92**). Further investigations into the biological activities of the asymmetrical analogues, confirmed that several of them showed better inhibitory potency and lower toxicity values compared to dicoumarol (**33**).

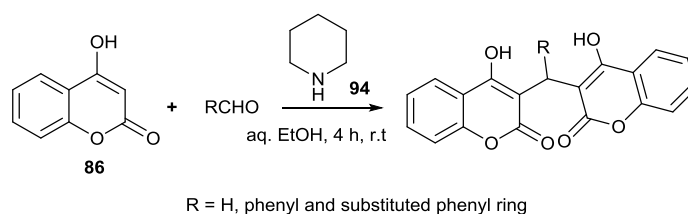


Reagents and conditions: (i) aromatic/aliphatic aldehydes, reflux, 24 h, 100°C; (ii)  $\text{NaCNBH}_3$ , methanol, reflux, 70°C, 20 h.

**Scheme 17:** Synthesis of symmetrical (**92**) and asymmetrical (**93**) analogues of dicoumarol.<sup>183</sup>

Anschutz<sup>184</sup> attempted condensation of 4-hydroxycoumarin with different aliphatic carbonyl compounds such as formaldehyde, acetaldehyde, propionaldehyde, butyraldehyde and acetone, however the latter three did not yield any product. The poor reactivity in these cases could be due to the electron donating ability of the alkyl groups giving rise to a less reactive electrophilic carbon.

Claudiu Supuran and co-workers reported the syntheses of analogues of dicoumarol by condensing various aromatic aldehydes with 4-hydroxycoumarin at room temperature in the presence of a catalytic amount of piperidine (**94**) as shown in Scheme 18. The products were obtained in excellent yields (74-96%).<sup>185</sup>



**Scheme 18:** Synthesis of dicoumarols using a catalytic amount of piperidine (**94**) in aqueous EtOH at room temperature.

## 2.3 New syntheses

In a search for new inhibitors of the enzyme NQO1 with biological activities comparable to that of dicoumarol, but with lower toxicity and fewer side effects, a range of symmetrical, asymmetrical and “halfway” stage analogues of dicoumarol were synthesized (Figure 66). These compounds were prepared using the sequence described by the Whitehead group. Their structural identities were confirmed using IR, NMR spectroscopy and mass spectrometry.

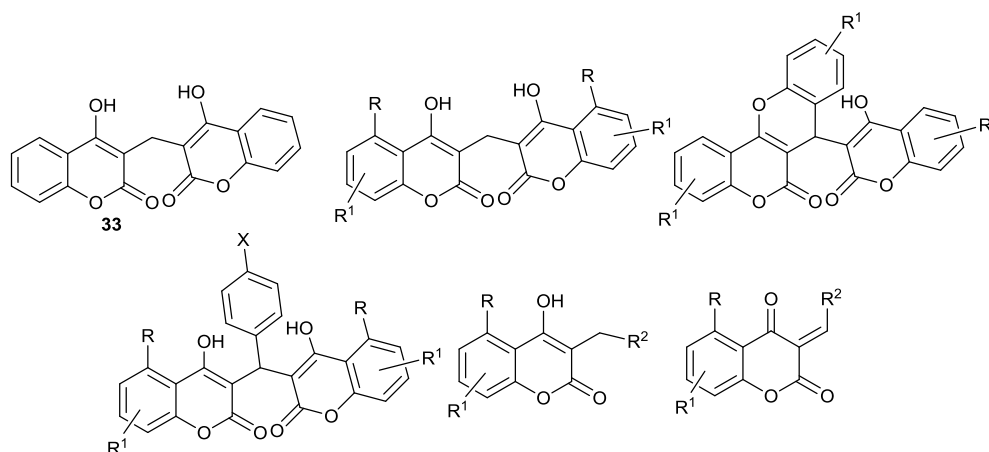


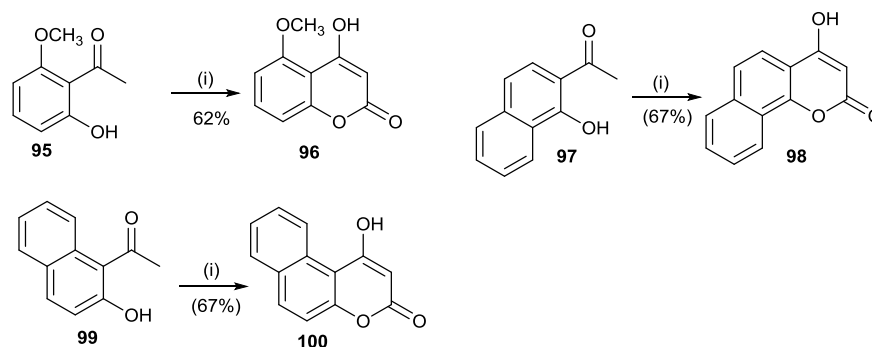
**Figure 66:** General structure of target compounds.

### 2.3.1 Synthesis of 4-hydroxycoumarin derivatives

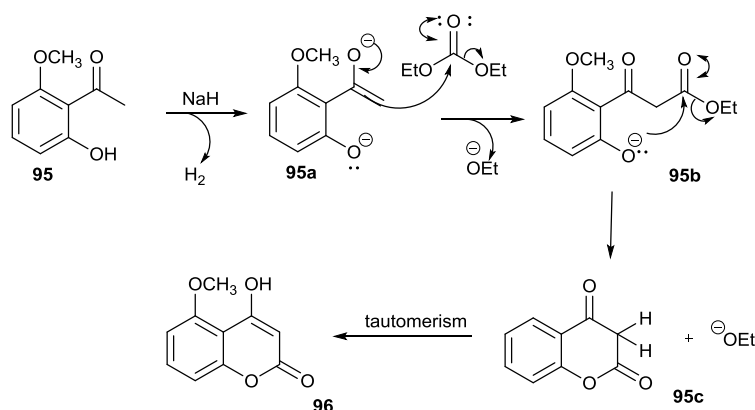
The 4-hydroxycoumarin derivatives which served as precursors for the target compounds were synthesized by reacting the appropriate acetophenone (**95**), (**97**) and



(**99**) with diethyl carbonate in the presence of sodium hydride (NaH) as illustrated in Scheme 19. A plausible mechanism for the reaction is depicted in Scheme 20.



**Scheme 19:** Reaction scheme for the syntheses of derivatives of 4-hydroxycoumarin (**96**, **98** and **100**). Reagents and conditions: (i) diethylcarbonate, sodium hydride, at reflux, 3h.



**Scheme 20:** Base-mediated cyclisation reaction of 2-hydroxy-6-methoxy acetophenone (**95**) to give (**96**). The mechanism is applicable to compounds (**98**) and (**100**).

In this reaction, the ‘hydride’ ion from sodium hydride abstracts the  $\alpha$ -hydrogen, of the acetophenone (**95**) to give the enolate anion (**95a**). The second step involves the nucleophilic attack of (**95a**) on the electrophilic carbon of the carbonyl of diethyl carbonate to form an intermediate  $\beta$ -keto ester (**95b**). The intermediate (**95b**) undergoes cyclisation *via* addition and elimination of ethoxide to give (**95c**) which undergoes rapid keto-enol tautomerisation to give (**96**). The structural identities of all the cyclized products were confirmed by <sup>1</sup>H NMR spectroscopy which indicated the presence of only one product. The <sup>1</sup>H NMR spectrum of compound (**96**), shown in Figure 67, is identical to the data reported by Carberry and co-workers.<sup>186</sup>

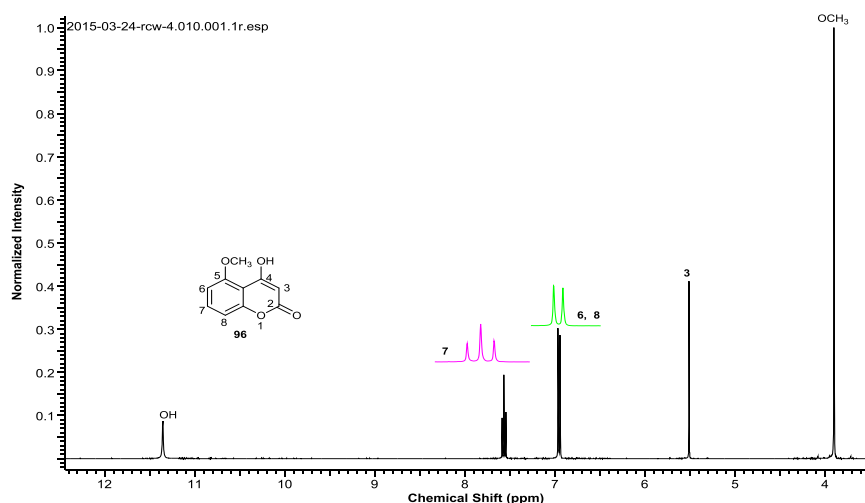
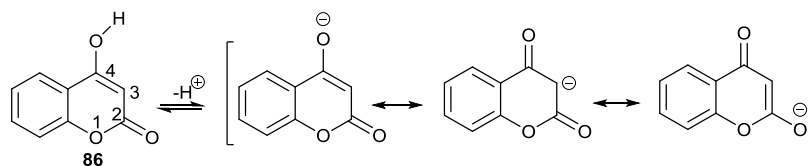


**Figure 67:**  $^1\text{H}$  NMR spectrum of compound (**96**) in  $\text{DMSO-d}_6$ ; 3, 6, 7 and 8 represent protons and their multiplicity.

The infra-red absorption spectra of (**96**), (**98**) and (**100**) in the solid state resembled that of a carboxylic acid with a broad O-H stretch between  $3200\text{--}3400\text{ cm}^{-1}$  and a  $\text{C=O}$  stretching frequency between  $1650\text{--}1700\text{ cm}^{-1}$ . The presence of a vinylogous carboxylic acid makes these compounds moderately strong acids.

### 2.3.2 Synthesis of symmetrical analogues of dicoumarol

The C-3 position of 4-hydroxycoumarin (**86**) and its derivatives, as depicted in Scheme 21, is reactive as a nucleophile as it is the central carbon atom of an enolic 1,3-dicarbonyl compound and it is this feature that facilitates the synthesis of symmetrical analogues of dicoumarol with general structure shown in Figure 68.



**Scheme 21:** Resonance forms of ionized 4-hydroxycoumarin.

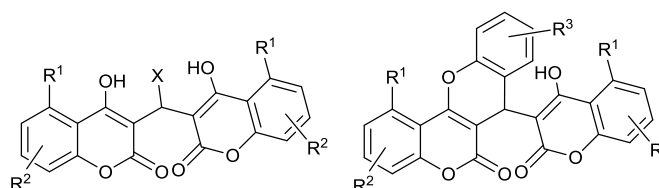
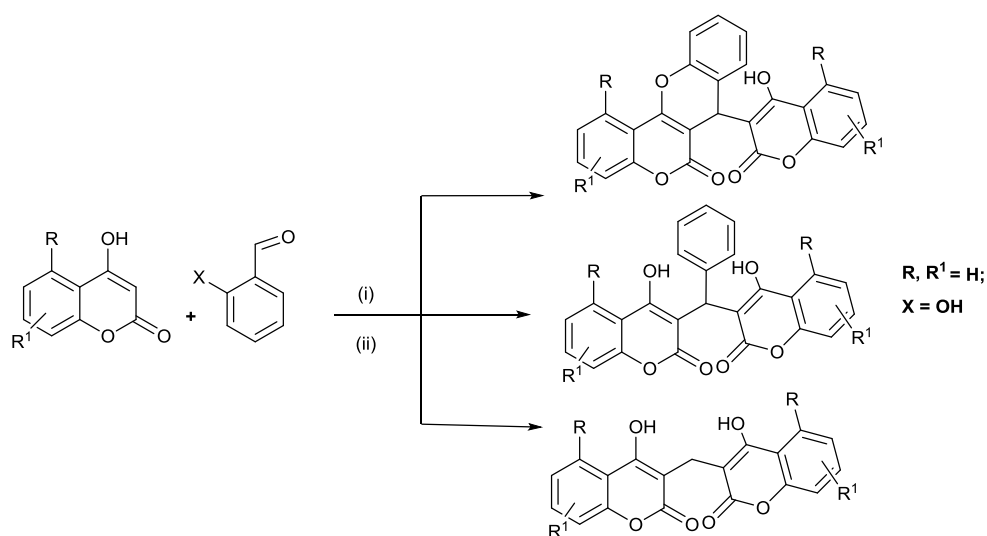


**Figure 68:** General structure of synthesized symmetric and asymmetrical dimer.

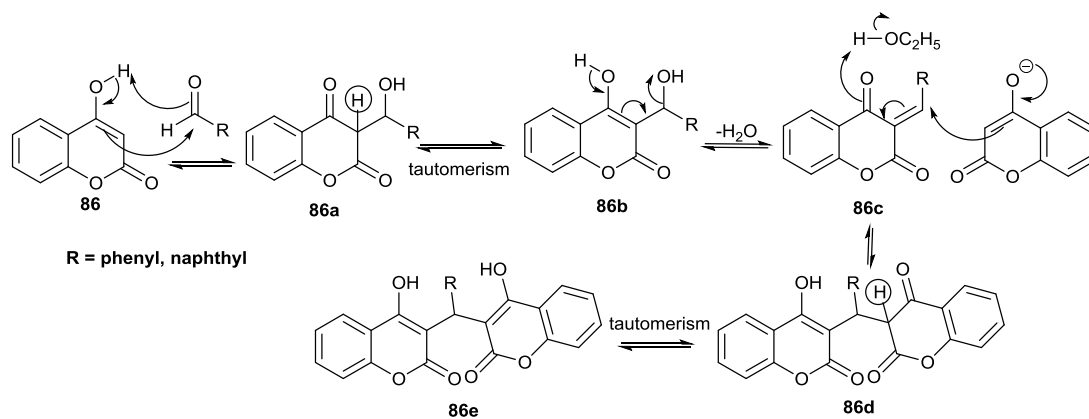
Dicoumarol and its analogues were synthesized using both thermal and microwave conditions from the reaction between an appropriate 4-hydroxycoumarin (2 equivalents) and substituted benzaldehyde (1 equivalent) as depicted in Scheme 22. The products were obtained in excellent yields (>70%). The use of microwave irradiation offers a lot of advantages over thermal heating. The concept of green chemistry is gaining momentum in the field of organic synthesis and microwave irradiation is an eco-friendly technique with advantages of improved yields, easy workup, considerably shortened reaction times, and minimum solvent usage and often without the usage of catalysts.



Reagents and conditions: (i) Thermal heating; coumarin 2 eq, aldehyde 1eq, ethanol, reflux at 85 °C, 24 hr. (ii) Microwave irradiation; coumarin 2 eq, aldehyde 1eq, ethanol, 85 °C, 10 mins.

**Scheme 22:** Synthesis of analogues of dicoumarol.

In contrast, reactions performed under thermal conditions, gave generally poor yields and in some cases no trace of product was observed after a short time compared to microwave conditions which gave >50% yield in under 10 minutes. The microwave technique therefore afforded a green chemistry protocol for the synthesis of dicoumarol and its analogues. A plausible mechanism for this reaction is shown in Scheme 23.



**Scheme 23:** General mechanism for condensation and dimerization reaction.

The first step involves the nucleophilic addition of 4-hydroxycoumarin (**86**) to the polarized carbonyl bond of the aldehyde to form aldol adduct (**86a**), followed by tautomerism to give (**86b**).  $\alpha,\beta$ -Unsaturated carbonyl compound (**86c**) is then formed by loss of water. The next step is the nucleophilic conjugate addition of a second molecule of 4-hydroxycoumarin to (**86c**) to form (**86d**) which subsequently undergoes keto-enol tautomerisation to give (**86e**).

### 2.3.2.1 Non planarity of symmetrical analogues of dicoumarol.

The two hydroxyl groups in the compounds with general structure shown in Figure 69 gave different chemical shifts (11.32 and 11.55ppm) with  $\text{CDCl}_3$  as the solvent.

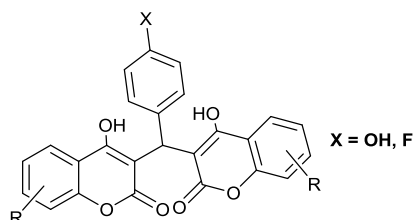


**Figure 69:** General structure of compounds with substituent (X) at *para*-position.

This difference was not noticed when  $\text{DMSO-d}_6$  was used as the solvent and this may be due to the interaction of the hydroxyl groups and the solvent. In order to confirm the assignment of the signals, a few drops of  $\text{D}_2\text{O}$  were added into the  $^1\text{H}$  NMR sample of (**101**) and the spectrum (Figure 70, B) revealed their disappearance which indicates that the two hydroxyl groups exist in different environments.

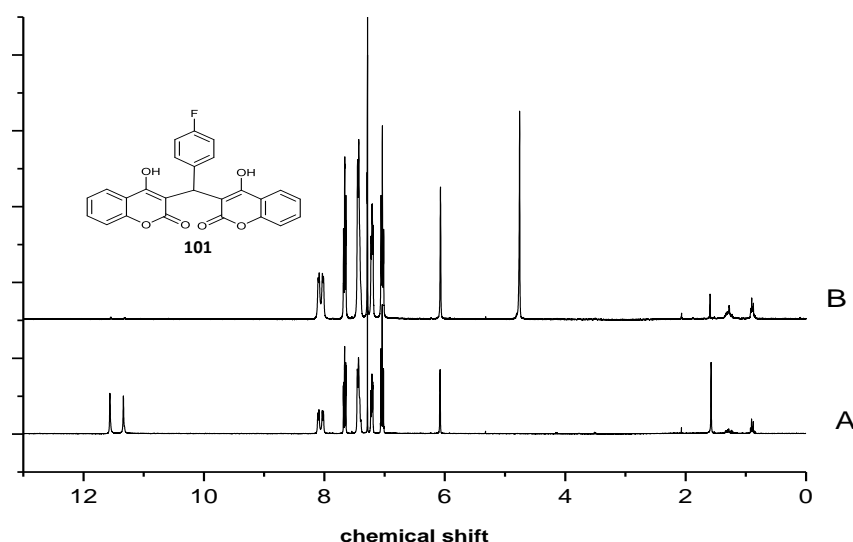


**Figure 70:**  $^1\text{H}$  NMR spectra of compound (**101**); ‘A’ represent  $^1\text{H}$  NMR spectrum of compound (**101**) in  $\text{CDCl}_3$  and ‘B’ is the  $^1\text{H}$  NMR spectrum after addition of  $\text{D}_2\text{O}$ .

In 1985, Godfroid and co-workers reported that dicoumarols substituted at the bridge methylene carbon (C5) displayed restricted rotation around the  $\text{C3C5}$  and  $\text{C3'C5'}$  as shown in Figure 71.<sup>187</sup>

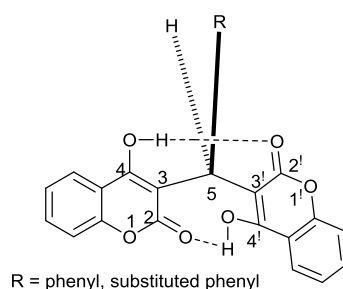


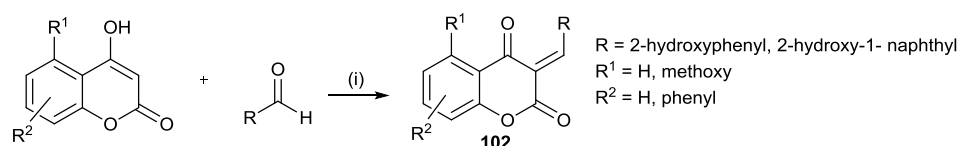
**Figure 71:** Structure of substituted dicoumarols at the methylene bridge.<sup>187</sup>

The team further explained that the hinderance to free rotation could be as a result of the following factors based on the calculated free activation energies at 37 °C:

- The barrier to rotation increased with increasing steric influence of the substituent (R)
- Intramolecular bonds also may exist between the two hydroxyl groups
- Increasing electron donating effect of the solvent can lower the barrier *via* the formation of intermolecular bonds between the hydroxyl groups and the solvent.

## 2.4 Synthesis of the “halfway stage” analogues of dicoumarol

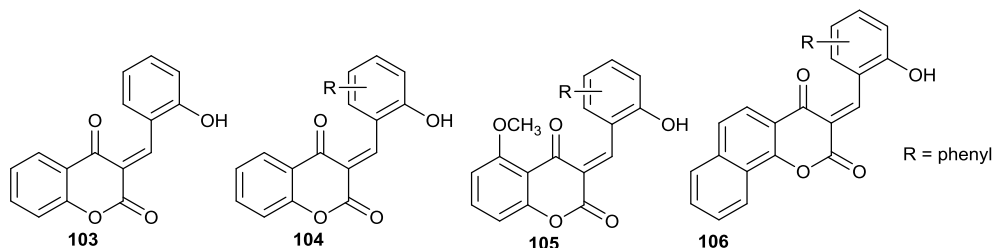
In continuation of the group’s ongoing efforts to prepare compounds with better inhibitory potency than dicoumarol, the synthesis of “halfway stage” analogues of dicoumarol (**102**) was carried out. The reactions were performed by reacting 1 equivalent of an appropriate 4-hydroxycoumarin and 1 equivalent of 2-hydroxyl benzaldehyde and 2-hydroxy-1-naphthaldehyde, using both thermal and microwave conditions as shown in Scheme 24.



Reaction conditions: (i) EtOH, reflux 80 °C, 45 mins.

**Scheme 24:** General method for the preparation of the “halfway stage” analogues (**102**) of dicoumarol.

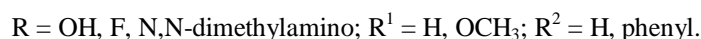
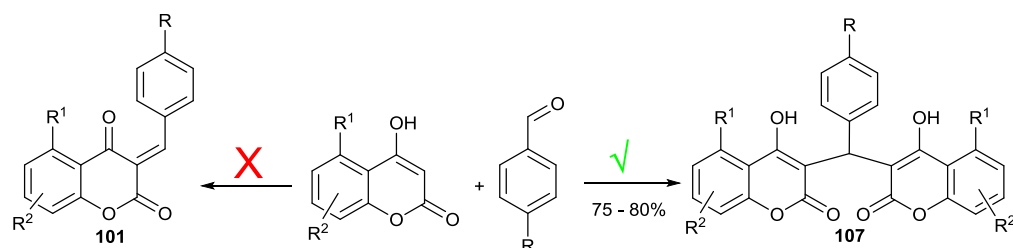
Generally, poor yields were obtained under both sets of conditions which is believed to be due to competitive dimer formation as illustrated in Table 4. This was more problematic under microwave than thermal conditions because heat transfer is faster compared to thermal conditions.



Compound	Conditions	Time (mins)	Temp (°C)	Yield (%)
<b>103</b>	(i) Microwave	30	80	20
	(ii) Thermal heating	45	80	28
<b>104</b>	(i) Microwave	30	80	31
	(ii) Thermal heating	45	80	41
<b>105</b>	(i) Microwave	30	80	28
	(ii) Thermal heating	45	80	33
<b>106</b>	(i) Microwave	30	80	26
	(ii) Thermal heating	45	80	34

**Table 4:** Comparison between the percentage yields obtained using microwave irradiation and thermal under reflux.

The reaction of 4-fluoro, 4-hydroxy and 4-dimethylamino benzaldehydes with 4-hydroxycoumarin in a 1:1 ratio, gave only the corresponding dimer (**107**) as depicted in Scheme 25. The reason for this is not understood.



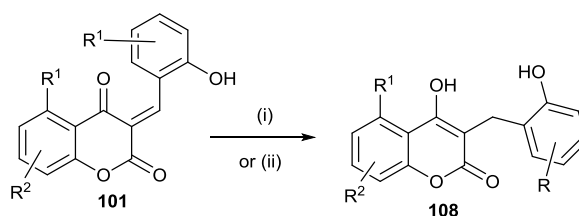
**Scheme 25:** Synthesis of “half-way stage” analogues (**101**) of dicoumarol using *para*-substituted aromatic aldehydes gave dimeric products (**107**) instead of (**101**).

#### 2.4.1 Reduction of the “halfway stage” analogues of dicoumarol

Some of the most synthetically important reducing agents are hydrides derived from aluminium and boron. As group three elements with six bonding electrons and an empty orbital, they can accept nucleophiles such as hydride ( $\text{H}^-$ ) to become stable tetravalent anion ( $\text{AlH}_4^-$  or  $\text{BH}_4^-$ ).  $\text{BH}_4^-$  reagents were used for the reduction of the “halfway stage” analogues (**101**) of dicoumarol.

$\text{BH}_4^-$  reagents were preferred due to the high reactivity of  $\text{LiAlH}_4$  which reacts violently with protic solvents such as methanol, ethanol and water.  $\text{LiBH}_4$  and  $\text{NaBH}_4$  are much milder than  $\text{LiAlH}_4$  and are commonly used in chemoselective reduction of aldehydes and ketones in the presence of esters. Although, esters can be reduced with  $\text{NaBH}_4$  this occurs at a much lower rate due to their natural electrophilicity.

Six equivalents of sodium borohydride were added to a solution of the “halfway stage” analogues (**101**) in methanol as solvent. In order to achieve complete conversion, the reactions were left to stir overnight and this gave compounds (**108**) in moderate yields (40-55%) as shown in Scheme 26.

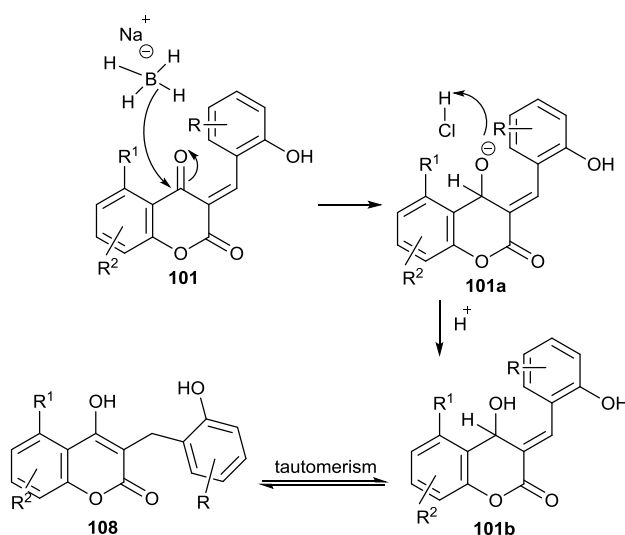


R, R<sup>2</sup> = H, phenyl ring; R<sup>1</sup> = H, OCH<sub>3</sub>

Reagents and conditions: (i) NaBH<sub>4</sub>/methanol, r.t., 24 h; (ii) LiBH<sub>4</sub>/THF, r.t., 24 h.

**Scheme 26:** Reduction of “halfway stage” analogues (**101**) to asymmetrical analogues (**108**) using NaBH<sub>4</sub>/LiBH<sub>4</sub>.

A possible mechanism for this reaction is depicted in Scheme 27. The first step involves nucleophilic attack of the hydride ion (H<sup>-</sup>) to the electrophilic carbon of the carbonyl group which gives an intermediate alkoxide anion (**101a**). In the workup step, the anion (**101a**) is protonated to give (**101b**) followed by rapid tautomerization to the final product (**108**). The overall reaction as depicted therefore, is a 1,2-addition reaction followed by tautomerism.



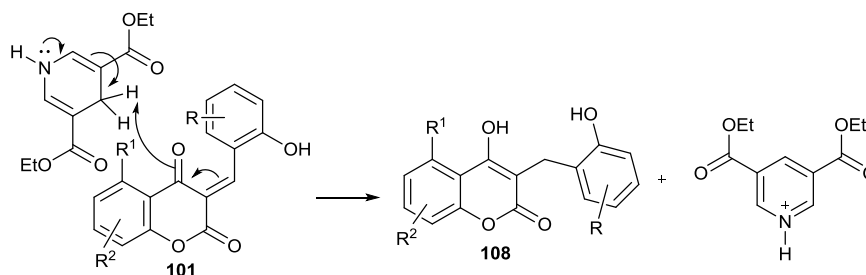
**Scheme 27:** Mechanism of reduction of “halfway stage” analogues of dicoumarol (**101**) with NaBH<sub>4</sub>/LiBH<sub>4</sub>.

#### 2.4.2 Reduction of “halfway stage” analogues of dicoumarol using Hantzsch’s ester

NQO1 enzyme detoxifies its substrates through hydrogen transfer using NADH/NADPH as electron donor. Similarly, a biomimetic approach involving the use of Hantzsch’s ester (**109**), an analogue of NADH was utilized for the reduction of the “halfway stage” analogues of dicoumarol (**101**). The successful reduction of

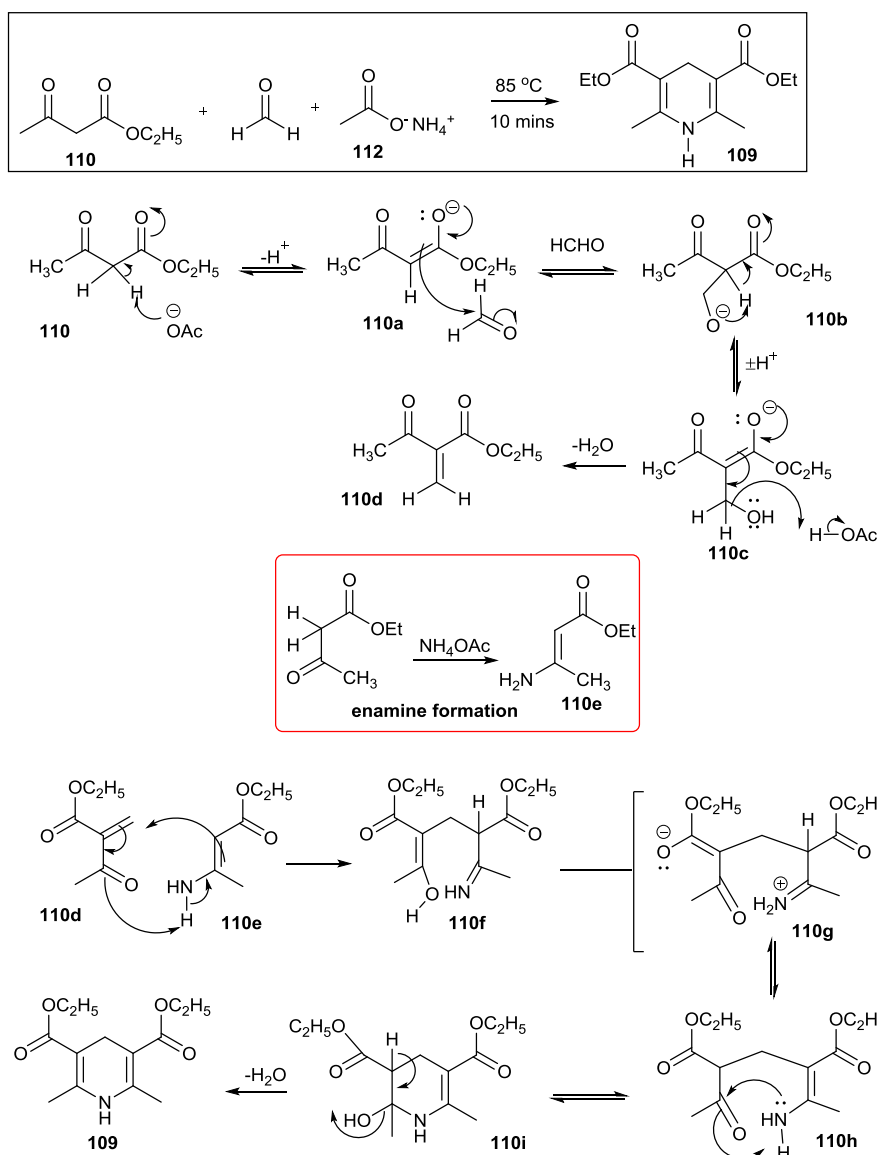


(**101**) with Hantzsch's ester (**109**) as depicted in Scheme 28, was an indication that the “halfway stage” analogues of dicoumarol (**101**) would undergo reduction by NQO1.



**Scheme 28:** Mechanism of the reduction of “halfway stage” (**101**) using Hantzsch's ester.

Hantzsch's ester (**109**), which have been utilized for efficient transfer hydrogenation of C=C, C=N and C=O bonds,<sup>188,189</sup> was first discovered in 1882 by Arthur Hantzsch.<sup>190,191</sup> The compound was synthesized by the reaction of ethyl acetoacetate (**110**), formaldehyde (**111**) and ammonium acetate (**112**) in a solvent-free single step reaction at 85 °C for 10 minutes as shown in Scheme 29.



**Scheme 29:** Mechanism of Hantzsch's ester synthesis.

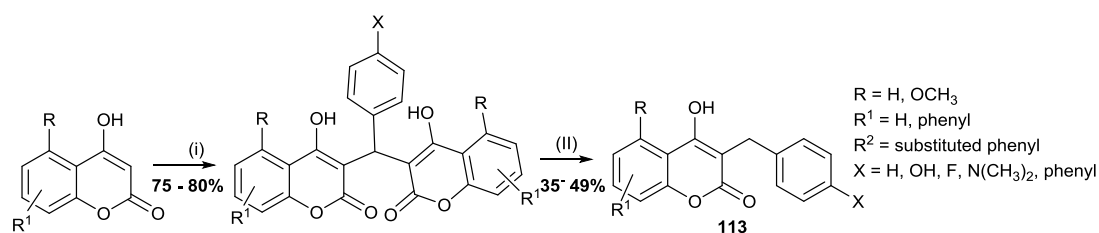
In this sequence, the most acidic proton ( $\alpha$ -proton) of the ethyl acetoacetate (**110**) is abstracted by acetate to form the intermediate enolate anion (**110a**). The enolate anion attacks the electrophilic carbonyl carbon of formaldehyde *via* an aldol condensation reaction to form intermediate (**110b**). This intermediate (**110b**) undergoes proton transfer to form (**110c**) which subsequently undergoes elimination of water to give (**110d**).

In the second step, the second molecule of ethyl acetoacetate undergoes enamine formation to give ethyl (*E*)-3-aminobut-2-enoate (**110e**) which then reacts with (**110d**) *via* Michael addition to enone to give (**110f**). Compound (**110f**) undergoes multiple

proton transfers to generate an intermediate (**110h**) followed by internal cyclisation and elimination of water to give the final product, Hantzsch's ester (**109**).

## 2.5 Reductive cleavage of C-C bond of symmetrical analogues of dicoumarol using $\text{NaBH}_3\text{CN}$

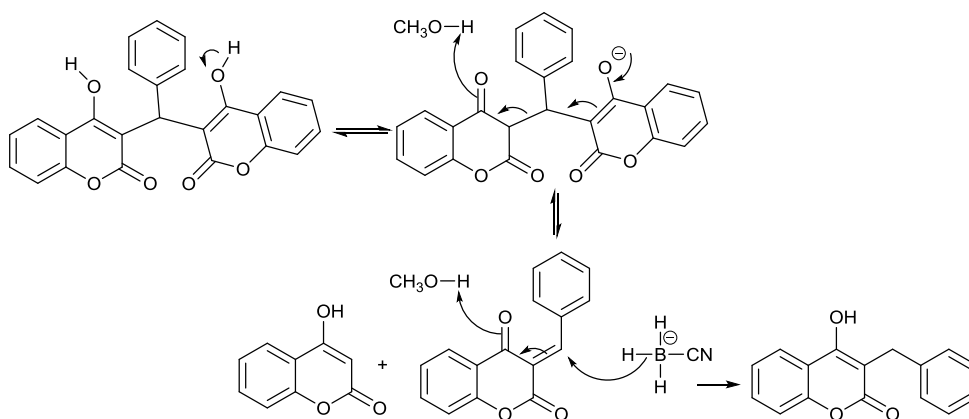
Asymmetrical analogues of dicoumarol with the general structure (**113**) were synthesized using the procedures previously adopted by the Whitehead research group.<sup>174</sup> This involved a two-step process which was initially reported in the literature by Appendino and co-workers and is illustrated in Scheme 30.<sup>192</sup>



Reagents and conditions: (i) 2 equivalents of hydroxycoumarin, 1 equivalent of aldehyde, 80 °C, 24 h.  
(ii) methanol,  $\text{NaBH}_3\text{CN}$ , 70 °C, 20 h.

**Scheme 30:** Synthesis of asymmetrical analogues of dicoumarol *via* C-C reductive cleavage.

This approach provides a strategy which allows ready access to asymmetrical analogues of dicoumarol (**113**) through a reaction sequence involving initial aldol condensation followed by 1,4-addition reaction. The symmetrical compounds which were previously synthesized according to (Scheme 18) were transformed into asymmetrical compounds with regeneration of 1 mole of 4-hydroxycoumarin by C-C cleavage using sodium cyanoborohydride. The crude products obtained were purified by flash column chromatography on silica gel using a solvent system of ethyl acetate and petroleum ether. Excess 4-hydroxycoumarin was removed by washing with saturated aqueous sodium bicarbonate solution. A plausible reaction mechanism for this reaction is shown in Scheme 31.



**Scheme 31:** Proposed mechanism for reductive C-C cleavage of symmetrical analogue of dicoumarol using  $\text{NaBH}_3\text{CN}$ .

Due to the presence of enolic hydroxyl groups dicoumarols can exist in different tautomeric forms as shown in Figure 72. The reductive fragmentation reaction however, can occur *via* either a monoprotonated (**114a**) or monodeprotonated (**114b**) semi-keto tautomer of the dicoumarol as illustrated in Figure 73.

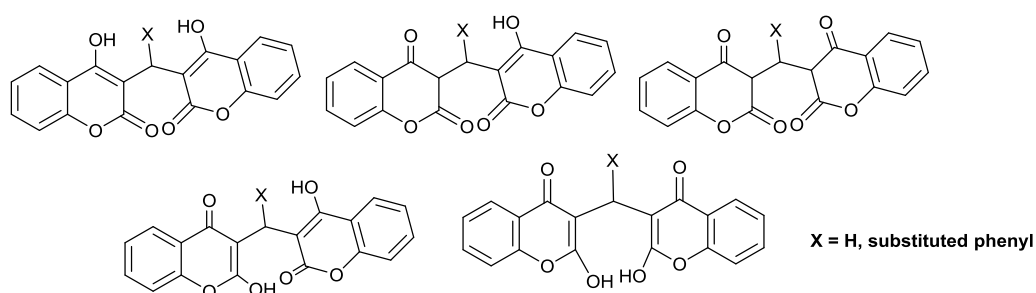


**Figure 72:** Different tautomers of dicoumarol and its analogues.<sup>193</sup>

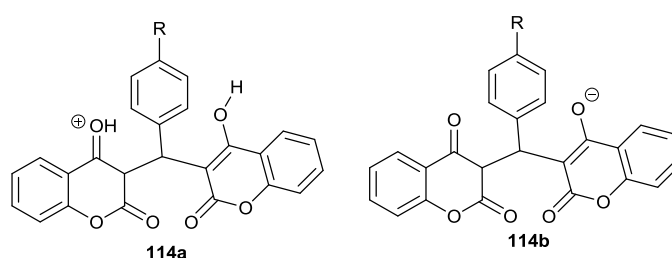


**Figure 73:** Dicoumarol analogue in a monoprotonated form (**114a**) (acid catalysis) and monodeprotonated form (**114b**) (base catalysis).<sup>194</sup>

In view of this, performing the reaction in the presence of strongly basic reducing agent like lithium aluminium hydride ( $\text{LiAlH}_4$ ) may lead to the formation of

dienolates (**114c**) as shown in Figure 74, and this will prevent the *retro*-Michael reaction from occurring.<sup>194</sup>

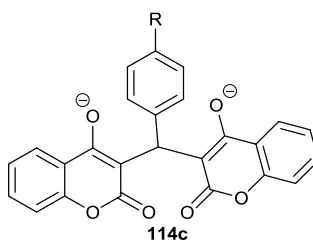


**Figure 74:** Structure of dienolates (deprotonated anions of enols, **114c**).

The reductive C-C bond cleavage with sodium cyanoborohydride suffered some limitations and, even though the desired product was obtained, the yield was very poor (< 35%). Furthermore, apart from a prolonged reaction time (18 hours), the procedure is atom uneconomical. For example, for every molecule of the desired product obtained, one molecule of 4-hydroxycoumarin was generated as a by-product. Lastly, the use of sodium cyanoborohydride is not environmentally friendly as it may liberate toxic hydrogen cyanide gas - as a result reactions were performed in a well ventilated fumehood.

## 2.6 Borrowing hydrogen methodology

The metal-catalyzed auto-transfer of hydrogen, otherwise known as ‘borrowing hydrogen methodology’, is a powerful tool for functional group interconversion. Following the discovery made by Grigg and co-workers,<sup>195</sup> who used alcohols as alkylating reagents, borrowing hydrogen methodology has emerged as a useful strategy in organic synthesis. The method has, to a significant extent, replaced traditional couplings and reductive aminations for the formation of C-C and C-N bonds respectively.<sup>196</sup>

Environmental regulation has emphasized the importance of using techniques involving high selectivity, high atom economy, excellent yields and that are environment friendly in organic synthesis.<sup>197,198</sup> This has led to intensive investigations into the development of new synthetic methods for the formation of C-C and C-N bonds. One of the most promising strategies is the direct metal-catalysed alkylation of esters, ketones, aldehydes and imines with alcohols.

The indirect functionalization of alcohols using catalytic amounts of metal complex and base, which produces only water as a by-product, is eco-friendly in contrast to standard C-C and C-N forming reactions. The reaction can be achieved using different metal catalysts such as ruthenium, rhodium, copper, iron and iridium complexes, where the iridium complex  $[\text{Cp}^*\text{IrCl}_2]_2$  (**115**), in particular, has been considered as the most effective (Figure 75).<sup>199,200</sup>

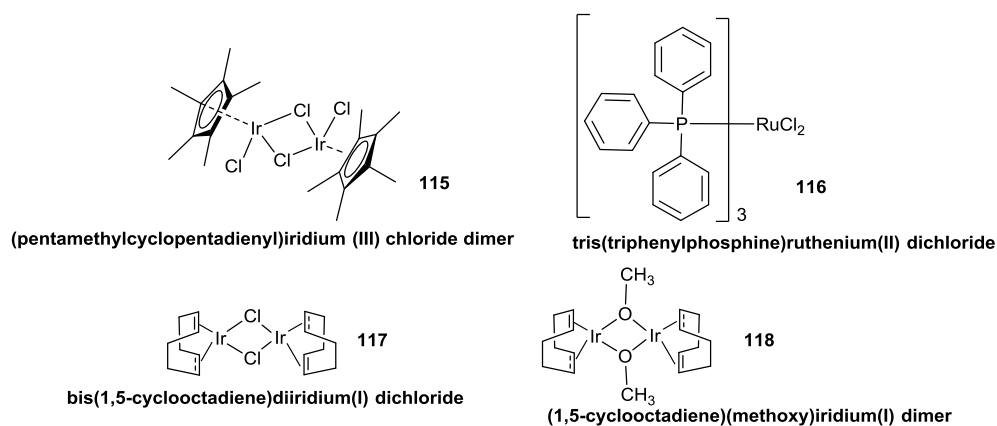
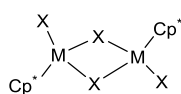


**Figure 75:** Catalysts used in "borrowing hydrogen" reaction.

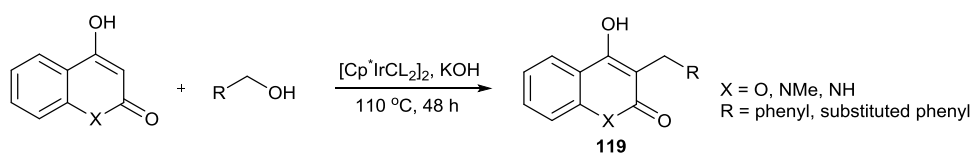
Early pioneering work by Maitlis and co-workers<sup>201</sup> demonstrated the catalytic potential of a series of halogen bridged dimers (Figure 76) in alkylation reactions. Fujii and his group<sup>202</sup> also reported the application of  $\text{Cp}^*\text{Ir}$  complex in *N*-heterocyclisation of primary amines with diols. In this synthesis a variety of five-, six-, and seven-membered cyclic amines were obtained in good to excellent yields.



X= Cl, I or Br; M= Ir, Rh, Ru.

**Figure 76:** halide bridge dimer used in metal catalysed borrowing hydrogen methodology.

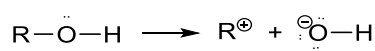
In 2009, Grigg and co-workers synthesized a range of asymmetrical analogues of dicoumarol (**119**) from the reaction between either 4-hydroxycoumarin or 4-hydroxy quinoline with several benzyl alcohols using a transition metal catalyst (Scheme 32).<sup>203</sup>



**Scheme 32:** General procedure for the synthesis of asymmetrical analogues of dicoumarol (**119**) derived from 4-hydroxycoumarin or 4-hydroxyquinoline.

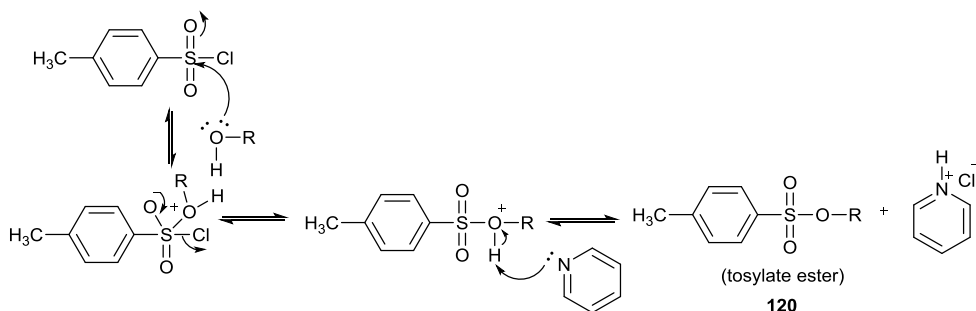
The products were mostly obtained in good to excellent yields (59-94%), except in some cases where halogenated aromatic alcohols (such as bromophenyl and chlorophenyl) were used, which gave lower yields (11-19%). The low yields were attributed to the electron withdrawing nature of the halogens and competitive dimer formation obtained *via* a Michael addition pathway.

Alcohols are generally poor electrophiles in dissociative alkylation reactions as their ionization is almost impossible because  $R^+$  is a high energy intermediate as depicted in Scheme 33. The activation of the 'OH' into a suitable leaving group is therefore required to enable nucleophilic substitution reactions to occur.

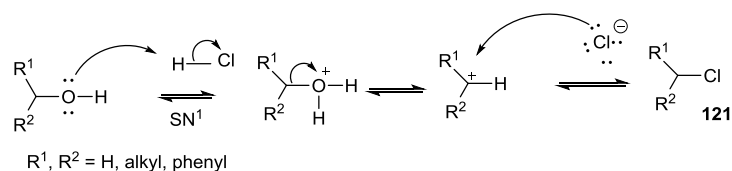


**Scheme 33:** ionization of an alcohol producing high energy charged intermediate ( $R^{(+)}$ ).

Previously, the activation of alcohol molecules has been accomplished by protonating the alcohol or converting it into a sulfonate ester (one of the most common being a tosylate ester **120**) or halide (**121**) as depicted in Schemes 34 and 35 respectively. Sulfonate and halide anions are both good leaving groups. These methods of alcohol activation have some limitations: apart from poor economy, protonation can deactivate the incoming nucleophile and the alkyl halides and alkylsulfonates that are generated as intermediates can also be mutagenic.<sup>204</sup>



**Scheme 34:** Mechanism of tosylate ester (**120**) formation.



**Scheme 35:** Mechanism of halide (**121**) formation.

Borrowing hydrogen methodology was therefore developed, as it provides a potential green pathway for the alkylation of alcohols using a metal catalyst. Through this reaction, the dimeric iridium catalyst ( $[\text{Cp}^*\text{IrCl}_2]_2$ ) (**122**), which is an 18 electron complex, undergoes activation by caesium carbonate. This results in the formation of an iridium-carbonate complex (**123**), a monomeric 16 electron complex, as illustrated in Figure 77. This occurs in order to allow coordination of the substrate alcohol.

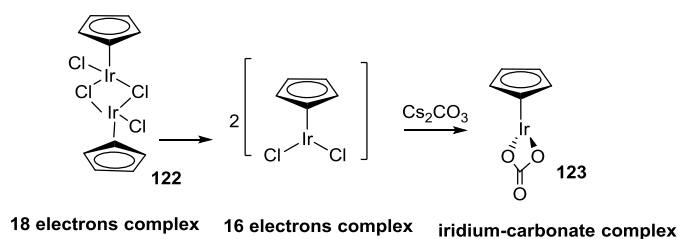
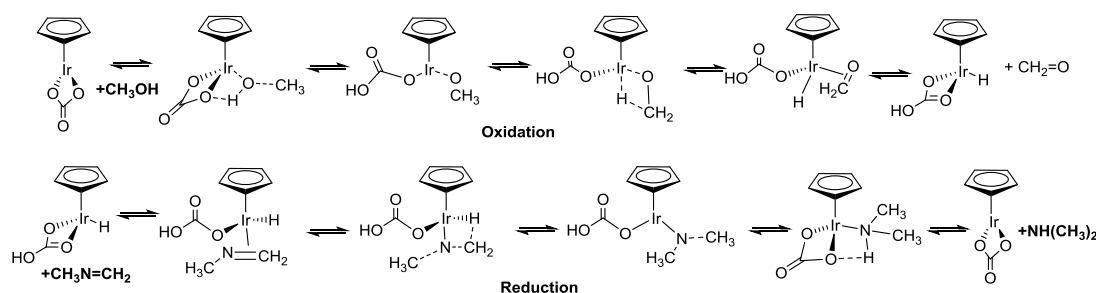


**Figure 77:** Dimer-monomer equilibrium.

The catalytic cycle occurs *via* three sequential stages: alcohol oxidation, double bond formation and reduction. The mechanistic pathway for the oxidation and reduction, as described by Eisenstein and co-workers for amine formation, is depicted in Scheme 36.<sup>205</sup>



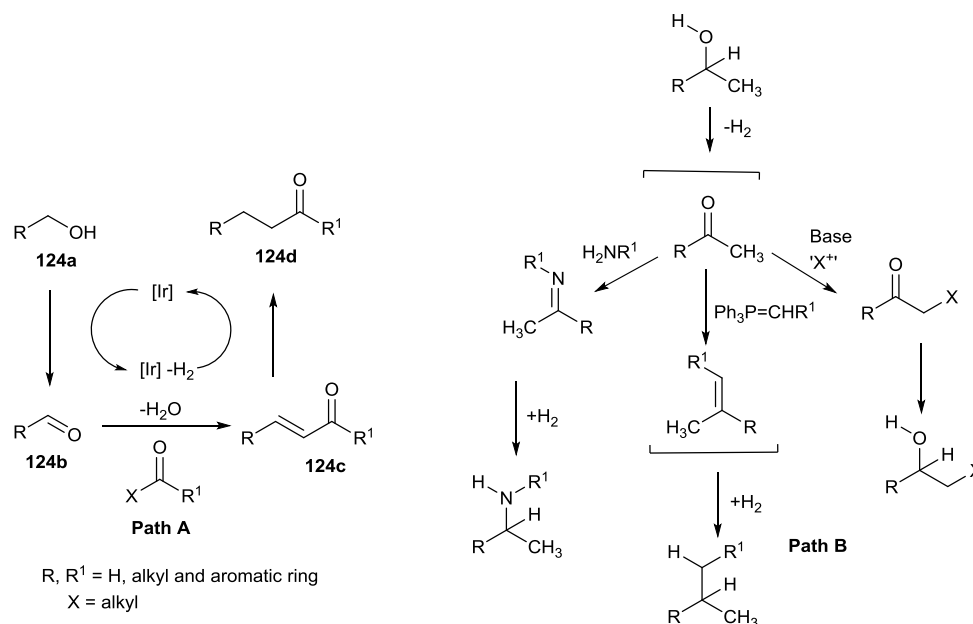
**Scheme 36:** The mechanistic sequence of alcohol oxidation and reduction by iridium-carbonate complexes (adapted from Eisenstein and co-workers).<sup>205</sup>

In the case of C-C bond formation, the metal catalyst alters the reactivity of the alcohol (**124a**) by removing two hydrogen atoms in a formal oxidation reaction as



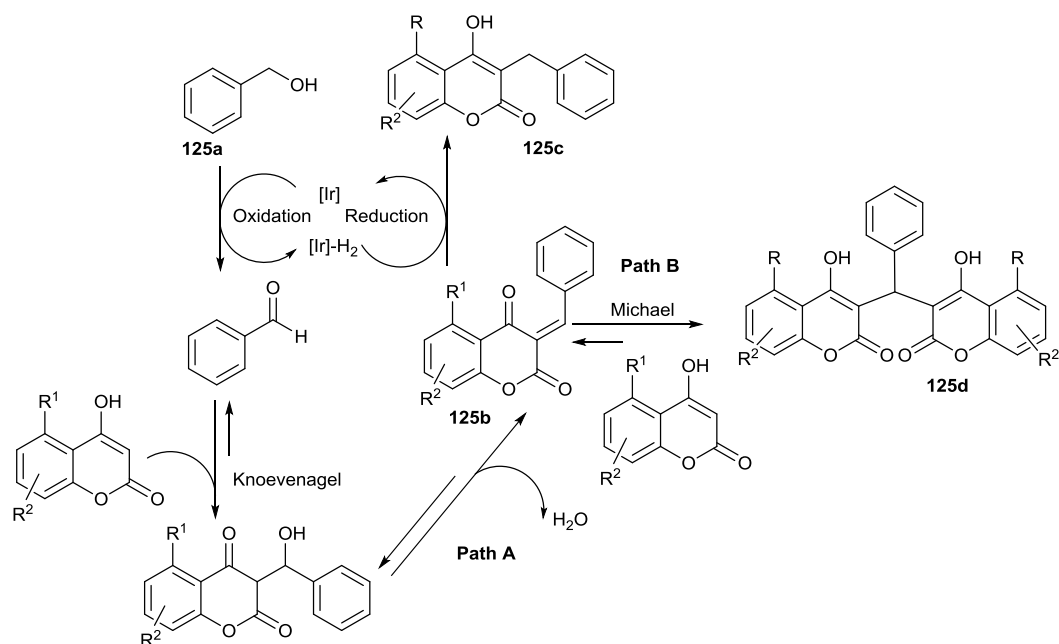
shown in Scheme 37, path A. This temporarily generates a reactive carbonyl compound (aldehyde or ketone **124b**), which permits bond formation to occur. The carbonyl undergoes aldol condensation reaction with a suitable substrate to form an  $\alpha,\beta$ -unsaturated intermediate (**124c**). In the final step, the  $\alpha,\beta$ -unsaturated intermediate is reduced with the return of two hydrogen atoms from the catalyst to the double bond giving an alkylated product (**124d**) without a net change in the overall oxidation state.<sup>206</sup>

In order to overcome the potential problem of residual unreacted alkene, isopropanol is added which acts as a hydrogen donor to replace any loss of hydrogen. Reactions are performed at a higher temperature for complete conversion. Alkylations of alcohols using borrowing hydrogen methodology have been achieved using ketones, nitriles and nitroalkanes as carbon nucleophiles.



**Scheme 37:** C-C bond formation using an iridium-catalysed “borrowing hydrogen” reaction (Path A) and the activation of alcohols (Path B) by borrowing hydrogen methodology (adapted from Williams and co-workers).<sup>206</sup>

In this research, C-3 alkylations of 4-hydroxycoumarin and its derivatives were performed using 5 mol% of iridium catalyst ( $[Cp^*IrCl_2]_2$ ) in the presence  $Cs_2CO_3$  as a base. A plausible catalytic cycle is depicted in Scheme 38.



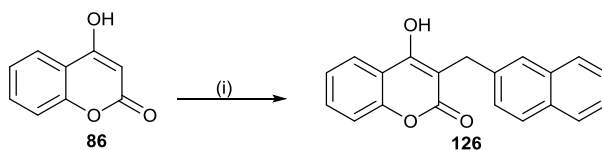
**Scheme 38:** Proposed mechanism for C-3 alkylation of 4-hydroxycoumarin and its derivatives using an iridium catalyst.

During the cycle, activation of the alcohol (**125a**) by catalytic dehydrogenation is followed by a Knoevenagel condensation and catalytic reduction (path 'A') to form the asymmetrical dicoumarol (**125c**). The reduction of intermediate compound (**125b**) to the desired product is in competition with a Michael addition reaction by the 4-hydroxycoumarin remaining in the reaction mixture through path 'B' which produces dimer (**125d**) as a by-product. The reaction therefore was left to react for a prolonged period of time (24 hours) in order to effect complete conversion.

One of the key challenges of the 'borrowing hydrogen methodology' arises from the use of excess of alcohols both as reagent and solvent, and as a result, a stoichiometric amount of reacting partners (alcohol, 2 equivalents) and (coumarin 1 equivalent) were applied. The result obtained gave lower yields (52-59%), whereas using 5 equivalents of alcohol gave higher yields (60-89%).

A second serious limitation of the 'borrowing hydrogen methodology' is the cost of the metal catalyst ( $[\text{Cp}^*\text{IrCl}_2]_2$ ) used. Consequently, effort was focussed on finding a less expensive catalyst with respect to the iridium complex. The ruthenium complex  $\text{Ru}(\text{PPh})_3\text{Cl}_2/\text{KOH}$  (**116**) was found to be inexpensive, easily available and has been reported to be effective for 'borrowing hydrogen' reaction.

In this project, optimization parameters such as solvent, base, time and temperature were investigated for the specific reaction of 4-hydroxycoumarin with naphthalene-2-ylmethanol using ruthenium catalyst (**116**) as shown in Scheme 39.



**Reaction condition:** (i) 4-hydroxycoumarin (1 eq); naphthalene-2-ylmethanol (1 eq), 2-methyl-2-butanol [4.0 M], ruthenium catalyst (5 mol%) and temperature (110 °C) for 24 h.

**Scheme 39:** General scheme for C-3 alkylation of 4-hydroxycoumarin using ruthenium catalyst (**116**) in the ‘borrowing hydrogen methodology’.

Initially the reaction was carried out at 110 °C for 24 hours using 5 mol% of  $\text{Ru}(\text{Ph}_3\text{P})_2\text{Cl}_2/\text{KOH}$  [4.0] and the  $^1\text{H}$  NMR spectrum of the crude product obtained showed only a trace of the product (**126**) (Figure 78). This is in contrast to the result obtained using  $([\text{Cp}^*\text{IrCl}_2]_2)/\text{Cs}_2\text{CO}_3$  complex which gave a complete conversion at 110 °C within 24 hours.

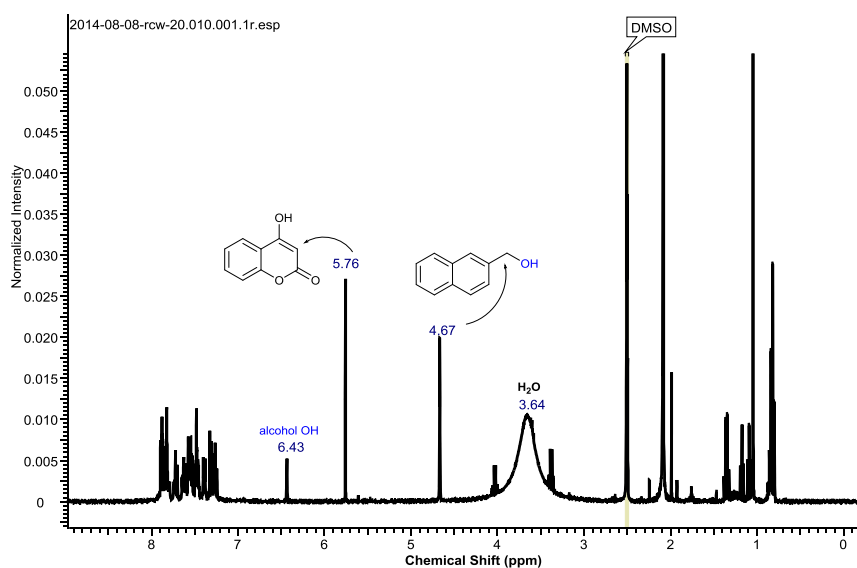


**Figure 78:**  $^1\text{H}$  NMR spectrum of crude reaction mixture involving naphthalene-2-ylmethanol and 4-hydroxycoumarin using  $\text{Ru}(\text{Ph}_3\text{P})_3\text{Cl}_2$  in borrowing methodology at a temperature of 110 °C.

Increasing the temperature of the reaction mixture to 140 °C for 24 hours resulted in an estimated yield of 81% of the desired product (**126**) from analysis of the  $^1\text{H}$  NMR spectrum of the crude product mixture as shown in Figure 79.

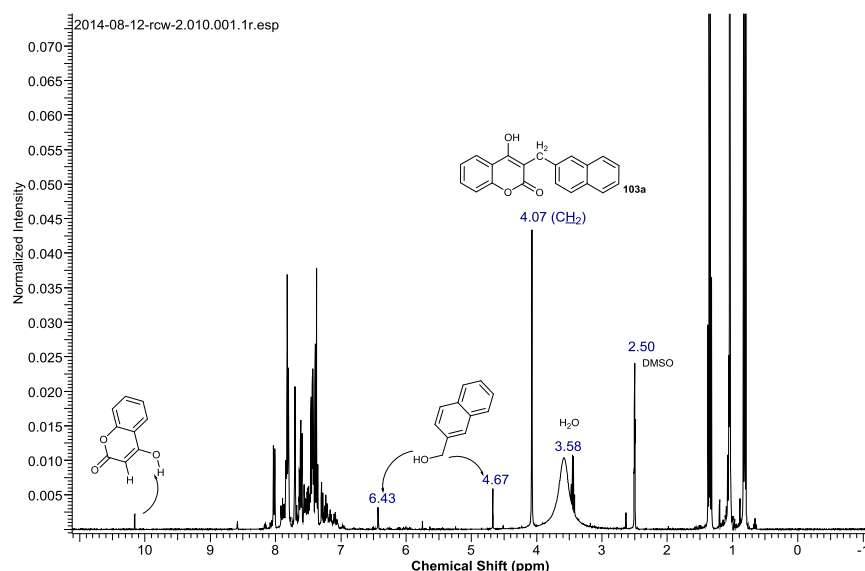


**Figure 79:** <sup>1</sup>H NMR spectrum of the crude reaction mixture involving naphthalene-2-ylmethanol and 4-hydroxycoumarin Ru(Ph<sub>3</sub>P)<sub>3</sub>Cl<sub>2</sub> as catalyst in “borrowing hydrogen methodology” at a temperature of 140 °C.

A comparison of the conversion achieved by changing the substrate concentration from 4.0 M to 0.5 M was made. The ratio of the product obtained with respect to residual alcohol and 4-hydroxycoumarin was linear with the best conversion at high concentration. Borrowing hydrogen methodology using the ruthenium catalyst was therefore more effective at high concentrations and elevated temperature and over a prolonged reaction time.

In summary, in contrast to reductive C-C cleavage of symmetrical analogues of dicoumarol using sodium cyanoborohydride (NaCNBH<sub>3</sub>), ‘borrowing hydrogen methodology’ afforded a higher yield for the asymmetrical analogues of dicoumarol and was more atom efficient.

## 2.7 Synthesis of an analogue of ‘antheminone A’ for prodrug design

As stated in the first chapter of this study, there is the possibility of a drug barrier to the target site due to the phospholipid nature of the cell membrane, causing poor penetration of the NQO1 inhibitor, and low toxicity to the cancer cells. In view of this, an analogue of antheminone A (**84a**) was synthesized and utilized for the preparation of potential prodrugs (**84b**) and (**84c**) as shown in Figure 80.

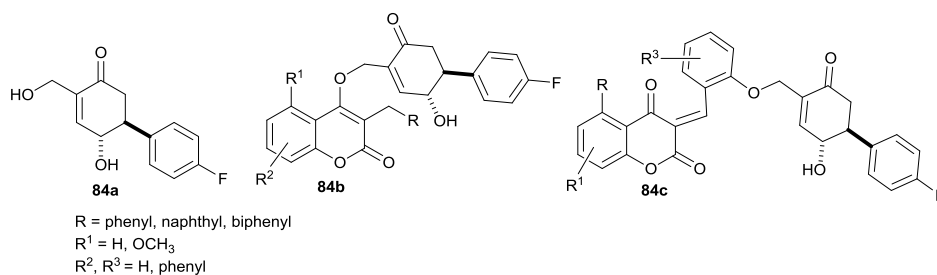
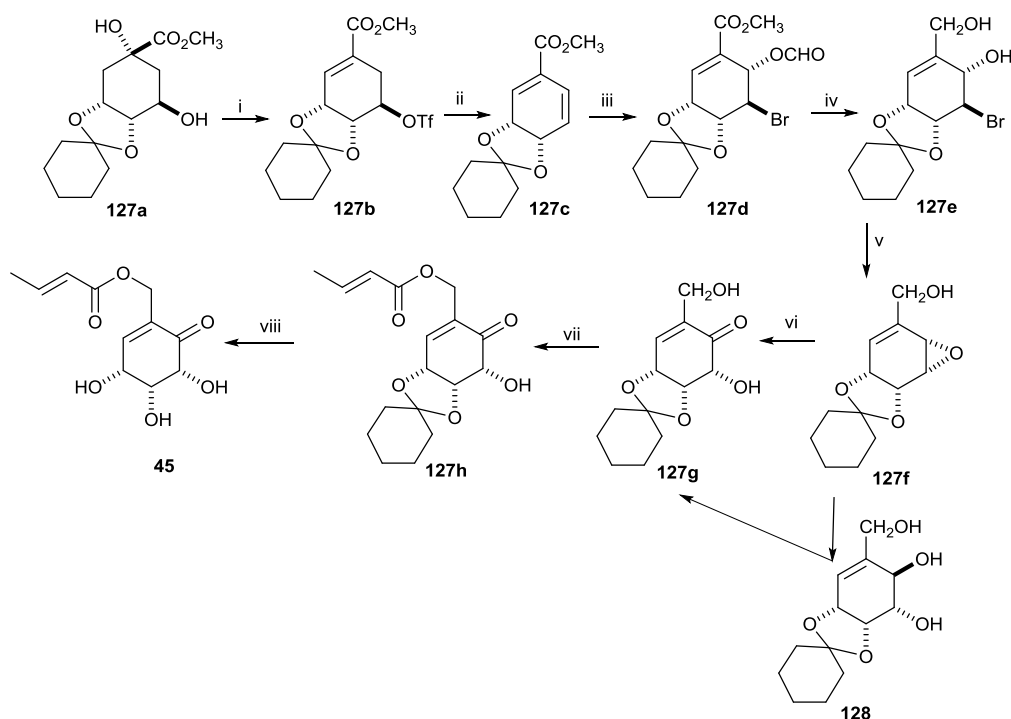


**Figure 80:** An analogue of antheminone A (**84a**) used in the synthesis of prodrugs (**84b**) and (**84c**).

In 2000, Ganem and co-workers<sup>207</sup> reported an efficient method for the synthesis of COTC (**45**), which involved an eight-step reaction sequence which proceeded in an overall yield of 73%. In this sequence, cyclohexylidene ketal protected (-)-methyl quinate (**127a**) was used as a precursor as shown in Scheme 40.



Reagents and conditions; (i) Tf<sub>2</sub>O, py, DCM, 65%; (ii) CsOAc, DMF; (iii) NBS-H<sub>2</sub>O, DMF, 72% over 2 steps; (iv) DIBAL-H, benzene-toluene, 65%; (v) LiN(TMS)<sub>2</sub>, THF, -78 °C, 87%; (vi) CH<sub>3</sub>SO<sub>3</sub>H, DMSO, r.t., 1.5 h then Et<sub>3</sub>N, r.t., 5 mins, 71%; (vii) crotonic anhydride, DCC, DMAP, THF, 54%; (viii) 1:1 TFA:H<sub>2</sub>O, 73%.

**Scheme 40:** An eight-step reaction sequence for the synthesis of COTC (**45**).

The group observed that in their attempt to carry out ring opening of epoxide (**127f**) to (**127g**) using DMSO in the presence of boron trifluoride etherate or triflic acid, an intermediate diol product (**128**) was obtained instead of the desired enone (**127h**).

Reacting diol (**128**) with  $(\text{Bu}_3\text{Sn})_2\text{O}$  and  $\text{Br}_2$  gave the desired product (**127g**) in 51% yield. Similarly, the direct conversion of (**127f**) to (**127g**) was achieved using methanesulfonic acid/DMSO followed by an excess of  $\text{Et}_3\text{N}$  at room temperature. The crotonylation of the primary hydroxyl group of (**127g**) with crotonic anhydride, followed by deprotection with TFA:  $\text{H}_2\text{O}$  gave COTC (**45**) in 73% yield.

### 2.7.1 Previous syntheses by the Whitehead group

The antitumor properties of both COTC and the antheminones have stimulated scientific interest in the synthesis of analogues. Over the past decade, the Whitehead group have successfully synthesized various analogues of both COTC and the antheminones which were found to be potent towards non-small lung cancer cell lines A549 and H460. To mention some of the compounds synthesized by the group (Figure 81), compounds (**131**) and (**132**) are among the new analogues related to COTC and the diols (**129**) and (**130**) are structurally related to the antheminones.

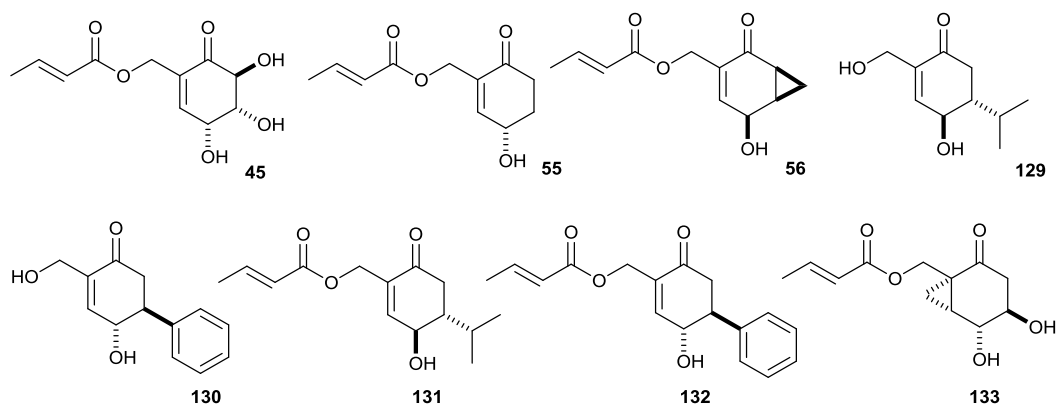
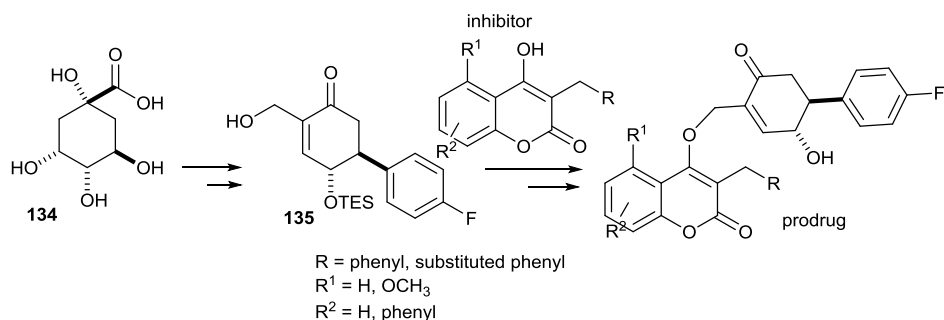


**Figure 81:** Analogues of COTC (**45**) antheminones synthesized by the Whitehead group.<sup>208</sup>

During the research programme described herein, the NQO1 inhibitors described previously were to be modified by coupling them with an analogue of antheminones A with the aim of overcoming poor cell penetration of these inhibitors. It was anticipated that activation of these prodrugs by GST/GSH, which are both up-regulated in most solid cancers, would release the NQO1 inhibitor as well as generating a cytotoxic exocyclic enone from the antheminone moiety.

The synthesis of an analogue of antheminone A, (**135**), was therefore carried out using (-)-quinic acid **134** as the starting material as outlined in Scheme 41. The

synthesis was carried out using procedures developed previously by the Whitehead group with little modifications in some cases.

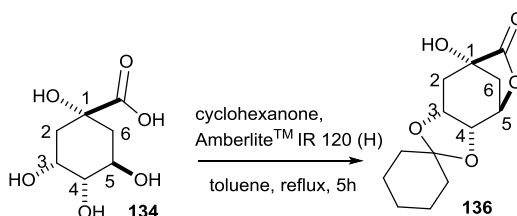


**Scheme 41:** Synthetic approach to a prodrug for release of an inhibitor of NQO1

### 2.7.2 Synthesis of $\gamma$ -lactone

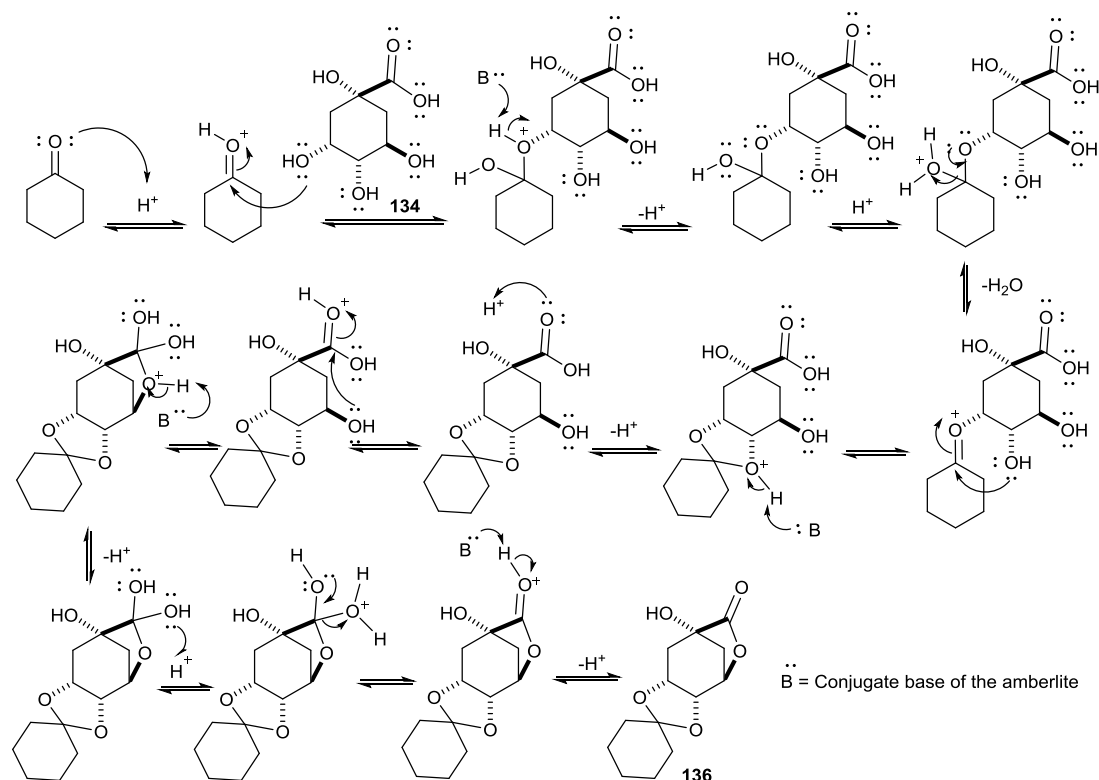
The conversion of (-)-quinic acid (**134**) to cyclohexylidene quinide (**136**) followed a modified reaction sequence developed by the Whitehead group. The  $\gamma$ -lactone (**136**) had previously been synthesized by Gero's procedure by boiling a mixture of (-)-quinic acid (**134**), cyclohexanone and acid catalyst (Amberlite™ IR 120 (H) resin) in a mixture of benzene and DMF.<sup>209</sup> An alternative procedure developed by the Whitehead group utilizes toluene as a reaction medium due to the health and safety issues associated with the use of benzene.

The *cis*-1,2-diol group of (-)-quinic acid (**134**) was selectively protected with cyclohexanone in the presence of an acid catalyst (Amberlite™ IR 120 (H) resin) as shown in Scheme 42. The reaction proceeded with concomitant lactonisation, *via* intramolecular condensation of the *syn* carboxylic acid at C1 and hydroxyl group at C5, to afford the known cyclohexylidene quinide (**136**) in 62% yield.



**Scheme 42:** Synthesis of cyclohexylidene ketal (**136**).

The removal of water using a Dean and Stark trap assisted in driving the reaction to completion by application of Le Chatelier's principle.<sup>209</sup> The mechanism for the lactonisation reaction is shown in scheme 43.



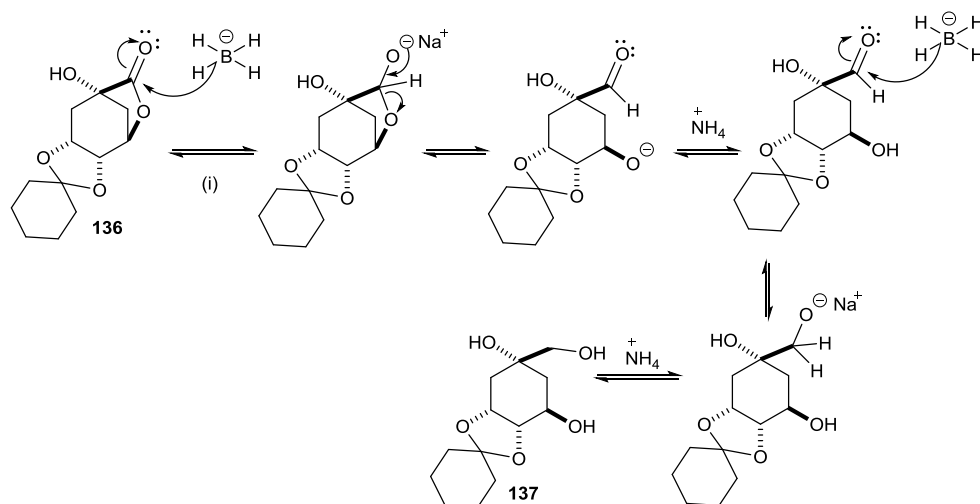
**Scheme 43:** Mechanism of formation of cyclohexylidene ketal (**136**) from (-)-quinic acid (**134**).

### 2.7.3 Conversion of $\gamma$ -lactone to hydroxyketone

#### 2.7.3.1 Reductive ring opening in $\gamma$ -lactone

The reductive ring opening of  $\gamma$ -lactone (**136**) was achieved by adopting the procedure described by Schulz and co-workers.<sup>210</sup> Usually, the reduction of ester and lactone is carried out using a strong reducing agent such as lithium aluminium hydride. In 2000, Schulz and co-workers reported the reduction of lactone (**136**) to triol (**137**) using the mild reducing reagent  $\text{NaBH}_4$ , in methanol as solvent. The reduction was successful due to the presence of the electron withdrawing hydroxyl group adjacent to the carbonyl which increases its electrophilic nature and reactivity towards nucleophilic attack by the hydride ion. The mechanism is depicted in Scheme 44.





Reagents and conditions: (i) methanol, NaBH<sub>4</sub> (10 eq), r.t., 20 h.

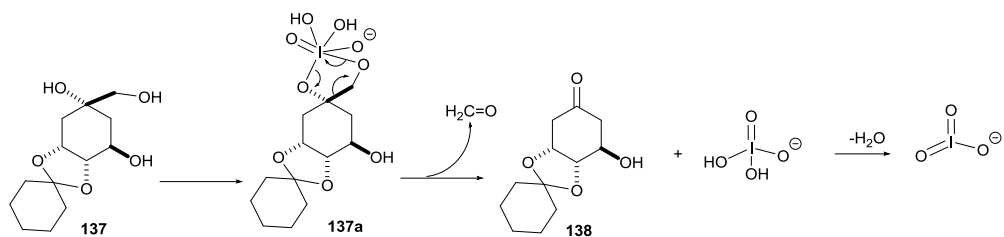
**Scheme 44:** Mechanism of formation of triol (**137**).

#### 2.7.4 Oxidative cleavage of triol

The oxidative cleavage of the vicinal diol moiety of (**137**) was accomplished using sodium periodate (NaIO<sub>4</sub>). Although this reagent has its limitations, such as poor solubility in apolar solvents, it is commonly used for the oxidative cleavage of vicinal 1,2-diols. It is easier to handle when compared to HIO<sub>4</sub> and is also inexpensive. In 1981, Gupta and his co-workers<sup>211</sup> solved the issue of insolubility by introducing silica gel-supported NaIO<sub>4</sub>. This procedure was later found to have some problems such as requiring longer reaction times and producing poor yields following the removal solvent.

Based on these findings, Daumas and co-workers<sup>212</sup> developed an alternative procedure, using wet silica gel-supported NaIO<sub>4</sub>. The mixture of silica gel and NaIO<sub>4</sub> dissolved in water and the vicinal diol (**137**) in DCM, however, produced colloidal forms upon stirring. To overcome this, in 1996, Shing and his team introduced a free flowing silica gel-supported NaIO<sub>4</sub>. The advantage of this procedure is that it doesn't usually require a final purification process.<sup>213</sup>

During this project, oxidative cleavage was performed using the free-flowing powder form of silica gel-supported sodium periodate.<sup>208</sup> The reaction gave hydroxy ketone (**138**) in 88% yield over two steps from lactone (**136**) as shown in Scheme 45.



Reagents and conditions: DCM, silica gel-supported NaIO<sub>4</sub> dissolved in water, stir at r.t., 4 h.

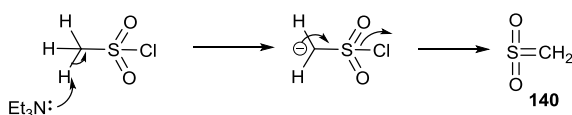
**Scheme 45:** Mechanism of the oxidative cleavage of triol (**137**) to hydroxyl ketone (**138**).

During this reaction, vicinal 1,2-diol (**137**) reacts with NaIO<sub>4</sub> to form a 5-membered cyclic periodate ester (**137a**) which undergoes a cheletropic loss of H<sub>2</sub>IO<sub>4</sub><sup>(-)</sup> resulting in cleavage of the C-C bond to form hydroxyketone (**138**) and formaldehyde.

### 2.7.5 Elimination of $\beta$ -hydroxyl

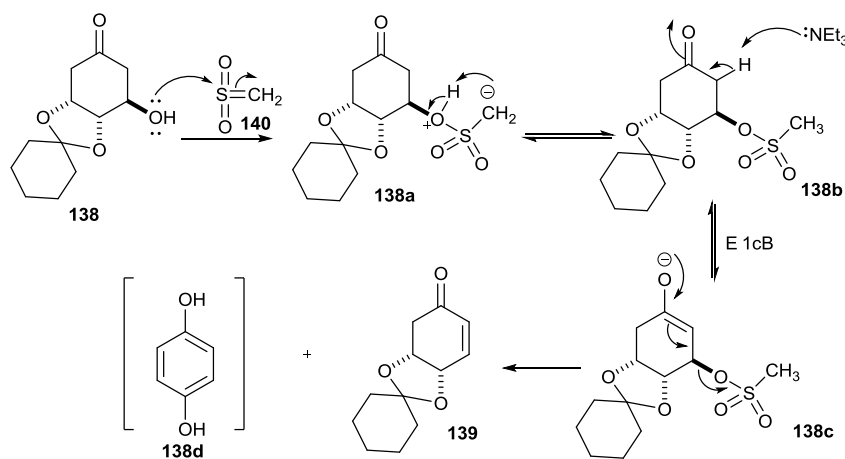
The hydroxide ion (OH<sup>-</sup>) is a relatively strong base compared to anions derived from strong acid and as a result it is a poor leaving group. To change it into a better leaving group, it can be reacted with methanesulfonyl chloride in the presence of triethylamine to generate a mesylate intermediate. In 1989, this procedure was described by Danishefsky and co-workers<sup>214</sup> for the preparation of enone (**139**) which proceeded in 72% yield.

The reaction commences with the *in situ* generation of a strongly electrophilic sulfene intermediate (**140**) via an E1<sub>C</sub>B mechanism as shown in Scheme 46.



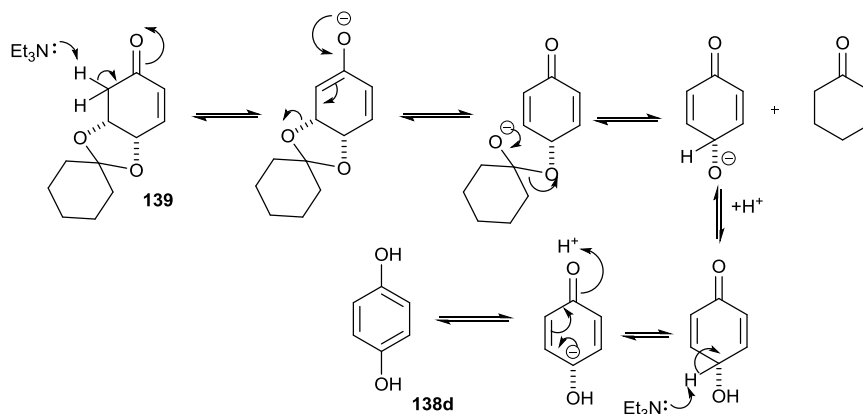
**Scheme 46:** Mechanism for the *in situ* formation of sulfene intermediate (**140**) via an E1<sub>C</sub>B mechanism.

The electrophilic sulfene intermediate (**140**) undergoes a nucleophilic attack by the free hydroxyl group of the hydroxyketone (**138**) to give sulfonate ester (**138b**). Subsequent deprotonation by triethylamine gives enolate (**138c**) which rapidly undergoes elimination of mesylate (CH<sub>3</sub>SO<sub>3</sub><sup>-</sup>) to give enone (**139**) as shown in Scheme 47.



**Scheme 47:** Mechanism of formation of enone (**139**).

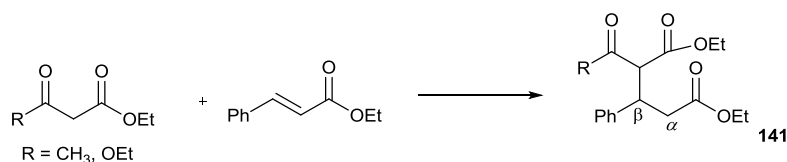
A significant difficulty was encountered during the synthesis of enone (**139**) which was a consequence of the unstable nature of the compound. To prevent this, both the crude and pure enone were stored in the freezer to retard any reaction with the residual triethylamine which can lead to elimination of cyclohexanone resulting in aromatisation to give hydroquinone (**138d**) as an impurity as depicted in Scheme 48.



**Scheme 48:** Mechanism of formation of hydroquinone (**138d**).

### 2.7.6 1,4-conjugate addition

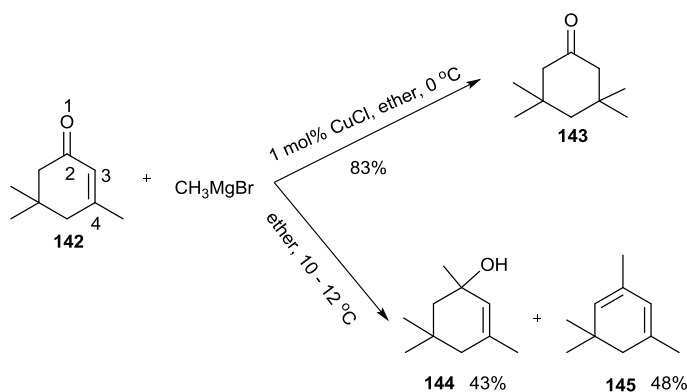
Conjugate additions have a relatively long history which first started with work by Komnesons in 1883.<sup>215</sup> They became an important methodology in organic synthesis following extensive research conducted by Arthur Michael in 1887. The subsequently named ‘Michael reaction’ involved conjugate addition of a carbon nucleophile in a protic solvent such as ethanol using a catalytic amount of a base (sodium hydroxide, alkoxide or a trialkylamine) to give a  $\beta$ -substituted product (**141**) (Scheme 49).<sup>216</sup>



**Scheme 49:** Conjugate addition to an  $\alpha,\beta$ -unsaturated ester giving a  $\beta$ -substituted product (**141**).

Studies have revealed that base-catalysed conjugate addition reaction can be accompanied by a poor level of selectivity and in some cases byproducts can be formed. High levels of stereoselectivity however can be achieved by careful selection of the reacting partners. Several transition metal catalyzed reactions have been developed in order to solve the problematic regioselectivity (e.g 1,2- vs 1,4-addition) and stereoselectivity.

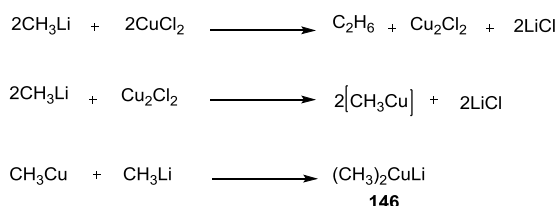
In 1941, Kharasch and co-workers performed conjugate addition reactions on  $\alpha,\beta$ -unsaturated enone (**142**) using Grignard reagents. The reactions were trialled both in the presence and absence of a copper(I) salt. Interestingly, the group discovered that in the presence of CuCl, the product (**143**) was obtained in an excellent yield (83%), whereas in the absence of CuCl, 1,2 adducts (**144**) and (**145**) were obtained instead (Scheme 50).<sup>217</sup>



**Scheme 50:** Reaction of  $\alpha,\beta$ -unsaturated enone (**142**) with CH<sub>3</sub>MgBr in the presence and absence of copper(I) salt according to Kharasch and co-workers.<sup>217</sup>

The generally accepted explanation for this is that Grignard reagents are relatively hard nucleophiles, likewise the electrophilic carbonyl carbon. To obtain a 1,4-conjugate addition product the Grignard reagent must be converted to a softer nucleophile by reacting with Cu(I) salt, since C-4 is a soft electrophile.

The first organocopper compound described in the literature was prepared by Reich in 1923.<sup>218</sup> In 1936, Henry Gilman demonstrated the possibility of utilizing organocopper reagents in organic synthesis.<sup>219</sup> Gilman observed that methyl lithium could react with copper(II) chloride to give copper (I) chloride and ethane. The copper(I) chloride in turn underwent another reaction with methyl lithium to give methyl copper (CH<sub>3</sub>Cu). Further reaction of methyl copper with methyl lithium gave a 'stable' lithium diorganocopper reagent (CH<sub>3</sub>)<sub>2</sub>CuLi otherwise known as a Gilman reagent (**146**) (Scheme 51).<sup>220</sup>



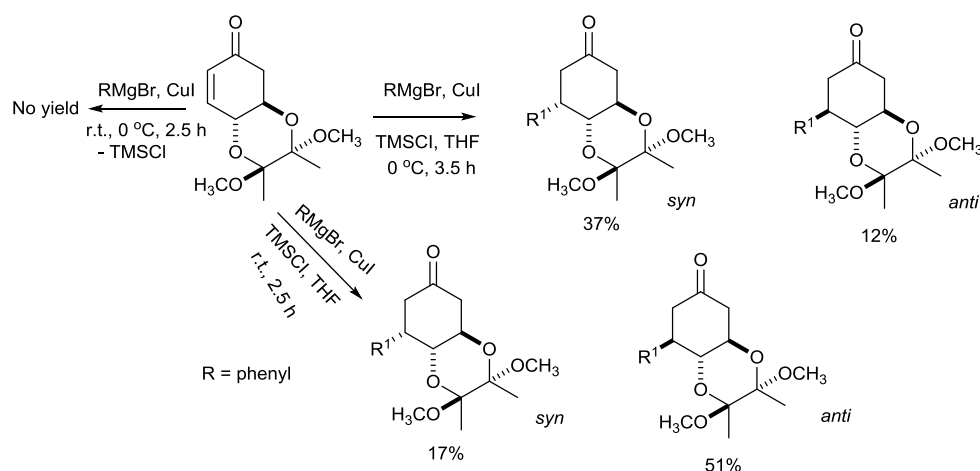
**Scheme 51:** Synthetic pathway for formation of a Gilman reagent (**146**).<sup>220</sup>

In 1966, House and co-workers carried out a similar reaction described in Scheme 50 above using the organocopper reagent ((CH<sub>3</sub>)<sub>2</sub>CuLi). The group observed a remarkable increase in the rate of reaction as well as improved overall yields compared to the CH<sub>3</sub>MgBr reagent used by Kharasch. The team reported that organocuprates were the reactive species responsible for the conjugate addition and, by analogy, that they may also have been the reactive species involved in Kharasch's earlier studies.<sup>221</sup>

Wider application of organocopper reagents in organic synthesis was retarded due to a lack of reproducible results caused by the use of impure salts. Organocopper reagents are thermally unstable and may explode because of their sensitivity to air and moisture. It was also revealed that in conjugate addition reactions, organocopper reagents may be less reactive or totally inactive compared to organocopper complexes.<sup>222,223</sup>

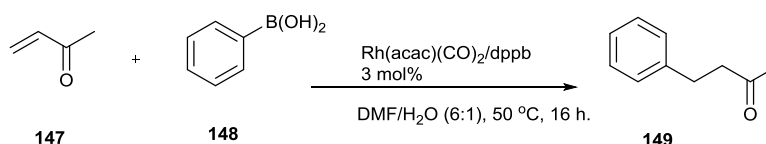
The Whitehead group have reported significant success using organocuprates (Gilman reagents) in the presence and absence of an additive (TMSCl), in several of their syntheses as depicted in Scheme 52. Unfortunately, they observed a poor level of stereoselectivity in certain cases which made their results inconclusive.<sup>224</sup> The

inconsistency in the use of organocuprate reagents shows that the reaction is somehow unpredictable and can be affected by the type of reagent, the additive and the reaction temperature. To overcome these limitations, rhodium catalysts were trialled due to their several advantages such as insensitivity to moisture and tolerance to other functional groups.



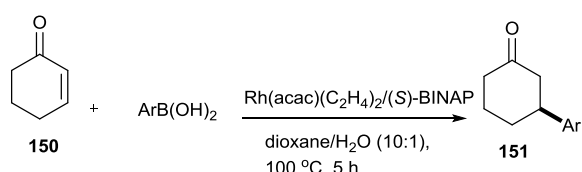
**Scheme 52:** Stereochemical outcome of the reactions with organocuprate reagents in the presence and absence of additive (TMSCl).<sup>224</sup>

In 1997, Miyuara and co-workers reported the first catalytic conjugate addition of aryl and alkenyl boronic acids reaction to an enone catalysed by a rhodium(I) complex. The rhodium(I) complex was generated *in situ* via the reaction of  $[\text{Rh}(\text{acac})(\text{CO})_2]$  and an achiral phosphine ligand. Further investigations into the efficiency of several ligands were carried out, and the results revealed that the bis(phosphine) ligands with large bite angles ( $\text{dppb} > \text{dppp} > \text{dppe}$ ) were the most effective. For example the reaction of but-3-en-2-one (**147**) and phenylboronic acid (**148**) using  $\text{Rh}(\text{acac})(\text{CO})_2$  and dppb gave 4-phenylbutan-2-one (**149**) in 99% yield as depicted in Scheme 53.<sup>225</sup>



**Scheme 53:** Reaction of but-3-en-2-one (**147**) and phenylboronic acid (**148**) using  $\text{Rh}(\text{acac})(\text{CO})_2/\text{dppb}$  to give 4-phenylbutan-2-one (**149**).

A year later, Miyuara and co-workers carefully investigated the reaction conditions (solvent, catalyst, ligand and temperature) for the reaction. In this investigation, the procedure used for the achiral reaction was modified by changing the rhodium catalyst to  $\text{Rh}(\text{acac})(\text{C}_2\text{H}_4)_2$ , using (*S*)-BINAP ligand and a 10:1 mixture of dioxane /water as solvent at 100 °C. The reaction of cyclohexenone (**150**) and 1.4 eq of phenylboronic acid in the presence of the rhodium catalyst at 100 °C in a 10:1 mixture of dioxane and water gave (*S*)-3-phenylcyclohexanone (**151**) in a 64% yield and 97% ee (Scheme 54).<sup>226</sup>



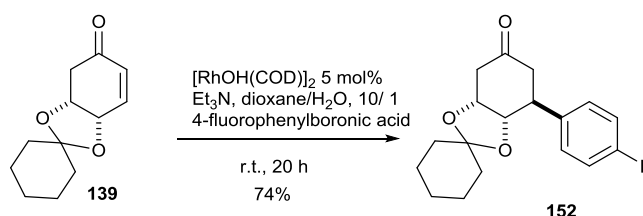
**Scheme 54:** Conjugate addition using  $\text{Rh}(\text{acac})(\text{C}_2\text{H}_4)_2/(\text{S})\text{-binap}$  and phenyl boronic acid.

The use of excess boronic acid, ranging from 2.5 to 5.0 equivalents, improved the yields from 93 to 99% respectively. Miyuara and co-workers also discovered that the reaction temperature had a significant effect on the overall yield. For example, at lower than 60 °C the 1,4-addition was very slow, giving the product in less than 3% yield, whereas the highest yields were obtained at 100 °C. An important observation made by the group was that the enantioselectivity (97% ee) was maintained between 40-120 °C. The use of organoboronic acids in 1,4-addition reactions described by Miyuara and co-workers has several advantages compared to 1,4-additions using organocuprates or organomagnesium reagents and these include:

- They are inert to oxygen and moisture and therefore allow the reaction to be carried out in a protic solvent or even in aqueous solvent.
- Organoboronic acids have wide compatibility with a variety of functional groups.
- They are much less reactive towards ketones in the absence or presence of a rhodium catalyst and consequently, there is no by-product formed as a result of 1,2-addition reaction.
- A remarkable advantage of the new strategy by Miyuara and co-workers was that the reaction could be catalysed by transition-metal complexes

coordinated with chiral ligands which resulted in a high level of enantioselectivity.

During these investigations described herein, 1,4-conjugate addition to enone (**139**) was carried out in the presence of Et<sub>3</sub>N and dioxane/H<sub>2</sub>O (10: 1) as shown in Scheme 55. The product (**152**) was obtained in a good yield of 74%.



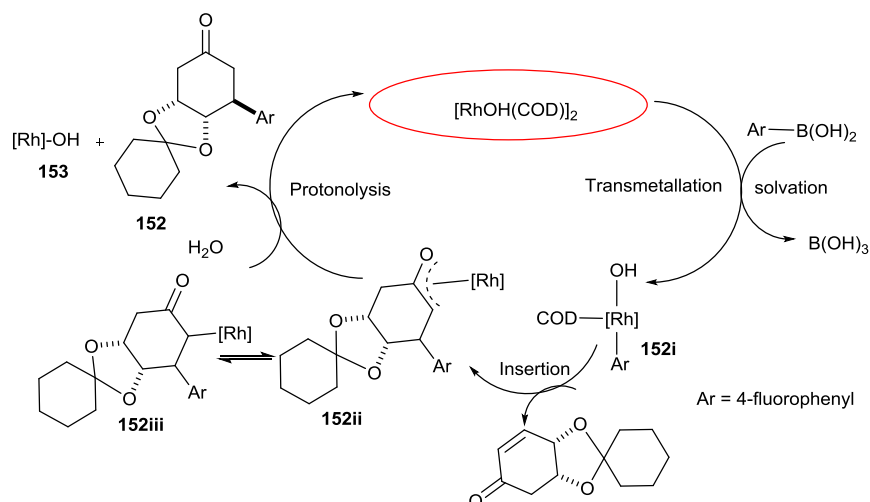
**Scheme 55:** Synthesis of fluorophenyl adduct (**152**).

### 2.7.7 The mechanistic cycle of rhodium-catalysed 1,4-addition

Transmetallation between the organoboronic acid and the rhodium-complex is the most important step that occurs in this C-C bond forming reaction. Water has been found to be vital in this transformation and in its absence there is no reaction as depicted in the mechanism on Scheme 56. The addition of Et<sub>3</sub>N accelerates the transmetallation step between the organoboronic acid and rhodium-complex which results in the formation of a rhodium-phenyl bond to give (**152i**) a key intermediate in the reaction.

The next step involves the insertion of the carbon-carbon double bond of the enone into the rhodium-phenyl bond to give an intermediate oxo-pi-allyl intermediate (**152ii**). This intermediate can undergo isomerisation to (**152iii**) which subsequently undergo protonolysis by water to give 1,4-addition product (**152**) and hydroxo-rhodium complex (**153**).

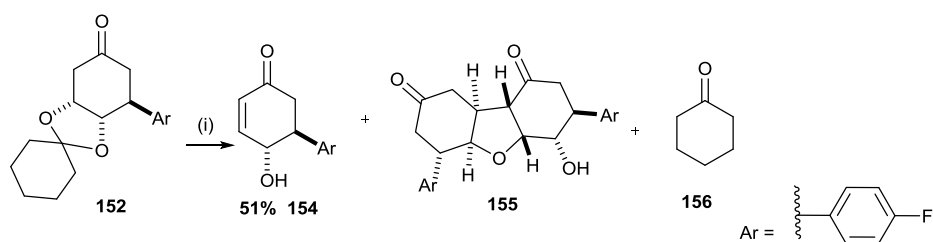




**Scheme 56:** Mechanistic cycle for the formation of conjugate adduct (**152**).

### 2.7.8 Eliminative removal of the cyclohexylidene protecting group

Eliminative deprotection of cyclohexylidene (**152**) was performed using a method adapted by the Whitehead group from an original procedure described by Danishefsky and co-workers.<sup>214</sup> During this reaction, two drop aliquots of NaOH were added into a solution of the conjugate adduct (**152**) in THF at 0 °C under nitrogen gas. Further two drop aliquots of NaOH were added every hour until the reaction had reached completion. The desired product (**154**) was obtained in an unpredictable yield (51%) due to formation of dimer (**155**) as depicted in Scheme 57.

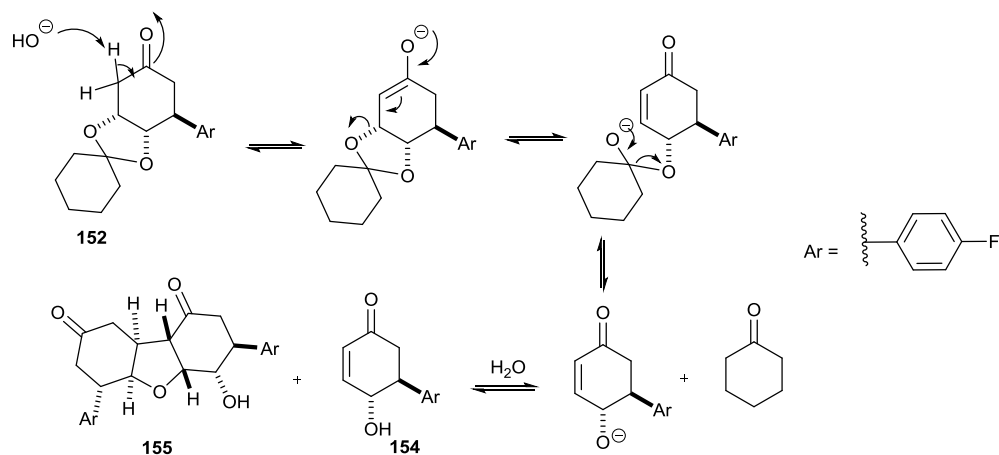


Reaction conditions: (i) THF, dil NaOH, 0 °C, 2 h.

**Scheme 57:** Eliminative deprotection of ketone (**152**) protecting group using a catalytic amount of base.

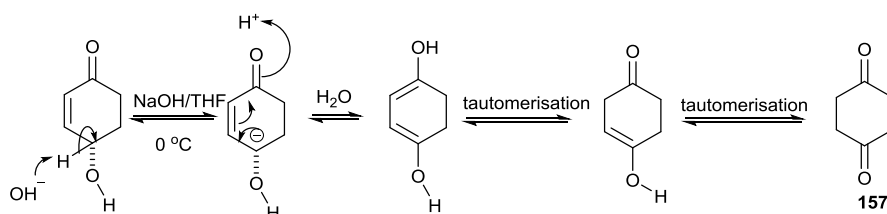
In order to optimize the yield, the reaction was carried out in the presence of excess NaOH or for a prolonged period of time (5 hours). In both cases, dimer (**155**) was the predominant product obtained. The highest yield was obtained in less than 2 hours by careful monitoring of the reaction by TLC every 30 minutes and the reaction was quenched as soon as the dimer started forming. The product (**154**) was obtained in a

moderate yield of 51%. A plausible mechanism for the formation of (**154**) is depicted in Scheme 58.



**Scheme 58:** Mechanism of deprotection of (**152**) to give  $\gamma$ -hydroxyenone (**154**).

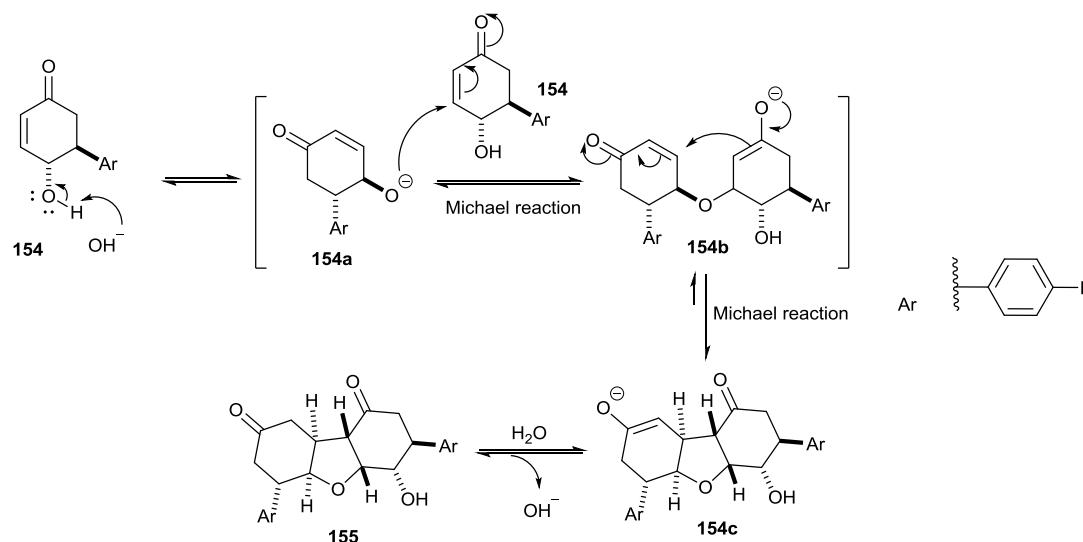
This elimination process was quite capricious and the yield unpredictable. Danishefsky and co-workers<sup>214</sup> attributed the poor yield to be a result of the instability of the alcohol towards tautomeric decomposition to 1,4-cyclohexanedione (**157**) as illustrated in Scheme 59.



**Scheme 59:** Mechanism for the formation of cyclohexane-1,4-dione (**157**).

Prior to the research study described herein, the Whitehead group conducted extensive investigations into deprotection of the conjugate adducts using a variety of bases such as DBU and  $\text{Et}_3\text{N}$ .<sup>224</sup> The group also observed that the yields (57-81%) were variable and sometimes unpredictable. Accidentally however, the group discovered that the major reason for the unpredictable nature of the NaOH mediated reaction was the ‘bipolar reactivity’ of the alcohol (**154**) which led to an unexpected dimerization reaction.

Further investigation revealed that when the conjugate adducts were left to react in the presence of NaOH over a prolonged period of time (18 hours), dimeric compounds were the only isolable products (obtained in 55-86%). The proposed mechanism for the formation of the dimer proceeded *via* a tandem “Michael-Michael” reaction of oxyanion (**154a**) with its conjugate acid (**154**) as depicted in Scheme 60.



**Scheme 60:** Proposed mechanism for the dimerization of alcohol (**154**).

Interestingly, the dimeric compound (**155**) was found to be structurally related to incarviditone (**158**) a natural product that is derived biosynthetically from rengyolone (**159**), both of which were isolated from *Incarvillea delevayi* in 2009 by Zhang and co-workers (Figure 82).<sup>227</sup> The team reported that incarviditone (**158**) showed moderate toxicity towards leukemia cell lines (HL-60 and 6T-CEM) and it was also non toxic to other cell lines such as HepG2, A549 and LOVO.

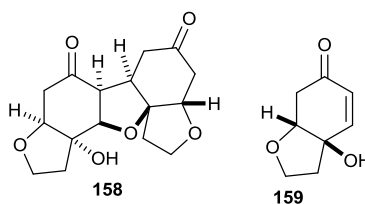


**Figure 82:** Structures of incarviditone (**158**) and rengyolone (**159**).

The toxicity of incarviditone prompted further studies into its structure and mode of biosynthesis. In 2012, Wu and Tang and co-workers carried out computational experiments and with the help of NMR and NOESY measurement, the group confirmed that the correct structure of incarviditone is (**160**) rather than the originally proposed structure (**158**) (Figure 83).<sup>228</sup>

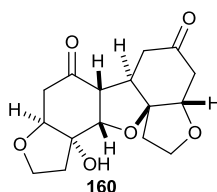


**Figure 83:** The revised structure of incarviditone (160) proposed by Wu and Tang and co-workers.

Further studies by the Whitehead group discovered that some of the synthesized dimeric compounds such as **(161)** and **(162)** (Figure 84), showed toxicity towards the A549 non-small-cell lung cancer cell line.

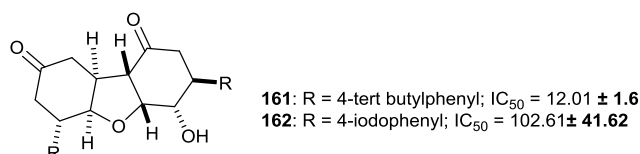
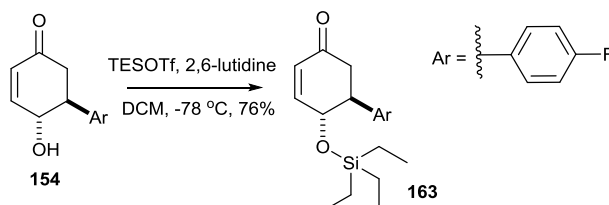


**Figure 84:** Structures of dimeric compounds **(161)** and **(162)** tested against small lung cancer cell line A549.

### 2.7.9 Triethylsilyl (TES) protection of the C-4 hydroxyl group

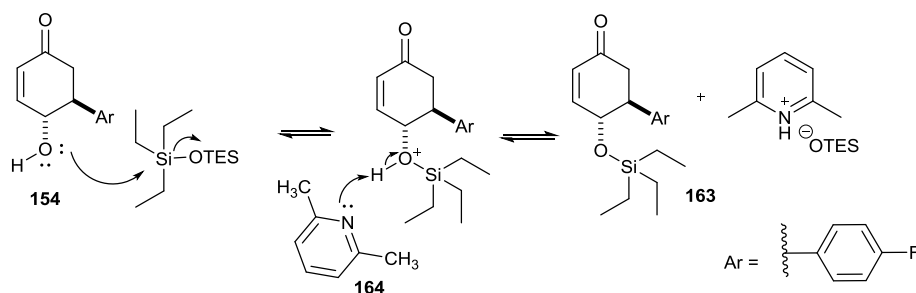
The free hydroxyl group at C-4 in compound **(154)** was protected in order to gain chemoselectivity in the subsequent reactions. A triethylsilyl ether (TES) was chosen as the protecting group due to the advantages it has over other protecting groups. For example, apart from being easier to remove at the end of the reaction, it is relatively stable under basic conditions and also improves the solubility of the product in the less polar solvents needed for the subsequent reactions.

The protection of the hydroxyl group at C-4 of compound **(154)** was performed with triethylsilyl trifluoromethanesulfonate (TESOTf) and 2,6-lutidine in DCM to give silyl ether **(163)** in 76% yield as shown in Scheme 61.



**Scheme 61:** Synthesis of triethylsilyl ether **(163)**.

2,6-Lutidine (**164**), which is a hindered and poorly nucleophilic base as a result of the adjacent methyl groups, neutralizes triflic acid generated by removing the acidic proton as demonstrated in the mechanism in Scheme 62.

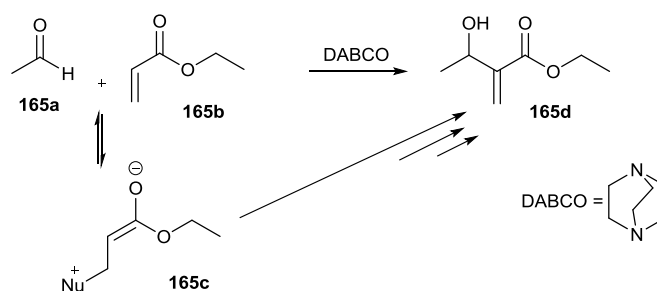


**Scheme 62:** Mechanism of formation of triethylsilyl ether (**163**).

## 2.8 Synthesis of Morita-Baylis-Hillman adduct

The Morita-Baylis-Hillman (MBH) reaction, which was first reported in the early nineteen seventies, is one of the more popular reactions for the formation of a carbon-carbon bond using an organocatalyst. It combines both aldol and Michael reactions in a single step to yield compounds with multiple functionalities. For example, the products have been used as precursors in the synthesis of medically important pharmaceutical compounds<sup>229,230</sup> as well as natural products.<sup>231</sup> The research investigation described herein however, involved the use of a MBH adduct for the synthesis of a novel prodrug which will be discussed later.

An example of a MBH reaction is that between acetaldehyde (**165a**) and ethyl acrylate (**165b**, Michael acceptor) catalysed by a Lewis base such as DABCO or DBU. The reaction results in the formation of carbon-carbon bond at the  $\alpha$ -position of the  $\alpha,\beta$ -unsaturated carbonyl (**165b**) with the carbonyl carbon of the aldehyde (**165a**) as depicted in Scheme 63.



**Scheme 63:** Morita-Baylis-Hillman reaction.

Although the MBH reaction is atom economical, it has some short-comings which include a slow reaction rate (up to 17 days), moderate yields and poor reactivity with enones as well as  $\alpha,\beta$ -unsaturated and hindered aldehydes. As a result, researchers have attempted to increase the reaction rate by using Lewis acids. This strategy was found to be very cumbersome because a Lewis base, can undergo Lewis acid/Lewis base interaction without actually increasing the rate of reaction. To achieve optimal reaction time, yield and to minimize environmental impact, water has been used as a reaction medium.<sup>232,233</sup>

The MBH reaction was previously conducted in polar solvents in order to increase equilibrium concentration of zwitterionic intermediate (**165c**) formed during the progress of the reaction.<sup>234</sup> Using aqueous media, however, may hinder the reaction rate due to poor solubility of the reactant. In view of this, it was suggested that a surfactant in water, which at the appropriate concentration forms a micellar solution may provide a better reaction medium.

Surfactants are amphiphilic molecules that contain both hydrophilic (water 'loving') and hydrophobic (water repelling) characteristics as shown in Figure 85.

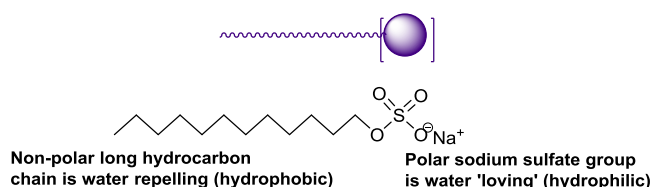


**Figure 85:** Structure of sodium dodecyl sulfate (SDS) used as a surfactant in the MBH reaction.

The prediction was that the lipophilic cyclohexyl ring and the relevant side chain would reside in the hydrophobic region of the surfactant tail, thus, allowing the reactive enone portion of the substrate (**163**) to reside in contact with the aqueous phase (hydrophilic area). Additional stabilisation of the zwitterionic intermediate (**163a**) would be provided by the polar head of the surfactant as demonstrated in Figure 86.

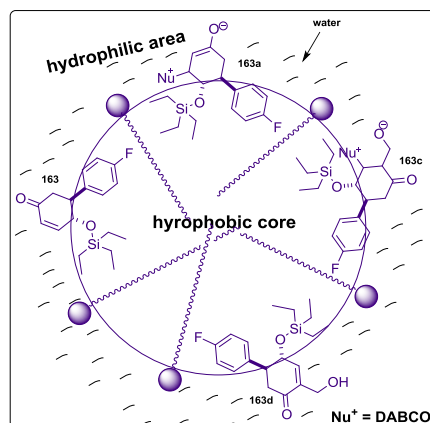
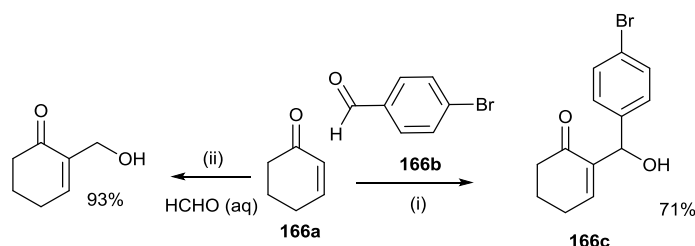


**Figure 86:** Representation of Morita-Baylis-Hillman reaction in micelles.

In order to confirm the effectiveness of this hypothesis, Williams and co-workers carried out studies on the reaction between cyclohexenone (**166a**) and substituted aromatic aldehyde (**166b**) under the new reaction conditions (i.e., sodium dodecyl sulfate (SDS), water and DMAP) as shown in Scheme 64. The group observed that the reaction in the presence of SDS was complete in less than 16 hours and gave the desired product (**166c**) in an excellent yield (71%) compared to a 17 day duration reported by Gatri and co-workers.<sup>234a</sup> Interestingly, in the absence of surfactant only a trace amount of the product was obtained.<sup>235</sup> Among the surfactants trialed, the team discovered that SDS was the most effective giving 63-85% yields with a range of substrates.

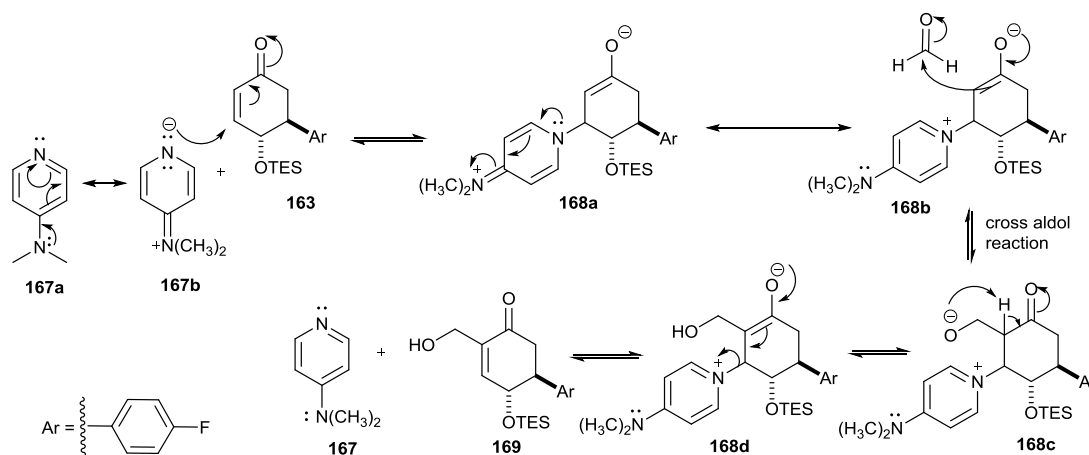


Reaction conditions: (i) SDS, DMAP, water, r.t., 16 h.

(ii) Imidazole, THF-H<sub>2</sub>O, r.t., 17 days.<sup>234a</sup>

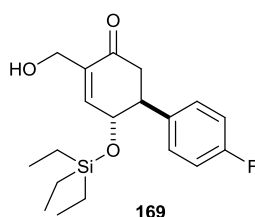
**Scheme 64:** MBH reaction of cyclohexanone (**166a**) with substituted aromatic aldehyde (**166b**) to give (**166c**).

In this research the protected cyclohexenone (**163**) was converted, in a slightly longer time of 22 hours, to (**169**) using a MBH reaction in the presence of SDS, DMAP and water at room temperature. The proposed mechanism for the reaction is depicted in Scheme 65.



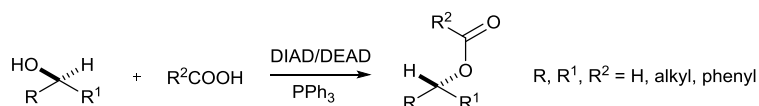
**Scheme 65:** Mechanism of the Morita-Baylis-Hillman reactions for the synthesis of (**169**).

In this catalytic cycle, the lone pair of the dimethylamino substituent of DMAP (**167a**) enhances the nucleophilicity of the nitrogen atom of the ring as illustrated by resonance form. Nucleophilic attack onto the double bond of the enone (**163**) gives intermediate (**168a**) which is in resonance with (**168b**). Subsequent reaction with formaldehyde *via* a cross aldol reaction form an intermediate **168c** which is followed by proton transfer to give (**168d**). The final step involves the elimination of DMAP to give MBH adduct (**169**).



## 2.9 Application of Mitsunobu reaction for the Prodrug synthesis

The Mitsunobu reaction, which was discovered in 1967, has been used for the conversion of primary and secondary alcohols to esters, ethers, thioethers and other compounds as shown in Scheme 66.<sup>236</sup> For this reaction to occur however, one of the reacting components (the nucleophile) must be sufficiently acidic to enable protonation of the DIAD/DEAD. This will prevent side reactions from occurring.



**Scheme 66:** General reaction scheme for the Mitsunobu reaction.



A range of compounds which had been selected as potential prodrugs (Figure 87) for this research programme were synthesized using the Mitsunobu reaction.

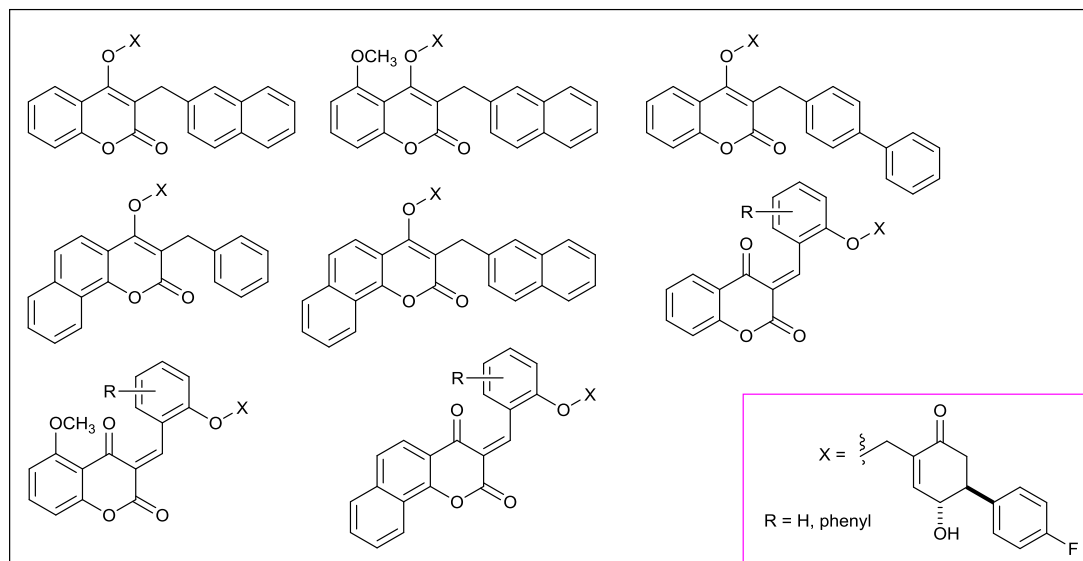
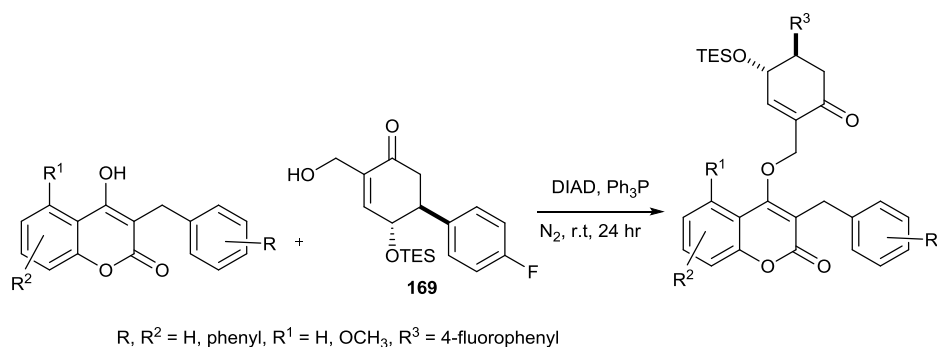


**Figure 87:** Structures of potential prodrugs.

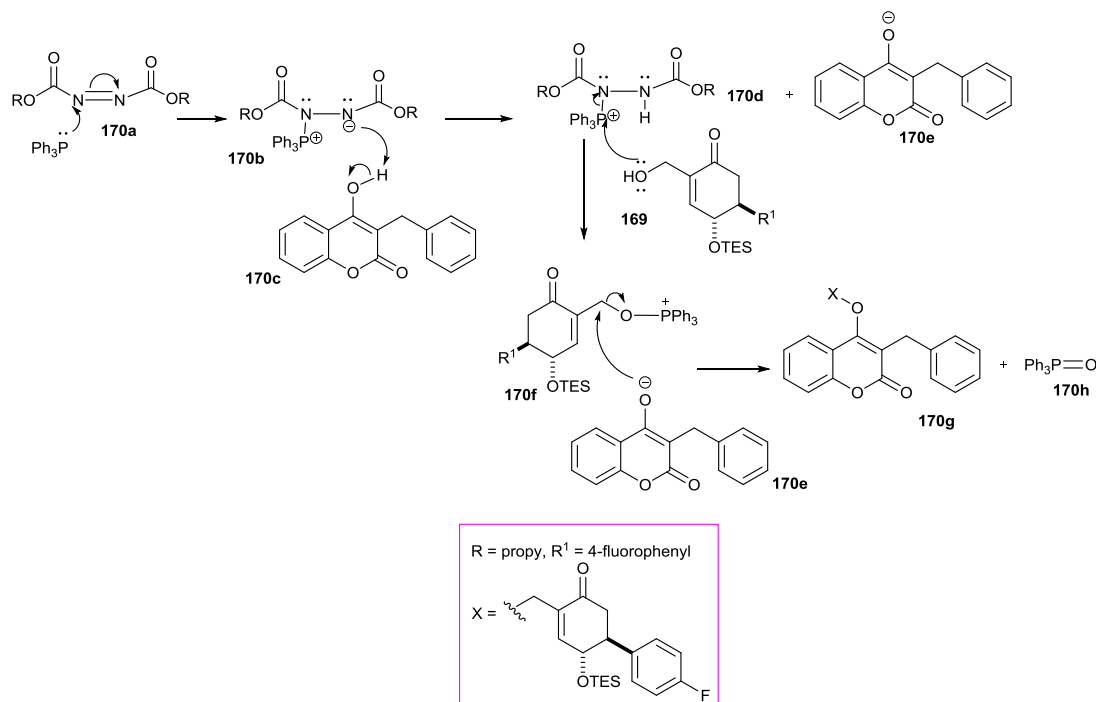
The reaction was carried out by reacting a selection of the NQO1 inhibitors with the Morita-Baylis-Hillman adduct (**169**), in the presence of DIAD and  $\text{Ph}_3\text{P}$  at room temperature under an atmosphere of nitrogen for 24 hours as shown in Scheme 67. During this reaction, the hydroxyl group of (**169**) is converted into a better leaving group that subsequently undergoes displacement *via* nucleophilic attack as depicted in Scheme 68.



**Scheme 67:** Synthesis of prodrugs.

The mechanism of this reaction is still under debate specifically concerning the intermediates and the role that they play. It is generally accepted that nucleophilic attack of  $\text{Ph}_3\text{P}$  on the electron deficient nitrogen atom of DIAD (**170a**) forms a triphenylphosphonium intermediate (**170b**). The intermediate (**170b**) is then

protonated by (**170c**) (pKa 4.75) to give a phosphonium intermediate (**170d**) and the carboxylate anion (**170e**). The phosphonium intermediate (**170d**) reacts with the alcohol oxygen of the Baylis-Hillman adduct (**169**), activating it as a very good leaving group (**170f**). Finally, the carboxylate anion (**170e**) undergoes S<sub>N</sub>2 displacement of triphenylphosphine oxide in (**170f**) to generate the desired compound (**170g**). It is generally accepted that phosphorus-oxygen double bond of (**170h**), which is one of the strongest bonds in chemistry, is the driving force for this reaction.



**Scheme 68:** Mechanism of the prodrug (**170g**) formation.

The protecting group (OTES) was removed by reacting (**170g**) with dilute trifluoroacetic acid for 30 minutes at room temperature and the crude material obtained was purified by silica-gel chromatography.

### 3.0 Chapter 3: Biological evaluation

#### 3.1 Introduction

According to the Federal Drug Agency (FDA), the half maximal inhibitory concentration ( $IC_{50}$ ) value represents the concentration of a drug that is required for 50% inhibition *in vitro*.<sup>237</sup> It is used to evaluate the potency of a drug in inhibiting biological activity such as that of enzymes.

Enzyme assay evaluation for NQO1 was carried out using techniques originally reported by Ernester and his co-workers in 1962,<sup>56</sup> which involved the reduction of cytochrome c by NQO1 in the presence of menadione using NADH as electron donor. The cytochrome c which acted as a terminal electron acceptor was inefficient in this role and as a result menadione (**31**) was included as an intermediate electron acceptor between reduced NQO1 (NQO1 is reduced by NADH) and cytochrome c. In this process, menadione (**31**) is reduced to menadiol (**31a**) by NQO1 and the menadiol (**31a**) formed subsequently reduces cytochrome c which results in a colour change from deep-red into a light orange-red in the presence of an inhibitor (Figure 88).

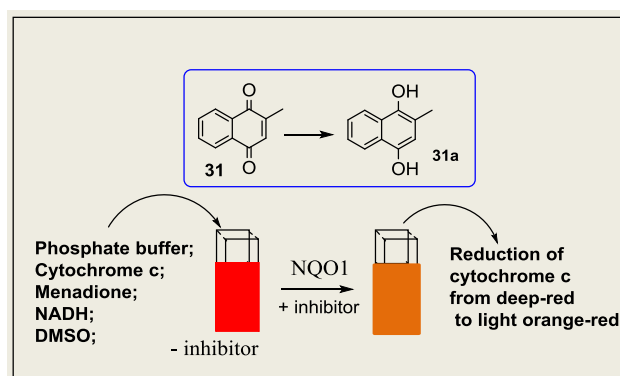


**Figure 88:** Evaluation of NQO1 activity using menadione (**31**) as intermediate electron acceptor and cytochrome c as the terminal electron acceptor.

The enzyme activity was monitored spectrophotometrically under *UV* light by monitoring the change in the absorbance at 550 nm. The experiment was carried out at constant enzyme concentration and different substrate concentrations in order to analyse structure-activity relationships (SARs).

### 3.2 Determination of IC<sub>50</sub> values

The IC<sub>50</sub> values were measured using nonlinear curve fitting as implemented in the program Excel (GraphPad Prism 5). Each measurement was made in triplicate and the experiments were repeated three times. The concentration-response plots obtained displayed a sigmoid response curve (Figure 89), and demonstrated moderate to good inhibitory potency for the NQO1 inhibitors. Low IC<sub>50</sub> values indicate that the compounds have good inhibitory potency while high values indicated poor inhibition.

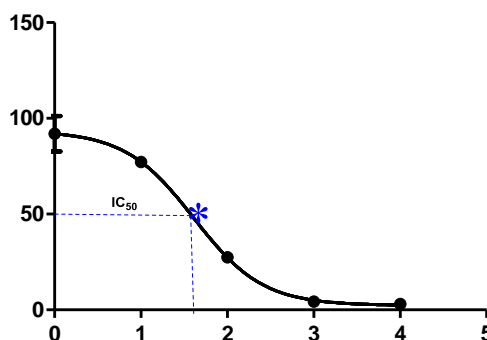
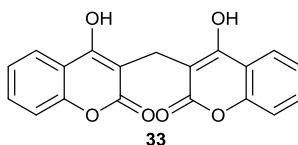


**Figure 89:** A sigmoid curve for the concentration-response plot of the enzyme assay.

### 3.3 Previous work in the Whitehead group

In 1967, Ernester and co-workers reported that dicoumarol (**33**) was the most potent inhibitor of NQO1 at that time (IC<sub>50</sub> = 2.6 nM).<sup>72</sup> Dicoumarol, however, suffered a lot of limitations such as poor selectivity towards cancer cells as it binds to many other proteins in circulating blood such as serum albumin. It caused side effects such as diarrhea, blurred vision, loss of hair, etc. Dicoumarol also caused off-target effects such as accumulation of intracellular superoxide and interference with mitochondrial function in oxidative phosphorylation.<sup>163</sup>



Human serum albumin (HSA), which is similar to Bovine serum albumin (BSA) in other mammals, is the most abundant protein in blood plasma and is produced in the liver. HSA is soluble, monomeric and constitutes about half of the blood serum protein. A drug in the blood plasma may exist in two different forms: bound or unbound. If the binding is reversible an equilibrium will exist between the bound and unbound form as shown below:



Albumin binding to a drug influences the fate of that drug in the body because it is the unbound or free drug, that diffuses through the capillary walls and reaches the target site and is also subject to elimination from the body.<sup>238</sup> In 2007, Trainer reported that the higher the concentration of the unbound drug in the blood plasma, the more effectively the drug will traverse the cell membrane or diffuse.<sup>239</sup>

In 1970, Colin reported a unique binding of dicoumarol to serum albumin which involved hydrophobic and electrostatic interactions.<sup>240</sup> In 1971, Garten and co-workers<sup>241</sup> conducted comparative studies of the binding of coumarin anticoagulants and related compounds to serum albumin. In this investigation, the group observed that coumarin binding was weak because the binding involved only the hydrophobic interaction.

A remarkable change occurred when 4-hydroxycoumarin was analysed, which resulted in a significant increase in the binding capacity. The group attributed this change to the presence of an ionisable hydroxyl group which generated a negatively charged oxygen atom capable of undergoing an electrostatic interaction with the cationic centres on the surface of the albumin protein.

Dicoumarol (**33**) with pKa values of 4.4 and 8.0<sup>242</sup> for the two hydroxy groups can exist either in a neutral (**33**), mono-anionic (**33i**) or di-ionic (**33ii**) state, and at blood plasma (pH 7.4), (**33i**) is the predominant form (Figure 90). As result of this, dicoumarol would show a greater degree of binding with the cationic centres on the surface of the serum albumin compared to coumarin itself.<sup>243</sup>

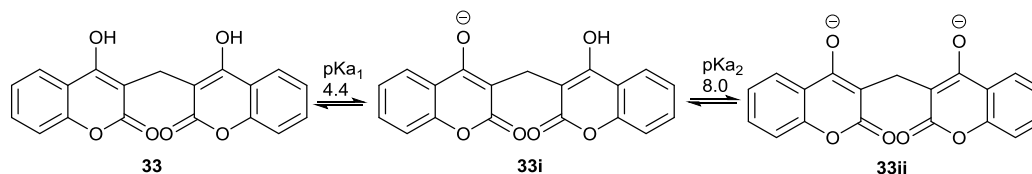
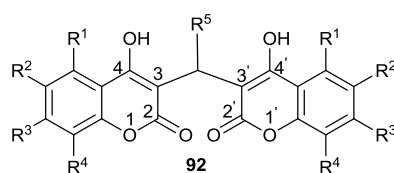


**Figure 90:** Neutral (**33**), mono-ionic (**33i**) or di-ionic (**33ii**) states of dicoumarol.<sup>242</sup>

This property of dicoumarol has stimulated scientific efforts to find novel NQO1 inhibitors with high selectivity for cancer cells and without problematic side and off-

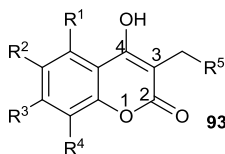
target effects. The research groups of Prof. Ian Stratford and Dr Roger Whitehead have carried out thorough investigations into the synthesis of suitable NQO1 inhibitors. In 2009, the groups synthesized a series of novel symmetrical (**92**) and asymmetrical analogues (**93**) of dicoumarol which had better inhibitory potency than dicoumarol itself.<sup>174</sup> In order to evaluate the extent to which serum albumin binding could affect the efficacy of these inhibitors, enzyme assays were conducted both in the presence and absence of BSA. Dicoumarol (**33**) and several of their derivatives such as (**92a**) and (**92b**) were assayed and (**92a**) displayed the greatest inhibitory potency in the presence of BSA ( $IC_{50} = 38 \text{ nM}$ ) as illustrated in Table 5.



Entry	R <sup>1</sup>	R <sup>2</sup>	R <sup>3</sup>	R <sup>4</sup>	R <sup>5</sup>	IC <sub>50</sub> (nM)	IC <sub>50</sub> + BSA (nM)
<b>33</b>	H	H	H	H	H	2.6 ± 1.6	404 ± 184
<b>92a</b>	OMe	H	H	H	H	2.8 ± 0.42	38 ± 2.1
<b>92b</b>	H	H	H	7,8-C <sub>4</sub> H <sub>4</sub>		0.18 ± 0.16	370 ± 198

**Table 5:**  $IC_{50}$  values of dicoumarol (**33**) and its derivatives (**92a**) and (**92b**).<sup>174</sup>

Further investigations into the asymmetrical analogues (**93**) of dicoumarol were also carried out by the research group of Stratford and Whitehead. In this investigation, the group observed that compounds with a naphthyl methyl substituent (**93a** and **93b**) showed better inhibitory potency than those with a benzyl substituent (**93c** and **93d**) as illustrated in Table 6.



Entry	R <sup>1</sup>	R <sup>2</sup>	R <sup>3</sup>	R <sup>4</sup>	R <sup>5</sup>	IC <sub>50</sub> (nM)	IC <sub>50</sub> + BSA (nM)
<b>93a</b>	H	Me	Me	H	2-naphthyl	2.5 ± 1.9	167 ± 83
<b>93b</b>	H	F	7,8-C <sub>4</sub> H <sub>4</sub>		2-naphthyl	2.2 ± 1.6	255 ± 151
<b>93c</b>	H	Me	Me	H	3,4-dimethyl phenyl	9.9 ± 4.4	192 ± 41
<b>93d</b>	H	Me	Me	H	Phenyl	39 ± 12	660 ± 108

**Table 6:**  $IC_{50}$  values of asymmetrical analogues (**93**) of dicoumarol.<sup>174</sup>

To evaluate these observations, the team conducted computational docking experiments in which both symmetrical (**92**) and asymmetrical analogues (**93**) were docked into the active site of the NQO1 enzyme. The results of this investigation suggested that the symmetrical analogue (**92**), which exists in a monoanionic form at pH 7.4, may have undergone an intramolecular hydrogen bond between the negative oxygen atom of C4 and the hydrogen atom of the hydroxyl group of C4', causing steric hinderance to the substrate conformation. The group therefore, concluded that this conformation of dicoumarol (Figure 91) and its derivatives may be the most stable in the NQO1 active site.

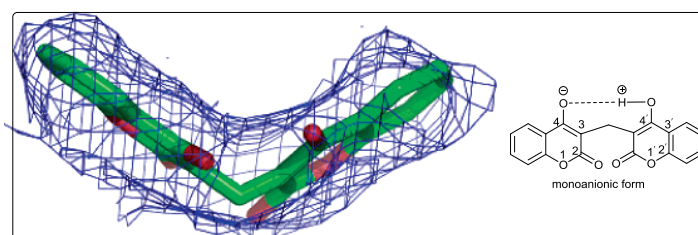


**Figure 91:** Electron density map around the dicoumarol in NQO1 active site.<sup>174</sup>

The team also attributed the potency of the asymmetrical analogues with a naphthyl ring (**93a** and **93b**) to be due to the hydrophobic interactions of the compounds with the amino acid residues of the active site. The hydrophobic nature of the active site suggested that NQO1 has better binding affinity to hydrophobic compounds.

### 3.4 IC<sub>50</sub> values of the novel synthesized compounds

Synthesis of NQO1 inhibitors has been the subject of numerous investigations. During the research programme described herein, four series of symmetrical, unsymmetrical dimer, asymmetrical and ‘halfway stage’ analogues of dicoumarol (Figure 92) were synthesized and assayed in the absence of BSA.

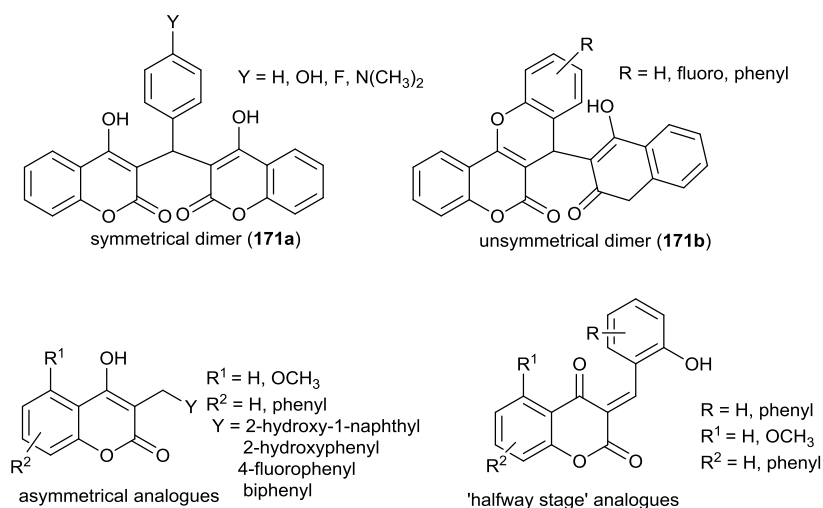


**Figure 92:** Structures of symmetrical unsymmetrical dimer, asymmetrical and ‘halfway stage’ analogues of dicoumarol.

Both symmetrical and unsymmetrical dimer analogues (**171a** and **171b**) of dicoumarol (Figure 93) were found to be ineffective as NQO1 inhibitors ( $IC_{50} > 1000$  nM).

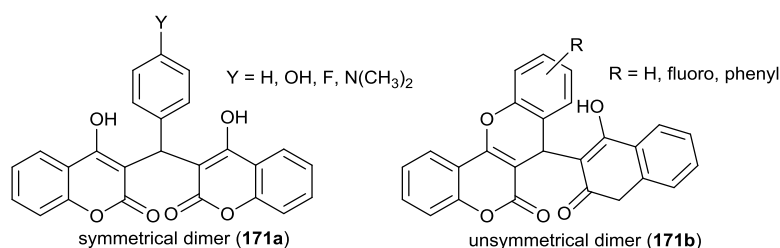
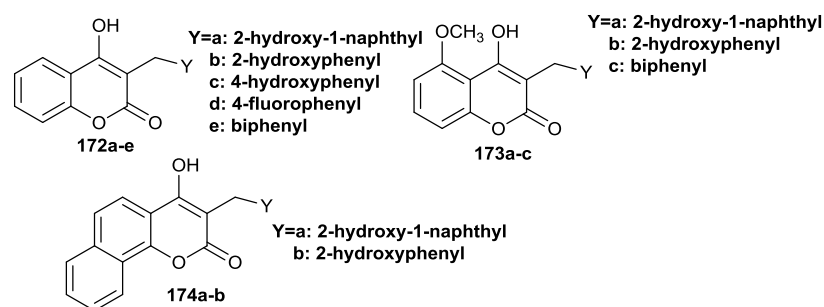


**Figure 93:** General structures of symmetrical and unsymmetrical dimer analogues (**171a** and **171b**) of dicoumarol.

Based on computational docking experiments, Stratford and co-workers proposed that the NQO1 inhibitors must be capable of hydrogen bonding interactions with the FAD cofactor and/or the key amino acid residues within the active site (Tyr-126, Tyr-128 and His-161).<sup>174</sup> A bulky substituted phenyl group would however, undergo steric clashes with the key amino acid residues within the active site, especially against the hydrophobic pocket which forms the internal wall of the binding site or FAD pocket.

The asymmetrical analogues (**172**, **173** and **174**) were also assayed and the results revealed that they are more effective as NQO1 inhibitors compared to symmetrical series (**171**) as illustrated in Table 7.





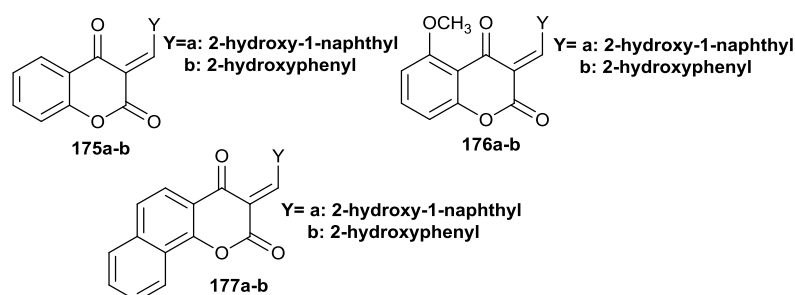
Entry	Y	NQO1, IC <sub>50</sub> (nM)
<b>172a</b>	2-hydroxy-1-naphthyl	11 ± 3
<b>172b</b>	2-hydroxyphenyl	940 ± 36
<b>172c</b>	4-hydroxyphenyl	464 ± 134
<b>172d</b>	4-fluorophenyl	528 ± 5
<b>172e</b>	Biphenyl	47 ± 3
<b>173a</b>	2-hydroxy-1-naphthyl	41 ± 21
<b>173b</b>	2-hydroxyphenyl	663 ± 286
<b>173c</b>	Biphenyl	79 ± 30
<b>174a</b>	2-hydroxy-1-naphthyl	19 ± 9
<b>174b</b>	2-hydroxyphenyl	74 ± 15

**Table 7:** IC<sub>50</sub> values of asymmetrical analogues of dicoumarol obtained by reduction using NaBH<sub>4</sub>/LiBH<sub>4</sub> and NaCNBH<sub>3</sub>.

Compounds (**172a**, **173a** and **174a**) bearing a substituted naphthyl ring displayed higher inhibitory potency than those with a substituted phenyl ring (**172b** and **173b**). These differences in the IC<sub>50</sub> values could be a result of the naphthyl ring undergoing hydrophobic interactions with the NQO1 enzyme. The phenyl ring is less hydrophobic than the naphthyl ring and this may be the reason that the analogues are less effective as NQO1 inhibitors. To make (**173b**) more hydrophobic, (**174a** and **174b**) were synthesized and assayed. Interestingly, the IC<sub>50</sub> value of (**174b**) improve from 940 ± 36 nM to 74 ± 15 nM thus confirming the importance of hydrophobic interactions of inhibitors at the NQO1 active site.

Introduction of a fluoro group (**172d**) gave a higher IC<sub>50</sub> value (528 ± 5 nM) when compared to (**172e**) which bears a biphenyl ring (47 ± 3 nM). This again suggested that the NQO1 active site binds more effectively to hydrophobic compounds.

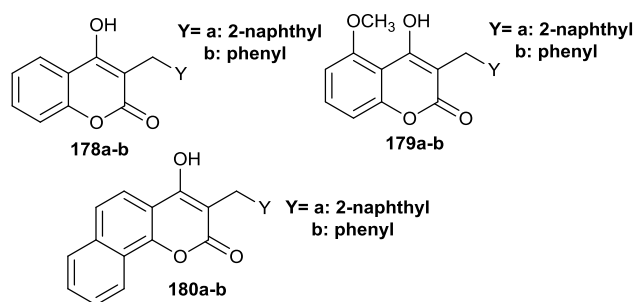
Further investigations were carried out on the “half-way stage” compounds (**175**, **176** and **177**) which had been synthesized. The compounds were assayed as NQO1 inhibitors in the absence of BSA and the IC<sub>50</sub> values obtained followed a similar trend to that previously discussed with the more hydrophobic compounds showing the greatest potency (Table 8).



Entry	Y	NQO1, IC <sub>50</sub> (nM)
<b>175a</b>	2-hydroxy-1-naphthyl	20 ± 6
<b>175b</b>	2-hydroxyphenyl	341 ± 115
<b>176a</b>	2-hydroxy-1-naphthyl	25 ± 10
<b>176b</b>	2-hydroxyphenyl	165 ± 88
<b>177a</b>	2-hydroxy-1-naphthyl	23 ± 5
<b>177b</b>	2-hydroxyphenyl	85 ± 49

**Table 8:** IC<sub>50</sub> values of the “half-way stage” analogues of dicoumarol.

Another set of asymmetrical analogues of dicoumarol, prepared using borrowing hydrogen methodology, were assayed in the absence of BSA and their IC<sub>50</sub> values are summarized in Table 9. In this case, the IC<sub>50</sub> values followed a similar trend with the naphthyl substituted compounds being more active as NQO1 inhibitors than those with phenyl substituents.



Entry	Y	NQO1, IC <sub>50</sub> (nM)
<b>178a</b>	2-naphthyl	55 ± 23
<b>178b</b>	Phenyl	416 ± 145
<b>179a</b>	2-naphthyl	47 ± 14
<b>179b</b>	Phenyl	898 ± 16
<b>180a</b>	2-naphthyl	6 ± 2
<b>180b</b>	Phenyl	125 ± 17

**Table 9:** IC<sub>50</sub> values of the asymmetrical analogues of diocoumarol prepared using ‘borrowing hydrogen methodology’.

In 2014, a previous postgraduate member of the Whitehead group carried out computational studies of the inhibitors (**179a**), (**180a**) with the enzyme NQO1.<sup>244</sup> In these experiments, the two inhibitors were stacked in a parallel orientation with the isoalloxazine ring of FAD, in the same manner to the binding mode of dicoumarol (**33**). It was found that (**179a**) had one polar active site interaction with Tyr 128, whereas, (**180a**) had two polar active site interactions with both Tyr 128 and His 161. The group therefore, attributed the difference in the IC<sub>50</sub> values to the absence of a polar active site interaction with His 161 in (**179a**). The team hypothesized that a NQO1-directed antitumor agent should be capable of hydrogen bonding interactions with the key amino acid residues (Tyr 126, 128 and His 161) and/or with the FAD cofactor.

### 3.5 Cytotoxicity assay

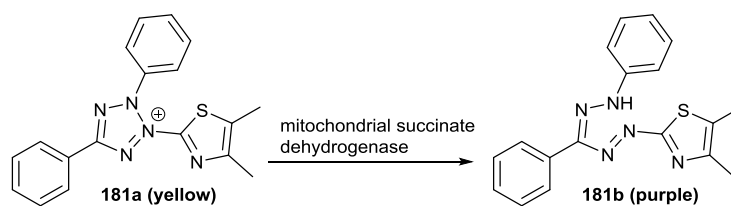
The use of cytotoxic drugs still remains an unavoidable therapeutic approach to the treatment of malignant tumors. Due to the remarkable inhibition of NQO1 by the asymmetrical and “halfway stage” analogues of dicoumarol, derivatives of these

compounds (Figure 87 above) were designed and synthesized and their antiproliferative activity towards a cancer cell line was analyzed. A non-small-cell adenocarcinoma cell line A549 was chosen for this study as a result of the following:

- It has up-regulation of NQO1 activity;<sup>245</sup>
- It has elevated levels of glutathione and glutathione transferase (GST/GSH). Since an analogue of antheminone A was used for the prodrug synthesis, GST/GSH are needed for conjugation to the prodrug and release of the NQO1 inhibitor.

### 3.5.1 MTT cell viability assay

The MTT cell viability is a colourimetric assay for measuring cell viability. In living cells, the enzyme mitochondrial succinate dehydrogenase is capable of reducing 3-(4,5-dimethylthiazol-2-yl)-2,5-diphenyl tetrazolium bromide (MTT, **181a**), a yellow dye, to insoluble formazan (**181b**) which shows a purple colouration (Scheme 69).<sup>246</sup> The amount of formazan crystal formed is dependent on the number of living cells. The experimental procedure is summarized in Chapter 5.



**Scheme 69:** Reduction of MTT dye (**181a**) (yellow) to formazan (**181b**) (purple) by mitochondrial succinate dehydrogenase.<sup>246</sup>

### 3.5.2 Evaluation of the IC<sub>50</sub> values of the novel compounds

An IC<sub>50</sub> value, in terms of an enzyme assay, represents the concentration of a drug that is required for 50% inhibition *in vitro*, whereas, in terms of cytotoxicity, it represents the concentration of a drug required to inhibit the growth of cells by 50%. For the MTT cell viability assay, it represents the concentration at which half of the cells seeded remain viable at the end of the analysis.

The MTT cell viability assay was carried out on thirteen compounds prepared during this project by another member of the Whitehead research group. The first set of compounds comprised COTC/antheminone hybrid analogues (**182**, **183** and **184**) depicted in Figure 94.

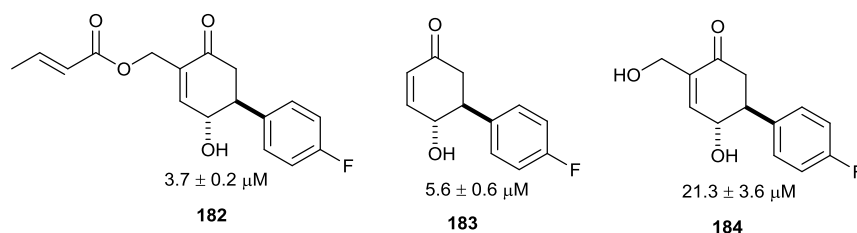


**Figure 94:** IC<sub>50</sub> values for the synthetic analogues (**182**) of COTC, (**183**) and (**184**) for antheminone A.

In this case, the COTC analogue (**182**) displayed higher toxicity towards the A549 cell line than (**183**) and the analogue of antheminone A (**184**). The reason for this significant difference in the IC<sub>50</sub> values may be due to the poor leaving group ability of the OH group in (**184**) which consequently cannot be displaced by GSH.

The asymmetrical analogues of dicoumarol (**172a** and **178a**), which showed a reasonable inhibitory potency ( $11 \pm 3$  nM and  $55 \pm 23$  nM respectively) towards NQO1, were inactive with respect to cytotoxicity. Compound (**178a**) was modified by synthesizing ‘prodrug’ (**185**), the IC<sub>50</sub> value of which showed moderate toxicity as illustrated in Figure 95.

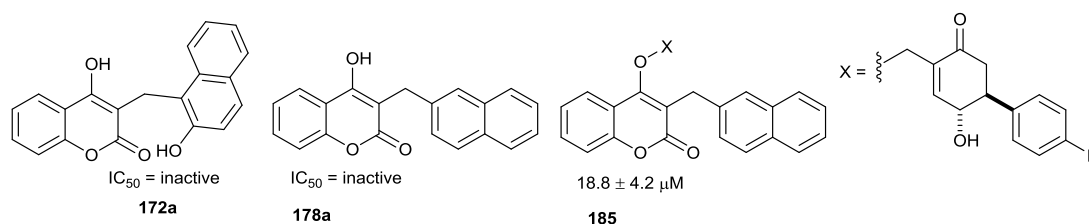


**Figure 95:** IC<sub>50</sub> value of the prodrug (**185**).

The “halfway stage” analogues of dicoumarol (**175a** and **177b**), which were also effective NQO1 inhibitor (IC<sub>50</sub> =  $20 \pm 6$  nM and  $85 \pm 49$  nM respectively), were tested for cell cytotoxicity. Compound (**175a**) showed moderate toxicity (IC<sub>50</sub> =  $9.2 \pm 0.2$  µM), whereas, compound (**177b**) was inactive. The reason for this significant difference is still unknown. Modification of the two compounds (**175a**) and (**177b**) as ‘prodrugs’ (**186**) and (**187**), gave the IC<sub>50</sub> values of  $2.9 \pm 0.3$  µM and  $3.0 \pm 0.4$  µM respectively which were more potent than the parent compounds (Figure 96).

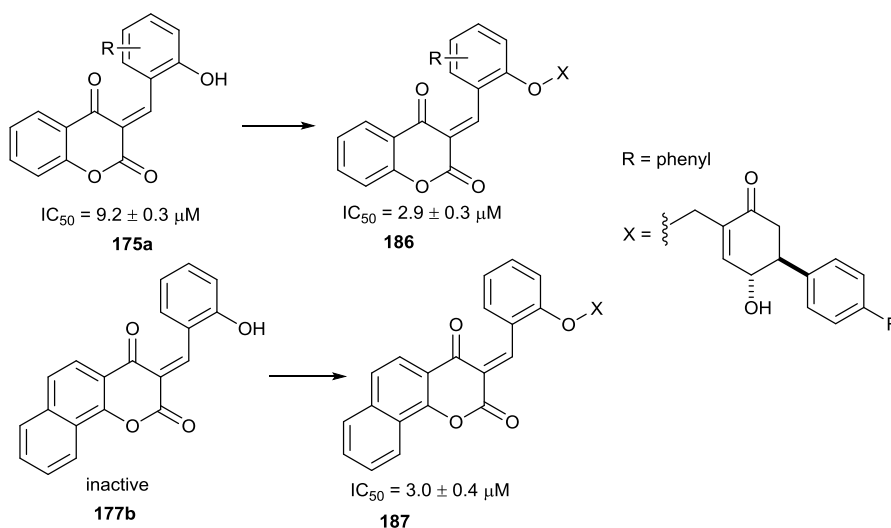


**Figure 96:**  $IC_{50}$  values of the “halfway stage” analogue of dicoumarol (175a) and the prodrug (186).

The potency of both the “halfway stage” (175a) and other prodrugs analyzed motivated further investigation into compounds with related structures as depicted in Figure 97. These compounds also displayed toxicity towards the A549 cancer cell line.

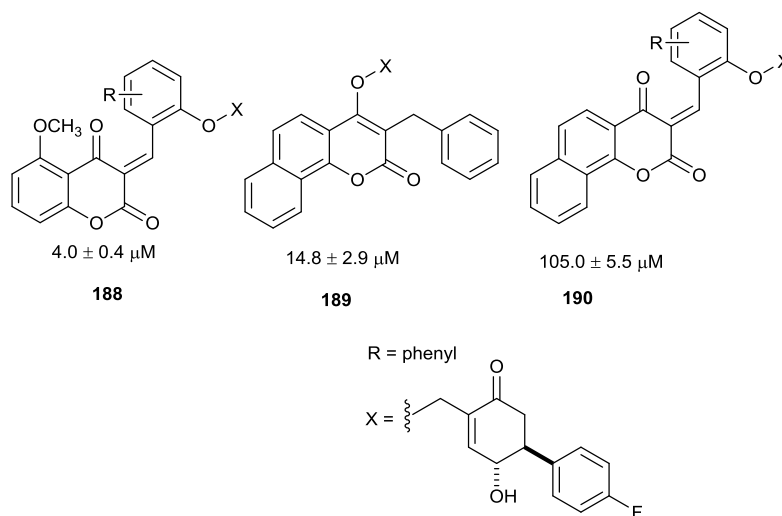


**Figure 97:** Potent inhibitors of NQO1 remodified as prodrug and their measured  $IC_{50}$  values for cell viability.

#### 4.0 Chapter 4: Conclusion and future work

Due to up-regulation of NQO1 in most solid tumors, it is believed that targeting this enzyme in chemotherapeutic treatment could help in the treatment of cancer. In 1967, Ernester and co-workers discovered that dicoumarol (**33**) was the most potent inhibitor of NQO1 ( $IC_{50} = 2.6 \text{ nM}$ ).<sup>72</sup> Dicoumarol suffered some limitations such as side effects and also off-target effects. These have led to more extensive investigations into finding novel effective inhibitors of NQO1 without problematic side and off-target effects like dicoumarol (**33**).

The research groups of Whitehead and Stratford have contributed immensely to these research investigations. For example, in the year 2009,<sup>174</sup> the collaborating team discovered that (**92a** and **92c**) are more effective inhibitors of NQO1 compared to dicoumarol (**33**) and its benzo derivative (**92b**) as illustrated in Figure 98.

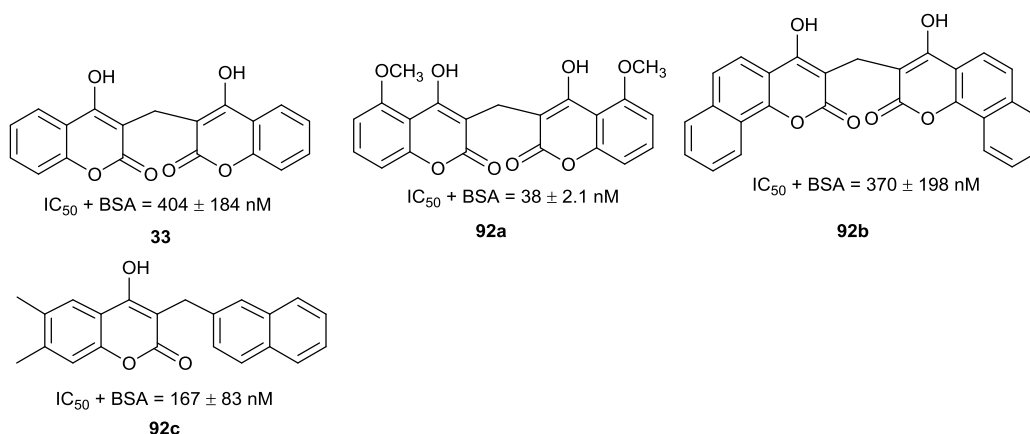


**Figure 98:**  $IC_{50}$  values of dicoumarol (**33**) and its derivatives (**92a**, **92b** and **92c**).

In the search for more potent inhibitors of NQO1, a variety of novel potent inhibitors (section 3.4) of NQO1 have been synthesized using different techniques such as ‘borrowing hydrogen methodology’, reductive C-C cleavage with  $NaBH_3CN$ ,  $LiBH_4$  and  $NaBH_4$ . Those compounds, which all contain a naphthyl ring have proved to be more potent than those consisting only phenyl rings as depicted in Tables 7, 8 and 9 (section 3.4).

Since the use of cytotoxic drugs is an unavoidable therapeutic method for the treatment of cancer, MTT assay was carried out on some of these inhibitors. Among the inhibitors assayed, (**175a**) is remarkable as it is not only effective as a NQO1

inhibitor ( $IC_{50} = 20 \pm 6$  nM), but it also displayed toxicity towards A549 cancer cell line ( $IC_{50} = 9.2 \pm 0.3$   $\mu$ M). To further understand the significant potency of (**175a**) towards the A549 cell line, another compound of related structure (**177b**) was synthesized and assayed. The results revealed that (**177b**) was inactive towards the A549 cell line. To conclude on this unique property displayed by (**175a**), MTT assays were carried out for (**172a**) and (**178a**) and both were inactive towards A549 as shown in Figure 99.

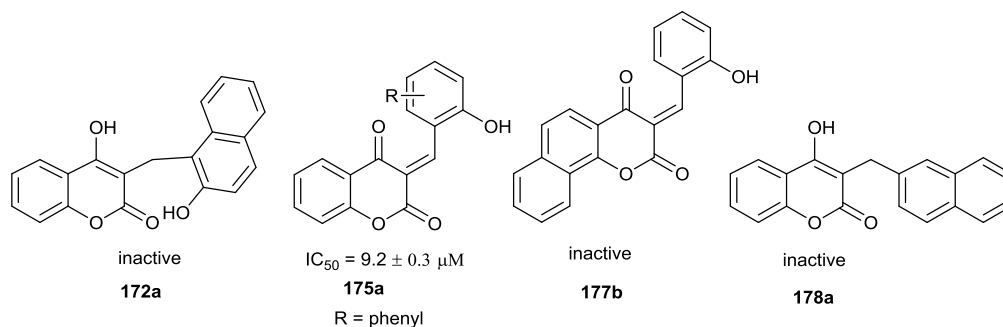


**Figure 99:** Cytotoxicity values of (**172a**, **175a**, **177b** and **178a**).

To gain access to their site of action, drugs must cross one or more barriers especially the plasma and the intracellular membranes of the cells. In view of this, some of the potent inhibitors were remodified by inclusion of a cytotoxic agent (**184**) derived from antheminone A, (**47**) as depicted in Figure 100. The inclusion of cytotoxic agent (**184**) was to help to deliver the inhibitors to their site of action.

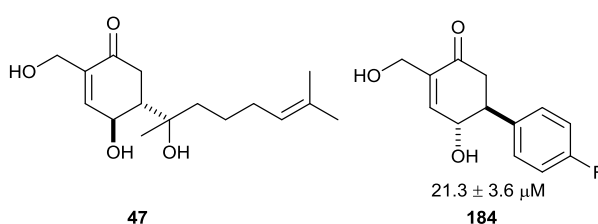


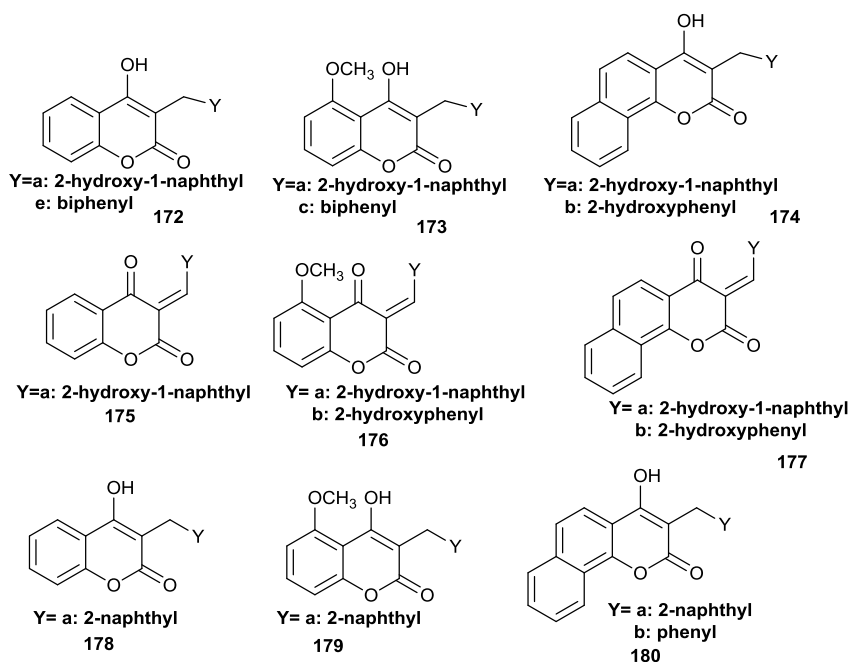
**Figure 100:** Cytotoxic agent (**184**) derived from antheminone A (**47**).

These prodrugs were synthesized *via* application of the Mitsunobu reaction which resulted in the synthesis of several novel prodrugs (**185**, **216**, **218**, **220**, **190**, **188**, **189**, **186** and **187**) as described in Chapter 5. These novel prodrugs displayed good potency towards A549 cell line which has up-regulated level of NQO1 activity.



The cytotoxicity properties of these novel prodrugs however, are yet to be understood. Since the A549 cell is up-regulated in NQO1 activity, it could be hypothesized that NQO1 played a significant role in the toxicity of these novel prodrugs. To verify this hypothesis, another mutant cell line which contain no NQO1 can be used in the MTT assay. Due to time limits, another member of the Whitehead research group will continue with this investigation.

In summary, 75 compounds have been synthesized. Out of these, 15 were effective inhibitors of NQO1 (Table 10).



Entry	Y	NQO1, IC <sub>50</sub> (nM)
<b>172a</b>	2-hydroxy-1-naphthyl	11 ± 3
<b>172e</b>	biphenyl	47 ± 3
<b>173a</b>	2-hydroxy-1-naphthyl	41 ± 21
<b>173c</b>	biphenyl	79 ± 30
<b>174a</b>	2-hydroxy-1-naphthyl	19 ± 9
<b>174b</b>	2-hydroxyphenyl	74 ± 15
<b>175a</b>	2-hydroxy-1-naphthyl	20 ± 6
<b>176a</b>	2-hydroxy-1-naphthyl	25 ± 10
<b>176b</b>	2-hydroxyphenyl	165 ± 88
<b>177a</b>	2-hydroxy-1-naphthyl	23 ± 5
<b>177b</b>	2-hydroxyphenyl	85 ± 49
<b>178a</b>	2-naphthyl	55 ± 23
<b>179a</b>	2-naphthyl	47 ± 14
<b>180a</b>	2-naphthyl	6 ± 2
<b>180b</b>	Phenyl	125 ± 17

**Table 10:** The effective inhibitors of NQO1.

The application of the Mitsunobu reaction has proven very efficient for the synthesis of prodrugs and this has led to the identification of a number of novel antitumor agents as depicted in Figure 101. Other potential anti-tumor agents synthesized are shown in Figure 102.

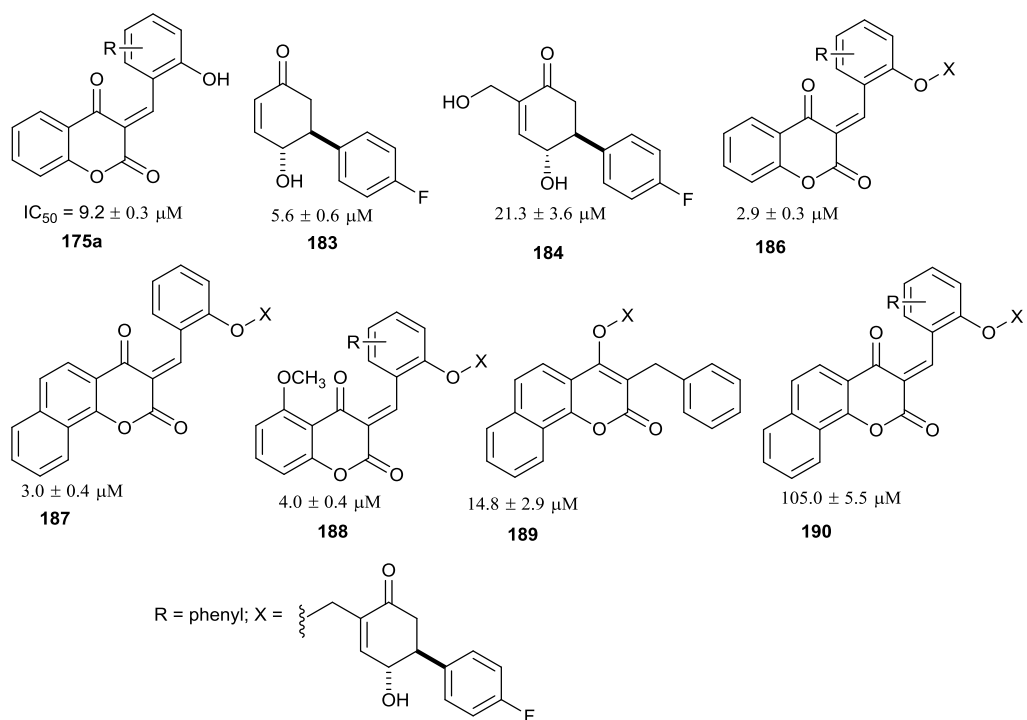


**Figure 101:** Structures of novel anti tumor agents.

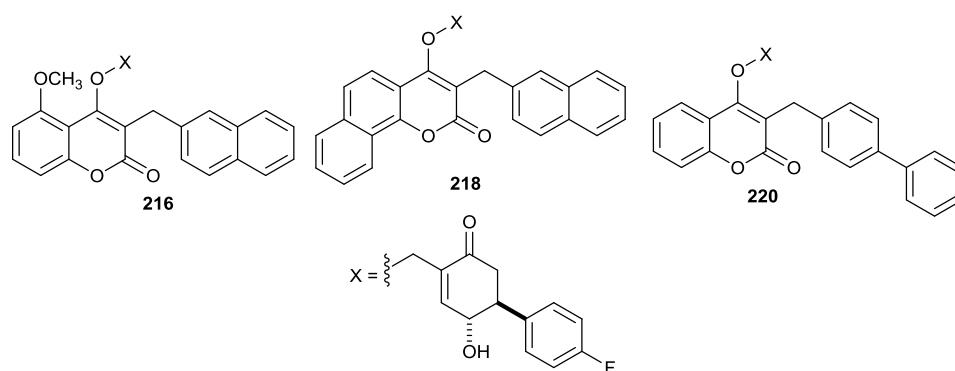


**Figure 102:** The potential anti tumor agents (**216**, **218** and **220**).

## **5.0 Chapter 5: Experimental Procedures**

### **5.1 Instrumentation**

Column chromatography was carried out using silica gel (Sigma-Aldrich) 40-63  $\mu\text{m}$  60Å or pH neutral alumina. The eluents used are reported in individual procedures.

Melting points were determined using a Sanyo Gallenkamp MPD.350 variable heater instrument and are uncorrected.

Infrared spectra were recorded in the solid state using a Bruker Alpha P FT-IR instrument. Absorption maxima were recorded in wavenumbers ( $\text{cm}^{-1}$ ) and the following abbreviations were used: weak (w), medium (m), strong (s) and broad (b).

$^1\text{H}$ -NMR spectroscopy was carried out using Bruker Avance 400 and 500 spectrometers. The chemical shift values ( $\delta_{\text{H}}$ ) are quoted in parts per million (ppm) to the nearest 0.01 ppm and referenced to the solvent residual peak. The coupling constant ( $J$ ) are given in Hz. Abbreviations used are: s-singlet, d-doublet, dd-doublet of doublets, q-quaternary carbon, t-triplet, td-triplet of doublets, m-multiplet. Proton assignments were assisted by DEPT,  $^1\text{H}$  COSY and HMQC.

$^{13}\text{C}$ -NMR spectroscopy was carried out using Bruker Avance (100 and 125 MHz) spectrometers. The chemical shifts ( $\delta_{\text{C}}$ ) are quoted in parts per million (ppm), with tetramethylsilane or the appropriate solvent peak as the reference peak.  $^{13}\text{C}$ -NMR spectra were assigned using DEPT and HMQC.

$^{19}\text{F}$ -NMR spectroscopy was carried out using Bruker Avance (376 MHz) spectrometers. The chemical shifts ( $\delta_{\text{F}}$ ) are quoted in parts per million (ppm), with tetramethylsilane or the appropriate solvent peak as the reference peak. Abbreviation used is: s-singlet.

Mass spectrometry was carried out by the Mass Spectrometry Laboratory at the School of Chemistry, University of Manchester. Molecular ions and their fragment ions are reported as mass/charge ( $m/z$ ) ratios and are within  $\pm 10$  ppm mass units for electrospray (ES) and high resolution mass spectrometry (HRMS). These were

obtained using a Micromass Platform II (ES), Waters QTOF (HRMS), and Thermo Finnegan MAT95XP (HRMS).

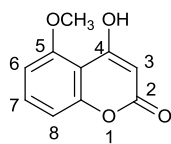
A Biotage Initiator TM microwave reactor (maximum power output of 300 W; operating frequency 2450 MHz) was used in the studies.

## 5.2 Reagents and conditions

All reagents used were obtained from commercial sources (Sigma-Aldrich Co., Alfa Aesar, Fisher Scientific, and ACROS Organics). The chemicals were handled according to the safety instructions and all reactions were carried out inside a fume cupboard. Microwave irradiation reactions were carried out using a Biotage® Initiator microwave synthesizer.

## 5.3 Experimental

### 5.3.1 Synthesis of 4-hydroxy-5-methoxy-2H-chromen-2-one, **191**.

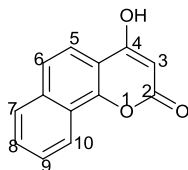


C<sub>10</sub>H<sub>8</sub>O<sub>4</sub>; Molecular weight: 192.17

2-Hydroxy-6-methoxyacetophenone (500 mg, 3.01 mmol) dissolved in diethylcarbonate (3 mL) was added to a suspension of sodium hydride (60% dispersion in mineral oil, 600 mg, 15.0 mmol) in diethylcarbonate (3 mL) and heated at 100 °C for 3 hours. The reaction mixture was left to cool to 0 °C in an ice bath and it was then quenched by dropwise addition of water until effervescence stopped. The aqueous layer was washed with diethyl ether (3 x 10 mL). Concentrated hydrochloric acid was added dropwise to the aqueous layer to adjust the pH to 4 and the resulting precipitate was collected by filtration, washed with water and left to dry overnight at 90 °C. The title compound (**191**) was isolated as an off-white solid (360 mg, 62%): Mp 155-157 °C [Lit.<sup>247</sup> 151-156 °C];  $\nu_{\max}/\text{cm}^{-1}$  3260 (w, OH), 1705 (s, C=O), 1640 (s, C=C);  $\delta_{\text{H}}$  (400 MHz; DMSO-*d*<sub>6</sub>) 3.89 (3H, s, OCH<sub>3</sub>), 5.50 (1H, s, C(3)H), 6.95 (2H, d, *J* 8.5, C(6)H and C(8)H), 7.56 (1H, t, *J* 8.5, C(7)H), 11.35 (1H, s, OH);  $\delta_{\text{C}}$  (100 MHz; DMSO-*d*<sub>6</sub>) 56.5 (OCH<sub>3</sub>), 90.8 (C(3)H), 105.0 (q), 106.7 (CH), 109.2 (CH),

133.0 (CH), 155.2 (q), 157.3 (q), 161.4 (q), 167.2 (C=O);  $m/z$  (+ES) 215.1 ( $[M+Na]^+$ , 100%); (Found 215.0329;  $C_{10}H_8O_4Na$  ( $[M+Na]^+$ ) requires 215.0320).

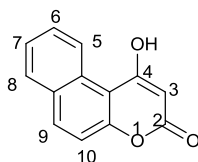
### 5.3.2 Synthesis of 4-hydroxy-2H-benzo[h]chromen-2-one, **192**



$C_{13}H_8O_3$ ; Molecular weight: 212.20

Using the procedure described for the synthesis of compound (**191**), 1-hydroxy-2-acetophenone (1.5 g, 8.06 mmol), diethylcarbonate (20 mL) and sodium hydride (1.8 g, 45.0 mmol), gave the title compound (**192**) as an off white solid (1.14 g, 67%): Mp 285-287 °C [Lit.<sup>248</sup> 287 °C];  $\nu_{max}/cm^{-1}$  3410 (br, s, OH), 1644 (s, C=O);  $\delta_H$  (400 MHz; DMSO- $d_6$ ) 5.70 (1H, s, C(3)H), 7.70-7.74 (2H, m, Ar-CH), 7.82-7.84 (2H, m, Ar-CH), 8.03-8.05 (1H, m, Ar-CH), 8.34-8.36 (1H, m, Ar-CH), 12.67 (1H, br, s, OH);  $\delta_C$  (100 MHz; DMSO- $d_6$ ) 90.6 (CH), 111.1 (q), 118.9 (CH), 121.7 (CH), 122.2 (q), 123.6 (CH), 127.3 (CH), 128.1 (CH), 128.8 (CH), 134.8 (q), 150.7 (q), 161.8 (q), 166.6 (q);  $m/z$  (-ES) 211.1 ( $[M-H]^-$ , 100%); (Found 211.0392;  $C_{13}H_7O_3$  ( $[M-H]^-$ ), requires 211.0395).

### 5.3.3 Synthesis of 1-hydroxy-3H-benzo[f]chromen-3-one, **193**

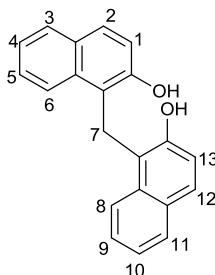


$C_{13}H_8O_3$ ; Molecular weight: 212.20

Using the procedure described for the synthesis of compound (**191**), 2-hydroxy-1-acetophenone (1.5 g, 8.06 mmol), diethylcarbonate (20 mL) and sodium hydride (1.8 g, 45.0 mmol) gave the title compound (**193**) as an off-white solid (1.14 g, 67%): Mp 285-286 °C [Lit.<sup>174</sup> 284 °C];  $\nu_{max}/cm^{-1}$  3376 (br, w, OH), 1650 (s, C=O);  $\delta_H$  (400 MHz; DMSO- $d_6$ ) 5.76 (1H, s, C(3)H), 7.53 (1H, d,  $J$  8.6, C(9)H or C(10)H), 7.60 (1H, ddd,  $J$  8.6, 7.0, 1.5, C(6)H or C(7)H), 7.70 (1H, ddd,  $J$  8.6, 7.0, 1.5, C(6)H or C(7)H), 8.04 (1H, dd,  $J$  8.6, 1.5, C(5)H or C(8)H), 8.21 (1H, d,  $J$  8.6, C(9)H or C(10)H), 9.29 (1H,

dd,  $J$  8.6, 1.5, C(5)H or C(8)H), 12.93 (1H, br, s, OH);  $\delta_C$  (100 MHz; DMSO- $d_6$ ) 91.7 (CH), 108.6 (q), 117.2 (CH), 125.6 (CH), 126.0 (CH), 128.3 (CH), 128.8 (q), 128.9 (CH), 130.3 (q), 134.2 (CH), 154.9 (q), 161.3 (q), 169.4 (C=O);  $m/z$  (-ES) 211.1 ([M-H]<sup>-</sup>, 100%); (Found 211.0392; C<sub>13</sub>H<sub>7</sub>O<sub>3</sub> ([M-H]<sup>-</sup>), requires 211.0395).

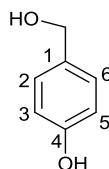
#### 5.3.4 Synthesis of 1,1'-methylenebis(naphthalen-2-ol), **194**



C<sub>21</sub>H<sub>16</sub>O<sub>2</sub>; Molecular weight: 300.35

A solution of 2-hydroxy-1-naphthaldehyde (500 mg, 2.90 mmol) and methanol (40 mL) was stirred for 10 minutes at room temperature. Sodium borohydride (220 mg, 5.81 mmol) was added portionwise, with stirring at 0 °C and the reaction mixture was then left to stir at room temperature for 24 hours. The progress of the reaction was monitored by TLC and after it had reached completion, dilute hydrochloric acid (0.1M, 10mL) was added. The resulting precipitate was collected by filtration and the crude product was isolated as a dark red solid (240 mg). This material was purified using flash column chromatography (petroleum: ethyl acetate, 4:1) and the title compound (**194**) was isolated as white solid (150 mg, 30%): Mp 202-204 °C [Lit.<sup>249</sup> 192-193 °C];  $\nu_{\max}/\text{cm}^{-1}$  3302 (s, br, OH), 1596 (s, C=C);  $\delta_H$  (400 MHz; DMSO- $d_6$ ) 4.70 (2H, s, C(7)H<sub>2</sub>), 7.08-7.14 (2H, m, Ar-CH), 7.16-7.20 (2H, m, Ar-CH), 7.28 (2H, d,  $J$  8.8, C(1)H and C(13)H or C(2)H and C(12)H), 7.59 (2H, d,  $J$  8.8, C(1)H and C(13)H or C(2)H and C(12)H), 7.65 (2H, dd,  $J$  8.8, 1.0, C(3)H and C(8)H or C(6)H and C(11)H), 8.19 (2H, d,  $J$  8.8, C(3)H and C(8)H or C(6)H and C(11)H), 10.13 (2H, s, 2 x OH);  $\delta_C$  (100 MHz; DMSO- $d_6$ ) 20.1 (CH(7)H<sub>2</sub>), 118.1 (CH), 119.4 (q), 122.1 (CH), 123.8 (CH), 125.4 (q), 127.4 (CH), 128.0 (CH), 128.4 (CH), 133.7 (q), 151.7 (q);  $m/z$  (+ES) 156.8 (C<sub>11</sub>H<sub>8</sub>O, 58%), 317.8 ([M+NH<sub>4</sub>]<sup>+</sup>, 30%).

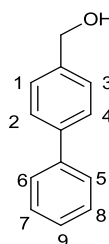
### 5.3.5 Synthesis of 4-(hydroxymethyl)phenol, **195**



C<sub>7</sub>H<sub>8</sub>O<sub>2</sub>; Molecular weight: 124.14

Using using the procedure for the synthesis of compound (**194**), 4-hydroxybenzaldehyde (2 g, 16.38 mmol) and sodium borohydride (1.3 g, 32.75 mmol) in methanol (30 mL) gave the title compound (**195**) as white solid (680 mg, 33%). Mp 115-117 °C (Lit.<sup>250</sup> 116-118 °C);  $\nu_{\max}/\text{cm}^{-1}$  3306-3436 (br, OH), 3022 (w, C-H), 1762 (s, C=C);  $\delta_{\text{H}}$  (400 MHz; DMSO-*d*<sub>6</sub>), 4.41 (2H, d, *J* 5.6, CH<sub>2</sub>OH), 5.01 (1H, t, *J* 5.6, CH<sub>2</sub>OH), 6.76 (2H, d, *J* 8.2, C(3)H and C(5)H), 7.16 (2H, d, *J* 8.2, C(2)H and C(6)H), 9.23 (1H, s, C(4)OH);  $\delta_{\text{C}}$  (100 MHz; DMSO-*d*<sub>6</sub>), 62.7 (CH<sub>2</sub>OH), 114.7 (C(3)H) and (C(5)H), 128.0 (C(2)H) and (C(6)H), 131.6 (q), 156.1 (q). *m/z* (-ES) 123.1 ([M- H]<sup>-</sup>, 85%).

### 5.3.6 Synthesis of [1,1'-biphenyl]-4-ylmethanol, **196**



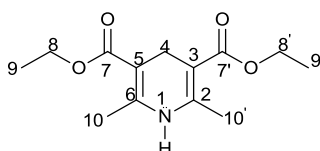
C<sub>13</sub>H<sub>12</sub>O; Molecular weight: 184.23

Lithium borohydride (144 mg, 6.59 mmol) was stirred in THF (8 mL) at room temperature under nitrogen gas for 15 minutes. A solution of 4-phenylbenzaldehyde (600 mg, 3.29 mmol) in THF (8 mL) was added gradually at 0 °C. After the addition was complete the reaction was allowed to stir at room temperature for 24 hours. The reaction was quenched by pouring onto cold 0.1 M HCl (10 mL) and organic material was then extracted into ethyl acetate (3 x 20 mL). The combined organic phases were dried over MgSO<sub>4</sub> and concentrated *in vacuo* to give the crude product as a white solid (560 mg). This material was purified by flash column chromatography (petroleum ether: ethyl acetate 5:1) to give the title compound (**196**) as white solid (550 mg, 91%): Mp 101-103 °C [Lit.<sup>251</sup> 103-106 °C];  $\nu_{\max}/\text{cm}^{-1}$  3221 (br, OH);  $\delta_{\text{H}}$  (400 MHz; DMSO-*d*<sub>6</sub>) 4.59 (2H, d, *J* 5.6, CH<sub>2</sub>OH), 5.29 (1H, t, *J* 5.6,



CH<sub>2</sub>OH), 7.37-7.40 (1H, m, Ar-CH), 7.44-7.51 (4H, m, Ar-CH), 7.65-7.70 (4H, m, Ar-CH);  $\delta_C$  (100 MHz; DMSO-*d*<sub>6</sub>); 62.6 (CH<sub>2</sub>), 126.4 (CH), 126.5 (CH), 127.0 (CH), 127.2 (CH), 128.9 (CH), 138.5 (q), 140.1 (q), 141.7 (q); *m/z* (-ES) 183.2 ([M-H]<sup>-</sup>), 38%).

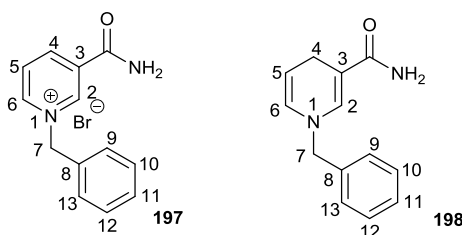
### 5.3.7 Synthesis of diethyl-2,6-dimethyl-1,4-dihydropyridine-3,5-dicarboxylate (Hantzsch's ester), **109**



C<sub>13</sub>H<sub>19</sub>NO<sub>4</sub>; Molecular weight: 253.29

A mixture of ethyl acetoacetate (988 mg, 7.59 mmol), ammonium acetate (430 mg, 5.58 mmol) and formaldehyde (110 mg, 3.66 mmol) was heated at 85°C for 10 minutes. After the product was collected by filtration and recrystallized from ethanol. The title compound (**109**) was isolated as a yellow solid (614 mg, 67%): Mp 178-180 °C [Lit.<sup>252</sup> 183-184 °C];  $\nu_{\max}$ /cm<sup>-1</sup> 3349 (s, N-H), 1691 (s, C=O), 1648 (s, C=C);  $\delta_H$  (400 MHz; CDCl<sub>3</sub>) 1.19 (6H, t, *J* 7.1, C(9)H<sub>3</sub> and C(9')H<sub>3</sub>), 2.10 (6H, s, C(10)H<sub>3</sub> and C(10')H<sub>3</sub>), 3.17 (2H, s, C(4)H<sub>2</sub>), 4.06 (4H, q, *J* 7.1, C(8)H<sub>2</sub> and C(8')H<sub>2</sub>), 5.11 (1H, s, N-H);  $\delta_C$  (100 MHz; CDCl<sub>3</sub>) 14.5 (CH), 19.2 (CH), 25.3 (CH), 61.5 (q), 99.5 (q), 141.0 (Ar-CH), 168.1 (C=O); *m/z* (-ES) 252.1 ([M-H]<sup>-</sup>, 100%); (+ES) (Found 276.1208; C<sub>13</sub>H<sub>19</sub>NO<sub>4</sub>Na ([M+Na]<sup>+</sup>), requires 276.1212).

### 5.3.8 Synthesis of 1-benzyl-1,4-dihydropyridine-3-carboxamide, **198**



C<sub>13</sub>H<sub>14</sub>N<sub>2</sub>O; Molecular weight: 214.26

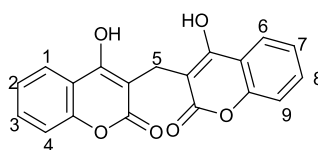
Benzylbromide (616 mg, 3.6 mmol) was added to a solution of nicotinamide (366 mg, 3.0 mmol) dissolved in a mixture of dioxane (8 mL) and methanol (2 mL). The reaction mixture was heated under reflux at 80 °C for 5 hours. The resulting precipitate was collected by filtration and washed with dioxane (2 x 5 mL) to give the title compound (**197**) as a silver white solid (790 mg, 90%). Sodium dithionite

(475 mg, 2.73 mmol) was added gradually to a solution of sodium carbonate (361 mg, 3.41 mmol) and pyridinium salt (**197**) (200 mg, 0.68 mmol) in water (5 mL) and the reaction was heated at reflux for 3 hours. The resulting precipitate was collected by filtration and washed with water (5 mL) to give the title compound (**198**) as a yellow solid (127 mg, 87%): Mp 110-112 °C [Lit.<sup>253</sup> 119-121 °C];  $\nu_{\max}/\text{cm}^{-1}$  3064 (w, NH), 1682 (m, C=O), 1600 (s, C=C);  $\delta_{\text{H}}$  (400 MHz;  $\text{CDCl}_3$ ) 3.07 (2H, d,  $J$  1.5, C(4)H<sub>2</sub>), 4.19 (2H, s, C(7)H<sub>2</sub>), 4.63-4.67 (1H, m, C(2)H or C(6)H), 5.22 (2H, br, s, NH<sub>2</sub>), 5.64 (1H, dd,  $J$  8.1, 1.5, C(5)H), 7.06 (1H, d,  $J$  1.5, C(2)H or C(6)H), 7.13-7.25 (5H, m, Ar-CH);  $\delta_{\text{C}}$  (100 MHz;  $\text{CDCl}_3$ ) 22.9 (CH), 57.4 (CH), 98.6 (q), 103.3 (CH), 127.2 (CH), 127.8 (CH), 128.8 (CH), 129.0 (CH), 137.2 (q), 140.1 (CH), 170.2 (C=O);  $m/z$  (-ES) 213.1 ( $[\text{M}-\text{H}]^-$ , 100%); (+ES) (Found 237.1004;  $\text{C}_{13}\text{H}_{14}\text{N}_2\text{ONa}$  ( $[\text{M}+\text{Na}]^+$ ), requires 237.1021).

**Method A:** General method for synthesis of symmetric dicoumarol analogue. The appropriate 4-hydroxycoumarin was reacted with formaldehyde (37% aqueous solution stabilized with 12% methanol). Ethanol was added to give a solution of 0.4M concentration with respect to 4-hydroxycoumarin. The reaction mixture was heated under reflux at 80 °C for 24 hours when it was allowed to cool to room temperature and the precipitate formed was collected by filtration, washed with ethanol and dried.<sup>254</sup>

**Method B:** The appropriate 4-hydroxycoumarin was reacted with formaldehyde (37% aqueous solution stabilized with 12% methanol). Ethanol was added to give a solution of 0.25M concentration with respect to 4-hydroxycoumarin. The reaction mixture was subjected to microwave irradiation at 80 °C for 4 hours. The resultant mixture was allowed to cool to room temperature and the precipitate formed was collected by filtration, washed with ethanol and dried.

### 5.3.9 Synthesis of 3,3'-methylenebis(4-hydroxy-2H-chromen-2-one, **33**

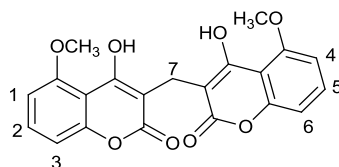


$\text{C}_{19}\text{H}_{12}\text{O}_6$ ; Molecular weight: 336.29

Using method A, 4-hydroxycoumarin (120 mg, 0.74 mmol) was reacted with formaldehyde (11 mg, 0.37 mmol) to give the title compound **33** as a white solid (90 mg, 72%).

Using method B, 4-hydroxycoumarin (120 mg, 0.74 mmol) was reacted with formaldehyde (11 mg, 0.37 mmol) to give the title compound (**33**) as a white solid (96 mg, 77%): Mp 291-293 °C [Lit.<sup>174</sup> 293-297 °C];  $\nu_{\max}/\text{cm}^{-1}$  3057 (bw, OH), 1650 (s, C=O);  $\delta_{\text{H}}$  (500 MHz; CDCl<sub>3</sub>) 3.85 (2H, s, C(5)H<sub>2</sub>), 7.35-7.39 (4H, m, Ar-CH), 7.59 (2H, ddd, *J* 8.2, 7.1, 1.6, C(2)H and C(7)H or C(3)H and C(8)H), 8.01 (2H, dd, *J* 8.2, 1.6, C(1)H and C(6)H or C(4)H and C(9)H), 11.31 (2H, s, 2 OH);  $\delta_{\text{C}}$  (126 MHz; CDCl<sub>3</sub>) 19.9 (C(5)H<sub>2</sub>), 102.9 (q), 116.5 (q), 116.7 (CH), 124.0 (CH), 124.8 (CH), 132.5 (CH), 152.4 (q), 164.4 (q), 168.7 (C=O); *m/z* (+ES) 337.1 ([M+H]<sup>+</sup>, 100%); (Found 359.0538; C<sub>19</sub>H<sub>12</sub>O<sub>6</sub>Na ([M+Na]<sup>+</sup>), requires 359.0532).

#### 5.3.10 Synthesis of 3,3'-methylenebis(4-hydroxy-5-methoxy-2H-chromen-2-one, **92a**)

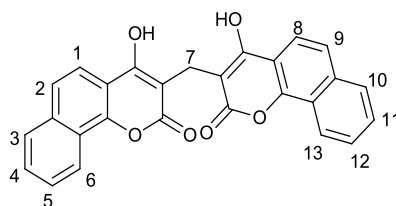


C<sub>21</sub>H<sub>16</sub>O<sub>8</sub>; Molecular weight: 396.35

Using method A, 4-hydroxy-6-methoxycoumarin (120 mg, 0.63 mmol) was reacted with formaldehyde (10 mg, 0.31 mmol) to give the title compound as a white powder (97 mg, 78%).

Using method B, 4-hydroxy-6-methoxycoumarin (120.0 mg, 0.63 mmol) was reacted with formaldehyde (9.4 mg, 0.31 mmol) to give the title compound (**92a**) as a white powder (100 mg, 81%): Mp 272-273 °C [Lit.<sup>174</sup> 261-263 °C];  $\nu_{\max}/\text{cm}^{-1}$  3286 (m, O-H), 1713 (s, C=O), 1650 (s, C=C);  $\delta_{\text{H}}$  (400 MHz; DMSO-*d*<sub>6</sub>) 3.67 (2H, s, C(7)H<sub>2</sub>), 3.97 (6H, s, 2OCH<sub>3</sub>), 6.98 (4H, dd, *J* 8.4, 0.9, C(1)H and C(3)H and C(4)H and C(6)H), 7.53 (2H, t, *J* 8.4, C(2)H and C(5)H), 10.08 (2H, br, s, 2 OH);  $\delta_{\text{C}}$  (100 MHz; DMSO-*d*<sub>6</sub>) 19.0 (C(7)H<sub>2</sub>), 57.3 (OCH<sub>3</sub>), 102.6 (q), 105.0 (q), 106.8 (CH), 110.0 (CH), 132.5 (CH), 153.3 (q), 156.4 (q), 161.1 (q), 162.3 (C=O); *m/z* (+ES) 397.1 ([M+H]<sup>+</sup>, 80%); (Found 419.0723; C<sub>21</sub>H<sub>16</sub>O<sub>8</sub>Na ([M+Na]<sup>+</sup>), requires 419.0743).

### 5.3.11 Synthesis of 3,3'-methylenebis(4-hydroxy-2H-benzo[h]chromen-2-one, **92b**

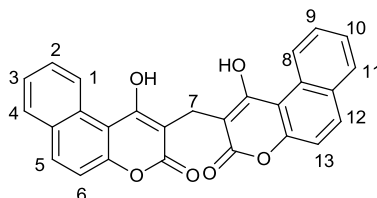


$C_{27}H_{16}O_6$ ; Molecular weight: 436.41

Using method A, 4-hydroxy-2H-benzo[h]chromen-2-one (120 mg, 0.56 mmol) was reacted with formaldehyde (9 mg, 0.3 mmol) to give the title compound (**92b**) as white solid (92 mg, 75%).

Using method B, 4-hydroxy-2H-benzo[h]chromen-2-one (120 mg, 0.556 mmol) was reacted with formaldehyde (9 mg, 0.3 mmol) to give the title compound (**92b**) as a white solid (96 mg, 78%): Mp 340-348 °C [Lit.<sup>174</sup> 279-281 °C];  $\nu_{\max}/\text{cm}^{-1}$  3063 (br, w, O-H), 1643 (s, C=O), 1560 (s, C=C);  $\delta_{\text{H}}$  (500 MHz; DMSO- $d_6$ ) 3.84 (2H, s, C(7)H<sub>2</sub>), 7.43-7.48 (2H, m, Ar-CH), 7.53 (2H, ddd,  $J$  7.8, 6.9, 0.8, C(4)H and C(11)H or C(5)H and C(12)H), 7.65-7.69 (2H, m, Ar-CH), 7.96 (2H, d,  $J$  8.8, C(1)H and C(8)H or C(2)H and C(9)H), 8.05 (2H, d,  $J$  8.8, C(1)H and C(8)H or C(2)H and C(9)H), 9.81 (2H, dd,  $J$  8.8, C(3)H and C(10)H or C(6)H and C(13)H);  $\delta_{\text{C}}$  (125 MHz; DMSO- $d_6$ ) 20.7 (C(7)H<sub>2</sub>), 117.5 (CH), 120.6 (q), 122.0 (q), 125.5 (CH), 127.0 (CH), 128.0 (CH), 129.0 (CH), 130.5 (q), 130.7 (q), 132.9 (d,  $J$  4.5, (CH)), 134.7 (q), 153.3 (q), 163.9 (C=O);  $m/z$  (+ES) 437.1 ([M+H]<sup>+</sup>, 100%); (Found 437.1011;  $C_{27}H_{17}O_6$  ([M+H]<sup>+</sup>), requires 437.1025).

### 5.3.12 Synthesis of 2,2'-methylenebis(1-hydroxy-3H-benzo[f]chromen-2-one, **199**

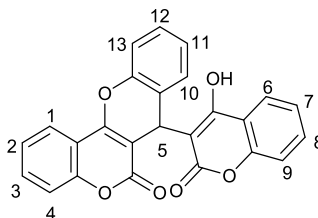


$C_{27}H_{16}O_6$ ; Molecular weight: 436.41

Using method B, 4-hydroxy-2H-benzo[h]chromen-2-one (120 mg, 0.56 mmol) was reacted with formaldehyde (9 mg, 0.3 mmol) to give the title compound (**199**) as a colourless solid (100 mg, 81%): Mp 340-348 °C [Lit.<sup>255</sup> decompose 300 °C];  $\nu_{\max}/\text{cm}^{-1}$

<sup>1</sup> 3063 (br, w, O-H), 1643 (s, C=O), 1560 (s, C=C); NMR could not be analysed due to poor solubility; *m/z* (+ES) 437.1 ([M+H]<sup>+</sup>, 100%); (Found 437.1011; C<sub>27</sub>H<sub>17</sub>O<sub>6</sub> ([M+H]<sup>+</sup>), requires 437.1025).

### 5.3.13 Synthesis of 7-(4-hydroxy-2-oxo-2H-chromen-3-yl)chromeno[4,3-b]chromen-6(7H)-one, **200**

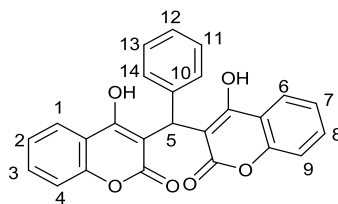


C<sub>25</sub>H<sub>14</sub>O<sub>6</sub>; Molecular weight: 410.37

Using method A, reaction of 4-hydroxycoumarin (500 mg, 3.0 mmol) and 2-hydroxybenzaldehyde (159 mg, 1.5 mmol) in ethanol (3 mL) gave the title compound (**200**) as a white solid (458 mg, 74%).

Using method B, reaction of 4-hydroxycoumarin (200 mg, 1.2 mmol) and 2-fluorobenzaldehyde (75 mg, 0.6 mmol) in ethanol (3 mL) at 85 °C for 10 minutes gave the title compound (**200**) as white solid (133 mg, 54%): Mp 253–255 °C [Lit.<sup>256</sup> 245 °C (decomp)]; *v*<sub>max</sub>/cm<sup>-1</sup> 3235 (br, OH), 1708 (s, C=O), 1600 (s, C=C); δ<sub>H</sub> (400 MHz; CDCl<sub>3</sub>) 5.38 (1H, s, C(5)H), 7.11-7.16 (2H, m, Ar-CH), 7.21 (1H, dd, *J* 8.3, 1.6, C(1)H or C(4)H or C(6)H or C(9)H), 7.29-7.33 (3H, m, Ar-CH), 7.41-7.53 (3H, m, Ar-CH), 7.64 (1H, ddd, *J* 8.3, 7.3, 1.6, C(2)H or C(3)H or C(7)H or C(8)H), 8.04 (1H, dd, *J* 8.3, 1.6, C(1)H or C(4)H or C(6)H or C(9)H), 8.17 (1H, dd, *J* 8.3, 1.6, C(1)H or C(4)H or C(6)H or C(9)H), 10.42 (1H, s, OH); δ<sub>C</sub> (126 MHz; CDCl<sub>3</sub>) 30.0 (C(5)H), 100.2 (q), 108.7 (q), 114.6 (q), 116.3 (CH), 116.3 (CH), 116.8 (q), 117.0 (CH), 121.4 (q), 123.4 (CH), 123.9 (CH), 124.4 (CH), 125.1 (CH), 125.6 (CH), 128.6 (CH), 132.0 (CH), 132.8 (CH), 151.0 (q), 152.1 (q), 153.1 (q), 158.8 (q), 161.2 (q), 161.4 (q), 166.2 (C=O); *m/z* (-ES), 409 ([M-H]<sup>-</sup>, 100%); *m/z* (+ES) (Found 433.0699; C<sub>25</sub>H<sub>14</sub>O<sub>6</sub>Na ([M+Na]<sup>+</sup>), requires 433.0700).

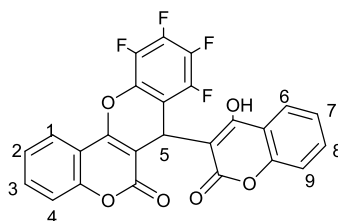
### 5.3.14 Synthesis of 3,3'-(phenylmethylene)bis[4-hydroxy-2H-chromen-2-one, **201**



$C_{25}H_{16}O_6$ ; Molecular weight: 412.39

Using method A, reaction of 4-hydroxycoumarin (250 mg, 1.50 mmol) and benzaldehyde (159 mg, 0.75 mmol) in ethanol (6 mL) gave the title compound (**201**) as a white solid (242 mg, 78%): Mp 210-212°C [Lit.<sup>257</sup> 215 °C];  $\nu_{\max}/\text{cm}^{-1}$  2700 (br, w, OH), 1670 (s, C=O), 1600 (s, C=C);  $\delta_H$  (400 MHz; DMSO- $d_6$ ) 6.3 (1H, s, C(5)H), 7.10-7.12 (3H, m, Ar-CH), 7.17-7.21 (2H, m, Ar-CH), 7.25-7.32 (4H, m, Ar-CH), 7.55 (2H, ddd,  $J$  8.2, 7.1, 1.6, C(2)H and C(7)H or C(3)H and C(8)H), 7.85 (2H, dd,  $J$  8.2, 1.6, C(1)H and C(6)H or C(4)H and C(9)H);  $\delta_C$  (126 MHz;  $CDCl_3$ ) 36.2 (C(5)H<sub>2</sub>), 103.9 (CH), 105.7 (CH), 116.5 (CH), 116.7 (CH), 116.9 (CH), 124.4 (CH), 124.9 (CH), 126.5 (CH), 126.9 (CH), 128.7 (CH), 132.9 (CH), 135.2 (CH), 152.3 (CH), 152.5 (q), 164.6 (q), 165.8 (q), 166.9 (q), 169.3 (C=O);  $m/z$  (-ES), 411.1 ([M-H]<sup>-</sup>, 50%);  $m/z$  (+ES) (Found 435.0856;  $C_{25}H_{16}O_6Na$  ([M+Na]<sup>+</sup>), requires 435.0845).

### 5.3.15 Synthesis of symmetric dicoumarol dimmer, **202**

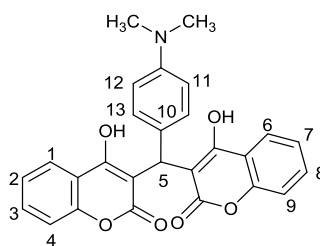


$C_{25}H_{10}F_4O_6$ ; Molecular weight: 482.34

Using method A, reaction of 4-hydroxycoumarin (250 mg, 1.54 mmol) and pentafluorobenzaldehyde (151 mg, 0.77 mmol) in ethanol (6 mL) gave the title compound (**202**) as a white solid (30 mg, 8%): Mp 270-272 °C;  $\nu_{\max}/\text{cm}^{-1}$  3178 (br, w, OH), 1716 (s, C=O), 1610 (s, C=C);  $\delta_H$  (400 MHz;  $CDCl_3$ ) 5.49 (1H, s, C(5)H), 7.25 (1H, dd,  $J$  8.3, 0.8, C(1)H or C(4)H or C(6)H or C(9)H), 7.35 (1H, ddd,  $J$  8.3, 7.2, 0.8, C(2)H or C(3)H or C(7)H or C(8)H), 7.46 (1H, dd,  $J$  8.3, 0.8, C(1)H or C(4)H or C(6)H or C(9)H), 7.48 (1H, ddd,  $J$  8.3, 7.2, 0.8, C(2)H or C(3)H or C(7)H or C(8)H), 7.53 (1H, ddd,  $J$  8.3, 7.2, 0.8, C(2)H or C(3)H or C(7)H or C(8)H), 7.68 (1H, ddd,  $J$

8.3, 7.2, 0.8, C(2)H or C(3)H or C(7)H or C(8)H), 8.03 (1H, dd, *J* 8.3, 0.8, C(1)H or C(4)H or C(6)H or C(9)H), 8.15 (1H, dd, *J* 8.3, 0.8, C(1)H or C(4)H or C(6)H or C(9)H), 10.11(1H, s, OH);  $\delta_C$  (126 MHz; CDCl<sub>3</sub>) 25.4 (C(5)H), 99.6 (q), 104.3 (q), 105.7 (q), 113.9 (q), 116.5 (q), 116.6 (CH), 117.2 (C H), 123.6 (CH), 124.4 (CH), 124.7 (CH), 125.7 (CH), 132.7 (CH), 133.7 (CH), 152.1 (CH), 153.2 (C-F), 157.8 (C-F), 161.6 (C-F), 162.5 (C-F), 165.4(C=O); *m/z* (-ES) 481.1 ([M-H]<sup>-</sup>, 100%); (Found 481.0341; C<sub>25</sub>H<sub>9</sub>O<sub>6</sub>F<sub>4</sub> ([M-H]<sup>-</sup>), requires 481.0335).

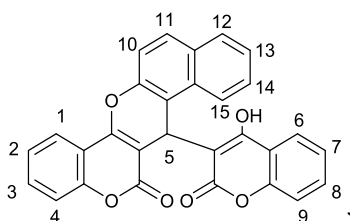
### 5.3.16 Synthesis of symmetric dicoumarol dimer, **203**



C<sub>27</sub>H<sub>21</sub>NO<sub>6</sub>; Molecular weight: 455.46

Using method A, reaction of 4-dimethylamino benzaldehyde (150 mg, 1.85 mmol) and 4-hydroxycoumarin (300 mg, 1.01 mmol) in a mixture of ethanol (10 mL) and 2 drops of piperidine gave the title compound (**203**) as a pink solid (390 mg, 86%): Mp 224-226 °C [Lit.<sup>258</sup> 206 °C];  $\nu_{\max}/\text{cm}^{-1}$  3000 (br, OH), 1650 (s, C=O), 1602 (s, C=C);  $\delta_H$  (400 MHz; DMSO-*d*<sub>6</sub>) 3.12 (6H, s, 2xCH<sub>3</sub>), 6.27 (1H, s, C(5)H), 7.21-7.37 (8H, m, Ar-CH), 7.52 (2H, ddd, *J* 8.4, 7.1, 1.6, C(2)H and C(7)H or C(3)H and C(8)H), 7.81 (2H, dd, *J* 8.4, 1.6, C(1)H and C(6)H or C(4)H and C(9)H);  $\delta_C$  (100 MHz; DMSO-*d*<sub>6</sub>) some signals coincident, 18.53 (CH<sub>3</sub>), 35.9 (C(5)H), 45.6 (q), 56.0 (q), 103.0 (q), 119.6 (CH), 115.6 (CH), 119.7 (CH), 123.0 (CH), 124.1 (CH), 128.2 (CH), 131.2 (q), 140.6 (q), 152.5 (q), 164.5 (q), 167.6 (C=O); *m/z* (-ES) 454.1 ([M-H]<sup>-</sup>, 100%); (Found 454.1275; C<sub>27</sub>H<sub>20</sub>NO<sub>6</sub> ([M-H]<sup>-</sup>), requires 454.1291).

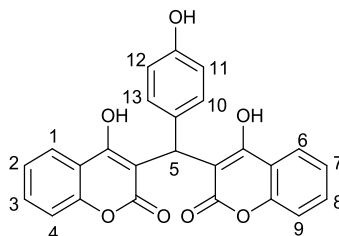
### 5.3.17 Synthesis of 7-(4-hydroxy-2-oxo-2H-chromen-3-yl)benzo[f]chromeno[4,3-b]chromen-6(7H)-one, **204**



C<sub>29</sub>H<sub>16</sub>O<sub>6</sub>; Molecular weight: 460.43

Using method A, reaction of 4-hydroxycoumarin (500 mg, 3.08 mmol) and 2-hydroxy-1-naphthadehyde (270 mg, 1.54 mmol) in ethanol (3 mL) gave the title compound (**204**) as a white solid (642 mg, 91%): Mp 305-307 °C;  $\nu_{\max}/\text{cm}^{-1}$  3200 (br, w, OH), 1712 (s, C=O), 1667 (s, C=C);  $\delta_{\text{H}}$  (400 MHz; CDCl<sub>3</sub>) 5.95 (1H, s, C(5)H), 7.14 (1H, d,  $J$  8.1, C(10)H or C(11)H), 7.32 (1H, ddd,  $J$  8.1, 7.3, 1.0, C(13)H or C(14)H), 7.40-7.50 (5H, m, Ar-CH), 7.53-7.57 (1H, m, Ar-CH), 7.67 (1H, ddd,  $J$  8.1, 7.3, 1.0, C(13)H or C(14)H), 7.73 (1H, d,  $J$  8.1, C(10)H or C(11)H), 7.83-7.89 (2H, m, Ar-CH), 8.11 (1H, dd,  $J$  8.1, 1.0, C(1)H or C(4)H or C(6)H or C(9)H), 8.21 (1H, dd,  $J$  8.1, 1.0, C(1)H or C(4)H or C(6)H or C(9)H), 10.56 (1H, s, OH);  $\delta_{\text{C}}$  (75 MHz; CDCl<sub>3</sub>) 27.8 (C(5)H), 100.4 (q), 108.1 (q), 113.3 (q), 114.6 (q), 116.2 (CH), 116.7 (CH), 117.03 (q), 122.3 (CH), 123.4 (CH), 123.8 (CH), 124.5 (CH), 125.1 (CH), 127.5 (CH), 128.8 (CH), 129.7 (CH), 130.9 (q), 131.6 (CH), 132.0 (q), 132.8 (CH), 149.2 (q), 152.2 (q), 153.1 (q), 158.7 (q), 160.9 (q), 166.2 (C=O),  $m/z$  (-ES) 459.1 ([M-H]<sup>-</sup>, 100%); (Found 459.0887; C<sub>29</sub>H<sub>15</sub>O<sub>6</sub> ([M-H]<sup>-</sup>), requires 459.0869).

### 5.3.18 Synthesis of 3,3'-((4-hydroxyphenyl)methylene)bis(4-hydroxy-2H-chromen-2-one, **205**



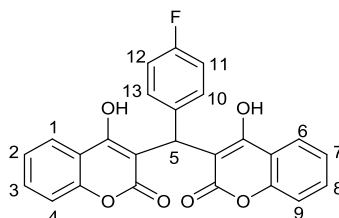
C<sub>25</sub>H<sub>16</sub>O<sub>7</sub>; Molecular weight: 428.39

Using method A, reaction of 4-hydroxycoumarin (243 mg, 1.50 mmol) and 4-hydroxybenzaldehyde (92 mg, 0.75 mmol) in ethanol (3 mL) gave the title compound (**205**) as pale yellow solid (210 mg, 65%): Mp 222-224 °C [Lit.<sup>259</sup> 222-224];  $\nu_{\max}/\text{cm}^{-1}$  3435 (br, OH), 1665 (s, C=O), 1600 (s, C=C);  $\delta_{\text{H}}$  (500 MHz; DMSO-*d*<sub>6</sub>) 6.19 (1H, s, C(5)H), 6.59 (2H, d,  $J$  8.6, C(10)H and C(13)H or C(11)H and C(12)H), 6.89 (2H, dd,  $J$  8.6, 1.0, C(1)H and C(4)H or C(6)H and C(9)H), 7.25-7.31 (4H, m, Ar-CH), 7.54 (2H, ddd,  $J$  8.6, 7.1, 1.0, C(2)H and C(3)H or C(7)H and C(8)H), 7.84 (2H, dd,  $J$  8.6, 1.0, C(1)H and C(4)H or C(6)H and C(9)H);  $\delta_{\text{C}}$  (125 MHz; DMSO-*d*<sub>6</sub>) 35.2 (C(5)H), 48.6 (q), 104.1 (q), 114.7 (CH), 115.7 (CH), 118.9 (q), 123.3 (CH), 123.9 (CH), 127.6 (CH), 131.3 (CH), 152.3 (q), 154.9 (q), 164.6 (q),



166.1 (C=O),  $m/z$  (+ES) 429 ( $[M+H]^+$ , 100%); (Found 429.0979;  $C_{25}H_{17}O_7$  ( $[M+H]^+$ ), requires 429.0974).

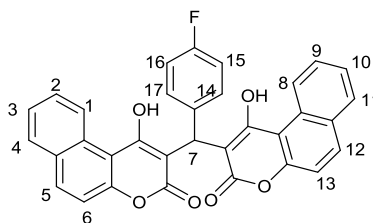
### 5.3.19 Synthesis of 3,3'-((4-fluorophenyl)methylene)bis(4-hydroxy-2H-chromen-2-one), **101**



$C_{25}H_{15}FO_6$ ; Molecular weight: 430.38

Using method A, reaction of 4-hydroxycoumarin (200 mg, 1.2 mmol) and 4-fluorobenzaldehyde (74 mg, 0.6 mmol) in ethanol (3 mL) gave the title compound (**101**) as a white solid (214 mg, 83%): Mp 219-221°C [Lit.<sup>260</sup> 213-215 °C];  $\nu_{\max}/\text{cm}^{-1}$  2870 (br, OH), 1670 (s, C=O), 1600 (s, C=C);  $\delta_H$  (400 MHz;  $CDCl_3$ ) 6.06 (1H, s, C(5)H), 7.00-7.04 (2H, m, Ar-CH), 7.18-7.21 (2H, m, Ar-CH), 7.41-7.43 (4H, m, Ar-CH), 7.65 (2H, ddd,  $J$  8.4, 7.2, 1.5, (C(2)H) and (C(7)H) or (C(3)H) and (C(8)H), 8.08 (2H, dd,  $J$  8.4, 1.5, C(1)H and C(4)H or C(6)H and C(9)H), 11.33 (1H, s, OH), 11.55 (1H, s, OH);  $\delta_C$  (100 MHz;  $CDCl_3$ ) 35.7 (C(5)H), 115.4 (CH), 115.6 (q), 116.7 (CH), 124.4 (CH), 124.9 (CH), 128.1 (d,  $J$  8.3, q), 128.2 (CH), 130.8 (d,  $J$  2.9, q), 132.9 (CH), 160.5 (C-F), 163.0 (C=O);  $m/z$  (+ES) 453 ( $[M+Na]^+$ , 100%); (Found 453.0762;  $C_{25}H_{15}O_6FNa$  ( $[M+Na]^+$ ), requires 453.0763).

### 5.3.20 Synthesis of 2,2'-((4-fluorophenyl)methylene)bis(1-hydroxy-3H-benzo[f]chromen-3-one), **206**

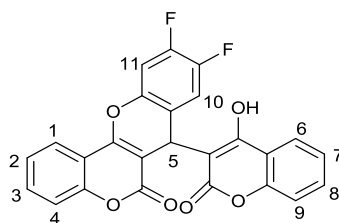


$C_{33}H_{19}FO_6F$ ; Molecular weight: 530.50

Using method B, reaction of 1-hydroxy-3H-benzo[f]chromen-3-one (150 mg, 0.71 mmol) and 4-fluorobenzaldehyde (44 mg, 0.35 mmol) in ethanol (6 mL) gave the title compound (**206**) as a cream powder (130 mg, 69%):  $\delta_H$  (400 MHz;  $CDCl_3$ ) 6.26 (1H, s, C(7)H), 7.01-7.05 (2H, m, Ar-CH), 7.28- 7.30 (2H, m, Ar-CH), 7.52-7.70

(5H, m, Ar-CH), 7.76 (1H, dd, *J* 8.4, 7.2, C(1)H or C(4)H or C(8)H or C(11)H), 7.91-7.95 (2H, m, Ar-CH), 8.09 (2H, d, *J* 9.1, C(14)H and C(17)H or C(15)H and C(16)H), 9.44 (1H, d, *J* 8.7, C(5)H or C(6)H or C(12)H or C(13)H), 9.55 (1H, d, *J* 8.7, C(5)H or C(6)H or C(12)H or C(13)H), 12.65 (1H, s, OH), 12.78 (1H, s, OH);  $\delta_C$  (100 MHz; CDCl<sub>3</sub>) 36.1 (C(7)H), 106.0 (q), 110.7 (q), 115.4 (CH), 115.6 (CH), 116.7 (CH), 126.3 (CH), 126.4 (CH), 127.2 (q), 127.3 (q), 128.3 (CH), 128.4 (CH), 128.9 (CH), 129.0 (CH), 131.2 (q), 135.2 (CH), 169.2 (C-F), 170.2 (C=O); *m/z* (-ES) 529.1 ([M-H]<sup>-</sup>, 50%); (Found 529.1101; C<sub>33</sub>H<sub>18</sub>O<sub>6</sub>F ([M-H]<sup>-</sup>), requires 529.1087).

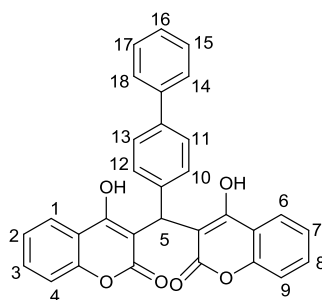
### 5.3.21 Synthesis of 9,10-difluoro-7-(4-hydroxy-2-oxo-2H-chromen-3-yl)chromeno[4,3-b]chromen-6(7H)-one, **207**



C<sub>25</sub>H<sub>12</sub>F<sub>2</sub>O<sub>6</sub>; Molecular weight: 446.36

Using method A, reaction of 4-hydroxycoumarin (200 mg, 1.2 mmol) and 2,4,5-trifluoro benzaldehyde (75 mg, 0.6 mmol) in ethanol (3 mL) gave the title compound (**207**) as a white solid (82 mg, 31%): Mp (290-292 °C);  $\nu_{\max}/\text{cm}^{-1}$  3065 (m, OH), 1700 (s, C=O), 1600 (s, C=C);  $\delta_H$  (400 MHz; CDCl<sub>3</sub>) 5.31 (1H, s, C(5)H), 6.95-6.99 (1H, m, Ar-CH), 7.15-7.19 (1H, m, Ar-CH), 7.24 (1H, dd, *J* 8.3, 0.8, C(1)H or C(4)H or C(6)H or C(9)H), 7.31-7.34 (1H, m, Ar-CH), 7.42-7.48 (2H, m, Ar-CH), 7.53 (1H, ddd, *J* 8.3, 7.2, 0.8, C(2)H or C(3)H or C(7)H or C(8)H), 7.67 (1H, ddd, *J* 8.3, 7.2, 0.8, C(2)H or C(3)H or C(7)H or C(8)H), 8.04 (1H, dd, *J* 8.3, 0.8, C(1)H or C(4)H or C(6)H or C(9)H), 8.11 (1H, dd, *J* 8.3, 0.8, C(1)H or C(4)H or C(6)H or C(9)H), 10.38 (1H, s, OH);  $\delta_C$  (100 MHz; CDCl<sub>3</sub>) 32.5 (C(5)H), 99.7 (q), 106.0 (CH), 106.2 (q), 107.8 (q), 114.2 (q), 116.2 (CH), 116.3 (CH), 116.7 (d, *J* 4.6, CH), 117.1 (CH), 117.6 (q), 117.7 (q), 117.8 (q), 123.2 (CH), 124.0 (CH), 124.4 (d, *J* 4.6, CH), 125.2 (CH), 132.3 (CH), 133.1 (q), 152.1 (q), 153.1 (q), 158.3 (q), 161.2 (C-F), 161.9 (C-F), 165.9 (C=O); *m/z* (+ES) 447.1 ([M+H]<sup>+</sup>, 100%); (Found 469.0508; C<sub>25</sub>H<sub>12</sub>O<sub>6</sub>F<sub>2</sub>Na ([M+Na]<sup>+</sup>), requires 469.0500).

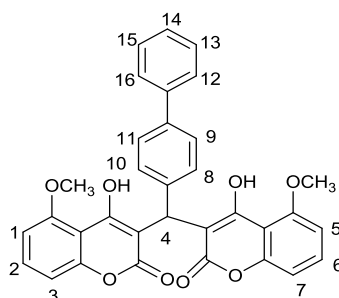
### 5.3.22 Synthesis of 3,3'-([1,1'-biphenyl]-4-ylmethylene)bis(4-hydroxy-2H-chromen-2-one), **208**



$C_{31}H_{20}O_6$ ; Molecular weight: 488.49

Using method A, reaction of 4-hydroxycoumarin (300 mg, 1.85 mmol) and 4-phenylbenzaldehyde (169 mg, 0.93 mmol) in ethanol (13 mL) gave the title compound (**208**) as a white solid (380 mg, 84%): Mp 228-230 °C [Lit<sup>261</sup> 227-229 °C];  $\nu_{\max}/\text{cm}^{-1}$  1665 (s, C=O), 1604 (s, C=C);  $\delta_{\text{H}}$  (400 MHz, DMSO- $d_6$ ), 6.36 (1H, s, C(5)H), 7.21 (2H, d,  $J$  8.6, C(10)H and C(12)H) or C(11)H and C(13)H), 7.28-7.35 (5H, m, Ar-CH), 7.43 (2H, t,  $J$  7.7, C(15)H and C(17)H), 7.50 (2H, d,  $J$  8.6, C(10)H and C(12)H or C(11)H and C(13)H), 7.62-7.66 (4H, m, Ar-CH), 7.88 (2H, dd,  $J$  8.6, 1.5, C(1)H and C(6)H or C(4)H and C(9)H);  $\delta_{\text{C}}$  (100 MHz; DMSO- $d_6$ ) 35.8 (C(5)H), 103 (q), 115.8 (CH), 118.4 (q), 118.7 (q), 123.5 (q), 123.4 (CH), 124.0 (CH), 126.3 (CH), 126.4 (CH), 127.3 (CH), 127.0 (CH), 128.8 (CH), 131.5 (CH), 140.1 (q), 152.3 (q), 164.7 (q), 166.0 (q);  $m/z$  (-ES) 487.1 ( $[\text{M}-\text{H}]^-$ , 50%); (Found 487.1193;  $C_{31}H_{19}O_6$  ( $[\text{M}-\text{H}]^-$ ), requires 487.1182).

### 5.3.23 Synthesis of 3,3'-([1,1'-biphenyl]-4-ylmethylene)bis(4-hydroxy-5-methoxy-2H-chromen-2-one), **209**

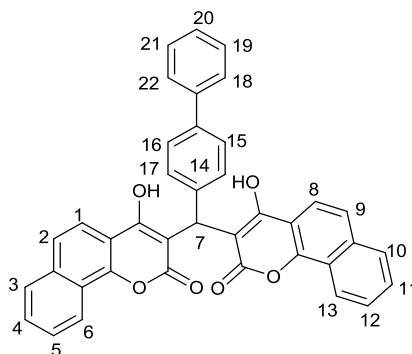


$C_{33}H_{24}O_8$ ; Molecular weight: 548.54

Using method A, reaction of 4-hydroxy-6-methoxycoumarin (121 mg, 0.63 mmol) and 4-phenylbenzaldehyde (57 mg, 0.32 mmol) in ethanol (6 mL) gave the title compound (**209**) as a white solid (57 mg, 33%): Mp 285-287 °C;  $\nu_{\max}/\text{cm}^{-1}$  3316 (br,

m, OH), 1687 (s, C=O), 1637 (s, C=C);  $\delta_H$  (500 MHz;  $CDCl_3$ ) 4.01 (6H, s,  $2OCH_3$ ), 6.30 (1H, s, C(4)H), 6.78 (2H, d,  $J$  8.4, C(8)H and C(10)H or C(9)H and C(11)H), 7.04 (2H, d,  $J$  8.4, C(8)H and C(10)H or C(9)H and C(11)H), 7.37-7.43 (4H, m, Ar-CH), 7.46 (2H, t,  $J$  8.4, C(2)H and C(6)H), 7.51 (2H, d,  $J$  8.4, C(1)H and C(5)H or C(3)H and C(7)H), 7.59 (2H, d,  $J$  8.4, C(1)H and C(5)H or C(3)H and C(7)H), 10.21 (2H, s, 2OH);  $\delta_C$  (125 MHz;  $CDCl_3$ ) 36.8 (C(4)H), 56.9 (OCH<sub>3</sub>), 104.7 (q), 105.7 (CH), 105.8 (q), 110.8 (CH), 126.9 (d,  $J$  6.4, (CH)), 127.1 (CH), 127.9 (CH), 128.6 (CH), 131.8 (CH), 138.8 (d,  $J$  4.5, (q)), 141.3 (q), 154.0 (q), 156.5 (q), 163.4 (d,  $J$  10.9);  $m/z$  (+ES) 549 ( $[M+H]^+$ , 80%); (Found 571.1345;  $C_{33}H_{24}O_8Na$  ( $[M+Na]^+$ ), requires 571.1369).

### 5.3.24 Synthesis of 3,3'-([1,1'-biphenyl]-4-ylmethylene)bis(4-hydroxy-2H-benzo[h]chromen-2-one, **210**



$C_{39}H_{24}O_6$ ; Molecular weight: 588.60

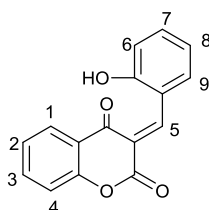
Using method A, reaction of 4-hydroxy-2H-benzo[h]chromen-2-one (124 mg, 0.56 mmol) and 4-phenylbenzaldehyde (53 mg, 0.29 mmol) in ethanol (5 mL) gave the title compound (**210**) as white solid (70 mg, 41%): Mp 257-259 °C;  $\nu_{max}/cm^{-1}$  3025 (br, w, OH), 1665 (s, C=O), 1626 (s, C=C);  $\delta_H$  (400 MHz;  $DMSO-d_6$ ) 6.46 (1H, s, C(7)H), 7.28-7.32 (3H, m, Ar-CH), 7.42 (2H, t,  $J$  7.7, C(19)H and C(21)H), 7.51 (2H, d,  $J$  8.6, C(14)H and C(17)H or C(15)H and C(16)H), 7.62 (2H, d,  $J$  8.6, C(14)H and C(17)H or C(15)H and C(16)H), 7.66-7.71 (4H, m, Ar-CH), 7.78 (2H, d,  $J$  8.6, C(1)H and C(8)H or C(2)H and C(9)H), 7.93 (2H, d,  $J$  8.6, C(1)H and C(8)H or C(2)H and C(9)H), 8.01-8.03 (2H, m, Ar-CH), 8.38-8.41 (2H, m, Ar-CH);  $\delta_C$  (100 MHz;  $DMSO-d_6$ ) 36.5 (C(7)H), 104.1 (q), 114.9 (q), 121.0 (CH), 122.1 (CH), 122.8 (q), 123.3 (CH), 126.8 (d,  $J$  17.3, (CH)), 127.4 (d,  $J$  9.1, (CH)), 127.9 (CH), 128.5 (d,  $J$  11.8, (CH)), 129.3 (CH), 134.9 (q), 137.6 (q), 140.7 (q), 141.3 (q), 149.5 (q), 165

(q), 168.2 (C=O);  $m/z$  (-ES) 587.2 ([M-H]<sup>-</sup>, 100%); (Found 589.1657; C<sub>39</sub>H<sub>25</sub>O<sub>6</sub>Na ([M+Na]<sup>+</sup>), requires 589.1651).

**Method C:** General procedure for the synthesis of half-way stage of dicoumarol. The appropriate 4-hydroxycoumarin (1 equivalent) was reacted with the appropriate aldehyde (1 equivalent). Ethanol was added to give a solution of 0.1 M with respect to hydroxycoumarin. The reaction mixture was heated under reflux at 80 °C for 30-60 minutes when it was allowed to cool to room temperature and the precipitate formed was collected by filtration, washed with methanol and dried.

**Method D:** The appropriate 4-hydroxycoumarin (1 equivalent) was reacted with the appropriate aldehyde (1 equivalent). Ethanol was added to give a solution of 0.5M concentration with respect to 4-hydroxycoumarin. The reaction mixture was subjected to microwave irradiation at 80 °C for 30 minutes. The resulting mixture was allowed to cool to room temperature and the precipitate formed was collected by filtration, washed with methanol and dried.

### 5.3.25 Synthesis of (*E*)-3-(2-hydroxybenzylidene)chroman-2,4-dione, **175b**



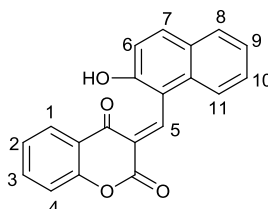
C<sub>16</sub>H<sub>10</sub>O<sub>4</sub>; Molecular weight: 266.25

Using method C, reaction of 4-hydroxycoumarin (540 mg, 3.33 mmol) and 2-hydroxy benzaldehyde (407 mg, 3.33 mmol) in ethanol (30 mL) gave the title compound (**175b**) as a yellow foam (250 mg, 28%).

Using method D, reaction of 4-hydroxycoumarin (540 mg, 3.33 mmol) and 2-hydroxy benzaldehyde (407 mg, 3.33 mmol) gave the title compound (**175b**) as a yellow solid (180 mg, 20%): Mp 171-173 °C [Lit.<sup>262</sup> 173-175 °C];  $\nu_{\max}/\text{cm}^{-1}$  3300 (br, OH), 1714 (s, C=O), 1650 (s, C=C);  $\delta_{\text{H}}$  (400 MHz; CDCl<sub>3</sub>) 6.91 (1H, ddd,  $J$  8.0, 7.2, 1.1, C(7)H, or C(8)H), 7.07-7.09 (1H, m, Ar-CH), 7.39 (1H, ddd,  $J$  8.0, 7.2, 1.1, C(7)H or C(8)H), 7.43-7.45 (1H, m, Ar-CH), 7.53-7.57 (2H, m, Ar-CH), 7.60 (1H, dd,  $J$  8.0, 1.6, C(1)H or C(4)H), 7.68 (1H, ddd,  $J$  8.0, 7.2, 1.6, C(2)H or C(3)H), 7.98 (1H, s, C(5)H), 11.75 (1H, s, OH);  $\delta_{\text{C}}$  (100 MHz; CDCl<sub>3</sub>), 117.1 (CH), 117.9 (q),

118.7 (CH), 118.9 (q), 119.2 (CH), 125.2 (CH), 126.4 (q), 129.1 (CH), 132.6 (CH), 133.7 (CH), 137.6 (CH), 144.3 (C(10)H, 154.6 (q), 158.1 (q), 163.3 (q), 196.2 (C=O);  $m/z$  (+ES), 289.05 ( $[M+Na]^+$ , 100 %); (Found 289.0477;  $C_{16}H_{10}O_4Na$  ( $[M+Na]^+$ ), requires 289.0475).

### 5.3.26 Synthesis of (*E*)-3-((2-hydroxynaphthalen-1-yl)methylene)chroman-2,4-dione, **175a**

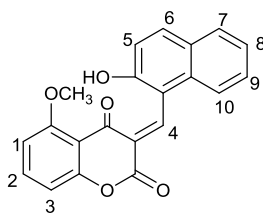


$C_{20}H_{12}O_4$ ; Molecular weight: 316.31

Using method C, 4-hydroxycoumarin (500 mg, 3.08 mmol) was reacted with 2-hydroxy-1-naphthaldehyde (530 mg, 3.08 mmol) and the resulting precipitate was recrystallized from 1,4-dioxane to give the title compound (**175a**) as a yellow foam (400 mg, 41%).

Using Method D, reaction of 4-hydroxycoumarin (500 mg, 3.08 mmol) and 2-hydroxy-1-naphthaldehyde (530 mg, 3.08 mmol) gave the title compound (**175a**) as a yellow solid (300 mg, 31%): Mp 247-249 °C [Lit.<sup>263</sup> 235-237 °C];  $\nu_{max}/cm^{-1}$  3080 (br, w, OH), 1704 (s, C=O), 1570 (s, C=C);  $\delta_H$  (400 MHz; DMSO- $d_6$ ) 6.94-6.98 (2H, m, aro CH), 7.48-7.53 (1H, m, Ar-CH), 7.64-7.68 (2H, m, Ar-CH), 7.74-7.78 (2H, m, Ar-CH), 8.11 (1H, d,  $J$  7.6, C(6)H or C(7)H), 8.31 (1H, d,  $J$  7.6 C(6)H or C(7)H), 8.64 (1H, d,  $J$  8.3, C(1)H or C(4)H), 9.12 (1H, s, C(5)H), 10.78 (1H s, OH);  $\delta_C$  (100 MHz; DMSO- $d_6$ ) 112.7 (CH), 116.6 (CH), 117.1 (CH), 119.3 (CH), 122.5 (CH), 123.2 (CH), 126.4 (CH), 127.8 (CH), 128.7 (CH), 129.0 (CH), 129.2 (CH), 130.0 (CH), 131.3 (CH), 134.7 (CH), 135.5 (CH), 138.9 (C(10)H, 154.1 (q), 158.1 (q), 159.1 (q), 192.6 (C=O);  $m/z$  (+ES) 339.0 ( $[M+Na]^+$ , 100%), 317.0 ( $[M+H]^+$ , 85%); (Found 339.0633;  $C_{20}H_{12}O_4Na$  ( $[M+Na]^+$ ), requires 339.0626).

### 5.3.27 Synthesis of (*E*)-3-((2-hydroxynaphthalen-1-yl)methylene)-5-methoxychroman-2,4-dione, **176a**

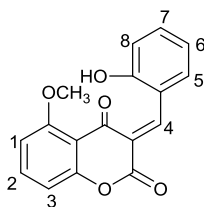


C<sub>21</sub>H<sub>15</sub>O<sub>5</sub>; Molecular weight: 347.34

Using method C, reaction of 4-hydroxy-5-methoxy-2H-chromen-2-one (60 mg, 0.31 mmol) and 2-hydroxy-1-naphthaldehyde (50 mg, 0.31 mmol) gave the title compound (**176a**) as yellow foam (35 mg, 33%).

Using method D, reaction of 4-hydroxy-5-methoxy-2H-chromen-2-one (60 mg, 0.31 mmol) and 2-hydroxy-1-naphthaldehyde (50 mg, 0.31 mmol) gave the title compound (**176a**) as yellow foam (30 mg, 28%): Mp 234-236 °C;  $\nu_{\max}/\text{cm}^{-1}$  3057 (w, OH), 1730 (s, C=O), 1560 (s, C=C);  $\delta_{\text{H}}$  (400 MHz; CDCl<sub>3</sub>) 3.69 (3H, s, OCH<sub>3</sub>), 6.40 (1H, d, *J* 8.3, C(5)H or C(6)H), 6.55-6.60 (1H, m, Ar-CH), 7.44 (1H, t, *J* 8.1, C(2)H), 7.53 (1H, d, *J* 8.3, C(5)H or C(6)H), 7.60-7.64 (1H, m, Ar-CH), 7.75 (1H, ddd, *J* 8.3, 7.2, 1.0, C(8)H or C(9)H), 7.96 (1H, d, *J* 8.1, C(1)H or C(3)H), 8.08 (1H, d, *J* 8.1, C(1)H or C(3)H), 8.34 (1H, d, *J* 8.3, C(7)H or C(10)H), 8.71 (1H, s, C(4)H), 12.03 (1H, s, OH);  $\delta_{\text{C}}$  (100 MHz; CDCl<sub>3</sub>) 56.0 (OCH<sub>3</sub>), 58.5 (q), 101.8 (CH), 111.0 (CH), 114.4 (q), 113.0 (q), 116.7 (CH), 121.7 (CH), 126.4 (CH), 128.8 (CH), 129.2 (CH), 129.5 (q), 130.4 (q), 134.4 (CH), 136.9 (CH), 137.5 (CH), 154.4 (q), 158.4 (q), 161.2 (q), 164.0 (q), 194.6 (C=O); *m/z* (+ES) 369.1 ([M+Na]<sup>+</sup>, 100%); (Found 369.0751; C<sub>21</sub>H<sub>14</sub>O<sub>5</sub>Na ([M+Na]<sup>+</sup>), requires 369.0739).

### 5.3.28 Synthesis of (*E*)-3-(2-hydroxybenzylidene)-5-methoxychroman-2,4-dione, **176b**

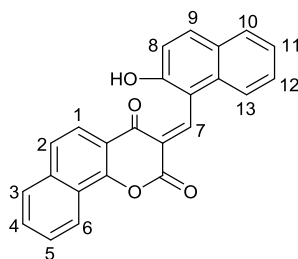


C<sub>17</sub>H<sub>12</sub>O<sub>5</sub>; Molecular weight: 296.27

Using method D, reaction of 4-hydroxy-5-methoxy-2H-chromen-2-one (65 mg, 0.34 mmol) and 2-hydroxy benzaldehyde (41 mg, 0.34 mmol) gave the title compound

(**176b**) as a yellow foam (31 mg, 30%): Mp 178-180 °C;  $\nu_{\max}/\text{cm}^{-1}$  3046 (w, OH), 1718 (s, C=O), 1592 (s, C=C);  $\delta_{\text{H}}$  (400 MHz;  $\text{CDCl}_3$ ) 3.68 (3H, s,  $\text{OCH}_3$ ), 6.37-6.39 (1H, m, Ar-CH), 6.66 (1H, dd,  $J$  8.6, 0.8, C(1)H or C(3)H), 7.33-7.45 (3H, m, Ar-CH), 7.59-7.63 (2H, m, Ar-CH), 7.88 (1H, s, C(4)H), 12.07 (1H, s, OH);  $\delta_{\text{C}}$  (100 MHz;  $\text{CDCl}_3$ ) 56.0 ( $\text{OCH}_3$ ), 101.8 ( $\underline{\text{CH}}$ ), 111.0 ( $\underline{\text{CH}}$ ), 111.2 (q), 116.7 ( $\underline{\text{CH}}$ ), 118.6 (q), 124.8 ( $\underline{\text{CH}}$ ), 129.0 ( $\underline{\text{CH}}$ ), 131.9 (q), 132.7 ( $\underline{\text{CH}}$ ), 137.6 ( $\underline{\text{CH}}$ ), 140.3 ( $\underline{\text{CH}}$ ), 154.2 (q), 158.3 (q), 161.1 (q), 164.2 (q), 194.4 (C=O);  $m/z$  (+ES) 319.1 ( $[\text{M}+\text{Na}]^+$ , 100%); (Found 319.0579;  $\text{C}_{17}\text{H}_{12}\text{O}_5\text{Na}$  ( $[\text{M}+\text{Na}]^+$ ), requires 319.0582).

### 5.3.29 Synthesis of (*E*)-3-((2-hydroxynaphthalen-1-yl)methylene)-H-benzo[h]chromene-2,4(3H)-dione, **177a**



$\text{C}_{24}\text{H}_{14}\text{O}_4$ ; Molecular weight: 366.36

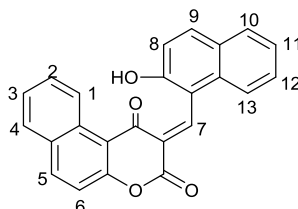
Using method C, reaction of 4-hydroxy-2H-benzo[h]chromen-2-one (200 mg, 0.94 mmol) and 2-hydroxy-1-naphthaldehyde (162 mg, 0.94 mmol) gave the title compound (**177a**) as orange foam (118 mg, 34%).

Using method D, reaction of 4-hydroxy-2H-benzo[h]chromen-2-one (200.0 mg, 0.94 mmol) and 2-hydroxy-1-naphthaldehyde (162 mg, 0.94 mmol) gave the title compound (**177a**) as orange foam (90 mg, 26%): Mp 250-252 °C;  $\nu_{\max}/\text{cm}^{-1}$  3058 (m, OH), 1713 (s, C=O), 1570 (s, C=C);  $\delta_{\text{H}}$  (400 MHz;  $\text{CDCl}_3$ ) 7.51 (1H, d,  $J$  9.0, C(8)H or C(9)H), 7.56-7.60 (3H, m, Ar-CH), 7.64 (1H, ddd,  $J$  8.2, 7.0, 1.4, C(11)H or C(12)H), 7.69 (1H, ddd,  $J$  8.2, 7.0, 1.4, C(11)H or C(12)H), 7.75 (1H, ddd,  $J$  8.2, 6.9, 1.4, C(4)H or C(5)H), 7.78 (1H, d,  $J$  8.1, C(1)H or C(2)H), 7.99 (1H, d,  $J$  8.1, C(1)H or C(2)H), 8.15 (1H, d,  $J$  9.0, C(8)H or C(9)H), 8.28 (1H, d,  $J$  8.2, C(3)H or C(6)H), 8.54 (1H, d,  $J$  8.2, C(3)H or C(6)H), 8.86 (1H, s, C(7)H), 13.67 (1H, s, OH);  $\delta_{\text{C}}$  (100 MHz;  $\text{CDCl}_3$ ) 110.7 (q), 110.9 (q), 114.9 ( $\underline{\text{CH}}$ ), 116.7 ( $\underline{\text{CH}}$ ), 119.6 ( $\underline{\text{CH}}$ ), 122.8 ( $\underline{\text{CH}}$ ), 123.3 (q), 123.5 (q), 124.1 ( $\underline{\text{CH}}$ ), 124.3 ( $\underline{\text{CH}}$ ), 124.7 ( $\underline{\text{CH}}$ ), 125.7 ( $\underline{\text{CH}}$ ), 127.1 ( $\underline{\text{CH}}$ ), 127.4 (d,  $J$  1.8,  $\underline{\text{CH}}$ ), 128.5 (q), 129.0 ( $\underline{\text{CH}}$ ), 133.4 ( $\underline{\text{CH}}$ ), 135.9 (q), 138.8 ( $\underline{\text{CH}}$ ),



153.3 (q), 156.3 (q), 162.3 (q), 194.1 (C=O);  $m/z$  (+ES), 367.0 ( $[M+H]^+$ , 80%); (Found 389.0794;  $C_{24}H_{14}O_4Na$  ( $[M+Na]^+$ ), requires 389.0790).

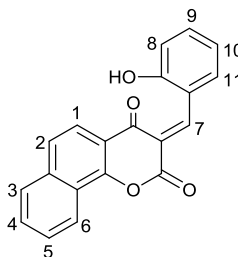
### 5.3.30 Synthesis of (*E*)-2-((2-hydroxynaphthalen-1-yl)methylene)-1H-benzo[f]chromene-1,3(2H)-dione, **211**



$C_{24}H_{14}O_4$ ; Molecular weight: 366.36

Using method D, reaction of 1-hydroxy-3H-benzo[f]chromen-3-one (500 mg, 2.36 mmol) and 2-hydroxy-1-naphthaldehyde (410 mg, 2.36 mmol) gave the title compound (**211**) as orange foam (250 mg, 29%): Mp (235 °C);  $\nu_{\max}/\text{cm}^{-1}$  3305 (br, m, OH), 1706 (s, C=O), 1651 (m, C=C);  $\delta_H$  (400 MHz; DMSO- $d_6$ ) 7.17 (1H, d,  $J$  9.1, C(8)H or C(9)H), 7.39 (1H, ddd,  $J$  8.4, 7.1, 1.3, C(11)H or C(12)H), 7.50 (1H, ddd,  $J$  8.4, 7.1, 1.3, C(2)H or C(3)H), 7.63-7.69 (2H, m, Ar-CH), 7.77 (1H, ddd,  $J$  8.4, 7.1, 1.3, C(2)H or C(3)H), 7.89 (1H, d,  $J$  8.4, C(10)H or C(13)H), 7.96 (1H, d,  $J$  8.4, C(10)H or C(13)H), 8.02 (1H, d,  $J$  8.6, C(5)H or C(6)H), 8.11 (1H, d,  $J$  8.6, C(5)H or C(6)H), 8.33 (1H, d,  $J$  8.4, C(1)H or C(4)H), 8.63 (1H, d,  $J$  8.4, C(1)H or C(4)H), 9.24 (1H, s, C(7)H), 10.53 (1H, s, OH);  $\delta_C$  (100 MHz; DMSO- $d_6$ ) 113.2 (q), 117.0 ( $\underline{\text{CH}}$ ), 118.6 ( $\underline{\text{CH}}$ ), 119.3 (q), 122.9 ( $\underline{\text{CH}}$ ), 123.8 ( $\underline{\text{CH}}$ ), 124.2 ( $\underline{\text{CH}}$ ), 127.0 ( $\underline{\text{CH}}$ ), 127.7 (q), 128.1 ( $\underline{\text{CH}}$ ), 128.5 (q), 128.8 ( $\underline{\text{CH}}$ ), 129.5 ( $\underline{\text{CH}}$ ), 129.6 ( $\underline{\text{CH}}$ ), 129.8 (q), 130.4 (q), 132.3 (q), 133.5 ( $\underline{\text{CH}}$ ), 136.0 ( $\underline{\text{CH}}$ ), 141.2 ( $\underline{\text{CH}}$ ), 155.2 (q), 155.8 (q), 158.3 (q), 192.3 (C=O);  $m/z$  (+ES), 367.1 ( $[M+H]^+$ , 100%); (Found 367.0962;  $C_{24}H_{15}O_4$  ( $[M+H]^+$ ), requires 367.0970).

### 5.3.31 Synthesis of (*E*)-3-(2-hydroxybenzylidene)-2H-benzo[h]chromene-2,4(3H)-dione, **177b**



C<sub>20</sub>H<sub>12</sub>O<sub>4</sub>; Molecular weight: 316.31

Using method D, reaction of 4-hydroxy-2H-benzo[h]chromen-2-one (300 mg, 1.42 mmol) and 2-hydroxy-benzaldehyde (150 mg, 1.42 mmol) gave the title compound (**177b**) as yellow foam (140 mg, 31%): Mp 226-228 °C;  $\nu_{\max}/\text{cm}^{-1}$  1719 (s, C=O), 1582 (s, C=C);  $\delta_{\text{H}}$  (500 MHz; CDCl<sub>3</sub>) 7.25 (1H, dd,  $J$  7.6, 1.4, C(8)H or C(11)H), 7.37-7.39 (1H, m, Ar-CH), 7.43-7.46 (2H, m, Ar-CH), 7.56-7.59 (1H, m, Ar-CH), 7.63 (1H, dd,  $J$  7.6, 1.4, C(8)H or C(11)H), 7.66-7.70 (2H, m, Ar-CH), 7.77 (1H, d,  $J$  8.2, C(1)H or C(2)H), 8.04 (1H, s, C(7)H), 8.52 (1H, d,  $J$  8.2, C(1)H or C(2)H), 13.59 (1H, s, OH);  $\delta_{\text{C}}$  (125 MHz; CDCl<sub>3</sub>) 112.7 (d,  $J$  2.7, q), 117.1 (CH), 118.1 (q), 118.7 (d,  $J$  4.5 CH), 124.7 (d,  $J$  3.6, CH), 125.1 (CH), 125.9 (d,  $J$  4.5, CH), 126.2 (CH), 126.8 (q), 127.6 (CH), 129.1 (CH), 130.9 (d,  $J$  3.6, CH), 133.6 (CH), 137.9 (d,  $J$  2.7, q), 144.3 (d,  $J$  3.6, CH), 154.6 (q), 158.2 (q), 164.2 (C=O);  $m/z$  (+ES), 317.0 ([M+H]<sup>+</sup>, 100%); (Found 339.0645; C<sub>20</sub>H<sub>12</sub>O<sub>4</sub>Na ([M+Na]<sup>+</sup>), requires 339.0633).

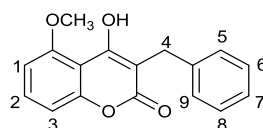
**Method E:** General procedures for the synthesis of asymmetrical analogues of dicoumarol. A solution of 4-hydroxycoumarin (1 eq), an appropriate aromatic alcohol (5 eq), pentamethyl cyclopentadienyl iridium(III)chloride dimer ([Cp\*IrCl<sub>2</sub>]<sub>2</sub>) (5 mol%), caesium carbonate (10 mol%), isopropanol (20 mol%) in toluene (1.4 M) was heated under reflux at 110 °C for 24 hours under nitrogen. The resultant mixture was concentrated *in vacuo* and purification of the crude product was carried out using flash column chromatography on silica gel (ethyl acetate: petroleum ether) or by washing with cold methanol.<sup>254</sup>

**Method F:** Sodium cyanoborohydride (5 eq) was added to a suspension of symmetrical analogues of dicoumarol (1 eq) in methanol (20 mL) and the reaction mixture was heated under reflux for 18 hours at 70 °C under nitrogen. The resulting solution was concentrated under *vacuo* in a ventilated fume hood. Saturated NH<sub>4</sub>Cl solution (15 mL) was added to the residue and organic material was extracted into ethyl acetate (4x20 mL). The combined organic extracts were washed with saturated NH<sub>4</sub>Cl solution (3x20 mL), brine (20 mL), dried over MgSO<sub>4</sub> and concentrated in *vacuo* to give the crude product. This crude material was purified by flash column chromatography on silica gel (petroleum: ethyl acetate).<sup>254</sup>

**Method G:** A solution of LiBH<sub>4</sub> (2 eq) or NaBH<sub>4</sub> (6 eq) was stirred in THF or methanol respectively at room temperature under nitrogen gas for 10 minutes. A

solution of an appropriate half way stage compound (1 eq) in THF or methanol (5 mL) was added dropwise at 0 °C and the reaction mixture was then allowed to stir for 24 hours at room temperature. The reaction was quenched by pouring into cold HCl (0.1M: 10 mL) and the resulting mixture was concentrated *in vacuo* to give dark brown oil. Ethyl acetate (20 mL) was added and the resulting suspension filtered. The residue was washed with ethyl acetate (3x10 mL), dried over MgSO<sub>4</sub> and concentrated *in vacuo* to give a crude product. This crude material was further purified by flash silica column chromatography (petroleum: ethyl acetate).

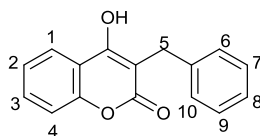
### 5.3.32 Synthesis of 3-benzyl-4-hydroxy-5-methoxy-2H-chromen-2-one, 179b



C<sub>17</sub>H<sub>14</sub>O<sub>4</sub>; Molecular weight: 282.29

Using method E, reaction of 4-hydroxy-5-methoxy-2H-chromen-2-one (136 mg, 0.71 mmol) and benzyl alcohol (384 mg, 3.55 mmol) gave the title compound (**179b**) as a cream coloured solid (178 mg, 89%): Mp 170-172 °C;  $\nu_{\text{max}}/\text{cm}^{-1}$  3320 (br, w, OH), 1686 (s, C=O), 1643 (s, C=C);  $\delta_{\text{H}}$  (400 MHz; CDCl<sub>3</sub>) 3.91 (2H, s, C(4)H<sub>2</sub>), 4.06 (3H, s, OCH<sub>3</sub>), 6.78 (1H, dd, *J* 8.4, 0.9, C(1)H or C(3)H), 7.01 (1H, dd, *J* 8.4, 0.9, C(1)H or C(3)H), 7.16-7.20 (1H, m, Ar-CH), 7.25-7.28 (2H, m, Ar-CH), 7.40-7.44 (3H, m, Ar-CH), 9.73 (1H, s, OH);  $\delta_{\text{C}}$  (126 MHz; CDCl<sub>3</sub>) 29.2 (C(4)H<sub>2</sub>), 57.0 (OCH<sub>3</sub>), 105.3 (CH), 105.4 (CH), 111.2 (CH), 126.1 (CH), 128.2 (CH), 128.9 (CH), 131.5 (CH), 140.1 (q), 151.2 (q), 153.6 (q), 155.8 (q), 161.1 (q), 163.3 (C=O); *m/z* (-ES) 283.1 ([M-H]<sup>-</sup>, 100%); (+ES) (Found 305.0796; C<sub>17</sub>H<sub>14</sub>O<sub>6</sub>Na ([M+Na]<sup>+</sup>), requires 305.0790).

### 5.3.33 Synthesis of 3-benzyl-4-hydroxy-2H-chromen-2-one, 178b

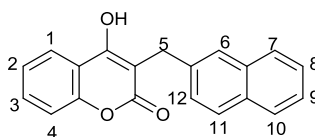


C<sub>20</sub>H<sub>12</sub>O<sub>4</sub>; Molecular weight: 252.26

Using method E, reaction of 4-hydroxycoumarin (136 mg, 0.84 mmol) and benzyl alcohol (454 mg, 4.19 mmol) gave the title compound (**178b**) as a white solid (111 mg, 52%): Mp 208–210 °C [Lit.<sup>264</sup> 207-209 °C];  $\nu_{\text{max}}/\text{cm}^{-1}$  3031 (br, OH), 1685 (s,

C=O), 1605 (s, C=C);  $\delta_{\text{H}}$  (400 MHz;  $\text{CDCl}_3$ ) 4.05 (2H, s, C(5)H), 7.28-7.34 (2H, m, Ar-CH), 7.36-7.38 (5H, m, Ar-CH), 7.55 (1H, ddd,  $J$  8.5, 7.6, 1.5, C(2)H or C(3)H), 7.75 (1H, dd,  $J$  8.5, 1.5, C(1)H or C(4)H);  $\delta_{\text{C}}$  (75 MHz;  $\text{DMSO}-d_6$ ) 29.1 (C(5)H), 104.1 (q), 116.0 (CH), 116.2 (CH), 123.3 (CH), 123.9 (CH), 125.6 (CH), 128.0 (CH), 128.1 (CH), 131.6 (CH), 139.7 (q), 152 (q), 160.4 (152 (q), 162.6 (C=O);  $m/z$  (-ES), 251 ( $[\text{M}-\text{H}]^-$ , 100%).

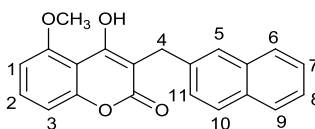
### 5.3.34 Synthesis of 4-hydroxy-3-(naphthalene-2-ylmethyl)-2H-chromen-2-one, **178a**



$\text{C}_{20}\text{H}_{14}\text{O}_3$ ; Molecular weight: 302.32

Using method E, reaction of 4-hydroxycoumarin (150 mg, 0.93 mmol) and 2-naphthalene methanol (270 mg, 1.71 mmol) gave the title compound (**178a**) as a white solid (168 mg, 60%): Mp 211 °C [Lit.<sup>174</sup> 202-204];  $\nu_{\text{max}}/\text{cm}^{-1}$  3054 (br, w, OH), 1650 (s, C=O), 1620 (s, C=C);  $\delta_{\text{H}}$  (400 MHz;  $\text{DMSO}-d_6$ ) 4.06 (2H, s, C(5)H), 7.36-7.45 (5H, m, Ar-CH), 7.63 (1H, ddd,  $J$  8.4, 7.2, 1.5, C(2)H or C(3)H or C(8)H or C(9)H), 7.69 (1H, s, C(6)H), 7.81-7.83 (3H, m, Ar-CH), 8.02 (1H, dd,  $J$  8.4, 1.5, C(1)H or C(4)H or C(7)H or C(10)H), 11.73 (1H, s, OH);  $\delta_{\text{C}}$  (100 MHz;  $\text{DMSO}-d_6$ ) 29.4 (C(5)H), 103.9 (q), 116.2 (CH), 116.3 (q), 123.4 (CH), 123.9 (CH), 125.2 (CH), 125.7 (CH), 125.9 (CH), 127.2 (CH), 127.3 (CH), 127.4 (CH), 127.6 (CH), 131.6 (q), 131.9 (CH), 133.0 (q), 137.4 (q), 152.1 (q), 160.8 (q), 162.9 (C=O);  $m/z$  (+ES) 325.1 ( $[\text{M}+\text{Na}]^+$ , 70%); (Found 325.0853;  $\text{C}_{20}\text{H}_{14}\text{O}_3\text{Na}$  ( $[\text{M}+\text{Na}]^+$ ), requires 325.0841).

### 5.3.35 Synthesis of 4-hydroxy-5-methoxy-3-(naphthalen-2-ylmethyl)-2H-chromen-2-one, **179a**

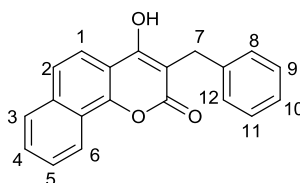


$\text{C}_{21}\text{H}_{16}\text{O}_4$ ; Molecular weight: 332.35

Using method E, reaction of 4-hydroxy-5-methoxy-2H-chromen-2-one (150 mg, 0.78 mmol) and 2-naphthalenemethanol (249 mg, 1.58 mmol) gave the title compound (**179a**) as a white solid (152 mg, 59%): Mp 157 °C;  $\nu_{\text{max}}/\text{cm}^{-1}$  3293 (s, OH), 1702 (s,

C=O), 1637 (s, C=C);  $\delta_{\text{H}}$  (400 MHz, DMSO- $d_6$ ) 3.99 (2H, s, C(4)H<sub>2</sub>), 4.06 (3H, s, OCH<sub>3</sub>), 7.07 (2H, d,  $J$  8.3, C(10)H and C(11)H), 7.47-7.53 (3H, m, Ar-CH), 7.63 (1H, t,  $J$  8.3, C(2)H), 7.78 (1H, s, C(5)H), 7.85-7.88 (3H, m, Ar-CH);  $\delta_{\text{C}}$  (100 MHz; DMSO- $d_6$ ) 29.0 (C(4)H<sub>2</sub>), 60.0 (OCH<sub>3</sub>), 103.2 (q), 104.4 (q), 106.5 (CH), 109.7 (CH), 125.2 (CH), 125.9 (CH), 127.2 (CH), 127.3 (CH), 127.4 (CH), 127.5 (q), 127.7 (CH), 131.6 (q), 132.5 (CH), 133.0 (q), 137.5 (q), 153.1 (q), 156.2 (q), 161.3 (q), 162.4 (C=O);  $m/z$  (+ES) 355.1 ([M]<sup>+</sup> Na<sup>+</sup>, 100%); (Found 355.0961 C<sub>21</sub>H<sub>16</sub>O<sub>4</sub> ([M+ Na]<sup>+</sup>), requires 355.0946).

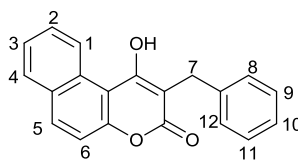
### 5.3.36 Synthesis of 3-benzyl-4-hydroxy-3,4-dihydro-2H-benzo[h]chromen-2-one, **180b**



C<sub>20</sub>H<sub>14</sub>O<sub>3</sub>; Molecular weight: 302.32

Using method E, reaction of 4-hydroxy-2H-benzo[h]chromen-2-one (120 mg, 0.57 mmol) and benzyl alcohol (306 mg, 2.83 mmol) gave the title compound (**180b**) as off-white solid (95 mg, 56%): Mp 260-262 °C [Lit.<sup>174</sup> 259 °C];  $\nu_{\text{max}}$ /cm<sup>-1</sup> 3028 (br, w, OH), 1606 (s, C=O), 1557 (s, C=C);  $\delta_{\text{H}}$  (400 MHz, DMSO- $d_6$ ) 3.95 (2H, s, C(7)H<sub>2</sub>), 7.15-7.18 (1H, m, Ar-CH), 7.24-7.29 (4H, m, Ar-CH), 7.70-7.73 (2H, m, Ar-CH), 7.88 (1H, d,  $J$  8.8, C(1)H or C(2)H), 8.01 (1H, d,  $J$  8.8, C(1)H or C(2)H), 8.06 (1H, dd,  $J$  5.8, 4.3, C(3)H or C(6)H), 8.34-8.37 (1H, m, Ar-CH);  $\delta_{\text{C}}$  (100 MHz; DMSO- $d_6$ ) 29.1 (C(7)H<sub>2</sub>), 103.8 (q), 116.6 (q), 119.4 (CH), 121.5 (CH), 122.1 (q), 123.6 (CH), 123.7 (CH), 125.9 (CH), 126.5 (CH), 127.3 (CH), 128.0 (CH), 128.1 (CH), 128.2 (CH), 128.5 (CH), 134.3 (q), 139.8 (q), 148.9 (q), 161.5 (q), 162.8 (q);  $m/z$  (+ES) 325.1 ([M+Na]<sup>+</sup>, 100%); (Found 325.0851; C<sub>20</sub>H<sub>14</sub>O<sub>3</sub>Na ([M+Na]<sup>+</sup>), requires 325.0841).

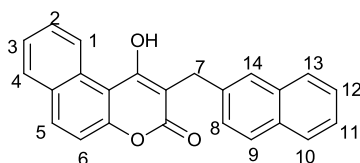
### 5.3.37 Synthesis of 3-benzyl-4-hydroxy-3,4-dihydro-2H-benzo[h]chromen-2-one, **212**



C<sub>20</sub>H<sub>14</sub>O<sub>3</sub>; Molecular weight: 302.32

Using method E, reaction of 1-hydroxy-3H-benzo[f]chromen-3-one (120 mg, 0.57 mmol) and benzyl alcohol (306 mg, 2.83 mmol) gave the title compound (**212**) as a white solid (95 mg, 56%): Mp 260-262 °C [Lit.<sup>174</sup> 259 °C];  $\nu_{\max}/\text{cm}^{-1}$  3047 (br, w, OH), 1646 (s, C=O), 1546 (s, C=C);  $\delta_{\text{H}}$  (400MHz; DMSO-*d*<sub>6</sub>) 4.03 (2H, s, C(7)H<sub>2</sub>), 7.14-7.27 (5H, m, Ar-CH), 7.53 (1H, d, *J* 8.8, C(5)H or C(6)H), 7.59 (1H, ddd, *J* 8.4, 7.1, 1.3, C(2)H or C(3)H), 7.69 (1H, ddd, *J* 8.4, 7.1, 1.3, C(2)H or C(3)H), 8.04 (1H, d, *J* 8.8, C(5)H or C(6)H), 8.17 (1H, d, *J* 8.4, C(1)H or C(4)H), 9.44 (1H, d, *J* 8.4, C(1)H or C(4)H), 11.96 (1H, s, OH);  $\delta_{\text{C}}$  (100 MHz; DMSO-*d*<sub>6</sub>) 29.4 (C(7)H<sub>2</sub>), 104.5 (q), 117.5 (CH), 117.5 (CH), 120.0 (CH), 125.9 (q), 126.4 (CH), 126.7 (CH), 128.3 (CH), 128.3 (CH), 128.6 (CH), 128.7 (CH), 129.5 (CH), 131.1 (CH), 131.7 (CH), 133.9 (CH), 138.5 (q), 140.0 (q), 153.4 (q), 162.8 (q), 168.0 (C=O); *m/z* (-ES) 301.2 ([M-H]<sup>-</sup>, 100%); (+ES) (Found 325.0857; C<sub>20</sub>H<sub>14</sub>O<sub>3</sub> ([M+Na]<sup>+</sup>), requires 325.0865).

### 5.3.38 Synthesis of 1-hydroxy-2-(naphthalene-2-ylmethyl)-3H-benzo[f]chromen-3-one, **213**

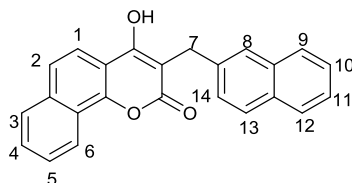


C<sub>24</sub>H<sub>16</sub>O<sub>3</sub>; Molecular weight: 352.38

Using method E, reaction of 1-hydroxy-3H-benzo[f]chromen-3-one (150 mg, 0.93 mmol) and 2-naphthalenemethanol (270 mg, 1.71 mmol) gave the title compound (**213**) as off-white solid (144 mg, 58%): Mp 270-272 °C;  $\delta_{\text{H}}$  (400 MHz; DMSO-*d*<sub>6</sub>) 4.21 (2H, s, C(7)H<sub>2</sub>), 7.40-7.49 (3H, m, Ar-CH), 7.54-7.62 (2H, m, Ar-CH), 7.68-7.71 (2H, m, Ar-CH), 7.81-7.85 (3H, m, Ar-CH), 8.05 (1H, d, *J* 7.6, C(5)H or C(6)H), 8.18 (1H, d, *J* 8.8, C(8)H or C(9)H), 9.44 (1H, d, *J* 8.8, C(8)H or C(9)H), 11.99 (1H,

br, s, OH);  $\delta_{\text{C}}$  (100 MHz; DMSO- $d_6$ ) 29.2 ( $\underline{\text{C}}(7)\text{H}_2$ ), 103.9 (q), 117.0 ( $\underline{\text{CH}}$ ), 125.2 ( $\underline{\text{CH}}$ ), 125.5 ( $\underline{\text{CH}}$ ), 125.9 ( $\underline{\text{CH}}$ ), 126.0 ( $\underline{\text{CH}}$ ), 126.3 ( $\underline{\text{CH}}$ ), 127.2 ( $\underline{\text{CH}}$ ), 127.3 ( $\underline{\text{CH}}$ ), 127.4 ( $\underline{\text{CH}}$ ), 127.7 ( $\underline{\text{CH}}$ ), 128.1 ( $\underline{\text{CH}}$ ), 129.0 (q), 129.1 ( $\underline{\text{CH}}$ ), 130.6 (q), 131.6 (q), 133.0 (q), 133.6 ( $\underline{\text{CH}}$ ), 137.1 (q), 153.0 (q), 162.4 (q), 164.6 (C=O);  $m/z$  (-ES) 351.3 ( $[\text{M}-\text{H}]^-$ , 100%); (Found 351.1020;  $\text{C}_{24}\text{H}_{15}\text{O}_3$  ( $[\text{M}-\text{H}]^-$ ), requires 351.1021).

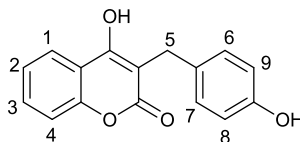
### 5.3.39 Synthesis of 4-hydroxy-3-(naphthalene-2-ylmethyl)-2H-benzo[h]chromen-2-one, 180a



$\text{C}_{24}\text{H}_{16}\text{O}_3$ ; Molecular weight: 352.38

Using method E, reaction of 4-hydroxy-2H-benzo[h]chromen-2-one (150 mg, 0.93 mmol) and 2-naphthalenemethanol (270 mg, 1.71 mmol) gave the title compound (**180a**) as off-white solid (144 mg, 58%): Mp 276-278 °C (Lit.<sup>174</sup> 260-263 °C);  $\nu_{\text{max}}/\text{cm}^{-1}$  3160 (br, w, OH), 1650 (s, C=O), 1607 (s, C=C);  $\delta_{\text{H}}$  (400 MHz, DMSO- $d_6$ ) 4.14 (2H, s,  $\text{C}(7)\underline{\text{H}}_2$ ), 7.41-7.51 (3H, m, Ar- $\underline{\text{CH}}$ ), 7.70-7.75 (3H, m, Ar- $\underline{\text{CH}}$ ), 7.82-7.89 (4H, m, Ar- $\underline{\text{CH}}$ ), 8.05 (2H, dd,  $J$  9.6, 4.6,  $\text{C}(9)\underline{\text{H}}$  and  $\text{C}(12)\underline{\text{H}}$ ), 8.38 (1H, dd,  $J$  9.6, 4.6,  $\text{C}(3)\underline{\text{H}}$  and  $\text{C}(6)\underline{\text{H}}$ ), 11.92 (1H, br, s, OH);  $\delta_{\text{C}}$  (100 MHz; DMSO- $d_6$ ) 29.4 ( $\underline{\text{C}}(7)\text{H}$ ), 103.6 (q), 111.7 (q), 119.5 ( $\underline{\text{CH}}$ ), 121.5 ( $\underline{\text{CH}}$ ), 122.1 (q), 123.6 ( $\underline{\text{CH}}$ ), 125.2 ( $\underline{\text{CH}}$ ), 125.7 ( $\underline{\text{CH}}$ ), 125.9 ( $\underline{\text{CH}}$ ), 126.9 (q), 127.3 (t,  $J$  5.1), 127.6 ( $\underline{\text{CH}}$ ), 128.0 ( $\underline{\text{CH}}$ ), 128.5 ( $\underline{\text{CH}}$ ), 131.6 (q), 133.0 (q), 134.3 (q), 137.4 (q), 150.6 (q), 161.7 (C=O);  $m/z$  (+ES) 375.1 ( $[\text{M}+\text{Na}]^+$ , 100%); (Found 375.1002;  $\text{C}_{24}\text{H}_{16}\text{O}_3\text{Na}$  ( $[\text{M}+\text{Na}]^+$ ), requires 375.0997).

### 5.3.40 Synthesis of 4-hydroxy-3-(4-hydroxybenzyl)-2H-chromen-2-one, 172c

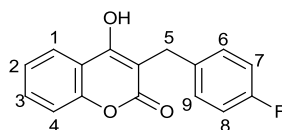


$\text{C}_{16}\text{H}_{12}\text{O}_4$ ; Molecular weight: 268.26

Using method F, reaction of 3,3'-((4-hydroxyphenyl)methylene)bis(4-hydroxy-2H-chromen-2-one, **71**) (122 mg, 0.29 mmol) and sodium cyanoborohydride (90 mg, 1.43 mmol) gave the title compound (**172c**) as a white solid (25 mg, 33%): Mp 208-

210 °C;  $\nu_{\max}/\text{cm}^{-1}$  3152 (br, w, OH), 1655 (s, C=O), 1568 (s, C=C);  $\delta_{\text{H}}$  (400 MHz; DMSO- $d_6$ ) 3.76 (2H, s, C(5)H<sub>2</sub>), 6.63 (2H, d,  $J$  8.3, C(6)H and C(7)H or C(8)H and C(9)H), 7.03 (2H, d,  $J$  8.3, C(6)H and C(7)H or C(8)H and C(9)H), 7.36 (2H, d,  $J$  8.1, Ar-CH), 7.60 (1H, td,  $J$  8.1, 1.5, C(2)H or C(3)H), 7.96 (1H, td,  $J$  8.1, 1.5, C(2)H or C(3)H), 9.14 (1H, s, OH);  $\delta_{\text{C}}$  (125 MHz; DMSO- $d_6$ ) 28.1 (C(5)H<sub>2</sub>), 104.9 (q), 114.9 (CH), 116.1 (CH), 116.3 (CH), 123.3 (CH), 123.8 (CH), 129.0 (CH), 129.8 (q), 131.7 (CH), 151.9 (q), 156.4 (q), 160.1 (q), 162.2 (C=O);  $m/z$  (-ES), 267.1 ([M-H]<sup>-</sup>, 100%); (Found 291.0638; C<sub>16</sub>H<sub>12</sub>O<sub>4</sub>Na ([M+Na]<sup>+</sup>), requires 291.0633).

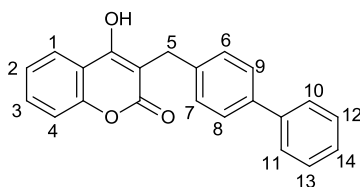
### 5.3.41 Synthesis of 3-(4-fluorobenzyl)-4-hydroxy-2H-chromen-2-one, 172d



C<sub>16</sub>H<sub>11</sub>O<sub>3</sub>F; Molecular weight: 270.25

Using method F, reaction of 3,3'-((4-fluorophenyl)methylene)bis(4-hydroxy-2H-chromen-2-one, **72**) (130 mg, 0.30 mmol) and sodium cyanoborohydride (95 mg, 1.51 mmol) in methanol (15.0 mL) gave the title compound (**172d**) as a white solid (27 mg, 33%): Mp 226-228 °C;  $\nu_{\max}/\text{cm}^{-1}$  3231 (br, OH), 1676 (s, C=O), 1603 (s, C=C);  $\delta_{\text{H}}$  (400MHz; DMSO- $d_6$ ) 3.86 (2H, s, C(5)H<sub>2</sub>), 7.05-7.09 (2H, m, Ar-CH), 7.25-7.29 (2H, m, Ar-CH), 7.33-7.36 (2H, m, Ar-CH), 7.59-7.64 (1H, m, Ar-CH), 7.98 (1H, d,  $J$  7.1, C(1)H or C(4)H);  $\delta_{\text{C}}$  (100 MHz; DMSO- $d_6$ ) 28.3 (C(5)H<sub>2</sub>), 115.2 (q), 115.4 (CH), 116.2 (d,  $J$  2.9, CH), 123.4 (CH), 124.4 (CH), 129.8 (CH), 129.9 (CH), 131.9 (CH), 135.8 (q), 135.9 (q), 152.5 (q), 161.1 (C-F), 163.3 (C=O);  $m/z$  (+ES), 293.0 ([M+Na]<sup>+</sup>, 100%); (Found 293.0583; C<sub>16</sub>H<sub>11</sub>O<sub>3</sub>FNa ([M+Na]<sup>+</sup>), requires 293.0590).

### 5.3.42 Synthesis of 3-([1,1'-biphenyl]-4-ylmethyl)-4-hydroxy-2H-chromen-2-one, 172e



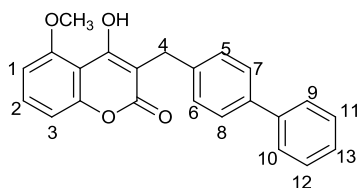
C<sub>22</sub>H<sub>16</sub>O<sub>3</sub>; Molecular weight: 328.36



Using method F, reaction of 3,3'-([1,1'-biphenyl]-4-ylmethylene)bis(4-hydroxy-2H-chromen-2-one, **96**) (130 mg, 0.27 mmol) and sodium cyanoborohydride (84 mg, 1.33 mmol) gave the the title compound (**172e**) as a white solid (45 mg, 52%).

Using method E, reaction of 4-hydroxycoumarin (65 mg, 0.40 mmol) and [1,1'-biphenyl]-4-yl methanol (369 mg, 2.01 mmol) gave the title compound (**172e**) as white solid (100 mg, 76%): Mp 225-227 °C [Lit.<sup>265</sup> 221-222 °C];  $\nu_{\max}/\text{cm}^{-1}$  3217 (br, w, OH), 1664 (s, C=O), 1626 (s, C=C);  $\delta_{\text{H}}$  (400MHz; DMSO- $d_6$ ) 3.93 (2H, s, C(5)H<sub>2</sub>), 7.30-7.45 (7H, m, Ar-CH), 7.55 (2H, d, *J* 8.1, C(6)H and C(7)H or C(8)H and C(9)H), 7.59-7.64 (3H, m, Ar-CH), 8.0 (1H, d, *J* 8.1, C(1)H or C(4)H);  $\delta_{\text{C}}$  (100 MHz; DMSO- $d_6$ ) 28.8 (C(5)H<sub>2</sub>), 104.1 (q), 116.2 (CH), 123.3 (CH), 123.9 (CH), 126.4 (CH), 126.5 (CH), 127.1 (CH), 127.2 (q), 128.7 (CH), 128.8 (CH), 131.9 (CH), 140.1 (q), 152.0 (q), 160.6 (q), 162.9 (C=O); *m/z* (+ES) 351.1 ([M+Na]<sup>+</sup>, 100%); (Found 351.1012; C<sub>22</sub>H<sub>16</sub>O<sub>3</sub>Na ([M+Na]<sup>+</sup>), requires 351.0997).

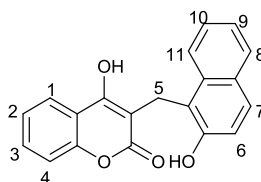
### 5.3.43 Synthesis of 3-([1,1'-biphenyl]-4-ylmethyl)-4-hydroxy-5-methoxy-2H-chromen-2-one, **173c**



C<sub>23</sub>H<sub>18</sub>O<sub>4</sub>; Molecular weight: 358.39

Using method F, reaction of 3,3'-([1,1'-biphenyl]-4-ylmethylene)bis(4-hydroxy-5-methoxy-2H-chromen-2-one, **99**) (46 mg, 0.09 mmol) and sodium cyanoborohydride (26 mg, 0.42 mmol) gave the title compound (**173c**) as a white solid (15 mg, 50%): Mp (172-174 °C);  $\nu_{\max}/\text{cm}^{-1}$  3325 (s, w, O-H), 2950 (w, alkyl C-H), 1685 (s, C=O), 1644 (s, C=C);  $\delta_{\text{H}}$  (400MHz; DMSO- $d_6$ ) 3.80 (2H, s, C(4)H<sub>2</sub>), 4.02 (3H, s, OCH<sub>3</sub>), 7.03 (2H, d, *J* 8.3, C(5)H and C(6)H or C(7)H and C(8)H), 7.31-7.37 (3H, m, Ar-CH), 7.41-7.45 (2H, m, Ar-CH), 7.54 (2H, d, *J* 8.3, C(5)H and C(6)H or C(7)H and C(8)H), 7.58-7.61 (3H, m, Ar-CH), 10.26 (1H, s, br, OH);  $\delta_{\text{C}}$  (100 MHz; DMSO- $d_6$ ) 28.4 (C(4)H<sub>2</sub>), 57.0 (OCH<sub>3</sub>), 103.4 (q), 106.5 (CH), 109.7 (CH), 126.5 (CH), 126.6 (CH), 127.1 (CH), 128.7 (CH), 128.8 (CH), 132.5 (CH), 137.9 (q), 139.2 (q), 140.1 (q), 153.0 (q), 156.1 (q), 161.1 (q), 162.3 (C=O); *m/z* (+ES) 359.1 ([M+H]<sup>+</sup>, 100%); (Found 381.1116; C<sub>23</sub>H<sub>18</sub>O<sub>4</sub>Na ([M+Na]<sup>+</sup>), requires 381.1103).

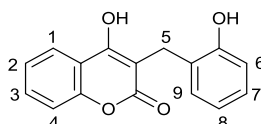
#### 5.3.44 Synthesis of 4-hydroxy-3-((2-hydroxynaphthalen-1-yl)methyl)-2H-chromen-2-one, **172a**



C<sub>20</sub>H<sub>14</sub>O<sub>4</sub>; Molecular weight: 318.32

Using method G, reaction of compound (**69**) (350 mg, 1.11 mmol) and sodium borohydride (252 mg, 6.65 mmol) in methanol (5 mL) gave the title compound (**172a**) as a white solid (150 mg, 43%): Mp 250-252 °C;  $\nu_{\max}/\text{cm}^{-1}$  2980 (br, w, OH), 1650 (s, C=O), 1600 (s, C=C);  $\delta_{\text{H}}$  (400 MHz; DMSO-*d*<sub>6</sub>) 4.23 (2H, s, C(5)H<sub>2</sub>), 7.20 (1H, d, *J* 8.6, C(6)H or C(7)H), 7.26-7.35 (3H, m, Ar-CH), 7.43 (1H, ddd, *J* 8.5, 7.0, 1.4, C(9)H or C(10)H), 7.57 (1H, ddd, *J* 8.5, 7.0, 1.4, C(9)H or C(10)H), 7.70 (1H, d, *J* 8.6, C(6)H or C(7)H), 7.77 (1H, dd, *J* 8.5, 1.4, C(8)H or C(11)H), 7.87 (1H, dd, *J* 8.5, 1.4, C(8)H or C(11)H), 8.35 (1H, d, *J* 8.5, C(1)H or C(4)H);  $\delta_{\text{C}}$  (100 MHz; DMSO-*d*<sub>6</sub>) 19.7 (C(5)H<sub>2</sub>), 103.5 (q), 116.0 (CH), 116.1 (q), 117.6 (q), 117.8 (CH), 122.8 (CH), 123.2 (CH), 123.8 (CH), 123.9 (CH), 126.3 (CH), 128.2 (CH), 128.2 (CH), 128.7 (q), 131.9 (CH), 133.4 (q), 151.3 (q), 151.8 (q), 161.5 (q), 163.1 (C=O); *m/z* (-ES) 317.2 ([M-H]<sup>-</sup>, 100%); (+ES) (Found 319.0970; C<sub>20</sub>H<sub>15</sub>O<sub>4</sub> ([M+H]<sup>+</sup>), requires 319.0975).

#### 5.3.45 Synthesis of 4-hydroxy-3-(2-hydroxybenzyl)-2H-chromen-2-one, **172b**

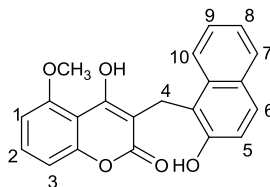


C<sub>16</sub>H<sub>12</sub>O<sub>4</sub>; Molecular weight: 268.26

Using method G, reaction of LiBH<sub>4</sub> (54 mg, 2.48 mmol) and compound (**175b**) (380 mg, 1.43 mmol) in THF (5 mL) gave the title compound (**172b**) as a white solid (70 mg, 18%): Mp 236-238 °C [Lit.<sup>266</sup> 238 °C];  $\nu_{\max}/\text{cm}^{-1}$  2940 (br, w, O-H), 1653 (s, C=O), 1600 (s, C=C);  $\delta_{\text{H}}$  (400 MHz; DMSO-*d*<sub>6</sub>) 3.78 (2H, s, C(5)H<sub>2</sub>), 6.66 (1H, td, *J* 7.8, 1.0, C(7)H or C(8)H), 6.80 (1H, dd, *J* 7.8, 1.0, C(6)H or C(9)H), 6.83-6.85 (1H, m, Ar-CH), 7.00 (1H, td, *J* 7.8, 1.0, C(7)H or C(8)H), 7.35-7.39 (2H, m, Ar-CH), 7.62 (1H, td, *J* 7.8, 1.0, C(2)H or C(3)H), 7.94 (1H, dd, *J* 7.8, 1.0, C(1)H or C(4)H);  $\delta_{\text{C}}$  (100 MHz; DMSO-*d*<sub>6</sub>) 23.8 (C(5)H<sub>2</sub>), 102.8 (q), 114.7 (q), 116.1 (CH), 116.4

(CH), 118.9 (CH), 123.3 (CH), 123.8 (CH), 125.4 (q), 126.8 (CH), 128.0 (CH), 131.7 (CH), 152.0 (q), 154.9 (q), 161.1 (q), 162.9 (C=O);  $m/z$  (+ES) 269.1 ( $[M+H]^+$ , 100%); (Found 291.0628;  $C_{16}H_{12}O_4Na$  ( $[M+Na]^+$ ), requires 291.0633).

#### 5.3.46 Synthesis of 4-hydroxy-3-((2-hydroxynaphthalen-1-yl)methyl)-5-methoxy-2H-chromen-2-one, **173a**

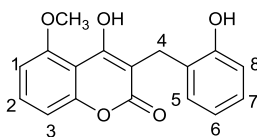


$C_{21}H_{16}O_5$ ; Molecular weight: 348.35

Using method G, reaction of sodium borohydride (230 mg, 6.07 mmol) and compound (**176a**) (350 mg, 1.01 mmol) in methanol (12 mL) gave the title compound (**173a**) as a white solid (140 mg, 40%).

**Method H:** Suspension of compound (**176a**) (31 mg, 0.09 mmol) in methanol (3 mL) was stirred for 10 minutes at room temperature under nitrogen. 1-benzyl-1,4-dihydropyridine-3-carboxamide, (**198**) (40 mg, 0.19 mmol) was added gradually at 0 °C and then the reaction mixture was stirred at room temperature for 24 hours. The progress of the reaction was monitored by TLC and once the reaction had completed, dilute HCl (0.1M, 7 mL) was added to quench the reaction. The crude material was collected by filtration as a brown solid (23 mg). This crude material was purified by flash column chromatography (petroleum: ethyl acetate 2:1) to give the title compound (**173a**) as a white solid (10 mg, 32%): Mp 218-220 °C;  $\nu_{max}/cm^{-1}$  3233 (br, w, OH), 1660 (s, C=O), 1635 (s, C=C);  $\delta_H$  (400 MHz;  $CDCl_3$ ) 4.13 (3H, s,  $OCH_3$ ), 4.21 (2H, s, C(4)H<sub>2</sub>), 6.81 (1H, d,  $J$  8.3, C(5)H), 7.01 (1H, d,  $J$  8.4, C(1)H or C(3)H), 7.31-7.35 (2H, m, Ar-CH), 7.43 (1H, t,  $J$  8.4, C(2)H), 7.50-7.54 (1H, m, Ar-CH), 7.67 (1H, d,  $J$  8.4, C(6)H), 7.74 (1H, d,  $J$  8.4, C(7)H or C(10)H), 8.51 (1H, d,  $J$  8.4, C(7)H or C(10)H), 9.53 (1H, s, OH), 10.37 (1H, s, OH);  $\delta_C$  (100 MHz;  $CDCl_3$ ) 19.0 (C(4)H<sub>2</sub>), 56.2 ( $OCH_3$ ), 103.4 (q), 104.0 (CH), 104.9 (q), 110.2 (CH), 116.9 (q), 119.8 (CH), 121.7 (CH), 125.0 (q), 127.4 (CH), 127.7 (CH), 128.5 (CH), 131.2 (q), 132.7 (CH), 151.9 (q), 152.9 (q), 154.7 (q), 161.2 (q), 165.6 (C=O);  $m/z$  (+ES) 371.3 ( $[M+Na]^+$ , 100%), 349.3 ( $[M+H]^+$ , 63%).

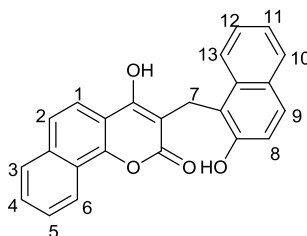
### 5.3.47 Synthesis of 4-hydroxy-3-(2-hydroxyl)-5-methoxy-2H-chromen-2-one, **173b**



C<sub>17</sub>H<sub>14</sub>O<sub>5</sub>; Molecular weight: 298.28

Using method G, reaction of compound (**176b**) (40 mg, 0.14 mmol) and sodium borohydride (10 mg, 0.27 mmol) in methanol (2 mL) gave the title compound (**173b**) as a white solid (20 mg, 50%): Mp 206-208 °C;  $\nu_{\text{max}}/\text{cm}^{-1}$  3286 (w, O-H), 1661 (s, C=O), 1635 (s, C=C);  $\delta_{\text{H}}$  (400 MHz; CDCl<sub>3</sub>) 3.79 (2H, s, C(4)H<sub>2</sub>), 4.03 (3H, s, OCH<sub>3</sub>), 6.73-6.77 (2H, m, Ar-CH), 6.87 (1H, dd, *J* 8.1, 1.0, C(12)H or C(15)H), 6.96 (1H, d, *J* 8.3, C(1)H or C(3)H), 7.03-7.07 (1H, m, Ar-CH), 7.34-7.40 (2H, m, Ar-CH), 8.52 (1H, s, OH), 9.95 (1H, s, OH);  $\delta_{\text{C}}$  (100 MHz; CDCl<sub>3</sub>) 24.2 (C(4)H<sub>2</sub>), 57.2 (OCH<sub>3</sub>), 104.8 (q), 105.1 (q), 106.0 (CH), 111.2 (CH), 117.6 (CH), 120.1 (CH), 125.6 (q), 128.2 (CH), 131.5 (CH), 132.2 (CH), 153.1 (q), 155.2 (q), 155.8 (q), 162.5 (q), 166.4 (q); *m/z* (+ES) 297.1 ([M-H]<sup>-</sup>, 100%); (+ES) (Found 299.0905; C<sub>17</sub>H<sub>15</sub>O<sub>5</sub> [M+H]<sup>+</sup>), requires 299.0919).

### 5.3.48 Synthesis of 4-hydroxy-3((2-hydroxynaphthalen-1-yl)methyl)-2H-benzo[h]chromen-2-one, **174a**

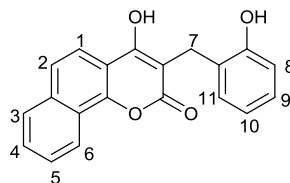


C<sub>24</sub>H<sub>15</sub>O<sub>4</sub>; Molecular weight: 367.37

Using method G, reaction of compound (**177a**) (150 mg, 0.41 mmol) and sodium borohydride (93 mg, 2.46 mmol) in methanol (12 mL) gave the title compound (**174a**) as a white solid (80 mg, 53%): Mp 284 °C;  $\nu_{\text{max}}/\text{cm}^{-1}$  2999 (br, w, O-H), 1657 (s, C=O), 1596 (s, C=C);  $\delta_{\text{H}}$  (400 MHz; DMSO-*d*<sub>6</sub>) 4.30 (2H, s, C(7)H<sub>2</sub>), 7.24 (1H, d, *J* 8.8, C(8)H or C(9)H), 7.29 (1H, ddd, *J* 8.1, 6.8, 1.3, C(11)H or C(12)H), 7.47 (1H, ddd, *J* 8.1, 6.8, 1.3, C(11)H or C(12)H), 7.66-7.74 (3H, m, Ar-CH), 7.77-7.81 (2H, m, Ar-CH), 7.89 (1H, d, *J* 8.3, C(1)H or C(2)H), 7.98-8.02 (1H, m, Ar-CH), 8.31-8.35 (1H, m, Ar-CH), 8.44 (1H, d, *J* 8.3, C(3)H or C(6)H);  $\delta_{\text{C}}$  (100 MHz; DMSO-*d*<sub>6</sub>) 20.2

( $\underline{\text{C}}(7)\text{H}_2$ ), 102.2 (q), 103.6 (q), 118.2 (d,  $J$  3.7,  $\underline{\text{CH}}$ ), 119.7 ( $\underline{\text{CH}}$ ), 122.0 ( $\underline{\text{CH}}$ ), 122.5 (q), 123.3 ( $\underline{\text{CH}}$ ), 124.1 (q), 124.4 ( $\underline{\text{CH}}$ ), 126.8 ( $\underline{\text{CH}}$ ), 127.8 ( $\underline{\text{CH}}$ ), 128.5 ( $\underline{\text{CH}}$ ), 128.7 ( $\underline{\text{CH}}$ ), 129.0 ( $\underline{\text{CH}}$ ), 129.2 (q), 133.9 (q), 134.8 (q), 149.2 (q), 151.8 (q), 163.5 (C=O);  $m/z$  (+ES) 369.1 ( $[\text{M}+\text{H}]^+$ , 100%); (Found 369.1120;  $\text{C}_{24}\text{H}_{17}\text{O}_4$  ( $[\text{M}+\text{H}]^+$ ), requires 369.1103).

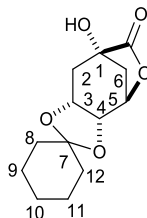
#### 5.3.49 Synthesis of 4-hydroxy-3-(2-hydroxybenzyl)-2H-benzo[h]chromen-2-one, **174b**



$\text{C}_{20}\text{H}_{14}\text{O}_4$ ; Molecular weight: 318.32

Using method G, reaction of compound (**177b**) (122 mg, 0.39 mmol) and lithium borohydride (17 mg, 0.77 mmol) in THF (7 mL) gave the title compound (**174b**) as brown crystal (90 mg, 74%): Mp 266-268 °C;  $\nu_{\text{max}}/\text{cm}^{-1}$  3269 (br, w, O-H), 1591 (s, C=O), 1526 (s, C=C);  $\delta_{\text{H}}$  (400 MHz;  $\text{DMSO}-d_6$ ) 3.61 (2H, s,  $\text{C}(7)\underline{\text{H}}_2$ ), 6.58-6.61 (2H, m, Ar- $\underline{\text{CH}}$ ), 6.92 (1H, td,  $J$  7.6, 1.5,  $\text{C}(9)\underline{\text{H}}$ ), 7.24 (1H, dd,  $J$  6.5, 1.2,  $\text{C}(11)\underline{\text{H}}$ ), 7.56-7.59 (2H, m, Ar- $\underline{\text{CH}}$ ), 7.62 (1H, d,  $J$  8.6,  $\text{C}(1)\underline{\text{H}}$  or  $\text{C}(2)\underline{\text{H}}$ ), 7.91-7.93 (2H, m, Ar- $\underline{\text{CH}}$ ), 8.28-8.30 (1H, m, Ar- $\underline{\text{CH}}$ ), 9.22 (1H, s, OH), 12.40 (1H, s, OH);  $\delta_{\text{C}}$  (100 MHz;  $\text{DMSO}-d_6$ ) 26.2 ( $\underline{\text{C}}(7)\text{H}_2$ ), 98.8, 114.2, 116.5, 117.1 ( $\underline{\text{CH}}$ ), 117.9 ( $\underline{\text{CH}}$ ), 122.0 (d,  $J$  14.7,  $\underline{\text{CH}}$ ), 126.1, 126.5 ( $\underline{\text{CH}}$ ), 127.0 ( $\underline{\text{CH}}$ ), 127.8 ( $\underline{\text{CH}}$ ), 129.9 ( $\underline{\text{CH}}$ ), 130.7 ( $\underline{\text{CH}}$ ), 133.9, 136.1, 156.6, 164.2 (C=O);  $m/z$  (+ES) 341.1 ( $[\text{M}+\text{Na}]^+$ , 100%); (Found 341.0793;  $\text{C}_{20}\text{H}_{14}\text{O}_4\text{Na}$  ( $[\text{M}+\text{H}]^+$ ), requires 341.0790).

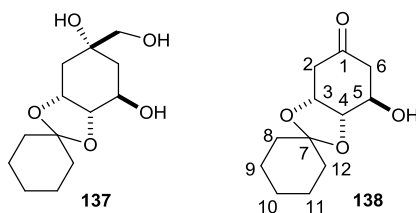
#### 5.3.50 Synthesis of (1S,3R,4R,5R)-3-O,4-O-Cyclohexylidene-7-oxo-6-oxabicyclo[3.2.1]octan- 1,3,4-triol, **136**



$\text{C}_{13}\text{H}_{18}\text{O}_5$ ; Molecular weight: 254.28

A mixture of (-)-quinic acid (5 g, 26.02 mmol) and cyclohexanone (15 mL, 158.7 mmol) in toluene (50 mL) were refluxed at 135 °C under N<sub>2</sub> in a flask fitted with a Dean and Stark trap and a condenser for 30 minutes. After the mixture was allowed to cool to room temperature, an amberlite<sup>®</sup> resin IR (5 g) (which was previously washed with methanol, filtered and washed again with diethyl ether and dried under vacuum) was added. The resulting suspension was heated at reflux for 5 hours at 135 °C and then allowed to cool to room temperature. The resin was filtered off and the filtrate was washed with a saturated solution of sodium bicarbonate (2 x 60 mL), water (2 x 60 mL), brine (60 mL), then dried over MgSO<sub>4</sub> and concentrated *in vacuo* to give the title compound (**136**) as a white solid (4.1 g, 62%): Mp 141-143 °C [Lit.<sup>267</sup> Mp 139-141 °C]; [ $\alpha$ ]<sub>D</sub><sup>30</sup> -41.7 (c 0.684 in CH<sub>2</sub>Cl<sub>2</sub>) [Lit.<sup>267</sup> [ $\alpha$ ]<sub>D</sub><sup>22</sup> -33.0 (c 1.05 in CHCl<sub>3</sub>)];  $\nu_{\text{max}}$ /cm<sup>-1</sup> 3426 (br, w, O-H), 2950 (s, C-H), 1766 (s, C=O);  $\delta_{\text{H}}$  (400 MHz; CDCl<sub>3</sub>) 1.33-1.66 (10H, m, 5x CH<sub>2</sub> of cyclohexane), 2.18 (1H, dd, *J* 14.5, 2.9, C(2)H<sub>ax</sub>), 2.28-2.40 (2H, m, C(2)H<sub>eq</sub> and C(6)H<sub>eq</sub>), 2.66 (1H, d, *J* 11.6, C(6)H<sub>ax</sub>), 4.30 (1H, ddd, *J* 6.3, 2.5, 1.4, C(4)H), 4.48 (1H, td, *J* 6.3, 2.9, C(3)H), 4.74 (1H, dd, *J* 6.3, 2.5, C(5)H);  $\delta_{\text{C}}$  (100 MHz; CDCl<sub>3</sub>) 23.5, 24.0, 25.0, 33.4 (4xCH<sub>2</sub> of cyclohexane), 34.4 (C(6)H<sub>2</sub>), 36.9 (C(10)H<sub>2</sub>), 38.4 (C(2)H<sub>2</sub>), 71.1 (C(3)H), 71.6 (C(1)), 71.7 (C(4)H), 76.0 (C(5)H), 179.0 (C=O); *m/z* (+ES) 277.1 ([M+Na]<sup>+</sup>, 100%).

### 5.3.51 Synthesis of 3-O,4-O-Cyclohexylidene-(3*R*,4*S*,5*R*)-trihydroxycyclohexanone, **138**



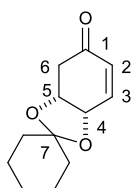
C<sub>12</sub>H<sub>18</sub>O<sub>4</sub>; Molecular weight: 226.27

To a solution of lactone (**136**) (4 g, 15.73 mmol) in methanol (200 mL) at 0 °C, sodium borohydride (6.1 g, 162.24 mmol) was added portionwise. Once effervescence had ceased, the reaction mixture was stirred at room temperature under N<sub>2</sub> for 20 hours. The reaction was quenched with a saturated aqueous solution of NH<sub>4</sub>Cl (60 mL). The resulting mixture was concentrated *in vacuo* to give a white solid. Ethyl acetate (100 mL) was added and the resulting suspension filtered. The residue was washed with ethyl acetate (3 x 50 mL) and the combined organic wastes

were dried over  $\text{MgSO}_4$  and concentrated *in vacuo* to give the unprufed product (**137**) as an off-white solid (4.5 g).

Sodium periodate (9.3 g, 43.53 mmol) was dissolved in hot water (10 mL). To the resulting suspension, silica gel (22 g) was added portionwise to give silica-supported sodium periodate as a free flowing powder. To this, dichloromethane (55 mL) was added, followed by a solution of compound (**137**) (4.5 g, 17.44 mmol) in dichloromethane (45 mL). The reaction mixture was stirred at room temperature under  $\text{N}_2$  for 1.5 hours, then it was filtered and the residue was washed with dichloromethane (3 x 55 mL). The filtrate was dried over  $\text{MgSO}_4$  and concentrated *in vacuo* to give the title compound (**138**) as a white solid (3.5 g, 88% over two steps): Mp 97-99 °C [Lit.<sup>268</sup> Mp 97-98 °C];  $[\alpha]_{\text{D}}^{30} +101.7$  (*c* 1.18 in  $\text{CH}_3\text{OH}$ ) [Lit.<sup>268</sup>  $[\alpha]_{\text{D}}^{22} +100.3$  (*c* 0.44 in  $\text{CH}_3\text{OH}$ )];  $\nu_{\text{max}}/\text{cm}^{-1}$  3456 (br, s, O-H), 2938 (s, C-H), 1709 (s, C=O);  $\delta_{\text{H}}$  (400 MHz;  $\text{CDCl}_3$ ) 1.46-1.61 (10H, m,  $5\times\text{CH}_2$  of cyclohexane), 2.08 (1H, br, s, OH), 2.38 (1H, ddd, *J* 17.9, 3.8, 2.0, C(6) $\underline{\text{H}}_{\text{eq}}$ ), 2.60-2.65 (2H, m, C(2) $\underline{\text{H}}_{\text{eq}}$  and C(6) $\underline{\text{H}}_{\text{ax}}$ ), 2.74 (1H, dd, *J* 17.2, 3.5 C(2) $\underline{\text{H}}_{\text{ax}}$ ), 4.18 (1H, ~q, *J* 2.8, C(5) $\underline{\text{H}}$ ), 4.24 (1H, dt, *J* 7.1, 2.3, C(4) $\underline{\text{H}}$ ), 4.63 (1H, d~t, *J* 6.8, 3.2, C(3) $\underline{\text{H}}$ );  $\delta_{\text{C}}$  (100 MHz;  $\text{CDCl}_3$ ) 23.5, 23.9, 25.1, 33.3, 36.3 ( $5\times\text{CH}_2$  of cyclohexane), 40.2 ( $\underline{\text{C}}(2)\text{H}_2$ ), 41.7 ( $\underline{\text{C}}(6)\text{H}_2$ ), 68.3 ( $\underline{\text{C}}(5)\text{H}$ ), 71.8 ( $\underline{\text{C}}(3)\text{H}$ ), 74.6 ( $\underline{\text{C}}(4)\text{H}$ ), 109.3 ( $\underline{\text{C}}(7)$ ), 208.4 ( $\underline{\text{C}}=\text{O}$ ); *m/z* (+ES) 249.1 ( $[\text{M}+\text{Na}]^+$ , 100%).

### 5.3.52 Synthesis of (3a*R*,7a*S*)-3a,4-dihydrospiro[benzo[d][1,3]dioxole-2,1'-cyclohexan]-5(7aH)-one, **139**

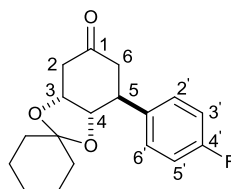


$\text{C}_{12}\text{H}_{16}\text{O}_3$ ; Molecular weight: 208.25

To a solution of the hydroxyketone (**138**) (3.5 g, 15.29 mmol) in dry dichloromethane (65 mL) at 0 °C under  $\text{N}_2$ , was added methanesulfonyl chloride (2 mL, 18.35 mmol) and triethylamine (6 mL, 44.48 mmol). The reaction mixture was stirred at room temperature for 4 hours and then quenched with water (20 mL) and extracted with dichloromethane (2 x 20 mL). The combined organic extracts were washed with water (2 x 20 mL), 0.1 M HCl (20 mL), brine (2 x 20 mL), dried over  $\text{MgSO}_4$  and concentrated *in vacuo* to give an orange oil residue. This residue was

purified by flash silica chromatography (ethyl acetate: petroleum ether 1:3) to give the title compound (**139**) as a white solid (2.4 g, 76%): Mp 62-64 °C [Lit.<sup>269</sup> Mp 55-58 °C];  $\nu_{\max}/\text{cm}^{-1}$  2931 (s, C-H), 1664 (s, C=O);  $\delta_{\text{H}}$  (400 MHz;  $\text{CDCl}_3$ ) 1.49-1.56 (10H, m, 5x $\text{CH}_2$  of cyclohexanone), 2.61 (1H, dd,  $J$  17.5, 3.9, C(6) $\underline{\text{H}}_{\text{ax}}$  or C(6) $\underline{\text{H}}_{\text{eq}}$ ), 2.88 (1H, ddd,  $J$  17.5, 2.6, 0.8, C(6) $\text{H}_{\text{ax}}$  or C(6) $\underline{\text{H}}_{\text{eq}}$ ), 4.58-4.66 (2H, m, C(4) $\underline{\text{H}}$  and C(5) $\underline{\text{H}}$ ), 5.94 (1H, dt,  $J$  10.3, 1.0, C(2) $\underline{\text{H}}$ ), 6.58 (1H, ddd,  $J$  10.3, 4.5, 2.5, C(3) $\underline{\text{H}}$ );  $\delta_{\text{C}}$  (100 MHz;  $\text{CDCl}_3$ ) 23.8, 23.9, 24.9, 36.0, 37.4 (5x $\text{CH}_2$  of cyclohexanone), 38.8 ( $\underline{\text{C}}(6)\text{H}_2$ ), 70.7 ( $\underline{\text{C}}(4)\text{H}$  or ( $\underline{\text{C}}(5)\text{H}$ )), 73.0 ( $\underline{\text{C}}(4)\text{H}$  or ( $\underline{\text{C}}(5)\text{H}$ )), 110.6 ( $\underline{\text{C}}(7)$ ), 128.7 ( $\underline{\text{C}}(2)\text{H}_2$ ), 146.1 ( $\underline{\text{C}}(3)\text{H}$ ), 195.6 (C=O);  $m/z$  (+ES) 263 ( $[\text{M}+\text{Na}+\text{MeOH}]^+$ , 70%), 231 ( $[\text{M}+\text{Na}]^+$ , 100%).

### 5.3.53 Synthesis of (3a*S*, 4*S*, 7a*R*)-4-(4-fluorophenyl)tetrahydrospiro[benzo[d][1,3]dioxole-2, 1'-cyclohexan]-6(3a*H*)-one, **152**



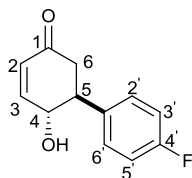
$\text{C}_{18}\text{H}_{21}\text{O}_3\text{F}$ ; Molecular weight: 304.36

To a solution of enone (**139**) (350 mg, 1.68 mmol) in dioxane: water (10:1), 3 mL was added 4-fluorophenyl boronic acid (587.2 mg, 4.20 mmol) and  $[\text{RhOH}(\text{cod})]_2$  (37.6 mg, 5 mol%), followed by triethylamine (0.2 mL, 1.58 mmol). The reaction mixture was stirred at room temperature for 20 hours. The solvents were evaporated *in vacuo* to give an orange residue which was purified by flash silica chromatography (ethyl acetate: petroleum ether 1:9) to give the title compound (**152**) as a thick yellow oil (380 mg, 74%):  $\nu_{\max}/\text{cm}^{-1}$  2935 (s, C-H), 1718 (s, C=O);  $\delta_{\text{H}}$  (400 MHz;  $\text{CDCl}_3$ ) 1.35-1.75 (10H, m, 5 x  $\text{CH}_2$  of cyclohexane), 2.45 (1H, dd,  $J$  17.3, 9.6, C(6) $\underline{\text{H}}_{\text{ax}}$ ), 2.57 (1H, dd,  $J$  17.3, 5.8, C(6) $\underline{\text{H}}_{\text{eq}}$ ), 2.64 (1H, dd,  $J$  14.5, 5.1, C(2) $\underline{\text{H}}_{\text{ax}}$  or C(2) $\underline{\text{H}}_{\text{eq}}$ ), 2.68 (1H, dd,  $J$  14.5, 5.1, C(2) $\underline{\text{H}}_{\text{ax}}$  or C(2) $\underline{\text{H}}_{\text{eq}}$ ), 3.31 (1H, ddd,  $J$  9.6, 5.8, 4.5, C(5) $\underline{\text{H}}$ ), 4.43 (1H, t,  $J$  6.6, C(4) $\underline{\text{H}}$ ), 4.51 (1H, dt,  $J$  4.5, 5.1, C(3) $\underline{\text{H}}$ ), 6.96 (2H, t,  $J$  8.6, C(3') $\underline{\text{H}}$  and C(5') $\underline{\text{H}}$ ), 7.13 (2H, dd,  $J$  8.6, 5.3, C(2') $\underline{\text{H}}$  and C(6') $\underline{\text{H}}$ );  $\delta_{\text{C}}$  (100 MHz;  $\text{CDCl}_3$ ) 23.6, 24.0, 25.1, 33.8, 37.1 (5x $\text{CH}_2$  of cyclohexane), 41.2 ( $\underline{\text{C}}(2)\text{H}_2$ ), 42.2( $\underline{\text{C}}(5)\text{H}_2$ ), 42.5 ( $\underline{\text{C}}(6)\text{H}_2$ ), 72.1 ( $\underline{\text{C}}(3)\text{H}_2$ ), 77.6 ( $\underline{\text{C}}(4)\text{H}_2$ ), 109.6 (cyclohexane  $\underline{\text{C}}$ ), 115.6 (d,  $J$  21,  $\underline{\text{C}}(3')\text{H}$  and  $\underline{\text{C}}(5')\text{H}$ ), 128.9 (d,  $J$  9, ( $\underline{\text{C}}(2')\text{H}$ ) and ( $\underline{\text{C}}(6')\text{H}$ )), 136.0 (d,  $J$  3,  $\underline{\text{C}}(1')\text{H}$ ),



161.8 (d,  $J$  244,  $\underline{\text{C}}(4^1\text{F})$ ), 208.4 (C=O);  $m/z$  (+ES) 327 ( $[\text{M}+\text{Na}]^+$ , 100%); (Found 327.1362;  $\text{C}_{18}\text{H}_{21}\text{O}_3\text{FNa}$  ( $[\text{M}+\text{Na}]^+$ ), requires 327.1367).

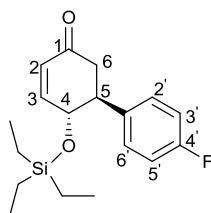
#### 5.3.54 Synthesis of (1*S*,6*R*)- 4'-fluoro-6-hydroxy-1,6-dihydro-[1,1'-biphenyl]-3(2*H*)-one, **154**



$\text{C}_{12}\text{H}_{11}\text{O}_2\text{F}$ ; Molecular weight: 206.21

To a stirring solution of compound (**152**) (350 mg, 1.15 mmol) in tetrahydrofuran (10 mL) at 0 °C under  $\text{N}_2$ , was added 3 drops of an aqueous solution of NaOH (0.5 M). The reaction mixture was stirred at 0 °C for 5 hours during which time a further 2 drops of NaOH (0.5 M) were added every 30 minutes. The reaction was quenched by the addition of a saturated aqueous solution of  $\text{NH}_4\text{Cl}$  (20 mL). Organic material was extracted into diethyl ether (2 x 20 mL). The combined organic extracts were washed with brine, dried over  $\text{MgSO}_4$  and evaporated *in vacuo* to give a brown residue. This material was purified by flash silica chromatography (ethyl acetate: petroleum ether 1:2) to give the title compound (**154**) as a waxy white solid (121 mg, 51%): Mp (101-103 °C);  $\nu_{\text{max}}/\text{cm}^{-1}$  3395 (br, w, O-H), 2930 (w, C-H), 1657 (s, C=O), 1604 (s, C=C);  $\delta_{\text{H}}$  (400 MHz;  $\text{CDCl}_3$ ) 2.68 (2H, d,  $J$  9.2,  $\underline{\text{C}}(6)\underline{\text{H}}_2$ ), 3.25 (1H, q,  $J$  9.2,  $\underline{\text{C}}(5)\underline{\text{H}}$ ), 4.65 (1H, ~d,  $J$  9.2,  $\underline{\text{C}}(4)\underline{\text{H}}$ ), 6.08 (1H, dd,  $J$  10.2, 2.4,  $\underline{\text{C}}(2)\underline{\text{H}}$ ), 7.00 (1H, dd,  $J$  10.2, 1.8,  $\underline{\text{C}}(3)\underline{\text{H}}$ ), 7.10 (2H, t,  $J$  8.6, 2 x Ar- $\underline{\text{H}}$ ), 7.28-7.31 (2H, m, 2 x Ar- $\underline{\text{CH}}$ );  $\delta_{\text{C}}$  (100 MHz;  $\text{CDCl}_3$ ) 43.1 ( $\underline{\text{C}}(6)\underline{\text{H}}_2$ ), 49.9 ( $\underline{\text{C}}(5)\underline{\text{H}}$ ), 71.9 ( $\underline{\text{C}}(4)\underline{\text{H}}$ ), 116.1 (d,  $J$  22,  $\underline{\text{C}}(3')\underline{\text{H}}$  and  $\underline{\text{C}}(5')\underline{\text{H}}$  or  $\underline{\text{C}}(1')$ ), 129.2 (d,  $J$  11,  $\underline{\text{C}}(2')\underline{\text{H}}$  and  $\underline{\text{C}}(6')\underline{\text{H}}$  or  $\underline{\text{C}}(1')$ ), 129.3 ( $\underline{\text{C}}(2)\underline{\text{H}}$ ), 135.3 (Ar- $\underline{\text{C}}$ ), 152.0 ( $\underline{\text{C}}(3)\underline{\text{H}}$ ), 162.2 (d,  $J$  256,  $\underline{\text{C}}(4^1\text{F})$ ), 197.8 (C=O);  $\delta_{\text{F}}$  (376 MHz;  $\text{CDCl}_3$ ) -114.3 (s, 1F);  $m/z$  (-ES) 205.0 ( $[\text{M}-\text{H}]^-$ , 100%); (+ES) (Found 224.1081,  $\text{C}_{12}\text{H}_{15}\text{O}_2\text{FN}$  ( $[\text{M}+\text{NH}_4]^+$ ), requires 224.1084).

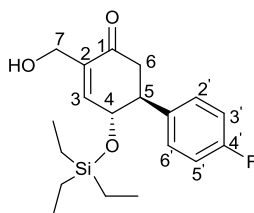
### 5.3.55 Synthesis of (1*S*,6*R*)- 4'-fluoro-6-hydroxy-6-((triethylsilyl)oxy)-1,6-dihydro-[1,1'-biphenyl]-3(2*H*)-one, **163**



C<sub>18</sub>H<sub>25</sub>O<sub>2</sub>SiF; Molecular weight: 320.47

To a solution of 2,6-lutidine (0.2 mL, 1.38 mmol) in distilled dichloromethane (6 mL), at -78 °C under N<sub>2</sub>, was added triethylsilyltrifluoromethane sulfonate (0.4 mL, 1.66 mmol) followed by a solution of compound (**154**) (121 mg, 0.59 mmol) in dichloromethane (5 mL). The reaction mixture was stirred at -78 °C for 30 minutes when it was quenched by the addition of a saturated aqueous solution of NH<sub>4</sub>Cl (10 mL) and allowed to warm to room temperature. The two layers were separated and the aqueous phase was extracted with dichloromethane (2 x 15 mL). The combined organic extracts were washed with brine (20 mL), dried over MgSO<sub>4</sub> and evaporated *in vacuo* to give the crude product as a brown oil. This crude product was purified by flash silica chromatography (ethyl acetate: petroleum ether 1:19) to give the title compound (**163**) as a yellow oil (143 mg, 76%); [ $\alpha$ ]<sub>D</sub><sup>30</sup> -131 (c 0.5, CH<sub>2</sub>Cl<sub>2</sub>):  $\nu_{\text{max}}$  (film)/cm<sup>-1</sup> 2955 (m, C-H), 1688 (s, C=O);  $\delta_{\text{H}}$  (400 MHz; CDCl<sub>3</sub>) 0.25-0.44 (6H, m, Si(CH<sub>2</sub>CH<sub>3</sub>)<sub>3</sub>), 0.77 (9H, t, *J* 7.8, Si(CH<sub>2</sub>CH<sub>3</sub>)<sub>3</sub>), 2.67 (1H, ddd, *J* 16.4, 4.8, 1.0, C(6)H<sub>eq</sub>), 2.71 (1H, dd, *J* 16.4, 13.4, C(6)H<sub>ax</sub>), 3.25 (1H, ddd, *J* 13.4, 9.6, 4.8, C(5)H), 4.51 (1H, dt, *J* 9.6, 2.0, C(4)H), 6.03 (1H, ddd, *J* 10.1, 2.0, 1.0, C(2)H), 6.84 (1H, dd, *J* 10.1, 2.0, C(3)H), 7.04 (2H, d, *J* 8.6, C(3')H and C(5')H), 7.21 (2H, d, *J* 8.6, C(2') and C(6')H);  $\delta_{\text{F}}$  (376 MHz; CDCl<sub>3</sub>) -115.47 (s, 1F);  $\delta_{\text{C}}$  (100 MHz; CDCl<sub>3</sub>) 4.4 Si(CH<sub>2</sub>CH<sub>3</sub>)<sub>3</sub>, 6.6 Si(CH<sub>2</sub>CH<sub>3</sub>)<sub>3</sub>, 42.8 (C(6)H), 49.9 (C(5)H), 72.8 (C(4)H), 115.4 (d, *J* 22, C(3')H and C(5')H or C(1')), 128.5 (C(2)H), 129.6 (d, *J* 11, C(2')H and C(6')H or C(1')), 136.6 (d, *J* 2.8, C(1')H), 153.7 (C(3)H), 162.1 (d, *J* 246, C(4')F), 198.3 (C=O);  $\delta_{\text{f}}$  (376 MHz; CDCl<sub>3</sub>) -115.5 (s); *m/z* (+ES) 343 ([M+Na]<sup>+</sup>, 100%).

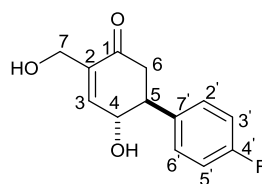
### 5.3.56 Synthesis of (1*S*,6*R*)- 4'-fluoro-4-(hydroxymethyl)-6-((triethylsilyl)oxy)-1,6-dihydro-[1,1'-biphenyl]-3(2*H*)-one, **169**



C<sub>19</sub>H<sub>27</sub>O<sub>3</sub>SiF; Molecular weight: 350.50

To a suspension of compound (**163**) (143 mg, 0.44 mmol) in water (2 mL), was added sodium dodecyl sulphate (48.7 mg, 0.17 mmol), and N,N-dimethylaminopyridine (54 mg, 0.45 mmol). The reaction mixture was stirred for 5 minutes at room temperature and then formaldehyde 37% (0.5 mL, 6.29 mmol) was added. The reaction mixture was stirred at room temperature for 24 hours after which the reaction was quenched by addition of brine (3 mL) and extracted with ethyl acetate (3 x 5 mL). The combined organic extracts were washed with brine (15 mL), dried over MgSO<sub>4</sub> and evaporated *in vacuo* to give the crude product as a yellow oil. This crude product was purified by flash silica chromatography (ethyl acetate: petroleum ether 1:2) to give the title compound (**169**) as a white solid (79 mg, 52%): Mp 62-64 °C; [ $\alpha$ ]<sub>D</sub><sup>29</sup> -91.6 (*c* 2.53, CH<sub>2</sub>Cl<sub>2</sub>);  $\nu_{\max}$  (film)/cm<sup>-1</sup> 3539 (br, O-H), 2956 (m, Ar-C-H), 2880 (m, aliph-C-H), 1671 (s, C=O);  $\delta_{\text{H}}$  (400 MHz; CDCl<sub>3</sub>) 0.24-0.43 (6H, m, Si(CH<sub>2</sub>CH<sub>3</sub>)<sub>3</sub>), 0.78 (9H, t, *J* 7.8, Si(CH<sub>2</sub>CH<sub>3</sub>)<sub>3</sub>), 2.68 (1H, dd, *J* 16.4, 4.5, C(6)H<sub>eq</sub>), 2.74 (1H, dd, *J* 16.4, 13.6, C(6)H<sub>ax</sub>), 3.24 (1H, ddd, *J* 13.6, 9.5, 4.5, C(5)H), 4.26 (1H, dt, *J* 13.6, 1.5, C(7)H<sub>a</sub>H<sub>b</sub>), 4.38 (1H, dt, *J* 13.6, 1.5, C(7)H<sub>a</sub>H<sub>b</sub>), 4.54 (1H, ~dq, *J* 9.5, 1.5, C(4)H), 6.77 (1H, d, *J* 1.5, C(3)H), 7.04 (2H, t, *J* 8.6, 2xAr-H), 7.22 (2H, dd, *J* 8.6, 5.3, 2xAr-H);  $\delta_{\text{F}}$  (376 MHz; CDCl<sub>3</sub>) -115.5 (s);  $\delta_{\text{C}}$  (100 MHz; CDCl<sub>3</sub>) 6.4 (Si(CH<sub>2</sub>CH<sub>3</sub>)<sub>3</sub>), 6.8 (Si(CH<sub>2</sub>CH<sub>3</sub>)<sub>3</sub>), 43.4 (C(6)H<sub>2</sub>), 50.0 (C(5)H), 61.2 (C(7)H<sub>2</sub>), 70.1 (C(4)H), 116.1 (d, *J* 22, C(3')H and C(5')H or C(1')), 129.2 (d, *J* 11, C(2')H and C(6')H or C(1')), 147.8 (C(3)H), 157.8 (C(2)H), (C(4)F) is not visible, 204.9 (C=O); *m/z* (+ES) 373.3 ([M+H]<sup>+</sup>, 100%); (Found 373.1611, C<sub>19</sub>H<sub>27</sub>O<sub>3</sub> NaSiF ([M+Na]<sup>+</sup>), requires 373.1602).

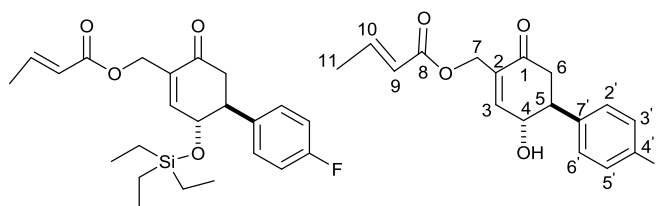
### 5.3.57 Synthesis of (1*S*, 6*R*)-4'-fluoro-6-hydroxy-4-(hydroxymethyl)-1,6-dihydro-[1,1'-biphenyl]-3(2*H*)-one, **184**.



C<sub>13</sub>H<sub>13</sub>O<sub>3</sub>F; Molecular weight: 236.24

A solution of compound (**169**) (49 mg, 0.14 mmol) in TFA: H<sub>2</sub>O (7:1, 1 mL) was stirred for 30 mins at room temperature. The solvents were concentrated *in vacuo* to give a crude brown oil which was purified by flash silica chromatography (ethyl acetate: petroleum ether 2:1) to give the title compound (**184**) as a colourless film (22 mg, 67%):  $\nu_{\max}$  (film)/cm<sup>-1</sup> 3347 (br, O-H), 1668 (s, C=O);  $\delta_{\text{H}}$  (400 MHz; CDCl<sub>3</sub>) 2.65-2.76 (2H, m, C(6)H<sub>2</sub>), 3.24 (1H, ~q, *J* 9.2, C(5)H), 4.30-4.40 (2H, m, C(7)H<sub>2</sub>), 4.67 (1H, dd, *J* 9.2, 1.5, C(4)H), 6.95 (1H, ~d, *J* 1.5, C(3)H), 7.06-7.12 (2H, m, Ar-CH), 7.26-7.29 (2H, m, Ar-CH);  $\delta_{\text{C}}$  (100MHz; CDCl<sub>3</sub>) 43.4 (C(6)H<sub>2</sub>), 49.9 (C(5)H), 61.0 (C(7)H<sub>2</sub>), 71.9 (C(4)H), 116.0 (d, *J* 22, C(3')H and C(5')H or C(1')), 129.2 (d, *J* 11, C(2')H and C(6')H or C(1')), 135.0 (d, *J* 3.7, C(7')), 137.6 (C(2)), 147.9 (C(3)H), (C(4')F) is not visible, 198.4 (C=O);  $\delta_{\text{F}}$  (376 MHz; CDCl<sub>3</sub>) -114.2 (s); *m/z* (+ES) 259 ([M+Na]<sup>+</sup>, 100%); (Found 259.0759, C<sub>13</sub>H<sub>13</sub>NaO<sub>3</sub>F ([M+Na]<sup>+</sup>), requires 259.0746).

### 5.3.58 Synthesis of ((1*S*,6*R*)-4'-fluoro-6-hydroxy-3-oxo-1,2,3,6-tetrahydro-[1,1'-biphenyl]-4-yl)methyl (*E*)-but-2-enoate, **182**

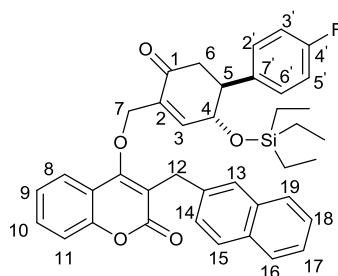


C<sub>17</sub>H<sub>17</sub>FO<sub>4</sub>; Molecular weight: 304.11

To a solution of alcohol (**169**) (88 mg, 0.25 mmol) in dichloromethane (1 mL), was added DMAP (3.5 mg, 0.03 mmol), pyridine (0.2 mL, 2.26 mmol) and crotonic anhydride (82  $\mu$ L, 0.56 mmol). The reaction mixture was left to react at room temperature with stirring for 2.5 hours. The reaction was quenched by the addition of a saturated aqueous solution of NaHCO<sub>3</sub> (2 mL) and diluted with water (3 mL) and dichloromethane (5 mL). The two layers were separated and the aqueous layer extracted with dichloromethane (3 x 5 mL). The combined organic extracts were

washed with brine (10 mL), dried over  $\text{MgSO}_4$  and evaporated *in vacuo* to give a crude brown oil. This crude product was purified by flash silica chromatography (ethyl acetate: petroleum ether 1:9);  $R_f$  0.32 to give a colourless oil (**214**) (35 mg). A solution of crude ester (**214**) (35 mg, 0.09 mmol) in TFA:  $\text{H}_2\text{O}$  (7:1, 2 mL) was stirred at room temperature for 45 minutes. The solvents were evaporated *in vacuo* to give the crude product as brown oil. This crude product was purified by flash silica chromatography (ethyl acetate: petroleum ether 1:2);  $R_f$  0.4 to give the title compound (**182**) as a colourless thick oil (29 mg, 38% over 2 steps):  $\nu_{\text{max}}$ /film  $\text{cm}^{-1}$  3432 (br, O-H), 1714 (s, C=O), 1675 (s, C=O);  $\delta_{\text{H}}$  (400 MHz;  $\text{CDCl}_3$ ) 1.91 (3H, dd,  $J$  6.9, 1.6, C(11) $\underline{\text{H}}_3$ ), 2.66-2.76 (2H, m, C(6) $\underline{\text{H}}_2$ ), 3.25 (1H, td,  $J$  10.0, 7.9, C(5) $\underline{\text{H}}$ ), 4.67 (1H, ~dq,  $J$  10.0, 1.6, C(4) $\underline{\text{H}}$ ), 4.85 (1H, ddd,  $J$  14.4, 3.8, 2.0, C(7) $\underline{\text{H}}_{\text{a}}\underline{\text{H}}_{\text{b}}$  O), 4.91 (1H, ddd,  $J$  14.4, 3.8, 2.0, C(7) $\underline{\text{H}}_{\text{a}}\underline{\text{H}}_{\text{b}}$  O), 5.90 (1H, dq,  $J$  15.4, 1.7, C(9) $\underline{\text{H}}$ ), 6.94 (1H, d,  $J$  1.3, C(3) $\underline{\text{H}}$ ), 7.00-7.04 (2H, m, C(9) $\underline{\text{H}}$  and C(10) $\underline{\text{H}}$ ), 7.08-7.12 (2H, m, 2 x Ar- $\underline{\text{H}}$ ), 7.26-7.29 (2H, m, 2 x Ar- $\underline{\text{H}}$ );  $\delta_{\text{C}}$  (100 MHz;  $\text{CDCl}_3$ ) 18.1 ( $\underline{\text{C}}$ (11) $\underline{\text{H}}_3$ ), 43.3 ( $\underline{\text{C}}$ (6) $\underline{\text{H}}_2$ ), 49.8 ( $\underline{\text{C}}$ (5) $\underline{\text{H}}$ ), 60.1 ( $\underline{\text{C}}$ (7) $\underline{\text{H}}_2$ ), 71.9 ( $\underline{\text{C}}$ (4) $\underline{\text{H}}$ ), 116.1 (d,  $J$  21,  $\underline{\text{C}}$ (14) $\underline{\text{H}}$ ) and ( $\underline{\text{C}}$ (16) $\underline{\text{H}}$ ), 122.1 ( $\underline{\text{C}}$ (9) $\underline{\text{H}}$ ), 129.2 (d,  $J$  8.1, ( $\underline{\text{C}}$ (13) $\underline{\text{H}}$ ) and ( $\underline{\text{C}}$ (17) $\underline{\text{H}}$ ), 134.3 ( $\underline{\text{C}}$ (12) $\underline{\text{H}}$ ), 145.8 ( $\underline{\text{C}}$ (3) $\underline{\text{H}}$ ), 148.0 ( $\underline{\text{C}}$ (10) $\underline{\text{H}}$ ), ( $\underline{\text{C}}$ (4')F) is not visible, 165.9 ( $\underline{\text{C}}$ (8)=O), 196.1 ( $\underline{\text{C}}$ (1)=O);  $\delta_{\text{F}}$  (376 MHz;  $\text{CDCl}_3$ ) -114.1 (s);  $m/z$  (+ES) 327.1 ( $[\text{M}+\text{Na}]^+$ , 100%); (Found 327.1016,  $\text{C}_{17}\text{H}_{17}\text{NaO}_4\text{F}$  ( $[\text{M}+\text{Na}]^+$ ), requires 327.1009).

### 5.3.59 Synthesis of 4-(((1*S*,6*R*)-4'-fluoro-3-oxo-6-((triethylsilyloxy)-1,2,3,6-tetrahydro-[1,1'-biphenyl]-4-yl)methoxy)-3-naphthalen-2-ylmethyl)-2H-chromen-2-one, **214**

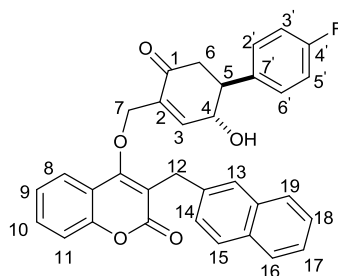


$\text{C}_{39}\text{H}_{39}\text{O}_5\text{SiF}$ ; Molecular weight: 634.81

To a solution of alcohol (**169**) (48.3 mg, 0.14 mmol) in dry THF (2 mL), under an atmosphere of nitrogen, was added triphenylphosphine (65 mg, 0.25 mmol) and 4-hydroxy-3-(naphthalene-2-ylmethyl)-2H-chromen-2-one (**178a**) (70 mg, 0.23 mmol). The reaction mixture was stirred at 0 °C for 30 minutes and then at room temperature

for 24 hours. The solvents were concentrated *in vacuo* to give the crude product as thick yellow oil. This crude product was purified by flash silica chromatography (ethyl acetate: petroleum ether 1:6) to give the title compound (**214**) as a thick white oil (48 mg, 55%).  $\nu_{\max}/\text{cm}^{-1}$  2955 (m, C-H), 2875 (w, C-H), 1717 (s, C=O);  $\delta_{\text{H}}$  (400 MHz;  $\text{CDCl}_3$ ) 0.23-0.42 (6H, m,  $\text{Si}(\text{CH}_2\text{CH}_3)_3$ ), 0.77 (9H, t,  $J$  7.8,  $\text{Si}(\text{CH}_2\text{CH}_3)_3$ ), 2.63 (2H, dd,  $J$  12.1, 9.3, C(6) $\underline{\text{H}}_2$ ), 3.21 (1H, ddd,  $J$  12.1, 9.3, 5.8, C(5)H), 4.18 (2H, d,  $J$  2.8, C(12) $\underline{\text{H}}_2$ ), 4.46 (1H, ~dq,  $J$  9.3, 1.5, C(4) $\underline{\text{H}}$ ), 4.71 (1H, ddd,  $J$  12.6, 3.0, 1.5, C(7) $\underline{\text{H}}_a$ ), 4.81 (1H, ddd,  $J$  12.6, 3.0, 1.5, C(7) $\underline{\text{H}}_b$ ), 6.97 (1H, d,  $J$  1.5, C(3) $\underline{\text{H}}$ ), 7.04 (2H, ~t,  $J$  8.6, C(2') $\underline{\text{H}}$  and C(6') $\underline{\text{H}}$  or C(3') $\underline{\text{H}}$  and C(5') $\underline{\text{H}}$ ), 7.14-7.17 (2H, m, Ar- $\underline{\text{CH}}$ ), 7.33 (1H, ddd,  $J$  8.2, 7.3, 1.0, C(9) $\underline{\text{H}}$  or C(10) $\underline{\text{H}}$  or C(17) $\underline{\text{H}}$  or C(18) $\underline{\text{H}}$ ), 7.39 (1H, dd,  $J$  8.2, 1.0, C(8) $\underline{\text{H}}$  or C(11) $\underline{\text{H}}$  or C(16) $\underline{\text{H}}$  or C(19) $\underline{\text{H}}$ ), 7.42-7.45 (2H, m, Ar- $\underline{\text{CH}}$ ), 7.48 (1H, dd,  $J$  8.2, 1.0, C(8) $\underline{\text{H}}$  or C(11) $\underline{\text{H}}$  or C(16) $\underline{\text{H}}$  or C(19) $\underline{\text{H}}$ ), 7.56 (1H, ddd,  $J$  8.2, 7.3, 1.0, C(9) $\underline{\text{H}}$  or C(10) $\underline{\text{H}}$  or C(17) $\underline{\text{H}}$  or C(18) $\underline{\text{H}}$ ), 7.74 (2H, d,  $J$  8.2, C(14) $\underline{\text{H}}$  and C(15) $\underline{\text{H}}$ ), 7.77-7.80 (3H, m, Ar- $\underline{\text{CH}}$ );  $\delta_{\text{C}}$  (100 MHz;  $\text{CDCl}_3$ ) 4.4 ( $\text{Si}(\text{CH}_2\text{CH}_3)_3$ ), 6.6 ( $\text{Si}(\text{CH}_2\text{CH}_3)_3$ ), 30.8 ( $\underline{\text{C}}(12)\text{H}_2$ ), 42.7 ( $\underline{\text{C}}(6)\text{H}_2$ ), 49.8 ( $\underline{\text{C}}(5)\text{H}$ ), 70.2 ( $\underline{\text{C}}(4)\text{H}$ ), 72.8 ( $\underline{\text{C}}(7)\text{H}_2$ ), 115.3 ( $\underline{\text{CH}}$ ), 115.5 ( $\underline{\text{CH}}$ ), 116.9 ( $\underline{\text{CH}}$ ), 117.0 ( $\underline{\text{CH}}$ ), 117.1 ( $\underline{\text{CH}}$ ), 123.4 ( $\underline{\text{CH}}$ ), 124.3 ( $\underline{\text{CH}}$ ), 125.5 ( $\underline{\text{CH}}$ ), 126.0 ( $\underline{\text{CH}}$ ), 126.7 ( $\underline{\text{CH}}$ ), 127.1 ( $\underline{\text{CH}}$ ), 127.6 (d,  $J$  3.7, ( $\underline{\text{CH}}$ )), 128.2 ( $\underline{\text{CH}}$ ), 129.4 ( $\underline{\text{CH}}$ ), 129.5 ( $\underline{\text{CH}}$ ), 131.8 ( $\underline{\text{CH}}$ ), 132.3 (q), 135.5(q), 133.6 (q), 136.0 (d,  $J$  3.7, (q)), 136.3 (q), 151.0 (q), 152.9 (q), 160.0 (d,  $J$  246.9,  $\underline{\text{C}}(4')\text{F}$ ), 163.0 (q), 163.6 (q), 196.4 (2x  $\underline{\text{C}}=\text{O}$ );  $m/z$  (+ES) 657.3 ( $[\text{M} + \text{Na}]^+$ , 100%).

### 5.3.60 Synthesis of 4-(((1*S*,6*R*)-4'-fluoro-6-hydroxy-3-oxo-1,2,3,6-tetrahydro-[1,1'-biphenyl]-4-yl)methoxy)-3-(naphthalen-2-ylmethyl)-2H-chromen-2-one, **185**

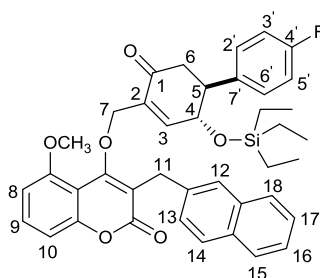


$\text{C}_{33}\text{H}_{25}\text{O}_5\text{F}$ ; Molecular weight: 520.55

A solution of compound (**214**) (40 mg, 0.06 mmol) in trifluoroacetic acid: water (7:1, 1 mL) was stirred for 30 minutes at room temperature. The solvents were concentrated under reduced pressure to give a brown oil. The residue was purified by

flash silica chromatography (ethyl acetate: petroleum ether 1:2) and the title compound (**185**) was isolated as a white foam (23 mg, 70%),  $R_f$  0.30: Mp 128-130 °C;  $[\alpha]_D^{30}$  -25.5 ( $c$  0.47 in  $\text{CH}_2\text{Cl}_2$ );  $\nu_{\text{max}}/\text{cm}^{-1}$  (film) 3433 (w, br, OH), 1682 (s, C=O), 1605 (s, C=C);  $\delta_{\text{H}}$  (400 MHz;  $\text{CDCl}_3$ ) 2.55 (1H, dd,  $J$  16.6, 13.9, C(6) $\underline{\text{H}}_{\text{eq}}$  or C(6) $\underline{\text{H}}_{\text{b}}$ ), 2.66 (1H, dd,  $J$  16.6, 4.3, C(6) $\underline{\text{H}}_{\text{ax}}$  or C(6) $\underline{\text{H}}_{\text{b}}$ ), 3.15 (1H, ddd,  $J$  13.9, 9.8, 4.3, C(5) $\underline{\text{H}}$ ), 3.71 (1H, s, OH), 4.18 (2H, s, C(12) $\underline{\text{H}}_2$ ), 4.52 (1H, ~dq,  $J$  9.8, 1.5, C(4) $\underline{\text{H}}$ ), 4.66 (1H, ddd,  $J$  12.4, 2.9, 1.5, C(7) $\underline{\text{H}}_{\text{aHb}}$ ), 4.75 (1H, ddd,  $J$  12.4, 2.9, 1.5, C(7) $\underline{\text{H}}_{\text{aHb}}$ ), 7.05-7.10 (3H, m, Ar- $\underline{\text{CH}}$ ), 7.16-7.20 (2H, m, Ar- $\underline{\text{CH}}$ ), 7.33 (1H, ddd,  $J$  8.2, 7.3, 1.0, C(9) $\underline{\text{H}}$  or C(10) $\underline{\text{H}}$  or C(17) $\underline{\text{H}}$  or C(18) $\underline{\text{H}}$ ), 7.39 (1H, dd,  $J$  8.2, 1.0, C(8) $\underline{\text{H}}$  or C(11) $\underline{\text{H}}$  or C(16) $\underline{\text{H}}$  or C(19) $\underline{\text{H}}$ ), 7.42-7.47 (3H, m, Ar- $\underline{\text{CH}}$ ), 7.48 (1H, d,  $J$  1.5, C(3) $\underline{\text{H}}$ ), 7.56 (1H, td,  $J$  8.2, 7.3, 1.0, C(9) $\underline{\text{H}}$  or C(10) $\underline{\text{H}}$  or C(17) $\underline{\text{H}}$  or C(18) $\underline{\text{H}}$ ), 7.73 (1H, s, C(13) $\underline{\text{H}}$ ), 7.76-7.80 (4H, m, Ar- $\underline{\text{CH}}$ );  $\delta_{\text{C}}$  (100 MHz;  $\text{CDCl}_3$ ) 30.8 (C(12) $\underline{\text{H}}_2$ ), 43.1 (C(6) $\underline{\text{H}}_2$ ), 49.6 (C(5) $\underline{\text{H}}$ ), 70.2 (C(7) $\underline{\text{H}}_2$ ), 71.8 (C(4) $\underline{\text{H}}$ ), 116.0 (C $\underline{\text{H}}$ ), 116.2 (C $\underline{\text{H}}$ ), 117.0 (d,  $J$  1.8, C $\underline{\text{H}}$ ), 123.4 (C $\underline{\text{H}}$ ), 124.3 (C $\underline{\text{H}}$ ), 125.5 (C $\underline{\text{H}}$ ), 126.1 (C $\underline{\text{H}}$ ), 126.7 (C $\underline{\text{H}}$ ), 127.1 (C $\underline{\text{H}}$ ), 127.6 (d,  $J$  3.7, C $\underline{\text{H}}$ ), 127.7 (C $\underline{\text{H}}$ ), 128.2 (q), 129.1 (q), 129.2 (d,  $J$  8.3, q), 131.8 (q), 132.2 (q), 133.5 (q), 134.0 (q), 136.5 (q), 150.0 (q), 152.9 (q), 160.2 (d, 248.6, C(4')F), 163.1(q), 196.0 (2x C=O);  $m/z$  (+ES) 521.3 ( $[\text{M} + \text{H}]^+$ , 100%); (Found 521.1759;  $\text{C}_{33}\text{H}_{26}\text{O}_5\text{F}$  ( $[\text{M}+\text{H}]^+$ ), requires 521.1753).

### 5.3.61 Synthesis of 4-(((1*S*,6*R*)-4'-fluoro-3-oxo-6-((triethylsilyl)oxy)-1,2,3,6-tetrahydro-1,1'-biphenyl]-4-yl)methoxy)-5-methoxy-3-(naphthalen-2-yl)-2H-chromen-2-one, **215**

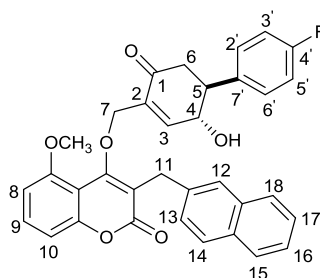


$\text{C}_{40}\text{H}_{41}\text{O}_6\text{SiF}$ ; Molecular weight: 664.83

To a solution of alcohol (**169**) (40 mg, 0.12 mmol) in distilled THF (1.5 mL), under an atmosphere of nitrogen, was added triphenylphosphine (60 mg, 0.23 mmol) and 4-hydroxy-5-methoxy-3-(naphthalene-2-ylmethyl)-2H-chromen-2-one (**179a**) (76 mg, 0.23 mmol). The reaction mixture was cooled to 0 °C and DIAD (40  $\mu\text{L}$ , 0.21 mmol) was added dropwise. The reaction mixture was stirred at 0 °C for 30 minutes and

then at room temperature for 24 hours. The solvents were concentrated *in vacuo* to give the crude product as a thick yellow oil. This crude product was purified by flash silica chromatography (ethyl acetate: petroleum ether 1:6) to give the title compound (**215**) as a white thick oil (48 mg, 63%):  $\nu_{\max}/\text{cm}^{-1}$  (film) 2955 (m, Ar C-H), 2875 (m, aliph C-H), 1714 (s, C=O), 1600 (s, C=C);  $\delta_{\text{H}}$  (400 MHz;  $\text{CDCl}_3$ ) 0.24-0.42 (6H, m,  $\text{Si}(\underline{\text{CH}_2\text{CH}_3})_3$ ), 0.77 (9H, t,  $J$  7.9,  $\text{Si}(\text{CH}_2\underline{\text{CH}_3})_3$ ), 2.60 (2H, dd,  $J$  12.1, 7.6, C(6)H<sub>2</sub>), 3.19 (1H, ddd,  $J$  12.1, 9.3, 5.8, C(5)H), 3.90 (3H, s, OCH<sub>3</sub>), 4.11 (2H, s, C(11)H<sub>2</sub>), 4.48 (1H, dd,  $J$  9.3, 1.8, C(4)H), 4.60 (1H, ddd,  $J$  12.9, 3.5, 1.8, C(7)H<sub>a</sub>H<sub>b</sub>), 4.68 (1H, ddd,  $J$  12.9, 3.5, 1.8, C(7)H<sub>a</sub>H<sub>b</sub>), 6.77 (1H, dd,  $J$  8.3, 1.0, C(8)H or C(10)H), 6.99 (1H, d,  $J$  1.8, C(3)H), 7.00-7.05 (3H, m, Ar-CH), 7.14 (2H, dd,  $J$  8.8, 5.3, C(2')H and C(6')H or C(3')H and C(5')H), 7.45 (1H, d,  $J$  8.3, C(13)H or C(14)H), 7.49 (1H, dd,  $J$  8.3, 1.0, C(8)H or C(10)H), 7.72 (1H, s, C(12)H), 7.74-7.78 (3H, m, Ar-CH);  $\delta_{\text{C}}$  (100MHz;  $\text{CDCl}_3$ ) 4.5 ( $\text{Si}(\underline{\text{CH}_2\text{CH}_3})_3$ ), 6.6 ( $\text{Si}(\text{CH}_2\underline{\text{CH}_3})_3$ ), 30.4 (C(11)H<sub>2</sub>), 42.8 (C(6)H<sub>2</sub>), 50.0 (C(5)H), 56.3 (OCH<sub>3</sub>), 69.7 (C(4)H), 72.8 (C(7)H<sub>2</sub>), 106.4 (CH), 107.5 (CH), 110 (CH), 115.2 (CH), 115.4 (CH), 117.3 (CH), 125.3 (CH), 125.9 (CH), 126.8 (CH), 127.3 (CH), 127.6 (d,  $J$  6.6, CH), 128.0 (CH), 128.2 (q), 128.3 (q), 129.4 (d,  $J$  8.1, CH), 129.5 (CH), 131.8 (CH), 132.2 (q), 133.6 (q), 136.2 (d,  $J$  2.9, q), 136.9 (q), 149.9 (CH), 154.7 (q), 156.1 (q), 160.4 (d,  $J$  248.2, C(4')F), 163.3 (q), 196.6 (2x C=O);  $\delta_{\text{F}}$  (376 MHz;  $\text{CDCl}_3$ ) -115.2 (s);  $m/z$  (+ES) 687.7 ( $[\text{M} + \text{Na}]^+$ , 100%).

### 5.3.62 Synthesis of 4-(((1*S*,6*R*)-4'-fluoro-6-hydroxy-3-oxo-1,2,3,6-tetrahydro-[1,1'-biphenyl]-4-yl)methoxy)-3-(naphthalen-2-ylmethyl)-2H-chromen-2-one, **216**



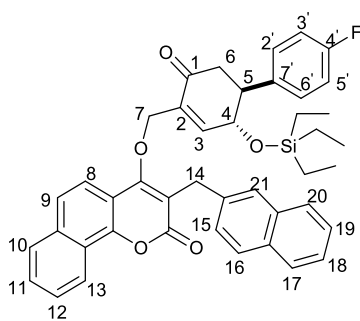
$\text{C}_{34}\text{H}_{27}\text{O}_6\text{F}$ ; Molecular weight: 550.57

A solution of compound (**215**) (30 mg, 0.05 mmol) in trifluoroacetic acid: water (7:1, 1 mL) was stirred for 30 minutes at room temperature. The solvents were concentrated under reduced pressure to give the crude product as a brown oil. This



crude product was purified by flash silica chromatography (ethyl acetate: petroleum ether 1:1) to give the title compound (**216**) as a white solid (16.8 mg, 67%): Mp 88-90 °C;  $\nu_{\text{max}}/\text{cm}^{-1}$  (film) 3435 (br, OH), 2931 (w, C-H), 1675 (s, C=O), 1600 (s, C=C);  $\delta_{\text{H}}$  (400 MHz;  $\text{CDCl}_3$ ) 2.06 (1H, s, OH), 2.50 (1H, dd,  $J$  16.4, 13.8, C(6) $\underline{\text{H}}_{\text{ax}}$ ), 2.62 (1H, dd,  $J$  16.4, 4.2, C(6) $\underline{\text{H}}_{\text{eq}}$ ), 3.13 (1H, ddd,  $J$  13.8, 9.8, 4.2, C(5) $\underline{\text{H}}$ ), 3.91 (3H, s,  $\text{OCH}_3$ ), 4.12 (2H, s, C(11) $\underline{\text{H}}_2$ ), 4.54 (1H, dd,  $J$  9.8, 1.8, C(4) $\underline{\text{H}}$ ), 4.59 (1H, ddd,  $J$  12.9, 3.8, 1.8, C(7) $\underline{\text{H}}_{\text{aHb}}$ ), 4.67 (1H, ddd,  $J$  12.9, 3.8, 1.8, C(7) $\underline{\text{H}}_{\text{aHb}}$ ), 6.78 (1H, dd,  $J$  8.3, 1.0, C(8) $\underline{\text{H}}$  or C(10) $\underline{\text{H}}$ ), 7.01 (1H, dd,  $J$  8.3, 1.0, C(8) $\underline{\text{H}}$  or C(10) $\underline{\text{H}}$ ), 7.07 (2H, ~t,  $J$  8.6, Ar-CH), 7.13 (C(3) $\underline{\text{H}}$ ), 7.16 (2H, dd,  $J$  8.6, 5.3, C(2') $\underline{\text{H}}$  and C(6') $\underline{\text{H}}$  or C(3') $\underline{\text{H}}$  and C(5') $\underline{\text{H}}$ ), 7.39-7.43 (2H, m, Ar-CH), 7.45-7.49 (2H, m, Ar-CH), 7.72 (1H, s, C(12) $\underline{\text{H}}$ ), 7.74-7.79 (3H, m, Ar-CH);  $\delta_{\text{C}}$  (100 MHz;  $\text{CDCl}_3$ ) 30.4 ( $\underline{\text{C}}$ (11) $\underline{\text{H}}_2$ ), 43.2 ( $\underline{\text{C}}$ (6) $\underline{\text{H}}_2$ ), 49.8 ( $\underline{\text{C}}$ (5) $\underline{\text{H}}$ ), 56.4 ( $\text{OCH}_3$ ), 69.7 ( $\underline{\text{C}}$ (4) $\underline{\text{H}}$ ), 71.9 ( $\underline{\text{C}}$ (7) $\underline{\text{H}}_2$ ), 106.5 ( $\underline{\text{C}}\underline{\text{H}}$ ), 107.4 (q), 110 ( $\underline{\text{C}}\underline{\text{H}}$ ), 115.9 ( $\underline{\text{C}}\underline{\text{H}}$ ), 116.1 ( $\underline{\text{C}}\underline{\text{H}}$ ), 117.1 (q), 125.4 ( $\underline{\text{C}}\underline{\text{H}}$ ), 126.0 ( $\underline{\text{C}}\underline{\text{H}}$ ), 126.7 ( $\underline{\text{C}}\underline{\text{H}}$ ), 127.3 ( $\underline{\text{C}}\underline{\text{H}}$ ), 127.6 ( $\underline{\text{C}}\underline{\text{H}}$ ), 128.0 ( $\underline{\text{C}}\underline{\text{H}}$ ), 129.1 ( $\underline{\text{C}}\underline{\text{H}}$ ), 129.2 (d,  $J$  8.1,  $\underline{\text{C}}\underline{\text{H}}$ ), 131.9 ( $\underline{\text{C}}\underline{\text{H}}$ ), 132.2 (q), 133.5 (q), 134.5 (q), 136.9 (q), 135.0 (q), 137.0 (q), 148.8 ( $\underline{\text{C}}\underline{\text{H}}$ ), 154.7 (q), 156.1 (q), 160.9 (d,  $J$  255,  $\underline{\text{C}}$ (4')F), 163.7 (q), 163.4 (q), 163.7 (q), 196.2 (2x C=O);  $\delta_{\text{F}}$  (376 MHz;  $\text{CDCl}_3$ ) -114.2 (s);  $m/z$  (+ES) 551.4 ( $[\text{M}+\text{H}]^+$ , 100%); (Found 573.1689;  $\text{C}_{34}\text{H}_{27}\text{O}_6\text{NaF}$  ( $[\text{M}+\text{Na}]^+$ ), requires 573.1698).

### 5.3.63 Synthesis of 4-(((1S,6R)-4'-fluoro-3-oxo-6-((triethylsilyloxy)-1,2,3,6-tetrahydro-[1,1'-biphenyl]-4-yl)methoxy)-3-(naphthalen-2-ylmethyl)-2H-benzo[h]chromen-2-one, **217**

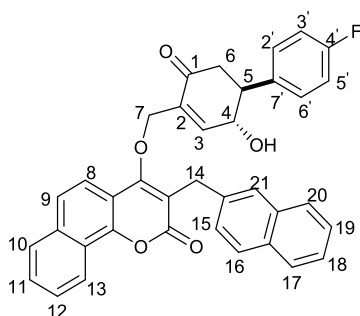


$\text{C}_{43}\text{H}_{41}\text{O}_5\text{SiF}$ ; Molecular weight: 684.27

To a solution of alcohol (**169**) (40 mg, 0.15 mmol) in distilled THF (2 mL), under an atmosphere of nitrogen, was added triphenylphosphine (60 mg, 0.23 mmol) and 4-hydroxy-3-methoxy-3-(naphthalene-2-ylmethyl)-2H-benzo[h]chromen-2-one (**180a**) (80.3 mg, 0.23 mmol). The reaction mixture was cooled to 0 °C and DIAD (40  $\mu\text{L}$ ,

0.21 mmol) was added dropwise. The reaction mixture was stirred at 0 °C for 30 minutes and then at room temperature for 24 hours. The solvents were concentrated *in vacuo* to give the crude product as a thick yellow oil. This crude product was purified by flash silica chromatography (ethyl acetate: petroleum ether 1:6) to give the title compound (**217**) as a thick white oil (90 mg, 70%):  $\nu_{\max}/\text{cm}^{-1}$  (film) 3053 (m, aro C-H), 2954 (m, aliph C-H), 1712 (s, C=O), 1605 (s, C=C);  $\delta_{\text{H}}$  (400 MHz;  $\text{CDCl}_3$ ) 0.23-0.42 (6H, m,  $\text{Si}(\text{CH}_2\text{CH}_3)_3$ ), 0.76 (9H, t,  $J$  7.8,  $\text{Si}(\text{CH}_2\text{CH}_3)_3$ ), 2.64 (2H, dd,  $J$  12.6, 9.6, C(6)H<sub>2</sub>), 3.22 (1H, ddd,  $J$  12.6, 9.3, 5.5, C(5)H), 4.24 (2H, d,  $J$  2.5, C(14)H<sub>2</sub>), 4.47 (1H, dd,  $J$  9.3, 1.4, C(4)H), 4.75 (1H, ddd,  $J$  12.6, 2.8, 1.4, C(7)H<sub>a</sub>H<sub>b</sub>), 4.85 (1H, ddd,  $J$  12.6, 2.8, 1.4, C(7)H<sub>a</sub>H<sub>b</sub>), 6.98 (1H, d,  $J$  1.4, C(3)H), 7.02-7.06 (2H, m, Ar-CH), 7.13-7.17 (2H, m, Ar-CH), 7.40-7.47 (2H, m, Ar-CH), 7.51 (1H, dd,  $J$  8.6, 1.5, C(17)H or C(20)H), 7.64-7.68 (2H, m, Ar-CH), 7.72-7.50 (6H, m, Ar-CH), 7.88-7.92 (1H, m, Ar-CH), 8.57-8.61 (1H, m, Ar-CH);  $\delta_{\text{C}}$  (100 MHz;  $\text{CDCl}_3$ ) 4.4 ( $\text{Si}(\text{CH}_2\text{CH}_3)_3$ ), 6.6 ( $\text{Si}(\text{CH}_2\text{CH}_3)_3$ ), 30.8 (C(14)H<sub>2</sub>), 42.8 (C(6)H<sub>2</sub>), 49.8 (C(5)H), 70.3 (C(4)H), 72.8 (C(7)H<sub>2</sub>), 115.3(CH), 115.5(CH), 117.0(q), 119.1 (CH), 122.5(CH), 125.4 (CH), 126.0 (CH), 126.7 (CH), 127.1, 127.6 (d,  $J$  5.2, CH), 127.8 (CH), 128.2 (CH), 129.4 (d,  $J$  8.1, CH), 131.8 (q), 133.4 (q), 133.6 (q), 136.0 (q), 137.3 (q), 151.1 (CH), 160.5 (d,  $J$  247.6, C(4')F), 162.6 (q), 196.4 (2x C=O);  $\delta_{\text{F}}$  (376 MHz;  $\text{CDCl}_3$ ) -115.1 (s);  $m/z$  (+ES) 685.3 ( $[\text{M}+\text{H}]^+$ , 50%).

#### 5.3.64 Synthesis of 4-(((1*S*,6*R*)-4'-fluoro-6-hydroxy-3-oxo-1,2,3,6-tetrahydro-[1,1'-biphenyl]-4-yl)methoxy)-3-(naphthalen-2-ylmethyl)-2H-benzo[*h*]chromen-2-one, **218**

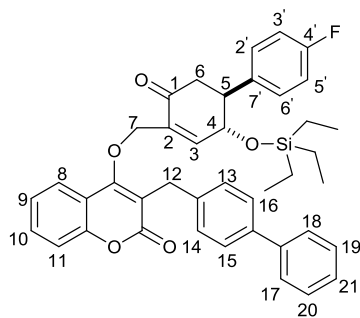


$\text{C}_{37}\text{H}_{27}\text{O}_5\text{F}$ ; Molecular weight: 570.60

A solution of compound (**217**) (23 mg, 0.04 mmol) in trifluoroacetic acid: water (7:1, 0.5 mL) was stirred for 30 minutes at room temperature. The solvents were concentrated under reduced pressure to give a brown oil. This residue was purified

by flash silica chromatography (ethyl acetate: petroleum ether 1:3) and the title compound (**218**) was isolated as an off-white solid (16.8 mg, 67%),  $R_f$  0.3:  $[\alpha]_D^{30}$  -30.22 ( $c$  0.45 in  $\text{CH}_2\text{CH}_2$ );  $\nu_{\text{max}}/\text{cm}^{-1}$  (film) 3416 (br, w, O-H), 1677 (s, C=O), 1603 (s, C=C);  $\delta_{\text{H}}$  (400 MHz;  $\text{CDCl}_3$ ) 2.55 (1H, dd,  $J$  16.6, 13.9, C(6) $\underline{\text{H}}_{\text{ax}}$ ), 2.66 (1H, dd,  $J$  16.6, 4.3, C(6) $\underline{\text{H}}_{\text{eq}}$ ), 3.16 (1H, ddd,  $J$  13.9, 10, 4.3, C(5) $\underline{\text{H}}$ ), 4.23 (2H, s, C(14) $\underline{\text{H}}_2$ ), 4.53 (1H, dd,  $J$  10, 1.5, C(4) $\underline{\text{H}}$ ), 4.72 (1H, ddd,  $J$  12.4, 2.8, 1.5, C(7) $\underline{\text{H}}_{\text{a}}$   $\underline{\text{H}}_{\text{b}}$ ), 4.81 (1H, ddd,  $J$  12.4, 2.8, 1.5, C(7) $\underline{\text{H}}_{\text{a}}$   $\underline{\text{H}}_{\text{b}}$ ), 7.00 (1H, d,  $J$  1.5, C(3) $\underline{\text{H}}$ ), 7.05-7.09 (2H, m, Ar- $\underline{\text{CH}}$ ), 7.14-7.19 (2H, m, Ar- $\underline{\text{CH}}$ ), 7.40-7.46 (2H, m, Ar- $\underline{\text{CH}}$ ), 7.49 (1H, dd,  $J$  8.6, 1.8, (C(10) $\underline{\text{H}}$ ) or (C(13) $\underline{\text{H}}$ ) or (C(17) $\underline{\text{H}}$ ) or (C(20) $\underline{\text{H}}$ )), 7.65-7.69 (2H, m, Ar- $\underline{\text{CH}}$ ), 7.73-7.80 (6H, m, Ar- $\underline{\text{CH}}$ ), 7.88-7.92 (1H, m, Ar- $\underline{\text{CH}}$ ), 8.54-8.57 (1H, m, Ar- $\underline{\text{CH}}$ );  $\delta_{\text{C}}$  (100 MHz;  $\text{CDCl}_3$ ) 30.8 ( $\underline{\text{C}}$ (14) $\underline{\text{H}}_2$ ), 43.1 ( $\underline{\text{C}}$ (6) $\underline{\text{H}}_2$ ), 49.6 ( $\underline{\text{C}}$ (5) $\underline{\text{H}}$ ), 70.3 ( $\underline{\text{C}}$ (4) $\underline{\text{H}}$ ), 71.8 ( $\underline{\text{C}}$ (7) $\underline{\text{H}}_2$ ), 116.0 (d,  $J$  3.7,  $\underline{\text{CH}}$ ), 116.2 ( $\underline{\text{CH}}$ ), 118.9 ( $\underline{\text{CH}}$ ), 122.4 ( $\underline{\text{CH}}$ ), 123.1 (q), 124.6 ( $\underline{\text{CH}}$ ), 125.5 ( $\underline{\text{CH}}$ ), 126.1 ( $\underline{\text{CH}}$ ), 126.6 ( $\underline{\text{CH}}$ ), 127.1 ( $\underline{\text{CH}}$ ), 127.4 ( $\underline{\text{CH}}$ ), 127.6 (d,  $J$  5.9,  $\underline{\text{CH}}$ ), 127.7 ( $\underline{\text{CH}}$ ), 127.8 ( $\underline{\text{CH}}$ ), 128.3 ( $\underline{\text{CH}}$ ), 128.9 ( $\underline{\text{CH}}$ ), 129.2 (d,  $J$  8.1,  $\underline{\text{CH}}$ ), 132.3 (q), 133.6 (q), 134.0 (q), 134.9 (q), 136.5 (q), 150.3 (d,  $J$  3.7,  $\underline{\text{CH}}$ ),  $\underline{\text{C}}$ (4')F is not visible, 196.3 (2x C=O);  $\delta_{\text{F}}$  (376 MHz;  $\text{CDCl}_3$ ) -114.0 (s);  $m/z$  (+ES) 593.3 ( $[\text{M}+\text{Na}]^+$ , 100%).

### 5.3.65 Synthesis of 3-([1,1'-biphenyl]-4-ylmethyl)-4-(((1*S*,6*R*)-4'-fluoro-3-oxo-6-((triethylsilyl)oxy)-1,2,3,6-tetrahydro-[1,1'-biphenyl]-4-yl)methoxy)-2H-chromen-2-one, **219**

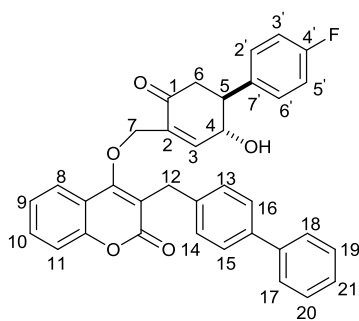


$\text{C}_{41}\text{H}_{41}\text{O}_5\text{SiF}$ ; Molecular weight: 660.84

To a solution of alcohol (**169**) (40 mg, 0.15 mmol) in dry THF (3 mL), under an atmosphere of nitrogen, was added triphenylphosphine (60 mg, 0.23 mmol) and 3-([1,1'-biphenyl]-4-ylmethyl)-4-hydroxy-2H-chromen-2-one (**172e**), (80 mg, 0.23 mmol). The reaction mixture was cooled to 0 °C and DIAD (40  $\mu\text{L}$ , 0.21 mmol) was added dropwise. The reaction mixture was stirred at 0 °C for 30 minutes and then at

room temperature for 24 hours. The solvents were concentrated *in vacuo* to give the crude product as a thick yellow oil. This crude product was purified by flash silica chromatography (ethyl acetate: petroleum ether 1:6) to give the title compound (**219**) as a thick white oil (47 mg, 62%),  $R_f$  0.3:  $\nu_{\max}/\text{cm}^{-1}$  (film) 2955 (m, Ar-C-H), 2875 (m, aliph-C-H), 1714 (s, C=O), 1608 (s, C=C);  $\delta_{\text{H}}$  (400 MHz;  $\text{CDCl}_3$ ) 0.26-0.45 (6H, m,  $\text{Si}(\text{CH}_2\text{CH}_3)_3$ ), 0.79 (9H, t,  $J$  7.8,  $\text{Si}(\text{CH}_2\text{CH}_3)_3$ ), 2.74 (2H, dd,  $J$  11.9, 6.3, C(6) $\underline{\text{H}}_2$ ), 3.29 (1H, ddd,  $J$  11.9, 9.3, 6.3, C(5) $\underline{\text{H}}$ ), 4.04 (2H, s, C(12) $\underline{\text{H}}_2$ ), 4.59 (1H, dd,  $J$  9.3, 1.5, C(4) $\underline{\text{H}}$ ), 4.73 (1H, ddd,  $J$  12.6, 2.8, 1.5, C(7) $\underline{\text{H}}_a\text{H}_b$ ), 4.82 (1H, ddd,  $J$  12.6, 2.8, 1.5, C(7) $\underline{\text{H}}_a\text{H}_b$ ), 7.06 (1H, d,  $J$  1.5, C(3) $\underline{\text{H}}$ ), 7.02-7.05 (2H, m, Ar- $\underline{\text{CH}}$ ), 7.20-7.24 (2H, m, Ar- $\underline{\text{CH}}$ ), 7.31-7.35 (2H, m, Ar- $\underline{\text{CH}}$ ), 7.38 (1H, d,  $J$  1.5, Ar- $\underline{\text{CH}}$ ), 7.40-7.44 (4H, m, Ar- $\underline{\text{CH}}$ ), 7.50-7.58 (5H, m, Ar- $\underline{\text{CH}}$ ), 7.79 (1H, dd,  $J$  7.9, 1.4, C(8) $\underline{\text{H}}$  or C(11) $\underline{\text{H}}$  or C(21) $\underline{\text{H}}$ );  $\delta_{\text{C}}$  (100 MHz;  $\text{CDCl}_3$ ) 4.5 ( $\text{Si}(\text{CH}_2\text{CH}_3)_3$ ), 6.6 ( $\text{Si}(\text{CH}_2\text{CH}_3)_3$ ), 30.3 ( $\underline{\text{C}}(12)\text{H}_2$ ), 42.9 ( $\underline{\text{C}}(6)\text{H}_2$ ), 49.9 ( $\underline{\text{C}}(5)\text{H}$ ), 70.3 ( $\underline{\text{C}}(4)\text{H}$ ), 72.9 ( $\underline{\text{C}}(7)\text{H}_2$ ), 115.3 ( $\underline{\text{CH}}$ ), 115.5 ( $\underline{\text{CH}}$ ), 117.0 (d,  $J$  5.9,  $\underline{\text{CH}}$ ), 117.3 (q), 123.3 ( $\underline{\text{CH}}$ ), 123.4 ( $\underline{\text{CH}}$ ), 124.3 ( $\underline{\text{CH}}$ ), 127.0 ( $\underline{\text{CH}}$ ), 127.1 ( $\underline{\text{CH}}$ ), 127.3 ( $\underline{\text{CH}}$ ), 127.3 ( $\underline{\text{CH}}$ ), 128.7 ( $\underline{\text{CH}}$ ), 129.0 ( $\underline{\text{CH}}$ ), 129.4 ( $\underline{\text{CH}}$ ), 129.5 (d,  $J$  8.1,  $\underline{\text{CH}}$ ), 131.8 (q), 133.6 (q), 137.9 (q), 139.4 (q), 140.9 (q), 151.2 ( $\underline{\text{CH}}$ ), 152.9 (q), 161.2 (d,  $J$  246.3,  $\underline{\text{C}}(4')\text{F}$ ), 163.2 (q), 196.4 (2x C=O);  $\delta_{\text{F}}$  (376 MHz;  $\text{CDCl}_3$ ) -115.0 (s);  $m/z$  (+ES) 683.4 ( $[\text{M}+\text{Na}]^+$ , 100%).

### 5.3.66 Synthesis of 3-([1,1'-biphenyl]-4-ylmethyl)-4-(((1S,6R)-4'-fluoro-6-hydroxy-3-oxo-1,2,3,6-tetrahydro-[1,1'-biphenyl]-4-yl)methoxy)-2H-chromen-2-one, **220**

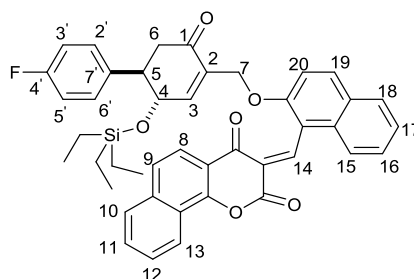


$\text{C}_{35}\text{H}_{27}\text{O}_5\text{F}$ ; Molecular weight: 546.58

A solution of compound (**219**) (39 mg, 0.06 mmol) in trifluoroacetic acid: water (7:1, 1 mL) was stirred for 30 minutes at room temperature. The solvents were concentrated under reduced pressure to give a brown oil. This residue was purified by flash silica chromatography (ethyl acetate: petroleum ether 1:2) to give the title

compound (**220**) as a white foam (23 mg, 71%),  $R_f$  0.2:  $\nu_{\max}/\text{cm}^{-1}$  3401 (w, br, O-H), 2961 (m, C-H), 1678 (s, C=O), 1607 (s, C=C);  $\delta_H$  (400 MHz;  $\text{CDCl}_3$ ) 2.05 (1H, s, OH), 2.72 (2H, dd,  $J$  12.4, 9.3, C(6) $\underline{H}_2$ ), 3.27 (1H, ddd,  $J$  12.4, 9.3, 5.5, C(5) $\underline{H}$ ), 4.05 (2H, s, C(12) $\underline{H}_2$ ), 4.68 (1H, dd,  $J$  9.3, 1.5, C(4) $\underline{H}$ ), 4.71 (1H, ddd,  $J$  13.4, 2.8, 1.5, C(7) $\underline{H}_a\text{H}_b$ ), 4.80 (1H, ddd,  $J$  13.4, 2.8, 1.5, C(7) $\underline{H}_a\text{H}_b$ ), 7.08 (2H, ~ t,  $J$  8.6, C(19) $\underline{H}$  and C(20) $\underline{H}$ ), 7.19 (1H, d,  $J$  1.5, C(3) $\underline{H}$ ), 7.24-7.28 (2H, m, Ar- $\underline{CH}$ ), 7.30-7.35 (2H, m, Ar- $\underline{CH}$ ), 7.37-7.43 (5H, m, Ar- $\underline{CH}$ ), 7.51-7.57 (5H, m, Ar- $\underline{CH}$ ), 7.79 (1H, dd,  $J$  7.9, 1.4, C(8) $\underline{H}$  or C(11) $\underline{H}$  or C(21) $\underline{H}$ );  $\delta_C$  (100 MHz;  $\text{CDCl}_3$ ) 30.2 (C(12) $\underline{H}_2$ ), 43.2 (C(6) $\underline{H}_2$ ), 49.7 (C(5) $\underline{H}$ ), 60.8 (C(4) $\underline{H}$ ), 70.3 (C(7) $\underline{H}_2$ ), 116.1 (C $\underline{H}$ ), 116.3 (C $\underline{H}$ ), 116.9 (q), 117.1 (q), 117.1 (C $\underline{H}$ ), 123.4 (C $\underline{H}$ ), 124.5 (C $\underline{H}$ ), 127.0 (C $\underline{H}$ ), 127.2 (d,  $J$  10.3, C $\underline{H}$ ), 127.3 (C $\underline{H}$ ), 128.8 (C $\underline{H}$ ), 128.9 (d,  $J$  18.4, q), 129.0 (C $\underline{H}$ ), 129.2 (d,  $J$  8.1, C $\underline{H}$ ), 129.3 (C $\underline{H}$ ), 131.9 (C $\underline{H}$ ), 134.1 (q), 134.7 (d,  $J$  2.9, q), 137.9 (q), 139.4 (q), 140.8 (q), 150.3 (C $\underline{H}$ ), 152.8 (q), 161.3 (d,  $J$  246.4, C(4')F), 163.2 (q), 164.1 (q), 196.3 (2x C=O);  $\delta_F$  (376 MHz;  $\text{CDCl}_3$ ) -114.0 (s);  $m/z$  (+ES) 548.6 ( $[\text{M}+2\text{H}]^+$ , 100%); (Found 569.1740;  $\text{C}_{35}\text{H}_{27}\text{O}_5\text{NaF}$  ( $[\text{M}+\text{Na}]^+$ ), requires 569.1725).

### 5.3.67 Synthesis of (E)-3-((2-(((1S,6R)-4'-fluoro-3-oxo-6-((triethylsilyloxy)-1,2,3,6-tetrahydro-[1,1'-biphenyl]-4-yl)methoxy)naphthalene)-2H-benzo[h]chromene-2,4(3H)-dione, **221**

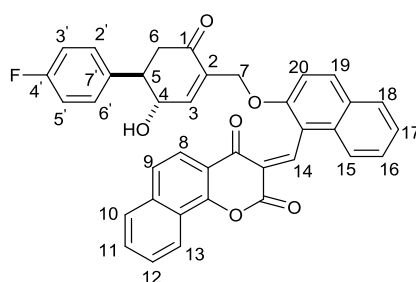


$\text{C}_{43}\text{H}_{39}\text{O}_6\text{SiF}$ ; Molecular weight: 698.85

To a solution of alcohol (**169**) (30 mg, 0.09 mmol) in distilled dichloromethane (3 mL), was added triphenylphosphine (50 mg, 0.19 mmol) and (Z)-3-((1-hydroxynaphthalen-2-yl)methylene)-2H-benzo[h]chromene-2,4(3H)-dione (**177a**) (60 mg, 0.17 mmol). DIAD (40  $\mu\text{L}$ , 0.21 mmol) was added dropwise, and the reaction mixture was stirred at room temperature for 24 hours. The solvents were concentrated *in vacuo* to give the crude product as a thick yellow oil which was purified by flash silica chromatography (ethyl acetate: petroleum ether 1:7) to give the title compound (**221**) as a thick yellow oil (39 mg, 65%),  $R_f$  0.3:  $\nu_{\max}/\text{cm}^{-1}$  (film)

2955 (m, Ar-C-H), 2875 (m, aliph-C-H), 1739 (s, C=O), 1676 (s, C=O);  $\delta_H$  (400 MHz; CDCl<sub>3</sub>) 0.21-0.40 (6H, m, Si(CH<sub>2</sub>CH<sub>3</sub>)<sub>3</sub>), 0.76 (9H, t,  $J$  7.9, Si(CH<sub>2</sub>CH<sub>3</sub>)<sub>3</sub>), 1.81 (1H, dd,  $J$  16.4, 14.2, C(6)H<sub>ax</sub>), 2.13 (1H, dd,  $J$  16.4, 3.8, C(6)H<sub>eq</sub>), 2.64 (1H, ddd,  $J$  14.2, 9.4, 3.8, C(5)H), 3.89 (1H, dd,  $J$  9.4, 1.9, C(4)H), 4.57 (1H, ddd,  $J$  13.4, 3.8, 1.9, C(7)H<sub>aH<sub>b</sub></sub>), 4.64 (1H, ddd,  $J$  13.4, 3.8, 1.9, C(7)H<sub>aH<sub>b</sub></sub>), 6.80 (1H, d,  $J$  1.9, C(3)H), 6.81-6.84 (2H, m, Ar-CH), 6.96 (2H, t,  $J$  8.6, C(11)H and C(12)H or C(16)H and C(17)H), 7.52-7.58 (2H, m, Ar-CH), 7.61-7.68 (2H, m, Ar-CH), 7.74-7.79 (2H, m, Ar-CH), 7.85-7.86 (1H, m, Ar-CH), 7.92 (1H, d,  $J$  8.2, C(8)H or C(9)H or C(19)H or C(20)H), 8.01 (1H, d,  $J$  8.2, C(8)H or C(9)H or C(19)H or C(20)H), 8.13-8.16 (2H, m, Ar-CH), 8.30 (1H, d,  $J$  8.4, C(8)H or C(9)H or C(19)H or C(20)H), 8.90 (1H, s, C(18)H);  $\delta_C$  (100 MHz; CDCl<sub>3</sub>) 4.4 (Si(CH<sub>2</sub>CH<sub>3</sub>)<sub>3</sub>), 6.6 (Si(CH<sub>2</sub>CH<sub>3</sub>)<sub>3</sub>), 42.1 (C(6)H<sub>2</sub>), 49.2 (C(5)H), 72.3 (C(4)H), 72.5 (C(7)H<sub>2</sub>), 113.1 (q), 115.0 (CH), 115.2 (CH), 117.1 (CH), 121.9 (CH), 123.1 (CH), 125.1 (CH), 125.6 (CH), 126.8 (d,  $J$  9.5, CH), 127.6 (q), 127.8 (q), 127.9 (q), 128.3 (CH), 128.7 (CH), 129.0 (CH), 129.2 (d,  $J$  8.8 CH), 129.6 (q), 130.2 (q), 133.5 (q), 134.7 (CH), 136.0 (d,  $J$  2.9, CH), 137.3 (q), 139.2 (CH), 149.7 (CH), 155.0 (q), 155.8 (q), 158.5 (q), 162.0 (d,  $J$  245.8, C-F), 191.5 (2x C=O), 196.0 (C=O);  $\delta_F$  (376 MHz; CDCl<sub>3</sub>) -115.3 (s);  $m/z$  (+ES) 721.2382 ([M+Na]<sup>+</sup>, 100%), requires 721.2398, C<sub>43</sub>H<sub>39</sub>O<sub>6</sub>FNaSi).

### 5.3.68 Synthesis of (*E*)-3-((2-(((1*R*,6*S*)-4'-fluoro-6-hydroxy-3-oxo-1,2,3,6-tetrahydro-[1,1'-biphenyl]-4-yl)methoxy)naphthalene-1-yl)methylene)-2H-benzo[*h*]chromene-2-one, **190**

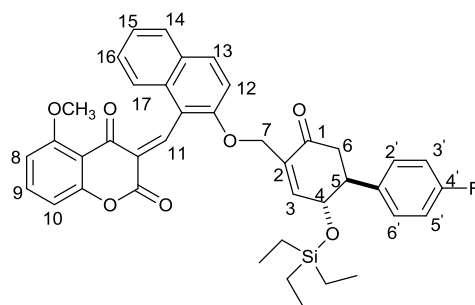


C<sub>37</sub>H<sub>25</sub>O<sub>6</sub>F; Molecular weight: 584.59

A solution of compound (**221**) (35 mg, 0.05 mmol) in trifluoroacetic acid: water (7:1, 1.5 mL) was stirred for 30 minutes at room temperature. The solvents were concentrated under reduced pressure to give the crude product as orange oil. This crude product was purified by flash silica chromatography (ethyl acetate: petroleum ether 1:2) and the title compound (**190**) was isolated as yellow solid (15 mg, 51%),

$R_f$  0.4:  $[\alpha]_D^{29}$  -72.9 ( $c$  0.45 in  $\text{CH}_2\text{Cl}_2$ );  $\nu_{\text{max}}/\text{cm}^{-1}$  3426 (m, a-C-H), 2923 (m, aliph-C-H), 1708 (s, C=O), 1668 (s, C=O), 1647 (s, C=C);  $\delta_{\text{H}}$  (400 MHz;  $\text{CDCl}_3$ ) 1.88 (1H, dd,  $J$  16.4, 14.4, C(6) $\underline{\text{H}}_{\text{ax}}$ ), 2.22 (1H, dd,  $J$  16.4, 3.9, C(6) $\underline{\text{H}}_{\text{eq}}$ ), 2.61 (1H, ddd,  $J$  14.4, 10.1, 3.9, C(5) $\underline{\text{H}}$ ), 3.77 (1H, dd,  $J$  10.1, 1.5, C(4) $\underline{\text{H}}$ ), 4.60 (1H, ddd,  $J$  15.4, 3.8, 1.5, C(7) $\underline{\text{H}}_{\text{aHb}}$ ), 4.62 (1H, ddd,  $J$  15.4, 3.8, 1.5, C(7) $\underline{\text{H}}_{\text{aHb}}$ ), 6.81 (2H, dd,  $J$  8.4, 5.4, C(15) $\underline{\text{H}}$  and C(18) $\underline{\text{H}}$ ), 6.91 (1H, d,  $J$  1.5, C(3) $\underline{\text{H}}$ ), 7.01 (2H, t,  $J$  8.6, C(11) $\underline{\text{H}}$  and C(12) $\underline{\text{H}}$  or C(16) $\underline{\text{H}}$  and C(17) $\underline{\text{H}}$ ), 7.56-7.59 (2H, m, Ar- $\underline{\text{CH}}$ ), 7.76-7.87 (3H, m, Ar- $\underline{\text{CH}}$ ), 7.94 (1H, d,  $J$  8.1, C(19) $\underline{\text{H}}$  or C(20) $\underline{\text{H}}$ ), 8.00 (1H, d,  $J$  8.1, C(19) $\underline{\text{H}}$  or C(20) $\underline{\text{H}}$ ), 8.12 (1H, d,  $J$  9.0, C(10) $\underline{\text{H}}$  or C(13) $\underline{\text{H}}$ ), 8.18 (1H, d,  $J$  8.4, C(8) $\underline{\text{H}}$  or C(9) $\underline{\text{H}}$ ), 8.31 (1H, d,  $J$  8.4, C(8) $\underline{\text{H}}$  or C(9) $\underline{\text{H}}$ ), 8.91 (1H, s, C(18) $\underline{\text{H}}$ );  $\delta_{\text{C}}$  (100 MHz;  $\text{CDCl}_3$ ) 42.7 (C(6) $\underline{\text{H}}_2$ ), 49.0 (C(5) $\underline{\text{H}}$ ), 71.4 (C(4) $\underline{\text{H}}$ ), 72.4 (C(7) $\underline{\text{H}}_2$ ), 113.1 (q), 115.7 (C $\underline{\text{H}}$ ), 115.9 (C $\underline{\text{H}}$ ), 117.2 (C $\underline{\text{H}}$ ), 121.8 (C $\underline{\text{H}}$ ), 123.1 (C $\underline{\text{H}}$ ), 125.3 (C $\underline{\text{H}}$ ), 125.5 (C $\underline{\text{H}}$ ), 126.8 (C $\underline{\text{H}}$ ), 126.9 (C $\underline{\text{H}}$ ), 127.7 (d,  $J$  1.5, q), 128.0 (q), 128.3 (C $\underline{\text{H}}$ ), 128.8 (C $\underline{\text{H}}$ ), 128.9 (d,  $J$  7.3, C $\underline{\text{H}}$ ), 129.1 (C $\underline{\text{H}}$ ), 129.3 (C $\underline{\text{H}}$ ), 129.6 (q), 134.1 (q), 134.9 (C $\underline{\text{H}}$ ), 137.3 (q), 139.2 (C $\underline{\text{H}}$ ), 148.2 (C $\underline{\text{H}}$ ), 155.1 (q), 155.8 (q), 158.6 (q), 162.1 (d,  $J$  247.2, C(4')F), 166.4 (q), 191.5 (C=O), 196.0 (2x C=O);  $\delta_{\text{F}}$  (376 MHz;  $\text{CDCl}_3$ ) -114.5 (s);  $m/z$  (+ES) 607.2 ( $[\text{M}+\text{Na}]^+$ , 100%); (Found 607.1542;  $\text{C}_{37}\text{H}_{25}\text{O}_6\text{NaF}$  ( $[\text{M}+\text{Na}]^+$ ), requires 607.1533).

### 5.3.69 Synthesis of (*E*)-3-((2-(((1*S*,6*R*)-4'-fluoro-3-oxo-6-((triethylsilyl)oxy)-1,2,3,6-tetrahydro-[1,1'-biphenyl]-4-yl)methoxy)naphthalen-1-yl)methylene)-5-methoxychromane-2,4-dione, **222**

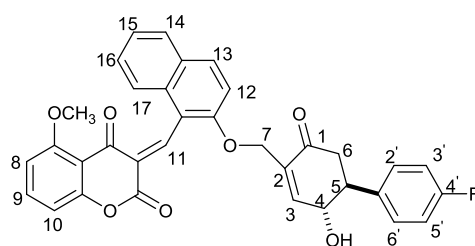


$\text{C}_{40}\text{H}_{39}\text{O}_7\text{SiF}$ ; Molecular weight: 678.24

To a solution of alcohol (**169**) (40 mg, 0.15 mmol) in dry dichloromethane (3 mL), was added triphenylphosphine (60 mg, 0.23 mmol) and (*E*)-3-((2-hydroxynaphthalen-1-yl)methylene)-5-methoxychromane-2,4-dione (**176a**), (60 mg, 0.17 mmol). DIAD (40  $\mu\text{L}$ , 0.21 mmol) was added dropwise, and the reaction mixture was stirred at room temperature for 24 hours. The solvents were concentrated *in vacuo* to give the crude product as a thick yellow oil. This crude

product was purified by flash silica chromatography (ethyl acetate: petroleum ether 1:2) to give the title compound (**222**) as a yellow oil (41 mg, 53%),  $R_f$  0.7:  $\delta_H$  (400 MHz;  $CDCl_3$ ) 0.13-0.32 (6H, m,  $Si(CH_2CH_3)_3$ ), 0.65 (9H, t,  $J$  7.8,  $Si(CH_2CH_3)_3$ ), 2.52 (2H, dd,  $J$  11.9, 6.9, C(6)H), 3.09 (1H, ddd,  $J$  11.9, 9.3, 6.9, C(5)H), 3.77 (3H, s,  $OCH_3$ ), 4.37 (1H, dd,  $J$  9.3, 1.9, C(4)H), 4.69 (1H, ddd,  $J$  13.6, 3.0, 1.9, C(7)H<sub>a</sub>H<sub>b</sub>), 4.79 (1H, ddd,  $J$  13.6, 3.0, 1.9, C(7)H<sub>a</sub>H<sub>b</sub>), 6.64 (1H, d,  $J$  8.6, C(8)H), 6.68 (1H, d,  $J$  8.6, C(10)H), 6.84 (1H, d,  $J$  1.9, C(3)H), 6.95-6.99 (2H, m, Ar-CH), 7.03-7.06 (2H, m, Ar-CH), 7.39 (1H, t,  $J$  8.6, C(9)H), 7.48 (1H, d,  $J$  9.1, C(12)H), 7.63 (1H, ddd,  $J$  8.3, 7.1, 1.0, C(15)H or C(16)H), 7.76 (1H, ddd,  $J$  8.3, 7.1, 1.0, C(15)H or C(16)H), 7.94 (1H, d,  $J$  8.3, C(14)H), 8.09 (1H, d,  $J$  9.1, C(13)H), 8.36 (1H, d,  $J$  8.3 C(17)H), 9.25 (1H, s, C(11)H);  $\delta_C$  (100 MHz;  $CDCl_3$ ) 4.4 ( $Si(CH_2CH_3)_3$ ), 6.5 ( $Si(CH_2CH_3)_3$ ), 42.8 (C(6)H), 49.7 (C(5)H), 56.0 ( $OCH_3$ ), 64.8 (C(4)H), 72.7 (C(7)H<sub>2</sub>), 104.5 (CH), 105.5 (CH), 113.0 (q), 115.1 (CH), 116.8 (CH), 118.9 (q), 121.7 (CH), 124.6 (q), 126.5 (CH), 129.1 (CH), 129.2 (CH), 129.4 (d,  $J$  8.1, CH), 129.9 (q), 130.2 (q), 131.8 (CH), 133.5 (q), 135.6 (CH), 136.3 (d,  $J$  3.7, (q)), 142.2 (CH), 149.7 (CH), 156.0 (q), 158.0 (q), 158.2 (q), 162.0 (d,  $J$  246.2, C(4')F), 189.8 (C=O), 196.7 (2x C=O);  $\delta_F$  (376 MHz;  $CDCl_3$ ) -115.5 (s);  $m/z$  (+ES) 701.2 ( $[M+Na]^+$ , 100%); (Found 701.2347;  $C_{40}H_{39}O_7NaFSi$  ( $[M+Na]^+$ ), requires 701.2330).

### 5.3.70 Synthesis of (*E*)-3-((2-(((1*S*,6*R*)-4'-fluoro-6-hydroxy-3-oxo-1,2,3,6-tetrahydro-[1,1'-biphenyl]-4-yl)methoxy)naphthalene-1-yl)methylene)-5-methoxychromane-2,4-dione, **188**



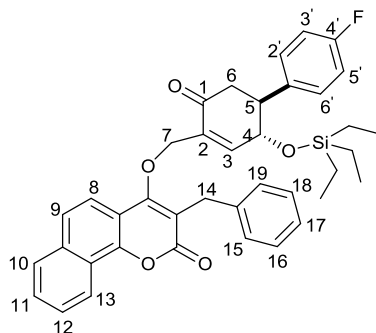
$C_{34}H_{25}O_7F$ ; Molecular weight: 564.56

A solution of compound (**222**) (33 mg, 0.05 mmol) in trifluoroacetic acid: water (7:1, 1.5 mL) was stirred for 30 minutes at room temperature. The solvents were concentrated under reduced pressure to give the crude product as orange oil. The crude product was purified by flash silica chromatography (ethyl acetate: petroleum ether 1:1) to give the title compound (**188**) as a yellow powder (16.4 mg, 59%),  $R_f$  0.4,  $[\alpha]_D^{29}$  -60.2 ( $c$  0.48 in  $CH_2Cl_2$ ):  $\nu_{max}/cm^{-1}$  1731 (s, C=O), 1682 (s, C=O), 1594 (s,



C-C);  $\delta_{\text{H}}$  (400 MHz;  $\text{CDCl}_3$ ) 2.53 (2H, dd,  $J$  12.4, 9.1, C(6)H<sub>2</sub>), 3.05 (2H, ddd,  $J$  12.4, 9.1, 5.5, C(5)H), 3.80 (3H, s, OCH<sub>3</sub>), 4.39 (1H, dd,  $J$  9.1, 1.9, C(4)H), 4.77 (2H, m, C(7)H<sub>2</sub>), 6.67 (2H, dd,  $J$  8.4, 4.2, C(8)H and C(10)H), 6.93 (1H, ~q,  $J$  3.3, 1.9, C(3)H), 6.99-7.03 (2H, m, Ar-CH), 7.07-7.10 (2H, m, Ar-CH), 7.39 (1H, t,  $J$  8.4, C(9)H), 7.47 (1H, d,  $J$  9.1, C(12)H), 7.62 (1H, td,  $J$  8.3, 7.1, 1.3, C(15)H) or C(16)H), 7.75 (1H, ddd,  $J$  8.3, 7.1, 1.3, C(15)H) or C(16)H), 7.93 (1H, d,  $J$  8.3, C(14)H) or C(17)H), 8.09 (1H, d,  $J$  9.1, C(13)H), 8.36 (1H, d,  $J$  8.3, C(14)H) or C(17)H), 9.25 (1H, s, C(11)H);  $\delta_{\text{C}}$  (100 MHz;  $\text{CDCl}_3$ ) 43.3 (C(6)H<sub>2</sub>), 49.4 (C(5)H), 56.1 (OCH<sub>3</sub>), 64.4 (C(4)H), 71.6 (C(7)H<sub>2</sub>), 104.7 (CH), 105.4 (CH), 113.1 (q), 115.7 (CH), 115.9 (CH), 116.8 (CH), 121.8 (CH), 124.7 (q), 126.6 (CH), 129.1 (t,  $J$  9.2, CH), 129.9 (q), 130.2 (q), 131.9 (CH), 134.0 (q), 135.8 (CH), 142.6 (CH), 148.7 (CH), 156.5 (q), 158.1 (q), 158.3 (q), 160.6 (d,  $J$  239.8, C(4')F), 190.1 (C=O), 196.4 (2x C=O);  $\delta_{\text{F}}$  (376 MHz;  $\text{CDCl}_3$ ) -114.8 (s);  $m/z$  (+ES) 565.2 ( $[\text{M}+\text{H}]^+$ , 100%); (Found 587.1489;  $\text{C}_{34}\text{H}_{25}\text{O}_7\text{NaF}$  ( $[\text{M}+\text{Na}]^+$ ) requires 587.1482).

### 5.3.71 Synthesis of 3-benzyl-4-(((1*S*,6*R*)-4'-fluoro-3-oxo-6-((triethylsilyl)oxy)-1,2,3,6-tetrahydro-[1,1'-biphenyl]-4-yl)methoxy)-2H-benzo[*h*]chromen-2-one, **223**

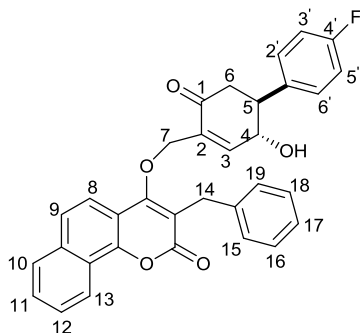


$\text{C}_{39}\text{H}_{39}\text{O}_5\text{SiF}$ ; Molecular weight: 634.81

To a solution of alcohol (**169**) (40 mg, 0.15 mmol) in dry tetrahydrofuran (3 mL), was added triphenylphosphine (50 mg, 0.19 mmol) and 3-benzyl-4-hydroxy-2H-benzo[*h*]chromen-2-one, (**180b**) (50 mg, 0.17 mmol). DIAD (40  $\mu\text{L}$ , 0.21 mmol) was added dropwise, and the reaction mixture was stirred at room temperature for 24 hours. The solvents were concentrated *in vacuo* to give the crude product as a thick yellow oil. The crude product was purified by flash silica chromatography (ethyl acetate: petroleum ether 1:6) to give the title compound (**223**) as a thick white oil (41 mg, 57%),  $R_f$  0.4:  $\nu_{\text{max}}/\text{cm}^{-1}$  (film) 2950 (m, Ar-C-H), 2874 (m, aliph-C-H), 1708 (s,

C=O), 1604 (s, C=C);  $\delta_{\text{H}}$  (400 MHz;  $\text{CDCl}_3$ ) 0.27-0.46 (6H, m,  $\text{Si}(\text{CH}_2\text{CH}_3)_3$ ), 0.79 (9H, t,  $J$  8.1,  $\text{Si}(\text{CH}_2\text{CH}_3)_3$ ), 2.76 (2H, dd,  $J$  12.4, 10.3, C(6) $\underline{\text{H}}_2$ ), 3.30 (1H, ddd,  $J$  12.4, 9.3, 5.3, C(5) $\underline{\text{H}}$ ), 4.06 (2H, s, C(12) $\underline{\text{H}}_2$ ), 4.60 (1H, dd,  $J$  9.3, 1.8, C(4) $\underline{\text{H}}$ ), 4.72 (1H, ddd,  $J$  12.6, 2.8, 1.8, C(7) $\text{H}_a\text{H}_b$ ), 4.81 (1H, ddd,  $J$  12.6, 2.8, 1.8, C(7) $\text{H}_a\text{H}_b$ ), 7.05 (1H, d,  $J$  1.8, C(3) $\underline{\text{H}}$ ), 7.07-7.10 (2H, m, Ar- $\underline{\text{CH}}$ ), 7.18-7.30 (5H, m, Ar- $\underline{\text{CH}}$ ), 7.39 (2H, d,  $J$  7.1, C(2') $\underline{\text{H}}$  and C(6') $\underline{\text{H}}$  or C(3') $\underline{\text{H}}$  and C(5') $\underline{\text{H}}$ ), 7.62-7.67 (2H, m, Ar- $\underline{\text{CH}}$ ), 7.73 (1H, d,  $J$  8.6, C(8) $\underline{\text{H}}$  or C(9) $\underline{\text{H}}$ ), 7.75 (1H, d,  $J$  8.6, C(8) $\underline{\text{H}}$  or C(9) $\underline{\text{H}}$ ), 7.87-7.90 (1H, m, Ar- $\underline{\text{CH}}$ ), 8.55-8.57 (1H, m, Ar- $\underline{\text{CH}}$ );  $\delta_{\text{C}}$  (100 MHz;  $\text{CDCl}_3$ ) 4.5 ( $\text{Si}(\text{CH}_2\text{CH}_3)_3$ ), 6.6 ( $\text{Si}(\text{CH}_2\text{CH}_3)_3$ ), 30.6 (C(12) $\underline{\text{H}}_2$ ), 42.9 (C(6) $\underline{\text{H}}_2$ ), 49.9 (C(5) $\underline{\text{H}}$ ), 70.3 (C(4) $\underline{\text{H}}$ ), 72.9 (C(7) $\underline{\text{H}}_2$ ), 112.5 (q), 115.3 (C $\underline{\text{H}}$ ), 115.5 (C $\underline{\text{H}}$ ), 116.8 (q), 119.1 (C $\underline{\text{H}}$ ), 122.5 (C $\underline{\text{H}}$ ), 123.1 (q), 124.3 (C $\underline{\text{H}}$ ), 126.5 (C $\underline{\text{H}}$ ), 127.2 (C $\underline{\text{H}}$ ), 127.8 (C $\underline{\text{H}}$ ), 128.6 (d,  $J$  2.9, C $\underline{\text{H}}$ ), 128.7 (C $\underline{\text{H}}$ ), 129.5 (d,  $J$  8.1, C $\underline{\text{H}}$ ), 133.6 (q), 134.8 (q), 136.1 (d,  $J$  3.7, q), 139.0 (q), 150.2 (q), 151.2 (C $\underline{\text{H}}$ ), 162.2 (d,  $J$  246.2, C(4')F), 163.7 (d,  $J$  15.5, q), 196.4 (2x C=O);  $\delta_{\text{F}}$  (376 MHz;  $\text{CDCl}_3$ ) -115.0 (s);  $m/z$  (+ES) 635.4 ( $[\text{M}+\text{H}]^+$ , 100%); (Found 635.2610;  $\text{C}_{39}\text{H}_{40}\text{O}_5\text{SiF}$  ( $[\text{M}+\text{H}]^+$ ) requires 635.2629).

### 5.3.72 Synthesis of 3-benzyl-4-(((1*S*,6*R*)-4'-fluoro-6-hydroxy-3-oxo-1,2,3,6-tetrahydro[1,1'-biphenyl]-4-yl)methoxy)-2H-benzo[*h*]chromen-2-one, **189**

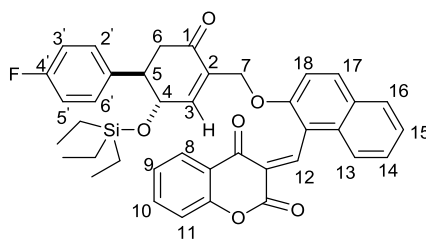


$\text{C}_{33}\text{H}_{25}\text{O}_5\text{F}$ ; Molecular weight: 520.17

A solution of compound (**223**) (35 mg, 0.06 mmol) in trifluoroacetic acid: water (7:1, 1.5 mL) was stirred for 30 minutes at room temperature. The solvents were concentrated under reduced pressure to give the crude material as an orange oil. The crude product was purified by flash silica chromatography (ethyl acetate: petroleum ether 1:1) to give the title compound (**189**) as a white solid (16.4 mg, 57%),  $R_f$  0.4.  $[\alpha]_{\text{D}}^{29}$  -26.4 ( $c$  0.48,  $\text{CH}_2\text{Cl}_2$ ):  $\nu_{\text{max}}/\text{cm}^{-1}$  3432 (br, m, O-H), 1676 (s, C=O), 1604 (s, C=C);  $\delta_{\text{H}}$  (400 MHz;  $\text{CDCl}_3$ ) 2.76 (2H, dd,  $J$  16.4, 9.8, C(6) $\underline{\text{H}}_2$ ), 3.29 (1H, td,  $J$  9.8, 6.8, C(5) $\underline{\text{H}}$ ), 4.06 (2H, s, C(12) $\underline{\text{H}}_2$ ), 4.70-4.73 (2H, m, C(7) $\underline{\text{H}}_2$ ) 4.79 (1H, ddd,  $J$  6.8,

2.0, C(4)H), 7.08 (1H, d, *J* 2.0, C(3)H), 7.10-7.13 (1H, m, Ar-CH), 7.19-7.22 (2H, m, Ar-CH), 7.29-7.32 (4H, m, Ar-CH), 7.38 (2H, d, *J* 7.3, C(8)H and C(9)H), 7.63-7.68 (2H, m, Ar-CH), 7.74 (2H, dd, *J* 13.1, 8.8, C(10)H and C(13)H), 7.87-7.91 (1H, m, Ar-CH), 8.54-8.58 (1H, m, Ar-CH);  $\delta_C$  (100 MHz; CDCl<sub>3</sub>) 30.6 (C(12)H<sub>2</sub>), 43.3 (C(6)H<sub>2</sub>), 49.8 (C(5)H), 70.3 (C(4)H), 72.0 (C(7)H<sub>2</sub>), 116.2 (d, *J* 20.6, CH), 116.3 (CH), 116.8 (q), 119.0 (CH), 122.5 (CH), 123.1 (q), 123.4 (q), 124.3 (CH), 125.8 (q), 126.5 (CH), 127.2 (CH), 127.8 (CH), 128.6 (CH), 128.7 (CH), 129.3 (d, *J* 8.1, CH), 134.2 (q), 134.8 (d, *J* 4.4, q), 139.1 (q), 149.9 (CH), 152.3 (d, *J* 2.9, q), 161.1 (d, *J* 247.7, C(4') F), 196.0 (2x C=O);  $\delta_F$  (376 MHz; CDCl<sub>3</sub>) -113.9 (s); *m/z* (+ES) 521.18 ([M+H]<sup>+</sup>, 100%); (Found 521.1771; C<sub>30</sub>H<sub>27</sub>O<sub>6</sub>F ([M+H]<sup>+</sup>) requires 521.1776).

### 5.3.73 Synthesis of (*E*)-3-((2-(((1*S*,6*R*)-4'-fluoro-3-oxo-6-(triethylsilyloxy)-1,2,3,6-tetrahydro-[1,1'-biphenyl]-4-yl)methoxy)naphthalene-1-yl)methylene)chromane-2,4-dione, **224**

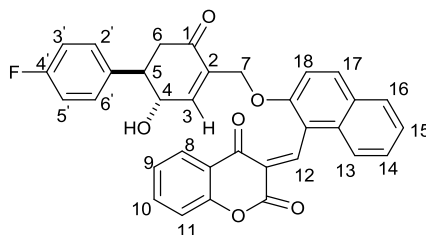


C<sub>39</sub>H<sub>37</sub>O<sub>6</sub>SiF; Molecular weight: 648.79

To a solution of alcohol (**169**) (40 mg, 0.15 mmol) in dry dichloromethane (3 mL), was added triphenylphosphine (50 mg, 0.19 mmol) and (*E*)-3-((2-hydroxynaphthalen-1-yl)methylene)chromane-2,4-dione (**175a**) (60 mg, 0.19 mmol). DIAD (40  $\mu$ L, 0.21 mmol) was added dropwise and the reaction mixture was stirred at room temperature for 24 hours. The solvents were concentrated *in vacuo* to give the crude product as a thick yellow oil. This crude product was purified by flash silica chromatography (ethyl acetate: petroleum ether 1:3) to give the title compound (**224**) as a thick yellow oil (43 mg, 58%), *R<sub>f</sub>* 0.4:  $\nu_{\max}/\text{cm}^{-1}$  2957 (m, Ar-C-H), 2875 (m, aliph-C-H), 1736 (s, C=O), 1681 (s, C=O);  $\delta_H$  (400 MHz; CDCl<sub>3</sub>) 0.07-0.26 (6H, m, Si(CH<sub>2</sub>CH<sub>3</sub>)<sub>3</sub>), 0.67 (9H, t, *J* 7.8, Si(CH<sub>2</sub>CH<sub>3</sub>)<sub>3</sub>), 1.99 (1H, dd, *J* 16.3, 13.6, C(6)H<sub>ax</sub>), 2.22 (1H, dd, *J* 16.3, 3.8, C(6)H<sub>eq</sub>), 2.77 (1H, ddd, *J* 13.6, 9.3, 3.8, C(5)H), 3.93 (1H, dd, *J* 9.3, 1.5, C(4)H), 4.55 (1H, ddd, *J* 11.9, 2.0, 1.5 C(7)H<sub>a</sub>H<sub>b</sub>), 4.75 (1H, ddd, *J* 11.9, 2.0, 1.5 C(7)H<sub>a</sub>H<sub>b</sub>), 6.66 (1H, d, *J* 1.5, C(3)H), 6.69-6.72 (2H, m, Ar-CH), 6.90-6.94 (2H, m, Ar-CH), 6.99 (1H, d, *J* 8.8, C(17)H or C(18)H), 7.15 (1H,

ddd,  $J$  8.1, 7.1, 1.0, C(14)H or C(15)H), 7.49 (1H, d,  $J$  8.8, C(17)H or C(18)H), 7.52-7.57 (1H, m, Ar-CH), 7.66 (1H, ddd,  $J$  8.1, 7.1, 1.0, C(14)H or C(15)H), 7.78 (2H, ddd,  $J$  8.6, 7.6, 1.5, C(9)H and C(10)H), 7.98 (1H, d,  $J$  8.1, C(13)H or C(16)H), 8.08 (1H, d,  $J$  8.6, C(8)H or C(11)H), 8.38 (1H, d,  $J$  8.6, C(8)H or C(11)H), 8.92 (1H, s, C(12)H);  $\delta_C$  (100 MHz; CDCl<sub>3</sub>) 4.3 (Si(CH<sub>2</sub>CH<sub>3</sub>)<sub>3</sub>), 6.6 (Si(CH<sub>2</sub>CH<sub>3</sub>)<sub>3</sub>), 42.3 (C(6)H<sub>2</sub>), 49.5 (C(5)H), 65.4 (C(4)H), 72.5 (C(7)H<sub>2</sub>), 112.5 (CH), 113.0 (q), 115.0 (CH), 115.2 (CH), 116.9 (CH), 121.6 (CH), 121.9 (CH), 126.6 (CH), 128.3 (q), 128.4 (q), 129.2 (d,  $J$  2.2, CH), 129.3 (d,  $J$  8.1, CH), 129.7 (q), 130.3 (q), 130.6 (CH), 133.2 (q), 134.2 (CH), 134.7 (CH), 139.2 (CH), 151.2 (CH), 155.0 (q), 157.8 (q), 159.5 (d,  $J$  247.8, C(4')F), 191.1 (C=O), 196.0 (2x C=O);  $\delta_F$  (376 MHz; CDCl<sub>3</sub>) -115.3 (s);  $m/z$  (+ES) 649.5968 ([M+H]<sup>+</sup>, 100%); (Found 649.2446; C<sub>39</sub>H<sub>38</sub>O<sub>6</sub>FSi ([M+H]<sup>+</sup>) requires 649.2422).

### 5.3.74 Synthesis of (*E*)-3-((2-(((1*S*,6*R*)-4'-fluoro-6-hydroxy-3-oxo-1,2,3,6-tetrahydro-[1,1'-biphenyl]-4-yl)methoxy)naphthalene-1-yl)methylene-2,4-dione, **186**

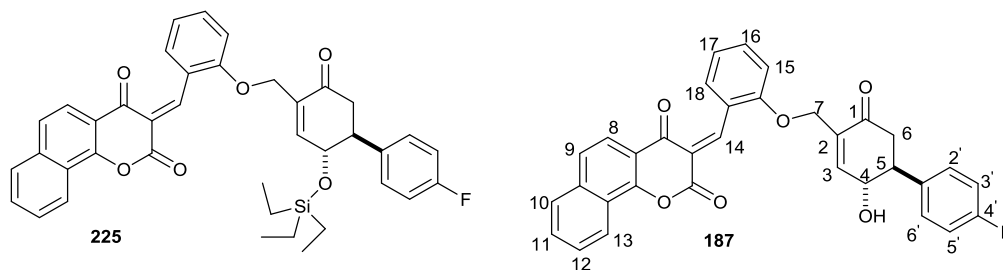


C<sub>33</sub>H<sub>23</sub>O<sub>6</sub>F; Molecular weight: 534.53

A solution of compound (**224**) (35 mg, 0.06 mmol) in trifluoroacetic acid: water (7:1, 1.5 mL) was stirred for 30 minutes at room temperature. The solvents were concentrated under reduced pressure to give the crude product as a thick yellow oil. The crude product was purified by flash silica chromatography (ethyl acetate: petroleum ether 1:2) to give the title compound (**186**) as a yellow powder (20 mg, 68%),  $R_f$  0.5:  $[\alpha]_D^{29}$  -65.4 ( $c$  0.5 in CH<sub>2</sub>Cl<sub>2</sub>):  $\nu_{max}/cm^{-1}$  1726 (s, C=O), 1676 (s, m, 1560 (s, Ar-C=O);  $\delta_H$  (400 MHz; CDCl<sub>3</sub>) 2.18 (1H, dd,  $J$  16.4, 14.1, C(6)H<sub>ax</sub>), 2.38 (1H, dd,  $J$  16.4, 4.1, C(6)H<sub>eq</sub>), 2.78 (1H, ddd,  $J$  14.1, 10.1, 4.1, C(5)H), 3.92 (1H, br, d,  $J$  10.1, C(4)H), 4.65 (1H, ddd,  $J$  12.6, 2.8, 1.5, C(7)H<sub>a</sub>H<sub>b</sub>), 4.75 (1H, ddd,  $J$  12.6, 2.8, 1.5, C(7)H<sub>a</sub>H<sub>b</sub>), 6.72 (1H, d,  $J$  1.5, C(3)H), 6.81-6.84 (2H, m, Ar-CH), 6.96-7.03 (3H, m, Ar-CH), 7.16 (1H, ddd,  $J$  8.6, 7.6, 0.8, C(18)H or C(19)H), 7.52-7.59 (2H, m, Ar-CH), 7.65 (1H, ddd,  $J$  8.6, 7.6, 0.8, C(18)H or C(19)H), 7.78 (2H, ddd,  $J$  8.3, 7.6,

1.8, C(13)H and C(14)H), 7.95 (1H, d, *J* 7.8, C(17)H or C(20)H), 8.09 (1H, d, *J* 8.3, C(12)H or C(15)H), 8.40 (1H, d, *J* 8.3, C(12)H or C(15)H), 9.02 (1H, s, C(16)H);  $\delta_c$  (125 MHz; CDCl<sub>3</sub>) 43.0 (C(6)H<sub>2</sub>), 49.3 (C(5)H), 64.7 (C(4)H), 71.4 (C(7)H<sub>2</sub>), 112.3 (CH), 113.2 (q), 115.8 (d, *J* 21.8, CH), 115.9 (CH), 116.8 (CH), 121.7 (CH), 121.9 (CH), 126.6 (CH), 128.1 (q), 128.4 (q), 128.9 (d, *J* 8.2, CH), 129.2 (d, *J* 6.4, CH), 129.8 (q), 130.2 (q), 130.7 (CH), 133.9 (q), 134.3 (CH), 134.8 (d, *J* 3.6, q), 134.9 (CH), 139.9 (CH), 149.0 (CH), 155.1 (q), 157.5 (q), 158.7 (q), 162.1 (d, *J* 248.9, C(4')F), 191.2 (C=O), 195.8 (2x C=O);  $\delta_F$  (471 MHz; CDCl<sub>3</sub>) -114.4 (s); *m/z* (+ES) 535.2 ([M+H]<sup>+</sup>, 100%); (Found 557.1391; C<sub>33</sub>H<sub>23</sub>O<sub>6</sub>FNa ([M+Na]<sup>+</sup>) requires 557.1376).

### 5.3.75 Synthesis of 3-((*E*)-2-(2-((1*S*,6*R*)-4'-fluoro-3-oxo-6-((triethylsilyl)oxy)-1,2,3,6-tetrahydro-[1,1'-biphenyl]-4-yl)ethyl)benzylidene)-2H-benzo[*h*]chromene-2,4(3*H*)-dione, **187**



C<sub>33</sub>H<sub>23</sub>O<sub>6</sub>F; Molecular weight: 534.53

To a solution of alcohol (**169**) (43.5 mg, 0.13 mmol) in dry dichloromethane (3 mL), was added triphenylphosphine (53 mg, 0.20 mmol) and (*E*)-3-((2-hydroxynaphthalen-1-yl)methylene)chromane-2,4-dione (**177b**), (60 mg, 0.19 mmol). DIAD (40  $\mu$ L, 0.20 mmol) was added dropwise, and the reaction mixture was stirred at room temperature for 24 hours. The solvents were concentrated *in vacuo* to give the crude product (**225**) as a thick yellow oil (56 mg).

A solution of the crude product (**225**) (56 mg, 0.09 mmol) in trifluoroacetic acid: water (7:1, 1.5 mL) was stirred for 30 minutes at room temperature, after which the solvents were concentrated under reduced pressure to give the crude product as a thick yellow oil. The crude product was purified by flash silica chromatography (ethyl acetate: petroleum ether 1:2) to give the title compound (**187**) as a yellow powder (26 mg, 39%, over 2 steps), *R<sub>f</sub>* 0.4; [ $\alpha$ ]<sub>D</sub><sup>29</sup> -38.8 (*c* 0.41, CH<sub>2</sub>Cl<sub>2</sub>);  $\nu_{\max}$ /cm<sup>-1</sup>

3454 (m, br, C-H), 1708 (s, C=O), 1671 (s, C=O), 1601 (s, C=C);  $\delta_{\text{H}}$  (400 MHz;  $\text{CDCl}_3$ ) 2.28 (1H, dd,  $J$  16.5, 14.2, C(6) $\underline{\text{H}}_{\text{ax}}$ ), 2.48 (1H, dd,  $J$  16.5, 3.8, C(6) $\underline{\text{H}}_{\text{eq}}$ ), 2.83 (1H, ddd,  $J$  14.2, 9.9, 3.8, C(5) $\underline{\text{H}}$ ), 4.16 (1H, dd,  $J$  9.9, 1.6, C(4) $\underline{\text{H}}$ ), 4.56-4.62 (2H, m, C(7) $\underline{\text{H}}_2$ ), 7.00 (1H, d,  $J$  1.6, C(3) $\underline{\text{H}}$ ), 7.05-7.10 (2H, m, Ar- $\underline{\text{CH}}$ ), 7.11-7.15 (2H, m, Ar- $\underline{\text{CH}}$ ), 7.37-7.41 (1H, m, Ar- $\underline{\text{CH}}$ ), 7.45 (1H, d,  $J$  8.3, C(15) $\underline{\text{H}}$  or C(18) $\underline{\text{H}}$ ), 7.56-7.59 (1H, m, Ar- $\underline{\text{CH}}$ ), 7.62-7.69 (3H, m, Ar- $\underline{\text{CH}}$ ), 7.77 (1H, d,  $J$  8.3, C(15) $\underline{\text{H}}$  or C(18) $\underline{\text{H}}$ ), 7.83 (1H, d,  $J$  8.5, C(8) $\underline{\text{H}}$  or C(9) $\underline{\text{H}}$ ), 7.92 (1H, d,  $J$  8.5, C(8) $\underline{\text{H}}$  or C(9) $\underline{\text{H}}$ ), 8.10 (1H, s, C(14) $\underline{\text{H}}$ ), 8.18 (1H, d,  $J$  8.2, C(10) $\underline{\text{H}}$  or C(13) $\underline{\text{H}}$ );  $\delta_{\text{C}}$  (125 MHz;  $\text{CDCl}_3$ ) 41.1 ( $\underline{\text{C}}$ (6) $\underline{\text{H}}_2$ ), 47.2 ( $\underline{\text{C}}$ (5) $\underline{\text{H}}$ ), 69.7 ( $\underline{\text{C}}$ (4) $\underline{\text{H}}$ ), 70.3 ( $\underline{\text{C}}$ (7) $\underline{\text{H}}_2$ ), 114.0 ( $\underline{\text{C}}\underline{\text{H}}$ ), 114.1 ( $\underline{\text{C}}\underline{\text{H}}$ ), 115.2 ( $\underline{\text{C}}\underline{\text{H}}$ ), 116.8 (q), 121.3 ( $\underline{\text{C}}\underline{\text{H}}$ ), 122.9 ( $\underline{\text{C}}\underline{\text{H}}$ ), 123.5 (d,  $J$  17.3, ( $\underline{\text{C}}\underline{\text{H}}$ )), 125.1 ( $\underline{\text{C}}\underline{\text{H}}$ ), 125.4 (q), 125.7 (q), 126.4 ( $\underline{\text{C}}\underline{\text{H}}$ ), 127.0 ( $\underline{\text{C}}\underline{\text{H}}$ ), 127.2 (d,  $J$  8.2,  $\underline{\text{C}}\underline{\text{H}}$ ), 127.4 (q), 127.6 ( $\underline{\text{C}}\underline{\text{H}}$ ), 131.4 (q), 132.1 (q), 133.2 (d,  $J$  2.7, q), 135.4 ( $\underline{\text{C}}\underline{\text{H}}$ ), 141.4 ( $\underline{\text{C}}\underline{\text{H}}$ ), 147.0 ( $\underline{\text{C}}\underline{\text{H}}$ ), 152.8 (q), 153.9 (q), 156.5 (q), 160.2 (d,  $J$  248.9,  $\underline{\text{C}}$ (4')F), 189.1 (C=O), 193.9 (2x C=O);  $\delta_{\text{F}}$  (471 MHz;  $\text{CDCl}_3$ ) -116.3 (s);  $m/z$  (+ES) 535.2 ( $[\text{M}+\text{H}]^+$ , 100%); (Found 557.1399;  $\text{C}_{33}\text{H}_{23}\text{O}_6\text{FNa}$  ( $[\text{M}+\text{Na}]^+$ ) requires 557.1376).

## **6.0 Experimental procedures for the enzyme and biological assays**

### **6.1 Application of menadione and cytochrome c in enzyme assay evaluation**

The procedure for this analysis was adapted from the sequence originally outlined by Ernester and his co-workers in 1962,<sup>56</sup> which involved the reduction of cytochrome c by NQO1 in the presence of menadione using NADH as electron donor. Cytochrome c which acted as a terminal electron acceptor was insufficient in this role and as a result menadione was included as an intermediate electron acceptor between reduced NQO1 and cytochrome c. Both the menadione and cytochrome c therefore acted as a substrate for the measurement of the NQO1 activity.

### **6.2 Preparation of chemicals and reagents for enzyme assay**

50 mM phosphate buffer (pH 6.8) was prepared using 50 mM potassium dihydrogen orthophosphate ( $\text{KH}_2\text{PO}_4$ ; VWR, UK) and 50 mM potassium hydrogen orthophosphate 3-hydrate ( $\text{K}_2\text{HPO}_4$ ; VWR, UK). The NQO1 enzyme was prepared in phosphate buffer with 250 mM sucrose and 5  $\mu\text{M}$  FAD to give a final enzyme concentration of 5 mg/mL. The enzyme was then aliquoted and stored at  $-80^\circ\text{C}$  for future use.

Serial dilution of the stock solutions of the synthetic dicoumarol analogues (10 mM concentration) were prepared in six cuvettes using DMSO to give concentrations ranging from 100 nM to 1 mM (0.1  $\mu\text{M}$  – 1000  $\mu\text{M}$ ). NQO1 enzyme was diluted in 50 mM phosphate buffer to give an enzyme activity within the 0.085 to 0.14 nM range.

### **6.3 Evaluation of NQO1 inhibition**

10  $\mu\text{L}$  of the dicoumarol analogue solution was added into six cuvettes containing phosphate buffer, cytochrome c, NADH and menadione as summarized in Table 11. The control cuvette contained 10  $\mu\text{L}$  of DMSO. The reaction was initiated by the addition of 10  $\mu\text{L}$  of NQO1 enzyme previously prepared and the six cuvettes were then inserted into the spectrophotometer. The reaction was monitored for colour change (deep-red to light orange-red) after a minute at 550 nm using a Beckman DU 650 spectrophotometer at room temperature. The rate of colour change correlates to the rate of NQO1 activity.

Component	MW (g/mol)	Stock	Weight Out	Diluent	Vol in cuvette ( $\mu$ l)
Buffer (PO <sub>4</sub> )pH 6.8	-	50 mM	-	dH <sub>2</sub> O	445
Cytochrome c	12,384 Da	140 $\mu$ M	1.734 mg/mL	Buffer	500
NADH	709.5	20 mM	14.18 mg/mL	Buffer	25
Menadione	172.18	10 mM	1.72 mg/mL	DMSO	10
NQO1	-	5 mg/mL	1:2500 dilution	Buffer	10
Inhibition	-	10 mM		DMSO	10

d = distill water

**Table 11:** Sequence for the enzyme assay analysis.

The IC<sub>50</sub> values were measured using nonlinear curve fitting as implemented in the program Excel (GraphPad Prism 5). Each measurement was made in triplicate and the experiments were repeated three times.

#### 6.4 MTT cell viability assay procedure

The MTT assay was carried out by another member of the Whitehead group. The experimental sequence for this evaluation is outlined below:

#### 6.5 Counting and seeding cells in haemocytometer

The A549 cell line was obtained from the American Type Culture Collection (ATCC) and grown in RPMI 1640 medium with 10% fetal bovin serum. Cells were seeded in 96-well flatbottom microtiter plates and then allowed to attach overnight (24 hours) at 37 °C with a 5% CO<sub>2</sub> in air humidified environment before the drug treatment. The concentration of cells in suspension was determined using a haemocytometer (Neubauer, Germany) (Figure 103) in order to determine the seeding density. A glass cover slip was positioned over the central area of the haemocytometer marked 'X' and 10  $\mu$ L of the cell suspension was then transferred at the edge of the chamber. Cell suspension was drawn under the cover-slip onto the grid *via* the capillary action while the cells in the four corner squares (A, B, C, D) were counted by placing the grid under a light microscope.



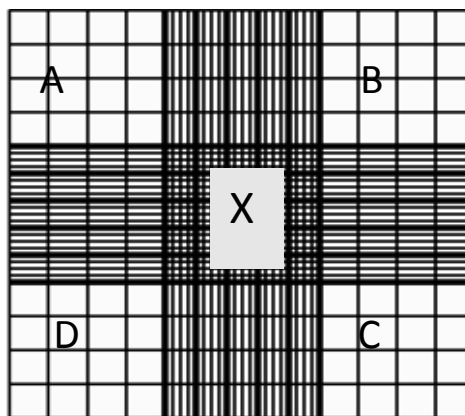


**Figure 103:** The haemocytometer grid

The cell concentration per mL was calculated using the following equation:

$$\text{Cells/ mL} = \text{Mean cell number of corner squares} \times 10^4$$

## 6.6 Treating the cells

The novel prodrugs to be analyzed were dissolved in DMSO (MTT solvent) to give a stock concentrations ranging from 25 mM to 250 nM. The serial dilutions were prepared in the growth medium from 100  $\mu\text{M}$  to 1 nM. 20  $\mu\text{L}$  of each dilution and DMSO as the solvent control were added to 180  $\mu\text{L}$  of cells in each sextuplicate across the microtiter plate in order to dilute the drug to final concentrations of 10  $\mu\text{M}$  to 0.1 nM.

## 6.7 Ending the viability assay

Cells were then treated with various concentrations of the drug and then kept in the incubator for 96 hours and the experiment was stopped by addition of (2.5 g/L) MTT solution to each well. The microtitre plates were left for another 4 hours until purple formazan precipitate is observed, which were then solubilized in 200  $\mu\text{L}$  of DMSO. The absorbances were determined at a wavelength of 540 nm using a multi-well scanning spectrophotometer. The optical density readings obtained depends on the number of viable cells.<sup>270</sup>

## References

1. M. Tavassoli, *Am. J. Pathol.*, 1980, **98**, 44.
2. Cell movement and the shaping of the vertebrate body in chapter 21 of molecular biology of the cell, fourth edition, edited by Bruce Albert (2002) published by Garland Science.
3. J. Bartkova, N. Rezaei and M. Lontos, *Nature*, 2006, **444**, 633-637.
4. J. Luo, N. L. Solimini and S. J. Elledge, *Cell*, 2009, **136**, 823-837.
5. Y. J. Surh, *Nature Rev. Cancer*, 2003, **3**, 768-780.
6. A. Teti, *J. Am. Soc. Nephrol.*, 1992, **2**, S83-S87.
7. R. Jinka, R. Kapoor, P. G. Sistla, T. A. Raj and G. Pande, *Inter. J. Cell Biol*, 2011, **2012**, 1-8.
8. D. Hanahan and R. A. Weinberg, *Cell*, 2011, **144**, 646-674.
9. D. Hanahan and R. A. Weinberg, *Cell*, 2000, **100**, 57-70.
10. M. B. Sporn, *Lancet*, 1996, **347**, 1377-1381.
11. J. Sariego, *The American Surgeon*, 2010, **76**, 1397-1401.
12. S. Neidle and G. N. Parkinson, *Curr. Opin. Biol.*, 2003, **13**, 275-283.
13. E. Bernstein, C. D. Allis and A. D. Goldberg, *Cell*, 2007, **128**, 635-638.
14. A. Bird, *Nature*, 2007, **447**, 396-398.
15. B. E. Benstein, A. Meissner and E. S. Lander, *Cell*, 2007, **128**, 669-681.
16. H. Oppermann, A. D. Levinson, H. E. Varmus, L. Levintow and J. M. Bishop, *Proc. Natl. Acad. Sci.*, 1979, **76**, 1804-1808.
17. S. E. Kern, K. W. Kinzler, A. Bruskin, D. Janosz, P. Friedman, C. Priwes and B. Vogelstein, *Science*, 1991, 252, 1708-1711.
18. Green and Douglas, "Means to an end", New York: Cold Spring Harbor Laboratory Press. ISBN: 2011, 978-8796-888-1.
19. A. Takaoka, S. Hayakawa, H. Yanai, D. Stoiber, H. Negishi, H. Kikuchi, S. Sasaki, K. Imai, T. Shibue, K. Honda and T. Taniguchi, *Nature*, 2003, **424**, 516-523.
20. John G. Barnes, "Synthesis of agents potentially useful in cancer chemotherapy", A thesis submitted to the University of Manchester for the degree of PhD in the Faculty of Medical and Human Sciences, 2011.
21. W. E. Mercer, M. T. Shields, M. Amin, G. J. Sauve, E. Apella, J. W. Romano and S. J. Ullrich, *Proc. Natl. Acad. Sci.* 1990, **87**, 6166-6170.
22. D. Michalovitz, O. Halevy and M. Oren, *Cell*, 1990, **62**, 671-680.
23. A. P. Read and T. Strachan, Chapter 18, Cancer genetic. Humam Molecular Genetics 2. New York. Wiley, ISBN. 1999, 0-471-33061-2.
24. Moshe Oren, *J. of FASEB*, 1992, **6**, 3169-3176.
25. P. D. Ray, B. W. Huang and Y. Tsuji, *Cell Signal*, 2012, **24**, 981-990.
26. T. Finkel, *J. Cell Biol.*, 2011, **194**, 7-15.
27. E. Racker, *Mol. Cell, Biochem.*, 1974, **5**, 17-23.
28. O. Warburg, K. Posener and E. Negelein, *Biochem. Zeitschr.*, 1924, 309-344.
29. G. L. Semenza, *Curr. Opin. Genet. Dev.*, 2010, **20**, 51-56.
30. Robert J. Gillies, Ian Robey and Robert A. Gatenby, *J. Nuclear Medicine*, 2008, **49**, 24S-42S.

31. Robert A. Gatenby and Robert J. Gillies, *Nat. Rev. Cancer*, 2004, **4**, 891-899.
32. S. Walenta, M. Wetterling, M. Lehrke, G. Schwickert, K. Sundfor, E. K. Rofstad and W. Mueller-Klieser, *Cancer Res.*, 2000, **60**, 916-921.
33. O. Warburg, *Klinische Wochenschrift*, 1925, 534-536.
34. P.P. Hsu and D. M. Sabatini, *Cell*, 2008, **134**, 703-707.
35. M. G. Vander Heiden, L. C. Cantley and C. B. Thompson, *Science*, 2009, **324**, 1029-1033.
36. G. L. Semenza, *Novartis Found. Symp.*, 2001, **240**, 251-260.
37. Jie Zheng, *Oncol. Letters*, 2012, **4**, 1151-1157.
38. R. A. Gaten and R. Gillies, *Nat. Rev. Cancer*, 2004, **4**, 891-899.
39. S. Walenta, M. Wetterling, M. Lehrke, G. Schwickert, K. Sundfor, E. K. Rofstad and W. Mueller-Klieser, *Cancer Res.*, 2000, **60**, 916-921.
40. W. H. Koppenol, P. L. Bounds and C. V. Dang, *Nat. Rev. Cancer*, 2011, **11**, 325-337.
41. G. E. Demetrakopoulos, B. Linn and H. Amos, *Biochem. Biophys. Res. Commun.*, 1978, **82**, 787-794.
42. A. Priebe, L. Tan, H. Wahl, A. Kueck, G. He, R. Kwok, A. Opiari and J. R. Liu, *Gynecol. Oncol.*, 2011, **122**, 389-95.
43. H. Shim, Y. S. Chun, B. C. Lewis and C. V. Dang, *Proc. Natl. Acad. Sci.*, 1998, **95**, 1511-1516.
44. L. Ernester and F. Navazio, *Acta. Chem. Scand.*, 1958, **12**, 595-602.
45. Merck Manual of Diagnosis and Therapy. Breast disorder: Breast Cancer. 2003. Retrieved 2008-02-05.
46. Breast Cancer Risk Factors, 2008. Retrieved, 2009-11-10.
47. V. Beral, D. Bull, R. Doll, R. Peto, G. Reeves, D. Skegg, G. Colditz, B. Hulka, C. Lavecchia, C. Magnusson, T. Miller, B. Peterson, M. Pike, D. Thomas and F. Van Leeuwen *Lancet*, 2002, **360**, 187-95.
48. F. Xue, W. C. Willett, B. A. Rosner, S. E. Hankinson and K. B. Michael, *Arch. Intern. Med.*, 2011, **171**, 125-133.
49. Male breast cancer treatment; National Cancer Institute, 2011, Retrieved 2011-02-26.
50. C. A. Thompson, G. L. Blackburn, R. T. Chlebowski, D. W. Nixon, A. Shapiro, M. K. Hoy, M. T. Goodman, A. E. Giulian, N. Karanja, P. McAndrew, C. Hudis, J. Butler, D. Merkel, A. Kristal, B. Caan, R. Michaelson, V. Vinciguerra, S. Del Prete, M. Winkler, R. Hall, M. Simon, B. L. Winters and R. M. Elashoff, *J. Natl. Cancer Inst.*, 2006, **98**, 1767-1776.
51. Update; When should women start regular mammograms? 40? 50? and how often is regular: National Research Centre for Women and Families. 2009.
52. M. B. Sporn and N. Suh, *Nature Rev. Cancer*, 2002, **2**, 537-543.
53. M. B. Sporn, *Cancer Res.*, 1991, **51**, 6215-6218.
54. J. Gronwald, N. Tung, W. D. Foulkes, K. Offit, R. Gershoni, M. Daly, C. S. Kim, H. Olsson, P. Ainsworth, A. Eisen, H. Saal, E. Fridman, O. Olopade, M. Osborne, J. Weitzel, H. Lynch, P. Ghadirian, J. Lubinski, P. Sun and S. A. Narod, *Int. J. Cancer*, 2006, **118**, 2281-2284.

55. Basics of Oncology, Springer, London, 2009.
56. L. Ernester, L. Danielson and M. Ljunggren, *Biochem. Biophys. Acta.*, 1962, **58**, 171-188.
57. L. Ernester, R. W. Estabrook, P. Hochstein and S. Orrenius, *Chem. Scr.*, 1987, **27A**, 1-207.
58. A. Begleiter and J. Fourie, *Method. Enzymol.*, 2004, **382**, 320-351.
59. C. Edlund, A. Elhammer and G. Dallner, *Bioscience Reports*, 1982, **2**, 861-865.
60. L. Ernester; in Pathophysiology of Lipid Peroxides and Related Free Radicals, ed. Yagi, K. (Karger, Basel), 1998, 149-158.
61. D. Ross; in Comprehensive Toxicology, ed. Guengerich, F. P. (Pergamon, New York), 1997, **3**, 179-197.
62. H. W. Moore and R. Czerniak, *Medicinal Research Reviews*, 1981, **1**, 249-280.
63. D. Ross, J. K. Kepa, S. L. Winski, H. D. Beall, A. Anwar and D. Siegel, *Chem. Biol. Interact.*, 2000, **129**, 77-79.
64. T. Iyanagi and I. Yamazaki, *Biochim. Biophys. Acta.*, 1970, **216**, 282-294.
65. P. Sanchez-Cruz and A. E. Alegria, *Chem. Res. Toxicol.*, 2009, **22**, 818-823.
66. N. P. E. Vermeulen, F. L. Boca Raton, CRC Press, Inc., 1996, 29-53.
67. C. Lind, P. Hochstein and L. Ernester: DT-diaphorase: properties, reaction mechanism, metabolic function. A progress report, In: T. E. King; H. S. Mason, M. Morrison, eds. Oxidases and related redox systems. Oxford Pergamon Press, 1982, 321-347.
68. R. Li, M. A. Bianchet, P. Talalay, L. M. Amzel, *Proc. Natl. Acad. Sci., USA*, 1995, **92**, 8846-50.
69. S. Deller, P. Macheroux and S. Sollner, *Cell. Mol. Life Sci.*, 2008, **65**, 141-160.
70. C. J. Moody, M. A. Colucci and G. D. Couch, *Org. Biomol. Chem.*, 2008, **6**, 637-656.
71. J. Segura-Aguilar, C. Lind, *Chem. Biol. Interact.*, 1989, **72**, 309-324.
72. L. Ernester, DT-diaphorase, *Methods Enzymol.*, 1967, **10**, 309-317.
73. C. Lind, E. Cadenas, P. Hochstein, L. Ernester, *Methods Enzymol.*; 1990, **186**, 287-301.
74. D. Ross; Quinone reductases in: F.P. Guengerich (Ed.), Comprehensive Toxicology, Vol.3. *Biotransformation*, Pergamon, New York; 1997, 179-198.
75. A. Morokutii, A. Lyskowski, S. Sollner, E. Pointner, T. B. Fitzpatrick, C. Kratky, K. Gruber and P. Macheroux, *J. Biochem.*, 2005, **44**, 13724-13733.
76. G. D. Buffinton, K. Ollinger, A. Brunmark and E. Cadenas, *Biochem. J.*, 1989, **257**, 561-571.
77. D. Ross and D. Siegel, *Methods Enzymol.*, 2004, **382**, 115-144.
78. G. Asher, J. Lotem, R. Kama, L. Sachs and Y. Shaul, *Proc. Natl. Acad. Sci.*, 2002, **99**, 3099-3104.
79. R. E. Beyer, J. Segura-Aguilar, S. Di Bernardo, M. Cavazzoni, R. Fato, D. Fiorentini, M. C. Galli, M. Stti, L. Landi, G. Lenaz, *Pro. Natl. Acad. Sci.*, 1996, **93**, 2528-32.

80. L. Landi, M. C. Galli, D. Fiorentini, J. Segura-Aguilar, R. E. Beyer, *Free Radic. Biol. Med.*, 1997, **22**, 329-35.
81. D. Siegel, D. L. Gustafson, D. L. Dehn, J. Y. Han, P. Boonchong, L. J. Berliner and D. Ross, *Mol. Pharmacol.*, 2004, **65**, 1238-1247.
82. A. T. Dinkova-Kostova and P. Talalay, *Arch. Biochem. Biophys.*, 2010, **501**, 116-123.
83. D. Ross, J. K. Kepa, S. L. Winski, H. D. Beall, A. Anwar and D. Siegel, *Proc. Chemico-Biological Interactions*, 2000, **129**, 77-97.
84. A. M. Benson, M. J. Hunkeler and P. Talalay, *Proc. Natl. Acad. Sci.*, 1980, **77**, 5216-5220.
85. P. Joseph, T. Xie, Y. Xu and A. K. Jaiswal, *Oncol. Res.*, 1994, **6**, 525-532.
86. P. Talalay, J. W. Fahey, W. D. Holtzclaw, T. Prestera and Y. Zhang, *Toxicol. Lett.*, 1995, **82-83**, 173-179.
87. Y. Zhang, P. Talalay, C. G. Cho and G. H. Posner, *Proc. Natl. Acad. Sci., USA*, 1992, **89**, 2399-2403.
88. R. Li, M. A. Bianchet, P. Talalay and L. M. Amzel, *Proc. Natl. Acad. Sci.*, 1995, **92**, 8846-8850.
89. G. Asher, O. Dym, P. Tsvetkov, J. Adler and Y. Shaul, *Biochemistry*, 2006, **45(20)**, 6372-6378.
90. S. Chen, P. S. Deing, J. M. Bailey and K. M. Swiderek, *Protein Sci.*, 1994, **3**, 51-57.
91. M. Faig, M. A. Bianchet, P. Talalay, S. Chen, S. Winski, D. Ross and L. M. Amzel, *Proc. Natl. Acad. Sci.*, 2000, **97**, 3177-3182.
92. M. F. Mendoza, N. M. Hollabaugh, S. U. Hettiarachchi and R. L. Mccarley, *Biochemistry*, 2012, **51(40)**, 8014-8026.
93. I. E. Parkinson, J. S. Bair, M. Cismesia and P. J. Hergenrother, *ACS Chem. Bio.*, 2013, **8**, 2173-2183.
94. K. A. Nolan, D. J. Timson, I. J. Stratford and R. A. Bryce, *Bioorg. Med. Chem. Lett.*, 2006, **16**, 6246-6254.
95. Z. Zhou, D. Fisher, J. Spidel, J. Greenfield, B. Patson, A. Fazal, C. Wigal, O. A. Moe and J. D. Madura, *Biochemistry*, 2003, **42**, 1985-1994.
96. B. L. Kuehl, J. W. Paterson, J. W. Peacock, M. C. Paterson, A. M. Rauth, *Br. J. Cancer*, 1995, **72**, 555-561.
97. J. L. Moran, D. Siegel and D. Ross, *Proc. Natl. Acad. Sci.*, 1999, **96**, 8150-8155.
98. M. J. Lafuente, X. Casterad, M. Trias, C. Ascaso, R. Molina, A. Ballesta, S. Zheng, J. K. Wiencke and A. Lafuente, *Carcinogenesis*, 2000, **21**, 1813-9.
99. R. A. Larson, Y. Wang, M. Banerjee, J. Wiemels, C. Hartford, M. M. Beau and M. T. Smith, *Blood* 1999, **94**, 803-807.
100. J. L. Wiemels, A. Pagnamenta, G. M. Taylor, O. B. Eden, F. E. Alexander and M. F. Greaves, *Cancer Res.*, 1999, **59**, 4095-9.
101. L. T. Hu, J. Stamberb and S. S. Pan, *Cancer Res.*, 1996, **56**, 5253-5259.
102. S. Liao and H. Williams-Ashmen, *Biochem. Biophys. Res. Commun.*, 1961, **4**, 208-213.

103. X. F. Liu, M. L. Liu, T. Iyanagi, K. Legesse, T. D. Lee and S. Chen, *Mol. Pharmacol.*, 1990, **37**, 911-915.
104. P. C. Presusch and D. M. Smalley, *Free Radic. Res. Commun.*, 1990, **8**, 401-415.
105. P. M. Hollander and L. Ernester, *Arch. Biochem. Biophys.*, 1975, **169**, 560-567.
106. S. Chen, K. Wu, D. Zhang, M. Sherman, R. Knox and C. S. Yang, *Mol. Pharmacol.*, 1999, **56**, 272-278.
107. S. Harada, H. Tachikawa and Y. Kawanishi, *Genet.*, 2003, **13**, 205-209.
108. A. K. Jaiswal, P. Burnett, M. Adenik and O. W. McBride, *Biochemistry*, 1990, **29**, 1899-1906.
109. A. K. Jaiwal, *Biol. Chem.*, 1994, **269**, 14502-14508.
110. Q. Zhao, X. L. Yang, W. D. Holtzclaw and P. Talalay, *Proc. Natl. Acad. Sci.*, 1997, **94**, 1669-1674.
111. D. J. Long and A. K. Jaiswal, *Chem. Boil. Interact.*, 2000, **129**, 99.
112. S. Harada, C. Fujii, A. Hayashi and N. Ohkoshi, *Biochem. Biophys. Res. Commun.*, 2001, 288, **887**-892.
113. Q. Zhao, X. L. Yang, W. D. Holtzclaw and P. Talalay, *Proc. Natl. Acad. Sci.*, 1997, **94**, 1669-1674.
114. J. J. Kwiek, T. A. Haystead and J. Rudolph, *Biochemistry*, 2004, **43**, 4538-4547.
115. R. J. Knox, T. C. Jenkins, S. M. Hobbs, S. Chiuan, R. G. Melton and J. Burke, *Cancer Res.*, 2000, **60**, 4179-4186.
116. F. Vella, G. Ferry, P. Delagrangue and J. A. Boutin, *Biochem. Pharmacol.*, 2005, **71**, 1-12.
117. L. Buryanovskyy, Y. Fu, M. Boyd, Y. Ma, T. C. Hsieh, J. M. Wu and Z. Zhang, *Biochemistry*, 2004, **43**, 11417-11426.
118. B. Leonid, Yue Fu, M. Boyd, Y. Ma, T. Hsieh, M. Joseph Wu and Z. Zhang, *Biochem.*, 2004, **43**, 11417-11426.
119. M. Abukhader, J. Heap, C. D. Matteis, B. Kellam, S. W. Doughty, N. Minton and M. Paoli, *J. Med. Chem.*, 2005, **48**, 7714-7719.
120. K. A. Nolan, M. C. Caraher and P. Mathew Humphries, Hoda Abdel-Aal Bettley, Richard A. Bryce and Ian J. Stratford, *Bioorg. Med. Lett.*, 2010, **20**, 7331-7336.
121. K. Wu, R. Knox, X. Z. Sun, P. Joseph, A. K. Jaiwal, D. Zhang, P. S. Deng and S. Chen, *Arch. Biochem. Biophys.*, 1991, **347**, 221-228.
122. S. Chen, K. Wu, D. Zhang, M. Sherman, R. Knox and C. S. Yang, *Mol. Pharmacol.*, 1999, **56**, 272-278.
123. L. Buryanovskyy, Y. Fu, M. Boyd, Y. Ma, T. C. Hsieh, J. M. Wu and Z. Zhang, *Biochem.*, 2004, **43**, 11417-11426.
124. P. R. Graves, J. J. Kwiek, P. Fadden, R. Ray, K. Hardenman, A. M. Coley, M. Foley and T. A. Haystead, *Mol. Pharmacol.*, 2002, **62**, 1364-1372.
125. P. L. Chesis, D. E. Levin, M. T. Smith, L. Ernester and B. N. Ames, *Proc. Natl. Acad. Sci.*, 1984, **81**, 1696-1700.

126. D. Schuetzle, W. O. Siegl, T. E. Jensen, M. A. Dearth, E. W. Kaiser, R. Gorse, W. Kreucher and E. Kulik, *Environ. Health Perspect.*, 1994, **102**, 3-12.
127. A. Brunmark and E. Cadenas, *Free Radic. Biol. Med.*, 1989, **7**, 435-477.
128. J. J. Schlager and G. Powis, *J. Cancer*, 1990, **45**, 403-409.
129. X. Zhang, L. X. Chen, L. Ouyang, Y. Cheng and B. Liu, *Cell Prolif.*, 2012, **45**, 466-476.
130. T. Takeuchi, H. Chimura, M. Hamada, H. Umezawa, O. Yoshioka, N. Oguchi, Y. Takahshi and A. J. Matsuda, *Antibio.*, 1975, **28**, 737-742.
131. A. Szent-Gyorgi, *Science*, 1968, **161**, 988-990.
132. F. A. French and B. L. Freedlander, *Cancer Res.*, 1958, **18**, 172-175.
133. T. Takeuchi, H. Chimura, M. Hamada, H. Umezawa, O. Yoshioka, N. Oguchi, Y. Takahshi and A. J. Matsuda, *J. Antibiol.*, 1975, **28**, 737-742.
134. K. T. Douglas, R. M. Phillips and T. K. M. Shing, *Anti-cancer Drug Des.*, 1992, **7**, 67.
135. C. L. Arthurs, G. A. Morris, M. Piacenti, R. G. Pritchard, I. J. Stretford, T. Tatic, R. C. Whitehead, K. F. Williams and N. S. Wind, *Tetrahedron*, 2010, **66**, 9049-9060.
136. K. T. Douglas and S. Shinkai, *Angew. Chem. Int. Ed. Engl.*, 1985, **24**, 31-44.
137. P. J. Thornalley, *Gen. Pharmac.*, 1996, **27**, 565-573.
138. L. G. Egyud and A. Szent-Gyorgyi, *Proc. Natl. Acad. Sci.*, 1966, **55**, 388-393.
139. J. P. Richard, *Biochem.*, 1991, **30**, 4581-4585.
140. H. Sakamoto, T. Mahima, A. Kizaki, S. Dan, Y. Hashimoto, M. Naito and T. Tsuruo, *Blood*, 2000, **95**, 3214-3218.
141. H. Sakamoto, T. Mahima, S. Sato, Y. Hashimoto, Y. Yamori and T. Tsuruo, *Clin. Cancer Res.*, 2001, **7**, 2513-2518.
142. E. Racker, *J. Biol. Chem.*, 1951, **190**, 685-696.
143. A. Prompella, A. Visvikis, A. Paolicchi, V. De-Tata and A. F. Casini, *Biochem. Pharmacol.*, 2003, **66**, 1499-1503.
144. A. Meister and M. Anderson, *Annul. Rev. Biochem.*, 1983, **52**, 711-760.
145. A. Pastore, P. Fiorella, L. Mattia, R. A. Lo, G. L. Maria, T. Giulia and F. Giorgio, *Clinical Chemistry*, 2003, **47**, 1467-1468.
146. W. Y. Yang, A. Begleiter, J. B. Johnson, L. G. Israels and M. R. Mowat, *Mol. Pharmacol.*, 1992, **41**, 625-630.
147. J. M. Estrela, A. Ortega and E. Obrador, *Crit. Rev. Cl. Lab. Sci.*, 2006, **43**, 143-181.
148. N. Traverso, R. Ricciarelli, M. Nitti, B. Marengo, A. L. Furfaro, M. A. Pronzato, U. M. Marinari and C. Domenicotti, *Oxid. Med. Cell. Longev.*, 2013, **2013**, 1-10.
149. C. F. M. Huntley, D. S. Hamilton, D. J. Creighton and B. Ganem, *Org. Lett.*, 2000, **2**, 3143-3144.
150. D. Kamiya, Y. Uchihata, E. Ichikawa, K. Kato and K. Umezawa, *Bioorg. Med. Chem. Lett.*, 2005, **15**, 1111-1114.
151. D. S. Hamilton, Z. Ding, B. Ganem and D. J. Creighton, *Org. Lett.*, 2002, **4**, 1209-1212.

152. E. Joseph, J. L. Eiseman, D. S. Hamilton, H. Wing, H. Tak, B. Ganem and D. J. Creighton, *J. Med. Chem.*, 2003, **46**, 194-196.
153. D. S. Hamilton, X. Zhang, Z. Ding, I. Hubatsch, B. Mannervik, K. N. Houk, B. Ganem and D. J. Creighton, *J. Am. Chem. Soc.*, 2003, **125**, 15049-15058.
154. Q. Zhang, Z. Ding, D. J. Creighton, B. Ganem and D. Fabris, *Org. Lett.*, 2002, **4**, 1459-1462.
155. F. Collu, L. Bonsignore, M. Casu, C. Floris, J. Gertsch and F. Cottiglia, *Bioorg. Med. Chem. Lett.*, 2008, **18**, 1559-1562.
156. Y. Shokoohinia, S. E. Sajjadi, A. R. Jassbi, H. Moradi, N. Ghassemi and B. Schneider, *Chemistry of Natural Compounds*, 2015, **51**, 491-494.
157. J. Jakupovic, M. Grenz, F. Bohlman and G. M. Mungai, *Phytochemistry*, 1990, **29**, 1213-1217.
158. A. A. Ahmed and A. A. Mohamoud, *Phytochemistry*, 1997, **45**, 533-535.
159. C. Zdero, F. Bohlmann and G. M. Mungai, *Phytochemistry*, 1991, **30**, 3297-3303.
160. F. Machumi, A. Yenesew, J. O. Midiwo, M. Heydenreich, E. Kleinpeter, B. L. Tekwani, S. I. Khan, L. A. Walker and I. Muhammad, *Nat. Pro. Commun.*, 2012, **7**, 1123-1126.
161. G. Schwartzman, B. Winograd and H. M. Pinedo, *Radiother. Oncol.*, 1988, **12**, 301-313.
162. K. A. Nolan, K. A. Scott, J. Barnes, J. Doncaster, R. C. Whitehead and I. J. Stratford, *Biochem. Pharmacol.*, 2010, **80**, 977-981.
163. P. Tsvetkov, G. Asher, V. Reiss, Y. Shaul, L. Sachs and J. Lotem, *Proc. Natl. Acad. Sci. USA*, 2005, **102**, 5535-5540.
164. V. J. Stella and K. W. Nti-Addae, *Adv. Drug Deliv. Rev.*, 2007, **59**, 677-694.
165. P. Ettmayer, G. L. Amidon, B. C.ement and B. Testa, *J. Med. Chem.*, 2004, **47**, 2393-2404.
166. A. Albert, *Nature*, 1958, **182**, 421-427.
167. T. A. Connors, *Gene. Ther.*, 1995, **2**, 702-709.
168. U. N. Harle and N. J. Gaikwad, *Nirali Prakashan Pune*, 2008, **15**, 1-19.
169. A. S. Kalgutkar, A. B. Marnett, B. C. Crews, R. P. Remel and L. J. Marnet, *J. Med. Chem.*, 2000, **43**, 2860-2880.
170. D. M. Brahmkar and S. B. Jaiswal, *A. Treatise Vallabh Prakashan Delhi*, 1995, **3**, 162-168.
171. M. L. O'Brein and K. D. Tew, *Eur. J. Cancer*, 1996, **32A**, 967-978.
172. S. Gunnarsdottir and A. A. Elfarrar, *J. Pharmacol. Exp. Ther.*, 1999, **290**, 950-957.
173. R. Gennaro and W. Alfanzo, *The Science and Practice of Pharmacy, Lippincott Williams and Wilkins*, 2003, **20**, 913-917.
174. K. A. Nolan, J. R. Doncaster, M. S. Dunstan, K. A. Scott, A. D. Frenkel, D. Siegel, D. Ross, J. Barnes, C. Levy, D. Leys, R. C. Whitehead, I. J. Stratford and R. A. Bryce, *J. Med. Chem.*, 2009, **52**, 7144-715.
175. R. S. Overmunn, M. A. Stahmann, C. F. Henbner, W. R. Sullivan, L. Spero, D. G. Doherty, M. Ikawa, L. Graf, S. Roseman and K. P. Link, *J. Biol. Chem.*,



- 1944, **153**, 5-24.
176. Z. H. Chohan, A. U. Shaikh, A. Rauf and C. T. Supuran, *J. Enzyme. Inbid. Med. Chem.*, 2006, **21**, 741-748.
  177. U. S. Weber, B. Steffen and C. P. Siegers, *Res. Commun. Mol. Pathol. Pharmacol.*, 1998, **99**, 193-206.
  178. E. Budzisz, E. Brzeninska, U. Krajewska and M. Rozalski, *Eur. J. Med. Chem.*, 2003, **38**, 597-603.
  179. M. A. Velasco-Velazquez, J. Agramonte-Hevia, D. Barrera, A. Jimenez-Orozco, M. J. Garcia-Mondragon and N. Mendoza-Patino, *Cancer Letts.*, 2003, **198**, 179-186.
  180. M. Ilia, C. M. Moessmer, I. Nicolova and N. Danchev, *Arch. Pharm. Chem. Life Sci.*, 2006, **339**, 319-326.
  181. R. A. Abramovitch and J. R. Gear, *Can. J. Chem.*, 1958, **36**, 1501.
  182. W. R. Sullivan, C. F. Huebner, M. A. Stahmann and K. P. Link, *J. Am. Chem. Soc.*, 1943, **65**, 2288-2291.
  183. N. S. Zeba and F. Farheen, *Catal. Sci. Technol.*, 2011, **1**, 810-816.
  184. G. Anschutz, *Ann.*, 1909, **367**, 217.
  185. M. K. Khalid, S. Iqbal, A. L. Muhammad, G. M. Maharvi, M. I. Choudhary, A. Rahman, H. Z. Chohan and C. T. Supuran, *J. Enzyme Inhibition and Med. Chem.*, 2004, **19**, 367-371.
  186. V. F. Traven, V. V. Negrebetsky, L. I. Vorobjeva and E. A. Carberry, *Can. J. Chem.*, 1997, **28**, 377-383.
  187. Claude Laruelle and Jean-Jacques Godfroid, *J. Med. Chem.*, 1975, **18**, 85-90.
  188. G. L. Zhao and A. Cordova, *Tetrahedron Lett.*, 2006, **47**, 7417-7421.
  189. S. G. Ouellet, J. B. Tuttle and D. W. C. MacMillan, *J. Am. Chem. Soc.*, 2005, **127**, 32-33.
  190. R. Lavilla, *J. Chem. Soc.*, 2002, **1**, 1141-1156.
  191. D. M. Stout and A. I. Meyers, *Chem. Rev.*, 1982, **82**, 223-228.
  192. G. Appendino, G. Cravotto, S. Tagliapietra, S. Ferraro, G. M. Nano and G. Palmisano, *Helv. Chim. Acta.*, 1991, **74**, 1451-1458.
  193. Alok Kumar. Sapan K. Jain and R. C. Rastogi, *J. Molecular Structure (Theochem)*, 2004, **678**, 55-61.
  194. M. A. Hermodson, W. M. Barker and K. P. Link, *J. Med. Chem.*, 1971, **14**, 167-169.
  195. R. Grigg, T. R. B. Mitchell, S. Suthiraiyakit, *Tetrahedron*, 1981, **37**, 4313.
  196. P. Fristrup, M. Tursky and R. Madsen, *Org. Biomol. Chem.*, 2012, **10**, 2569.
  197. S. L. Schreiber, *Science*, 2000, **287**, 1964-1969.
  198. D. R. Spring, *Org. Biomol. Chem.*, 2003, **1**, 3867-3870.
  199. K. Fujita and R. Yamaguchi, *Synl.*, 2005, 560-571.
  200. G. M. Zhao, H. L. Liu, Xu-ri Huang, D. Zhang and X. Yang, *RSC Adv.*, 2015, **5**, 22996-23008.
  201. J. Cook, J. E. Hamlin, A. Nutton and P. M. Maitlis, *J. Chem. Soc., Dalton Trans.*, 1981, 2342-2352.
  202. K. Fujita, T. Fujii and R. Yamaguchi, *Org. Lett.*, 2004, **6**, 3525-3528.

203. R. Grigg, S. Whitney, V. Sridharan, A. Keep and A. Derrick, *Tetrahedron*, 2009, **65**, 7468-7473.
204. A. Rath, *Adv. Synth. Catal.*, 2007, 1555.
205. D. Balcells, A. Nova, E. Clot, D. Gnanamagari, R. H. Crabtree and O. Eisenstein, *Organometallics*, 2008, **27**, 2529-2535.
206. M. Haniti, S. A. Hamid, P. A. Slatford and J. M. Y. Williams, *Adv. Synth. Catal.*, 2007, **349**, 1555-1575.
207. C. Frederick M. Huntley, Harold B. Wood and Bruce Ganem, *Tetrahedron Lett.*, 2000, **41**, 2031-2034.
208. C. L. Arthurs, G. A. Morris, N. Piacenti, R. G. Pritchard, I. J. Stratford, T. Tatic, R. C. Whitehead, K. F. Williams and N. S. Wind, *Tetrahedron*, 2010, **66**, 9049-9060.
209. D. Mercier, J. Leboul, J. Ceophax and S. D. Gero, *Carbohydr. Res.*, 1971, **20**, 299-304.
210. J. Schulz, M. W. Beaton and G. Gani, *J. Chem. Soc., Perkin Trans.1*, 2000, 943-945.
211. D. N. Gupta, P. Hodge and J. E. Davis, *J. Chem. Soc., Perkin Trans.1*, 1981, 2970-2973.
212. M. Daumas, Y. Vo-Quang, L. Vo-Quang and F. L. Gaffic, *Synthesis*, 1989, 64-65.
213. T. K. M. Shing and Y. L. Zong, *J. Org. Chem.*, 1997, **62**, 2622-2624.
214. J. E. Audia, L. Boisvert, A. D. Patten, A. Villalobos and S. J. Danishefsky, *J. Org. Chem.*, 1989, **54**, 3738-3740.
215. T. Komemnos, *Liebigs Ann. Chem.*, 1883, **218**, 145.
216. A. Michael, *J. Am. Chem.*, 1887, **9**, 112.
217. M. S. Kharasch and P. O. Tawney, *J. Am. Chem. Soc.*, 1941, **63**, 2308-2315.
218. J. Reich, *Compt. Rend.*, 1923, **177**, 322.
219. H. Gilman and J. M. Straley, *Rec. Trav. Chem.*, 1936, **55**, 821.
220. H. Gilman, R. G. Jones and L. A. Wood, *J. Org. Chem.*, 1952, **17**, 1630-1634.
221. H. O. House, L. W. Respass and G. M. Whitesides, *J. Org. Chem.*, 1966, **31**, 3128-3141.
222. N. T. Luong-Thui and H. Riviere, *Compt. Rend.*, 1968, **267**, 776.
223. N. T. Luong-Thui and H. Riviere, *Tetrahedron Lett.*, 1970, 1583.
224. R. C. Whitehead, S. Christou, E. Ozturk, R. G. Pritchard, P. Quale, I. J. Stratford and K. F. Williams, *Bioorg. Med. Chem. Lett.*, 2013, **23**, 5066-5069.
225. M. Sakai, H. Hayashi and N. Miyaara, *Organometallics*, 1997, **16**, 4229-4231.
226. Y. Takaya, M. Ogasawara and T. Hayashi, *J. Am. Chem. Soc.*, 1998, **120**, 5579-5580.
227. Y. Q. Chen, Y. H. Shen, Y. Q. Su, L. Y. Kong and W. D. Zhang, *Chem. Biodivers.*, 2009, **6**, 779-783.
228. K. Zhao, G. J. Cheng, H. Shang, X. Zhang, Y. D. Wu and Y. Tang, *Org. Lett.*, 2012, **14**, 4878-4881.
229. B. Das, N. Chowdhury, J. Banerjee and M. Anjoy, *Tetrahedron Lett.*, 2006, **47**, 6615-6618.

230. G. W. Amarante, P. Rezende, M. Cavallaro and F. Coelho, *Tetrahedron Lett.*, 2008, **49**, 3744-3748.
231. P. Wasnaire, M. Wiaux, R. Touillaux and I. E. Marko, *Tetrahedron Lett.*, 2006, **47**, 985-989.
232. H. S. Byun, K. C. Reddy and R. Bittman, *Tetrahedron Lett.*, 1994, **35**, 1371-1374.
233. C. Z. Yu, B. Liu and L. Q. Hu, *J. Org. Chem.*, 2001, **66**, 5413-5418.
234. J. Cai, Z. Zhou, G. Zhao and C. Tang, *Org. Lett.*, 2002, **4**, 4723-4725.
- 234a. R. Gatri and M. M. E. Gaied, *Tetrahedron Lett.*, 1998, **39**, 5965-5966.
235. B. D. Schwartz, A. Porzelle, K. S. Jack, J. M. Faber, I. R. Gentle and C. M. Williams, *Adv. Synth. Catal.*, 2009, **351**, 1148-1154.
236. O. Y. Mitsunobu and M. Bull, *Soc. Jpn.*, 1967, **40**, 2380-2382.
237. H. U. Bergmeyer, *Methods of Enzymatic Analysis*, 1974, **2**, 2066-72.
238. A. H. Antou and H. M. Solomon, *Acad. Sci.*, 1973, **226**, 1-362.
239. G. L. Trainer, *Expert Opinion on Drug Discovery*, 2007, **2**, 51-64.
240. C. F. Chignell, *Molecular Pharmacology*, 1970, **6**, 1-12.
241. S. Garten and W. D. Wosilait, *Biochemical Pharmacology*, 1971, **20**, 1661-1668.
242. K. Ghosh, D. Kar, R. Frohlich, A. P. Chattopadhyay, A. Samadder and A. R. Khuda-Bukhash, *Analyst*, 2013, **138**, 3038-3045.
243. S. Garten and W. D. Wosilait, *Comp. Gen. Pharma.*, 1972, **3**, 83-88.
244. S. M. Chee, PhD Thesis; The University of Manchester, 2014.
245. X. Huang, Y. Dong, E. A. Bey, J. A. Kilgore, J. S. Bair, L. S. Li, M. Patel, E. I. Parkinson, Y. Wang, N. S. Williams, J. Gao, P. J. Hergenrother and D. A. Boothman, *Cancer Res.*, 2012, **72**, 3038-3047.
246. T. Mosmann, *Journal of Immunological Methods*, 1983, **65**, 55-63.
247. N. J. Desai and S. Sethna, *J. Org. Chem.*, 1957, **22**, 388-90.
248. T. D. Connor and J. R. Sorenson, *J. Het. Chem.*, 1981, **18**, 587-590.
249. T. R. Kasturi, J. A. Sattiger and P. V. P. Pragnacharyulu, *Tetrahedron lett.*, 1995, **51**, 3051-3059.
250. M. R. Naimi-Jamal, *Europ. J. Org. Chem.*, 2009, **21**, 3567-72.
251. P. Andre Dieskau, *Europ. J. Org. Chem.*, 2011, **2011**, 5291-96.
252. B. E. Norcross, G. Clement and M. Weinstein, *J. Chem. Educ.*, 1969, **46**, 694-695.
253. D. Dennis Tanner, *J. Org. Chem.*, 1988, **53**, 1646-50.
254. G. Appendino, G. Gravotto, S. Tagliapietra, S. Ferraro, G.M. Nano and G. Palmisano, *Helv. Chim. Acta.*, 1991, **74**, 1451-58.
255. K. K. Bhargava, *Indian J. Chem.*, 1975, **13**, 321-2.
256. W. R. Sullivan, *J. Am. Chem. Soc.*, 1943, **65**, 2288-91.
257. Qadir, Salma, *Synth. Commun.*, 2008, **38**, 3490-99.
258. Gpmg, Gui-Xia, *Synth. Commun.*, 2009, **39**, 497-505.
259. Singh, Preashant, *Catalysis Lett.*, 2010, **134**, 303-308.
260. H. Mehrabi and H. Abusaidi, *J. Iran. Chem. Soc.*, 2010, **7**, 890-894.

261. H. Zhao, N. Neamati, H. Hong, A. Mazumder, S. Wang, S. Sunder, George W. A. Milne, Y. Pommier and T. R. Bure (Jr), *J. Med. Chem.*, 1997, **40**, 242-249.
262. K. Mehadi, F. Alireza, E. Saeed, S. Maliheli, D. Gholamreza, A. Babak, R. Ali, *Chem. Biol. Drug Des.*, 2011, **78**, 580-586.
263. M. Ilia, *Archiv der Pharmazie (Weinheim, Germany)*, 2006, **339**, 319-326.
264. B. D. Ramachary and K. Mamillapalli, *Org. Biomol. Chem.*, 2010, **8**, 2859-67.
265. A. Montagut-Romans, M. Boulven, M. Lemaire and F. Popowycz, *New J. Chem.*, 2014, **38**, 1794-1801.
266. M. Darius, *Bulletin de la Societe Chimique de France*, 1961, 1417-28.
267. D. Mercier, J. Leboul, J. Cleophax and S.D. Gero, *Carbohydr. Res.* 1971, **20**, 299-304.
268. J. Schultz, M. W. Beaton and D. Gani, *J. Chem. Soc., Perkin Trans. 1*, 2000, 943-954.
269. C. Colas, B. Quiclet-Sire, J. Cleophax, J. Delaumeny, A. Sepulchre and S. D. Gero, *J. Am. Chem. Soc.*, 1980, **102**, 857-858.
270. N. Robertson, I. J. Stratford, S. Houlbrook, J. Carmichael and G. E. Adams, *Biochem. Pharmacol.*, 1992, **44**, 409-412.

## List of figures, tables and schemes

Figure 1.	Cross section of a human cell.....	12
Figure 2.	Loss of normal cell growth control shown in red. The cells escape apoptosis and therefore progress to a tumor.....	13
Figure 3.	Cancer cell division.....	14
Figure 4.	Cross section of human liver taken at autopsy examination, showing multiple large pale tumor deposits.....	14
Figure 5.	Seven acquired capabilities of cancer cells (hallmark of cancer).....	15
Figure 6.	The cell cycle, showing G1, S, G2 and M phases. Cell growth occurs during G1 and G2, while DNA is synthesized in S phase. Cell division occurs during M phase (mitosis). G0 is a quiescent phase where the cell exists the cycle but can re-enter if the signals from the environment are adequate. Red dots indicate cell cycle checkpoints.....	17
Figure 7.	Angiogenesis causes blood vessels to grow more branches for transportation of nutrients, oxygen and evacuation of carbondioxide.....	18
Figure 8.	Structure of DNA with the protective telomeres at the end of the chromosomes.....	19
Figure 9.	Oncogene and cancer cell.....	21
Figure 10.	Structure of antioxidant compounds: glutathione (1), vitamin C(2) and vitamin E (3).....	22
Figure 11.	Emden-Meyerhof Paranas glycolytic pathways. Steps i and iii consume ATP while steps vii and x produce ATP. Steps vi-x occur twice per glucose molecule and therefore, producing a total of 2 ATP for the complete pathway.....	23
Figure 12.	Comparison of glucose metabolic pathways in normal and cancer cells.....	24
Figure 13.	Pentose phosphate pathway (PPP).....	25
Figure 14.	Structure of warfarin (4) and tamoxifen (5).....	28
Figure 15.	Structure of Flavin adenine dinucleotide (FAD, 6).....	29
Figure 16.	Compounds generally considered as NQO1-directed anti-tumor agents; mytomycin C (7), quinolinequinone (8), aziridinybenzoquinone (9) and CB1954 (10).....	30
Figure 17.	Structure of NADH and NADPH .....	30
Figure 18.	Structure of UDP-glucuronic acid (14).....	31
Figure 19.	Diagrammatic representation of the ‘ping-pong’ mechanism of NQO1.....	32
Figure 20.	Structures of NQO1 co-substrates.....	32
Figure 21.	Structure of butylated hydroxyanisole.....	33
Figure 22.	X-ray crystal structure of human NQO1 in complex with its inhibitor dicoumarol (purple) and FAD (red), green and blue $\alpha$ -helices and $\beta$ -sheets represent one monomer. The second monomer is represented by orange and yellow $\alpha$ -helices and $\beta$ -sheets.....	34

Figure 23.	Diagrammatic representation of the NQO1 dimer.....	34
Figure 24.	A single unit of NQO1 showing $\alpha$ -helices and twisted $\beta$ -sheet.....	35
Figure 25.	Representation of FAD-NQO1 interactions showing residues involved in hydrogen bonds (dashed lines) to the cofactor. FAD is secured by Tyr-104, Trp-105, Phe-106 and Leu-103.....	35
Figure 26.	Structural image of deoxynyboquinone (DNQ) in the NQO1 active site. DNQ is reduced by NQO1, thus preventing one electron reduction by cytochrome c reductases which would produce ROS...36	36
Figure 27.	The active site residues of human NQO1.....	36
Figure 28.	Structures of flavones; 7,8-dihydroxyflavone ( <b>29</b> ) and chrysin ( <b>30</b> )..	38
Figure 29.	Structures of menadione ( <b>31</b> ) and vitamin K <sub>1</sub> ( <b>32</b> ).....	38
Figure 30.	Interaction of dicoumarol with NQO1. Protein amino acid, FAD and dicoumarol are labelled (C) and (A) to represent the 1 <sup>st</sup> and 2 <sup>nd</sup> NQO1 monomers respectively. Nitrogen atoms are coloured in blue, oxygen in red and carbon in black. Residues making Van der Waals interactions with the dicoumarol are represented by a decorated arc. Hydrogen bonds are represented by dashed green lines along their distances.....	38
Figure 31.	Structure of warfarin ( <b>4</b> ), CB1954 ( <b>10</b> ), DCPIP ( <b>20</b> ), phenindone ( <b>34</b> ), ES936 ( <b>35</b> ) and cibacron blue ( <b>36</b> ).....	39
Figure 32.	Misfolded proteins and its degradation by proteasome.....	39
Figure 33.	X-ray crystal structure of NQO2. Zinc/ copper metal is represented in purple colour.....	41
Figure 34.	Structure of NRH ( <b>37a</b> ) and its analogues ( <b>37b-f</b> ).....	41
Figure 35.	Structure of ethylenediamine tetra-acetic acid (EDTA, <b>38</b> ).....	42
Figure 36.	Representation of the deep cavity of the active site of the NQO2 in its apo-form with the non-covalently bound FAD.....	42
Figure 37.	Structure of trans-resveratrol ( <b>39</b> ).....	43
Figure 38.	Representation of FAD interaction with CB1954 ( <b>10</b> ) in NQO2 active site. CB1954 makes two important electrostatic interactions with the protein residues such as Gly 149 and Asn 161. The site of reduction is in proximity to the FAD N5 (3.0 Å). Gly 149 holds the CB1954 strongly and thereby places the 4-nitro group in a better orientation for hydride transfer.....	44
Figure 39.	CB1954 at the active site of NQO2 in a parallel position with respect to the FAD moiety.....	44
Figure 40.	Resveratrol ( <b>39</b> ) in the binding pocket of NQO2 active site. The structure illustrates the $\pi$ - $\pi$ interaction of the FAD moiety with the resveratrol inhibitor. The green colour represents water molecules.....	44
Figure 41.	Predicted binding orientation of CB1954 ( <b>10</b> ) in the active site of NQO1. The diagram suggested different orientation of CB1954 in NQO1 compared with that of NQO2.....	45
Figure 42.	Structure of quinacrine ( <b>40</b> ) and chloroquine ( <b>41</b> ).....	46

Figure 43.	Structure of chrysoeriol ( <b>42</b> ), quercetin ( <b>43</b> ) and primaquine ( <b>44</b> )....	46
Figure 44.	Structures of COTC ( <b>45</b> ), gabosine ( <b>46</b> ), antheminone A ( <b>47</b> ), phorbasin B ( <b>48</b> ) and COMC ( <b>49</b> ).....	49
Figure 45.	Structure of methylglyoxal ( <b>50</b> ).....	50
Figure 46.	Structure of thiophenol ( <b>51</b> ), 2-mercaptoethanol ( <b>52</b> ) and cysteine ( <b>53</b> ).....	50
Figure 47.	Structure of mono-hydroxylated analogues of COTC ( <b>45</b> ).....	51
Figure 48.	Glutathione disulphide (GSSG, <b>62</b> ).....	54
Figure 49.	Chemotherapeutic anti-cancer agents: Cisplatin ( <b>63</b> ), Melphalan ( <b>64</b> ) and Chlorambucil ( <b>65</b> ).....	54
Figure 50.	Structure of COTC-GSH conjugate adduct ( <b>66</b> ).....	55
Figure 51.	X-ray crystal structure of $\pi$ GSTP1-1 showing the Tyr 108 residue in black colour which was proposed to be involved in the activation of glutathione (GSH).....	56
Figure 52.	Structure of antheminone A ( <b>47</b> ), antheminone B ( <b>69</b> ) and antheminone C ( <b>70</b> ).....	59
Figure 53.	Structure of some of the carvoacetone derivatives isolated ( <b>71</b> - <b>75</b> ).....	61
Figure 54.	Chemical structure of carvotacetone derivatives ( <b>76-79</b> ) that display antiplasmodial, antileishmanial and anticancer properties.....	62
Figure 55.	A simplified illustration of the prodrug concept. Barriers are any limitations that prevent optimal efficiency of the parent drug which has to be overcome for the development of a marketable drug. This is achieved by coupling the drug with a drug carrier moiety. The ideal prodrug yields the parent drug with high recovery ratios with the drug carrier moiety being either toxic or non-toxic.....	63
Figure 56.	Structure of symmetrical dicoumarol ( <b>33</b> ) and its derivatives ( <b>92a</b> ) and ( <b>92b</b> ).....	65
Figure 57.	General structure of asymmetrical dicoumarol used as NQO1 inhibitors.....	65
Figure 58.	General structure of target compounds.....	66
Figure 59.	Representation of cell membrane with phospholipid hydrophilic layer.....	66
Figure 60.	Structure of an analogue of antheminone A ( <b>84a</b> ), utilized for prodrug synthesis ( <b>84b</b> ) and ( <b>84c</b> ).....	67
Figure 61.	Structure of $\alpha$ -benzopyrene ( <b>85a</b> ) and $\gamma$ -benzopyrone ( <b>85b</b> ).....	68
Figure 62.	Structure of quercetin ( <b>43</b> ), 4-hydroxycoumarin ( <b>86</b> ), 7-hydroxy coumarin ( <b>87</b> ).....	68
Figure 63.	Structure of symmetrical analogues of dicoumarol.....	69
Figure 64.	General structure of “halfway stage” ( <b>91</b> ) analogues of dicoumarol.....	70
Figure 65.	Structures of symmetrical ( <b>92</b> ) and asymmetrical ( <b>93</b> ) analogues of dicoumarol.....	71
Figure 66.	General structure of the target compounds.....	72

Figure 67.	<sup>1</sup> H NMR spectrum of compound ( <b>96</b> ) in DMSO d <sub>6</sub> ; 3,6,7 and 8 represent protons and their multiplicity.....	74
Figure 68.	General structure of synthesized symmetrical dicoumarols.....	74
Figure 69.	General structure of compounds with substituent (X) at para-position.....	76
Figure 70.	<sup>1</sup> H NMR spectra of compound ( <b>101</b> ); ‘A’ represent <sup>1</sup> H NMR spectrum of compound ( <b>101</b> ) in CDCl <sub>3</sub> and ‘B’ is the <sup>1</sup> H NMR spectrum after addition of D <sub>2</sub> O.....	77
Figure 71.	Structure of substituted dicoumarols at the methylene bridge.....	77
Figure 72.	Different tautomers of dicoumarol and its analogues.....	84
Figure 73.	Dicoumarol analogue in a monoprotonated form ( <b>114a</b> ) (acid catalysis) and monodeprotonated form ( <b>114b</b> ) (base catalysis).....	84
Figure 74.	Structure of dienolates (deprotonated anions of enols, <b>114c</b> ).....	85
Figure 75.	Catalysts used in ‘borrowing hydrogen’ reaction.....	86
Figure 76.	Halide bridge dimer used in metal catalysed borrowing hydrogen methodology.....	86
Figure 77.	Dimer-monomer equilibrium.....	88
Figure 78.	<sup>1</sup> H NMR spectrum of crude reaction product involving ruthenium catalyst in ‘borrowing hydrogen methodology’ at a temperature of 110 °C.....	91
Figure 79.	<sup>1</sup> H NMR spectrum of crude reaction product involving ruthenium catalyst in ‘borrowing hydrogen methodology’ at a temperature of 140 °C.....	92
Figure 80.	Structure of analogue of antheminone A ( <b>84</b> ) used in prodrug synthesis ( <b>84a</b> ).....	93
Figure 81.	Analogues of COTC ( <b>45</b> ) and antheminones synthesized by the Whitehead group.....	94
Figure 82.	Structures of incarviditone ( <b>158</b> ) and rengyolone ( <b>159</b> ).....	107
Figure 83.	The revised structure of incarviditone ( <b>160</b> ) proposed by Wu and Tang and co-workers.....	108
Figure 84.	Structure of dimeric compounds ( <b>124e</b> ) and ( <b>124f</b> ) tested against lung cancer cell line (A549).....	108
Figure 85.	Structure of sodium dodecyl sulfate (SDS) used as a surfactant in the MBH reaction.....	110
Figure 86.	Representation of Morita-Baylis-Hillman reaction in micelles .....	111
Figure 87.	Structures of the potential prodrugs.....	113
Figure 88.	Evaluation of NQO1 activity using menadione ( <b>31</b> ) as intermediate electron acceptor and cytochrome c as the terminal electron acceptor.....	115
Figure 89.	A sigmoid curve for the concentration-response plot of the enzyme assay.....	116
Figure 90.	Neutral ( <b>33</b> ), mono-ionic ( <b>33i</b> ) or di-ionic ( <b>33ii</b> ) states of dicoumarol.....	117



Figure 91.	Electron density map around the dicoumarol in NQO1 active site.....	119
Figure 92.	Structures of symmetrical unsymmetrical dimer, asymmetrical and ‘halfway stage’ analogues of dicoumarol.....	120
Figure 93.	General structures of symmetrical and unsymmetrical dimer analogues ( <b>171a</b> and <b>171b</b> ) of dicoumarol.....	120
Figure 94.	IC <sub>50</sub> values for the synthetic analogues ( <b>182</b> ) of COTC, ( <b>183</b> ) and ( <b>184</b> ) for antheminone A.....	125
Figure 95.	IC <sub>50</sub> values of the prodrug ( <b>185</b> ).....	125
Figure 96.	IC <sub>50</sub> values of the “halfway stage” analogues of dicoumarol ( <b>175a</b> ) and the prodrug ( <b>186</b> ).....	126
Figure 97.	Potent inhibitors of NQO1 remodified as prodrug and their measured IC <sub>50</sub> values for cell viability.....	126
Figure 98.	IC <sub>50</sub> values of dicoumarol ( <b>33</b> ) and its derivatives ( <b>92a</b> , <b>92b</b> and <b>92c</b> ).....	127
Figure 99.	Cytotoxicity values of ( <b>172a</b> , <b>175b</b> and <b>178a</b> ).....	128
Figure 100.	Cytotoxic agent ( <b>184</b> ) derived from antheminone A ( <b>47</b> ).....	128
Figure 101.	Structures of novel anti tumor agents.....	131
Figure 102.	The potential anti tumor agents ( <b>216</b> , <b>218</b> and <b>220</b> ) .....	131
Figure 103.	The haemocytometer grid.....	194
Table 1.	Level of NQO1 activity in normal and tumor tissues. The values represent the activity inhibited by 1 $\mu$ M dicoumarol with dichloroindophenol (DCPIP) as the substrate. Units are nmol/min/mg protein.....	48
Table 2.	Bioactivity of COTC ( <b>45</b> ) and its analogues.....	51
Table 3.	Cytotoxic activities ( $\mu$ M) of antheminones A ( <b>47</b> ), antheminone B ( <b>69</b> ) and antheminones C ( <b>70</b> ) determined after 72 hours.....	60
Table 4.	Comparison between the %yields obtained using microwave irradiation and thermal under reflux.....	78
Table 5.	IC <sub>50</sub> values of dicoumarol ( <b>33a</b> ) and its derivatives ( <b>92a</b> ) and ( <b>92b</b> ).....	118
Table 6.	IC <sub>50</sub> values of asymmetrical analogues ( <b>93</b> ) of dicoumarol.....	118
Table 7.	IC <sub>50</sub> values of asymmetrical analogues of dicoumarol obtained using NaBH <sub>4</sub> /LiBH <sub>4</sub> and NaCNBH <sub>3</sub> .....	121
Table 8.	IC <sub>50</sub> values of the “halfway stage” analogues of dicoumarol.....	122
Table 9.	IC <sub>50</sub> values of the asymmetrical analogues of dicoumarol obtained by ‘borrowing hydrogen methodology’.....	123
Table 10.	The effective inhibitors of NQO1.....	130
Table 11.	Sequence of the enzyme assay analysis.....	192

Scheme 1.	One electron reduction of quinones ( <b>11</b> ) by cytochrome p450 reductase results in formation of semi-quinone radical intermediates ( <b>13</b> ), whereas two electron reduction forms hydroquinone ( <b>12</b> ).....	30
Scheme 2.	Reaction mechanism of human NQO1. The quinone reduction occurs via two hydride transfer steps: transfer of one hydride from the electron donor (NADH) to FAD and a second hydride from FADH to the quinone following a ‘ping-pong’ mechanism.....	31
Scheme 3.	Flavin mediated electron transfer from NADPH to an azo dye ( <b>24</b> ) to give the products: 2-amino benzoic acid and <i>N,N</i> -dimethyl benzene-1,4-diamine.....	33
Scheme 4.	Reduction of CB1954 ( <b>10</b> ) to 5-(aziridin-1-yl)-4-(hydroxyamino)-2-nitrobenzamide ( <b>10a</b> ) catalysed by NQO1 and NQO2.....	45
Scheme 5.	One electron reduction of quinone ( <b>11</b> ) to a semiquinone ( <b>13</b> ) caused by cytochrome p450 reductases.....	47
Scheme 6.	Nucleophilic displacement of the crotonyl moiety of COTC ( <b>45</b> ) by sulfhydryl containing compounds.....	50
Scheme 7.	The mechanism of methylglyoxal ( <b>50</b> ) detoxification by the glyoxalase system.....	53
Scheme 8.	Synthesis of reduced glutathione from its precursor amino acids; L-glutamic acid ( <b>59</b> ), L-cysteine ( <b>60</b> ) and glycine ( <b>61</b> ).....	53
Scheme 9.	Nucleophilic displacement of crotonate group by GSH.....	56
Scheme 10.	Mechanism of formation of an intermediate electrophilic exocyclic enone ( <b>68</b> ).....	57
Scheme 11.	Mechanism of alkylation of nucleic acids/proteins by an exocyclic enone ( <b>68</b> ) to give ( <b>69</b> ).....	57
Scheme 12.	An alternative mechanism for the reaction of COMC ( <b>49</b> ) and GSH in the presence of $\pi$ (hGSTP1-1).....	58
Scheme 13.	The assumed mechanism of action of antheminones A ( <b>47</b> ). The reaction is not chemically allowed because OH is a poor leaving group and thus cannot be displaced by GSH. The mechanism by which antheminone A exerts their antitumor effects is still unknown.....	60
Scheme 14.	The proposed mechanism of action of antheminones C ( <b>70</b> ) by Collu and co-workers.....	61
Scheme 15.	Prodrug ( <b>80</b> ) activation by GSH which releases cytotoxic thiopurine ( <b>81</b> ).....	64
Scheme 16.	Synthesis of analogues of dicoumarol using 5 mol% Zn(proline) <sub>2</sub> .....	70
Scheme 17.	Synthesis of symmetrical ( <b>92</b> ) and asymmetrical ( <b>93</b> ) analogues of dicoumarol.....	71
Scheme 18.	Synthesis of dicoumarols using a catalytic amount of piperidine ( <b>94</b> ) in aqueous EtOH at room temperature.....	72
Scheme 19.	Reaction scheme for the synthesis of derivatives of 4-hydroxycoumarin ( <b>96</b> ), ( <b>98</b> ) and ( <b>100</b> ).....	73

Scheme 20.	Base mediated cyclisation reaction of 2-hydroxy-6-methoxy acetophenone to give <b>(96)</b> . The mechanism is applicable to compound <b>(98)</b> and <b>(100)</b> .....	73
Scheme 21.	Resonance forms of ionized 4-hydroxycoumarin.....	74
Scheme 22.	Synthesis of analogues of dicoumarol.....	75
Scheme 23.	General mechanism for condensation and dimerization reaction.....	76
Scheme 24.	General method for the preparation of the “halfway stage” analogues <b>(102)</b> of dicoumarol.....	78
Scheme 25.	Synthesis of “half-way stage” analogues <b>(101)</b> of dicoumarol using <i>para</i> -substituted aromatic aldehydes gave dimeric products <b>(107)</b> instead of <b>(101)</b> .....	79
Scheme 26.	Reduction of “halfway stage” analogues <b>(101)</b> to give asymmetrical analogues <b>(108)</b> using NaBH <sub>4</sub> /LiBH <sub>4</sub> .....	80
Scheme 27.	Mechanism of reduction of “halfway stage” compounds <b>(101)</b> with NaBH <sub>4</sub> /LiBH <sub>4</sub> .....	80
Scheme 28.	Mechanism of reduction of the ‘halfway stage’ <b>(101)</b> using Hantzsch’s ester.....	81
Scheme 29.	Mechanism of Hantzsch’s ester synthesis <b>(109)</b> .....	82
Scheme 30.	Synthesis of asymmetrical analogues of dicoumarol <i>via</i> C-C reductive cleavage.....	83
Scheme 31.	Proposed mechanism for reductive C-C cleavage of symmetrical dimer using NaBH <sub>3</sub> CN.....	84
Scheme 32.	General procedure for the synthesis of asymmetrical analogues of dicoumarol <b>(119)</b> derived from 4-hydroxycoumarin or 4-hydroxyquinoline.....	87
Scheme 33.	Ionization of an alcohol producing high energy charged intermediate (R <sup>+</sup> ).....	87
Scheme 34.	Mechanism of tosylate ester <b>(120)</b> formation.....	87
Scheme 35.	Mechanism of halide <b>(121)</b> formation.....	88
Scheme 36.	The mechanistic sequence of alcohol oxidation and reduction by iridium-carbonate complex.....	88
Scheme 37.	C-C bond formation using an iridium-catalysed ‘borrowing hydrogen’ (Path A) and the activation of alcohols (Path B) by borrowing hydrogen methodology (Adapted from Williams and co-workers).....	89
Scheme 38.	Proposed mechanism for C-3 alkylation fo 4-hydroxycoumarin and its derivatives using iridium catalyst.....	90
Scheme 39.	General scheme for C-3 alkylation of 4-hydroxycoumarin using ruthenium catalyst <b>(116)</b> in the ‘borrowing hydrogen methodology’.....	91
Scheme 40.	An eight-step reaction sequence for the synthesis of COTC <b>(45)</b> .....	93
Scheme 41.	Synthetic approach to a prodrug for release of an inhibitor of NQO1.....	95

Scheme 42.	Synthesis of cyclohexylidene ketal ( <b>136</b> ).....	95
Scheme 43.	Mechanism of formation of cyclohexylidene ketal ( <b>136</b> ) from (-)-quinic acid ( <b>134</b> ).....	96
Scheme 44.	Mechanism of formation of triol ( <b>137</b> ).....	97
Scheme 45.	Mechanism of the oxidative cleavage of triol ( <b>137</b> ) to hydroxyl ketone ( <b>138</b> ).....	98
Scheme 46.	Mechanism for the in situ formation of sulfene intermediate ( <b>140</b> ) via E1 <sub>c</sub> B.....	98
Scheme 47.	Mechanism of formation of enone ( <b>139</b> ).....	99
Scheme 48.	Mechanism of formation of hydroquinone ( <b>138d</b> ).....	99
Scheme 49.	Conjugate addition of $\alpha,\beta$ -unsaturated ester given a $\beta$ -substituted product ( <b>141</b> ).....	100
Scheme 50.	Reaction of $\alpha,\beta$ -unsaturated enone ( <b>142</b> ) with CH <sub>3</sub> MgBr in the presence and absence of copper(1) salt according to Kharasch and co-workers.....	100
Scheme 51.	Synthetic pathway for the formation of a Gilman reagent ( <b>146</b> ).....	101
Scheme 52.	Stereochemical outcome of the reactions with organocuprate reagents in the presence and absence of additive (TMSCl).....	102
Scheme 53.	Reaction of but-3-en-2-one ( <b>147</b> ) and phenylboronic acid ( <b>148</b> ) using Rh(acac)(CO) <sub>2</sub> /dppb to give 4-phenylbutan-2-one ( <b>149</b> ).....	102
Scheme 54.	Conjugate addition using Rh(acac)(C <sub>2</sub> H <sub>4</sub> ) <sub>2</sub> /(S)-binap in the presence of boronic acid.....	103
Scheme 55.	Synthesis of fluorophenyl adduct ( <b>152</b> ).....	104
Scheme 56.	Mechanistic cycle for the formation of conjugate adduct ( <b>152</b> ).....	105
Scheme 57.	Eliminative deprotection of ketone ( <b>152</b> ) protecting group using a catalytic amount of base.....	105
Scheme 58.	Mechanism of deprotection of ( <b>152</b> ) to give $\gamma$ -hydroxyenone ( <b>154</b> ).....	106
Scheme 59.	Mechanism for the formation of cyclohexane-1,4-dione ( <b>157</b> ).....	106
Scheme 60.	Proposed mechanism for the dimerization of alcohol ( <b>154</b> ).....	107
Scheme 61.	Synthesis of triethylsilyl ether ( <b>163</b> ).....	108
Scheme 62.	Mechanism of formation of triethylsilyl ether ( <b>163</b> ).....	109
Scheme 63.	Morita-Baylis-Hillman reaction.....	109
Scheme 64.	MBH reaction of cyclohexanone ( <b>166a</b> ) with substituted aromatic aldehyde ( <b>166b</b> ) to give ( <b>166c</b> ) .....	111
Scheme 65.	Mechanism of the Morita-Baylis-Hillman reactions for the synthesis of ( <b>169</b> ).....	112
Scheme 66.	General reaction scheme for the Mitsunobu reaction.....	112
Scheme 67.	Synthesis of prodrugs.....	113
Scheme 68.	Mechanism of the prodrug ( <b>170g</b> ) formation.....	114

Scheme 69. Reduction of MTT dye ( <b>181a</b> ) (yellow) to formazan ( <b>181b</b> ) (purple) by mitochondrial succinate dehydrogenase.....	124
--	-----

